PHENYLENEDIAMINE PYRIDYL LIGANDS AND BORYL SUPPORT LIGANDS FOR ORTHO-DIRECTED IRIDIUM CATALYZED C–H BORYLATION

By

Alex C. O'Connell

A DISSERTATION

Submitted to
Michigan State University
in partial fulfillment of the requirements
for the degree of

Chemistry – Doctor of Philosophy

2022

ABSTRACT

PHENYLENEDIAMINE PYRIDYL LIGANDS AND BORYL SUPPORT LIGANDS FOR ORTHO-DIRECTED IRIDIUM CATALYZED C–H BORYLATION

By

Alex C. O'Connell

With organoboron compounds being useful components in the synthesis of pharmaceuticals, agrochemicals, and materials, it is imperative to find new catalytic strategies to design an effective system capable of borylating a broad range of (hetero)arene substrates in high yields and high selectivity. Traditional iridium-catalyzed systems borylate aromatic compounds and are directed by steric factors of the substrate. These steric-directed catalysts are hypothesized to have a singly open coordination site on the metal center where activation of the most accessible C–H bond can occur. In order to change regioselectivity from steric products to alternatives, new catalyst systems must be designed.

A phenylenediamine pyridyl framework was implemented for chelate-directed C–H borylation, where an aromatic substrate undergoes borylation of the *ortho* C–H bond, relative to a directing group. This ligand type has been explored and shown to have three major components that influence the reactivity, selectivity, and coordination of the ligand. These parts that make up the ligand were examined using a ligand screen, NMR studies, and stoichiometric reactions.

From the literature, it has been shown that double B,N-bidentate ligated catalysts work well for a broad substrate scope and produce borylated products whose substitution pattern is based on steric effects. Other variants of this system have used a single B,N-bidentate ligand to produce products borylated in the *ortho*-position relative to a directing

group on the substrate. To improve upon these catalytic systems, experiments were performed to optimize *ortho*-selectivity of the originally steric-directed catalyst containing two B,N-bidentate ligands by reducing the loading of the dimer boryl ligand. In doing so, regioselectivities can be completely switched from steric products to chelate products. This modification of ligand to metal ratio greatly effects selectivity and is a unique feature to dimer boryl ligands.

These phenylenediamine pyridyl ligands and boryl support ligands will be explored.

Dedicated to my family–
Thank you for everything you have done for me

ACKNOWLEDGMENTS

Well, graduate school has been quite the experience. Lots of ups and downs but it was a journey worthwhile. As with every journey, you meet friend and foe along the way…

Surviving graduate school would not have been possible without the love and support of my family. My mother and father (Cathy & Mike) and my brother (Zach) were the bedrock I could build my foundations on. Their encouragement and belief in me gave me the strength to keep going and push through. I thank them for their patience and understanding while I was away for so long.

To my friends Kiyo, Ryan, Tim, Reza, and Mona–you have all been tremendously helpful and it was truly a pleasure to work, converse, and spend time with you while at Michigan State. You all are what made grad school fun and exciting. I probably learned more about chemistry discussing ideas and concepts with you than in any classroom.

Lastly, I would like to acknowledge my advisor, committee members, and chemistry support staff for their aid in the graduation process, useful advice, and taking a part in my education.

Thank you all.

TABLE OF CONTENTS

LIST OF TABLES

LIST OF FIGURES

LIST OF SCHEMES

KEY TO ABBREVIATIONS

Å	Angstrom
Ar	Aryl
BDE	Bond dissociation enthalpy
B_2pin_2	Bis(pinacolato)diboron
Bz	Benzyl
°C	Degrees Celsius
CHB	C–H borylation
COD	1,5-Cyclooctadiene
COE	Cyclooctene
Cp	Cyclopentadiene
DCM	Dichloromethane
DG	Directing group
dtbpy	4,4’-di-*tert*-butyl-2,2’dipyridyl
EAS	Electrophilic aromatic substitution
equiv	Equivalent
h	Hour
HBpin	Pinacolborane
Ind	Indenyl
*i*Pr	isopropyl
K	Kelvin
kcal	kilocalorie

KIE	Kinetic isotope effect
Me	Methyl
Mes	Mesitylene
mg	Milligram
mL	Milliliter
mol	Mole
mmol	Millimole
mp	Melting point
m/*z*	Mass divided by charge of an ion
NMR	Nuclear magnetic resonance
Ph	Phenyl
ppm	Parts per million
rt	Room temperature
SMAP	Silica-supported monophosphine
SMCC	Suzuki-Miyaura Cross-Coupling
THF	Tetrahydrofuran
tmphen	3,4,7,8-tetramethyl-1,10-phenanthroline
^{t}Bu	*tert*-Butyl
Xyl	Xylene

Chapter 1. Introduction to C–H Borylation

1.1 C–H Activation and Functionalization

C–H activation and functionalization is a key chemical transformation in building complex molecules. Organic compounds are the foundation of nature and comprise the structures within pharmaceuticals and biologically active molecules, agrochemicals, and materials. With such an abundance and prevalence of this chemical class, it is important to be able to selectively diversify it into more valuable end products. However, selectively activating and functionalizing hydrocarbons entails challenges owing to their relatively inert nature. This is due to C–H bonds being nonpolar and of low basicity/acidity, compared to other chemical groups. For functionalizing aromatic compounds, aromaticity usually needs to be temporarily broken in order to activate the C(sp^2)–H and substitute a different functionality. Aromatic substitution reactions typically require stoichiometric amounts of metal for enhancement of the electrophile to be substituted on the ring and often use harsh basic or acidic conditions.[1,2] These conditions may have a negative impact or increase the difficulty of synthesis when sensitive functional groups are present on the substrate. This becomes especially apparent for late-stage functionalization of complex molecules. Because of these matters, a more direct and mild method for functionalizing hydrocarbon bonds for further diversification is desirable.[3]

1.2 Organoboron Compounds

Organoboron compounds are incredibly versatile in their ability to be easily transformed into other functionalities. The first prominent case of this was studied and disclosed by H. C. Brown who demonstrated organoboranes could be used as synthetic

intermediates to form alcohols.[4,5] He was awarded the Nobel Prize in 1979 for his pioneering work on organoboranes.

Another leading example, and Nobel winning work, highlighting organoboron's proficiency as a chemical intermediate was the Suzuki-Miyaura cross-coupling (SMCC) reaction. In this palladium-catalyzed reaction, aryl carbon-carbon bonds are formed using boronic acid and organohalide starting reagents. In medicinal chemistry, the SMCC reaction has become the most employed method for carbon-carbon bond formation.[5,6]

Boronic acids and esters have found tremendous usage in further diversifying organic molecules. From a starting aryl-boronic ester, the C–B group can be transformed into alcohols,[7] amines,[8,9] halogens,[10,11] cyano groups,[12,13] aryl groups,[14] and more (Scheme 1.1).

Scheme 1.1 Utility of aryl boronic acids/esters.

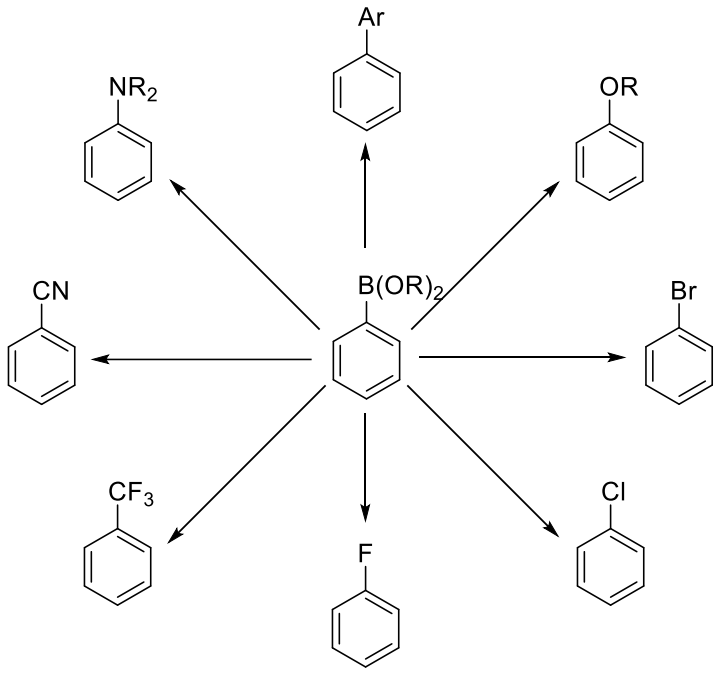

While organic boronic esters are valuable synthetic intermediates, their syntheses were not initially straightforward. Traditionally, the route to forming an aryl-boronic ester

was a three-step process (Scheme 1.2).[15] Starting from an arene, one must first perform a halogenation reaction, form a Grignard reagent, and finally quench the Grignard reagent with a boronic ester. With each additional step in a reaction, yields will be lowered, and waste streams increased.

Scheme 1.2 Synthetic route to aryl boronic esters.

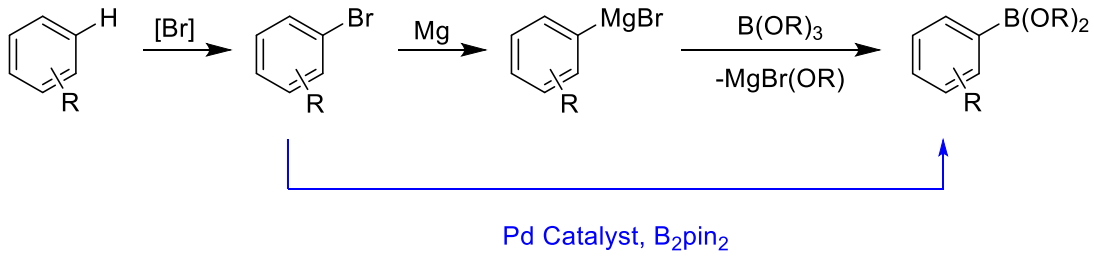

An alternative two-step route to these desired products is Miyaura borylation. By this method, an aryl halide is cross coupled with bis(pinacolato)diboron (B_2pin_2), forming the boronate.[16] This reaction uses a palladium catalyst under basic conditions.

1.3 Iridium Catalyzed C–H Borylation

Given that organoboron compounds are so versatile and important in chemistry, an efficient catalyst that has high functional group tolerance and could directly activate and functionalize a C–H bond into a C–$B(OR)_2$ group would be highly valuable. In 1994, the Hartwig group published computational data revealing that the transformation from hydrocarbon to organoborane is thermoneutral (Scheme 1.3), showing that this overall process could be a feasible synthetic route.[17]

Scheme 1.3 Reaction of methane with catecholborane (HBcat) or ethylene glycol borane (HBeg) to form the organoboron product. Bond dissociation enthalpies (BDE) in (kcal/mol).

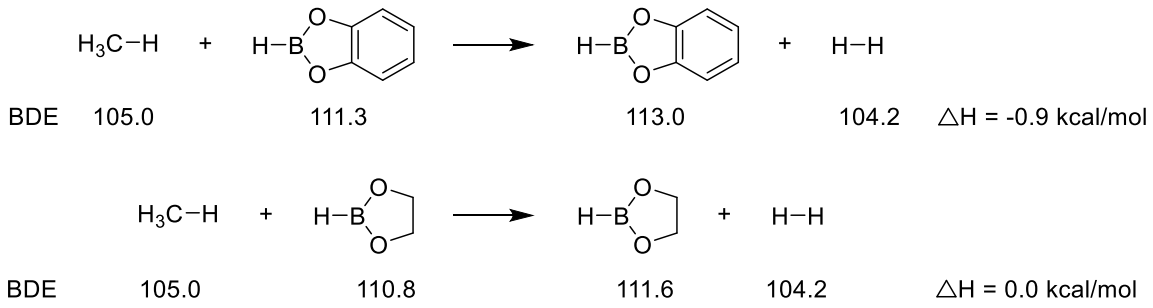

The first thermal catalyst for direct CHB reactions was reported by Smith and Iverson in 1999.[18] This landmark discovery presented an iridium catalyst borylating benzene using pinacolborane (HBpin) as the boron source, with H_2 gas being the sole byproduct (Scheme 1.4).

Scheme 1.4 First thermal CHB catalyst.

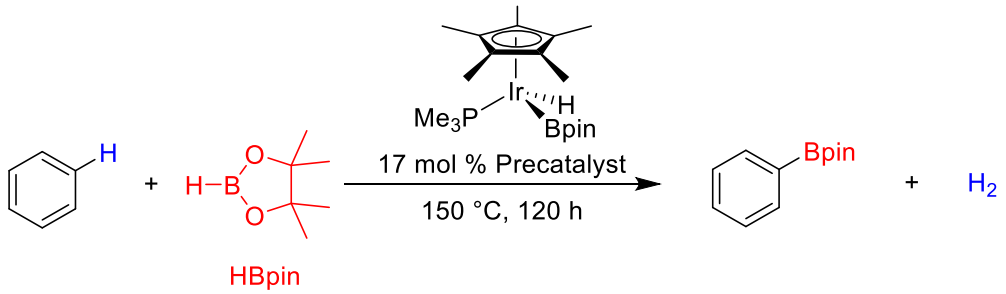

In 2002, the Smith and Maleczka group made further developments of the iridium catalyst system and established the usage of bidentate neutral donor ligands. Their system using (1,5-cyclooctadiene)(η^5-indenyl)iridium(I) precatalyst and bisphosphine ligand combination exhibited much higher turnover numbers (50-5000) and greater utility than the initial thermal catalyst. This new catalyst system was able to borylate a broad range of (hetero)arenes and the borylated products could be used in a one-pot synthesis for further functionalization via SMCC.[15] Since the inception of iridium-based catalyst

systems, numerous other catalysts have been developed using additional transition metals like Co,[19-21] Pd,[22,23] Rh,[24] and Fe.[25,26] Even with these alternatives, the iridium and L_2 ligand combination are still the most used and most studied catalysts due to their high efficacy, regio/chemoselectivities, and broad substrate scope.

1.4 Selectivity and Mechanistic Insights into Ir-Catalyzed C–H Borylation

In traditional Ir-catalyzed systems, aromatic substrates are borylated with selectivity that is complimentary to electrophilic aromatic substitution (EAS) reactions. In EAS chemistry, arenes are activated/functionalized at the ortho/para or meta sites of the substrate based on the electronic effects of its substituents. For Ir-catalyzed CHBs, regioselectivity is based on the steric factors of the substrate.[27] For example, borylating a monosubstituted arene will yield products with the boryl group in the meta and para positions in a 2:1 ratio. No (*or trace*) amounts of ortho borylated product will be present (Scheme 1.5).

Scheme 1.5 CHB reaction of a monosubstituted arene.

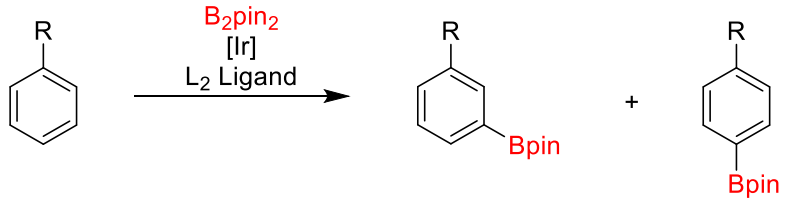

In 2002, Miyaura, Hartwig, and Ishiyama published on using $[Ir(Cl)cod]_2$ and 4,4'-di-*tert*-butyl-2,2'-dipyridyl (dtbpy) as a reactive catalyst for CHB. Complex (a) of Figure 1.1 was synthesized and characterized by X-ray crystallography. The structure revealed a trisboryl species ligated with dtbpy and cyclooctene (COE). This trisboryl complex was very reactive for CHBs and could perform catalysis at room temperature, while reactions usually required heating. It was proposed that by dissociation of COE, that a singly vacant

coordination site is created for activation of the least sterically hindered C–H bond (Figure 1.1).[28]

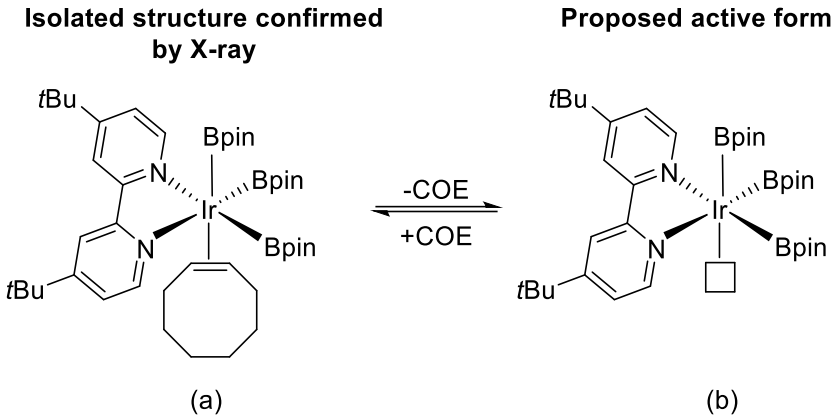

Figure 1.1 An (a) isolated trisboryl iridium complex and (b) its proposed active form.

Initial mechanistic studies of Ir-catalyzed CHB were done by Smith and Maleczka. They began by probing whether the catalytic cycle involved Ir^{I}/Ir^{III} species versus Ir^{III}/Ir^{V}. To probe this, they first performed borylations of benzene using either the Ir(I) complex, $Ir(Bpin)(PMe_3)_4$, and the Ir(III) complex, $Ir(Bpin)_3(PMe_3)_3$. In this reaction, both Ir complexes were capable of producing the arylboronic ester product. Although, when the substrate was changed to iodobenzene, only the Ir(III) complex could carry out the CHB while the Ir(I) complex yielded no borylation. From this, Smith and Maleczka proposed an Ir^{III}/Ir^{V} catalyst cycle.[15]

After these early insights, further investigative work was done by Hartwig and coworkers that provided more evidence of a Ir^{III}/Ir^{V} cycle. With the trisboryl iridium complex they performed extensive kinetic studies using B_2pin_2 as the boron source and arene substrates. Through these studies, they found that the trisboryl species reacts with arenes after reversible dissociation of COE and via kinetic isotope experiments that oxidative addition is the rate limiting step.[28] Computationally, Sasaki[29] calculated

transition states for various possible catalyst structures and came to the same conclusions of an Ir^{III}/Ir^{V} cycle and oxidative addition being the rate limiting step. The overall catalytic cycle based on the culmination of Smith and Maleczka's, Hartwig and coworkers', and computational data is presented in Scheme 1.6.

Scheme 1.6 Catalyst cycle for Ir-catalyzed CHBs.

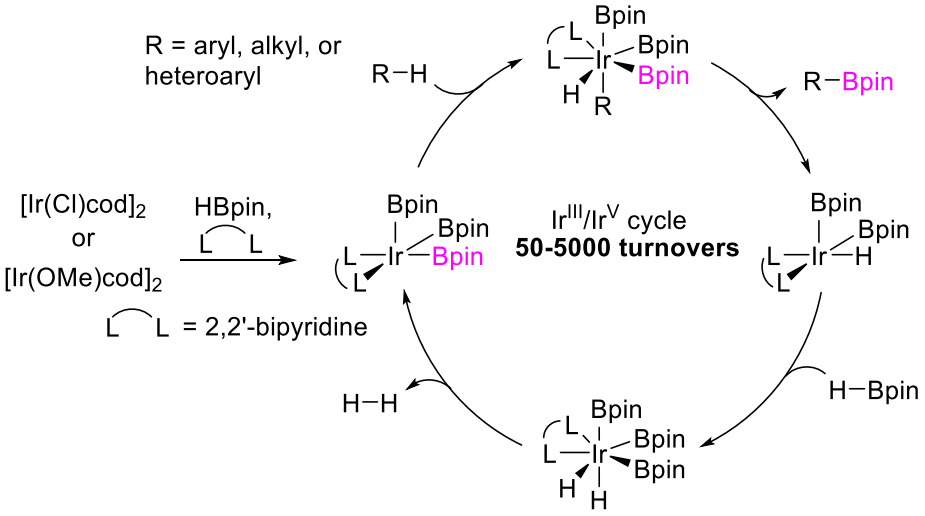

In this cycle, the active catalyst is a trisboryl 16 e^- species. The arene substrate undergoes oxidative addition and forms an Ir(V) species. Through reductive elimination, the organoboron product is expelled from the catalyst, returning it to the Ir(III) oxidation state. The boron source oxidatively adds to the metal, replenishing the lost boryl group creating an Ir(V) species. Lastly, HBpin or H_2 gas reductively eliminates (depending upon the boron source used) as the byproduct and completes the cycle for further catalysis.

1.5 Directed Iridium Catalyzed Borylations of Aromatic Compounds

In order to gain more regioselective control and greater options of which C–H bond is to be borylated, new catalyst designs were needed. For aromatic substrates, there are three main sites where CHB can be directed—*ortho*, *meta*, or *para* positions. Known strategies for each type are discussed below.

1.6 *ortho*-Directed CHB

The first type of directed CHB using [Ir] was seen in 2008 by the Hartwig group.[30] They showed that silyl groups could undergo metathesis with the boryl ligand on the metal. Once the silyl group is coordinated to the metal, the adjacent C–H bond is activated. Although this route had good selectivity, requiring substrates prefunctionalized with a silyl group was not ideal.

To circumvent this, 'chelate-directed' catalysis was explored. In this design, the catalyst is proposed to have two vacant coordination sites rather than one. A directing group on the substrate coordinates to one of the vacant sites of iridium and positions the *ortho* C–H bond near the second vacant site for activation.[31,32] Scheme 1.7 depicts a general reaction setup for the chelate-directed method.

Scheme 1.7 CHB reaction of a monosubstituted arene.

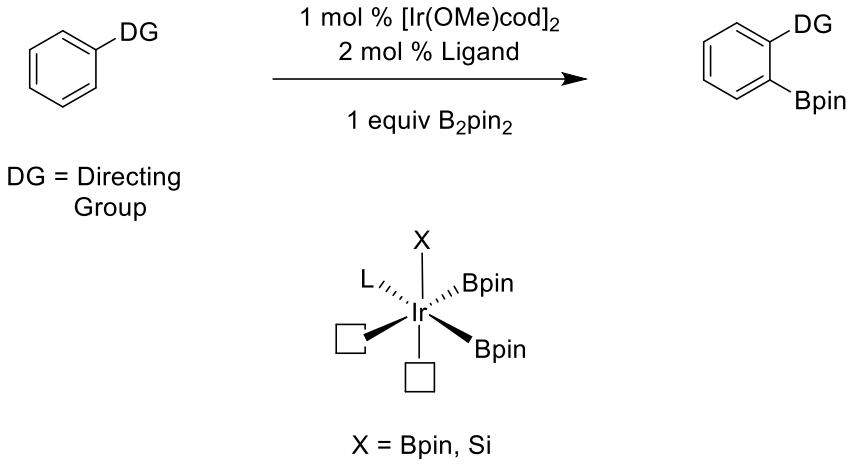

Chelate-directed catalysts are the most capable catalysts for *ortho* CHB and many ligand variations can be seen within the literature (Figure 1.2).[31-33]

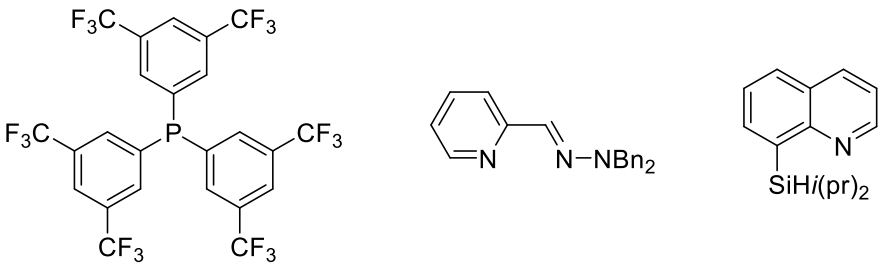

Figure 1.2 Ligands used for chelate-directed borylations—(a) monodentate phosphine ligand, (b) 'hemilabile' pyridyl hydrazone ligand, and (c) monoanionic quinoline silyl ligand.

Each of the ligands of Figure 1.2 are proposed to generate an active catalyst with two vacant coordination sites. Miyaura and Ishiyama's phosphine ligand above, with its electron trifluoromethyl groups, can dissociate from the metal freeing up a coordination site.[31] Lassaletta's pyridyl hydrazone ligand is proposed to be hemilabile where the less donating imine portion of the ligand can freely dissociate from the metal center and free the second vacant site for ortho selectivity.[32] Lastly, Smith and Maleczka's monoanionic quinoline silyl ligand replaces one of the anionic boryl ligands while maintaining stability of the ligand through chelation.[33]

The previous two approaches to directed borylation rely on a functionality of the substrate to directly interact with the metal center. A different approach would be for an interaction between the ligand of the catalyst and the substrate. This approach is termed 'outer-sphere' directed. For outer-sphere directed borylations, the ligand acts as an acceptor for interaction of the substrate. Prominent examples of this have been seen with H-bonding for *ortho* borylation of phenols[34] and anilines,[35] and Lewis acid-base pairs for borylation of compounds with a sulfur directing group.[36]

1.7 *meta*-Directed CHB

To perform *meta*-directed CHB, Kanai and coworkers designed a bipyridine ligand with a urea linked to it.[37] They found that a hydrogen-bonding interaction between the urea N–H and the lone pairs of a directing group (ester, ketone, amide, phosphate) could poise the substrate for meta borylation.

Phipps and coworkers also disclosed that ion-pairing interactions between an ammonium moiety of the substrate and a sulfate ion attached to a bipyridine ligand could direct CHBs for the meta site of aromatics (Figure 1.3).[38-40]

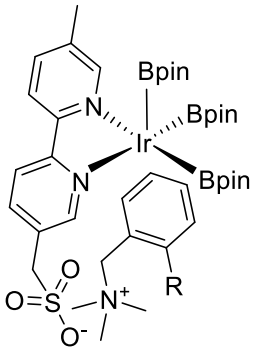

Figure 1.3 Ion-pairing strategy for *meta* CHB.

1.8 *para*-Directed CHB

In 2015, Itami and coworkers devised a method for achieving *para* selectivity by taking advantage of steric interactions between the substrate and a bulky bisphosphine ligand with xylene (Xyl) substituents. The cumbersome ligand can effectively inhibit activation of ortho and meta C–H bonds due to steric crowding near the coordination site on iridium.[41,42] Scheme 1.8 demonstrates this concept.

Scheme 1.8 Itami's bulky bisphosphine ligand for para CHB.

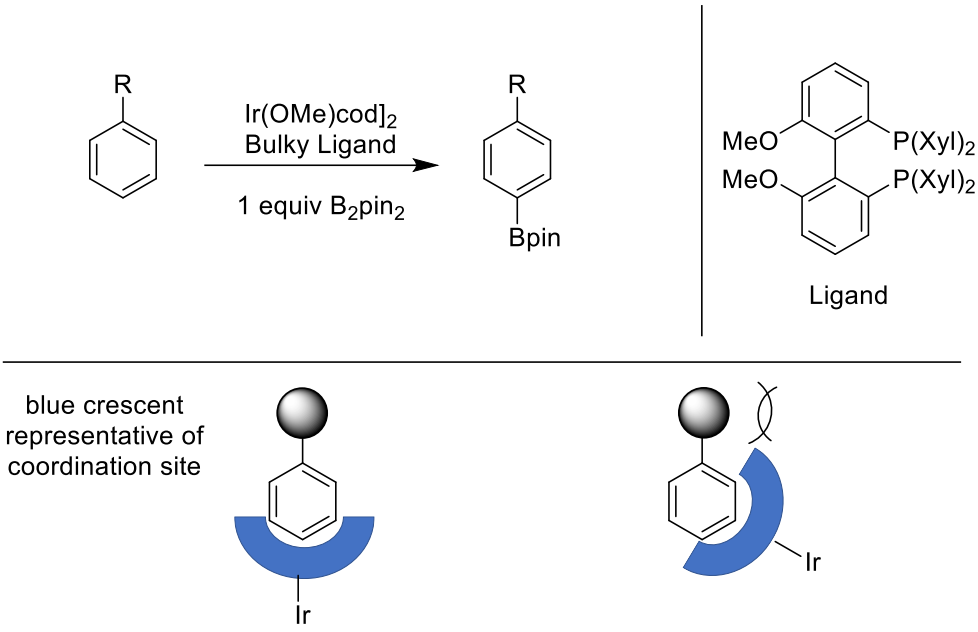

Aside from steric factors influencing selectivity, the Smith and Maleczka group and Phipps group concurrently showed that an ion-pairing method previously used for *meta* CHB, could also be implemented for *para* CHB. This was done by using an aryl sulfate as the substrate with an alkyl ammonium counterion to sterically shield the meta sites from CHB.[43,44]

Chattopadhyay group showed that *para* CHB could be achieved by noncovalent interactions. This method used an L-shaped ligand with a potassium ion substituent which acts as a Lewis acid. The attraction between the acidic ligand acceptor with the partially negative carbonyl oxygen of the phenyl ester substrate led to products that were borylated in the para position.[45] This (C=O···K−O) interaction worked well for many phenyl esters with varying steric, electronic, and substitution patterns of the aryl substrate. The catalyst system showed to work well for heteroarenes donning an ester directing group as well. Figure 1.4 shows the proposed catalyst for these CHBs.

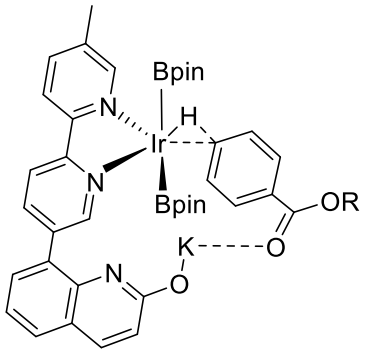

Figure 1.4 Non-covalent strategy for *para* CHB.

In summary, there are many possible routes and iterations for achieving ortho, meta, and para regioselectivities of aromatic compounds. Iridium precatalysts paired with phosphine or nitrogen ligands create very reactive and tunable systems to yield the desired organoboron product.

1.9 Directed Iridium Catalyzed Borylations of Aliphatic Compounds

Just like arylboronic esters, alkylboronic esters are an important class of compounds used as intermediates and are present in an array of useful pharmaceuticals like Ixazomib[46] and Vaborbactam,[47] which are used as anticancer and antibiotic therapeutics, respectively. Despite the great strides made for C(sp^2)–H CHB of (hetero)arenes, Ir catalysts for C(sp^3)–H borylation are not as well developed.

The first use of an iridium catalyst for C(sp^3)–H borylation was done by Hartwig using (η^6-mesitylene)Ir(Bpin)$_3$ and 3,4,7,8-tetramethyl-1,10-phenanthroline (tmphen) as precatalyst and ligand. This catalyst could borylate cyclic ethers and activation/functionalization occurred in the 3-position of the substrates (Scheme 1.9).[48]

Scheme 1.9 First iridium-catalyzed route for sp^3 CHBs using (η^6-mesitylene)Ir(Bpin)$_3$ with tmphen on cyclic ethers.

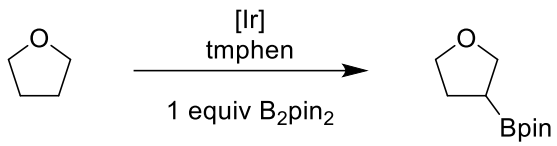

Another commonly used method for sp^3 borylations is the relay-directed method that was similarly used for sp^2 CHBs.[49,50] Again, in this system, the starting material to be borylated needs to have a silyl group installed in order to successfully carry out the borylation. In this catalysis, the silyl group replaces a boryl ligand on the metal and positions the aliphatic C –H bond near the metal for activation.

As mentioned previously for *ortho*-directed CHBs, chelate-directed catalysts are also capable of performing sp^3 borylations. In these systems, ensuring that there is a second coordination site is imperative. A heterogeneous catalyst that is efficient for this type of borylation was developed by Sawamura[51] and uses a monodentate silica-SMAP ligand (Scheme 1.10).

Scheme 1.10 Heterogeneous catalyst with Si-SMAP for sp^3 CHB.

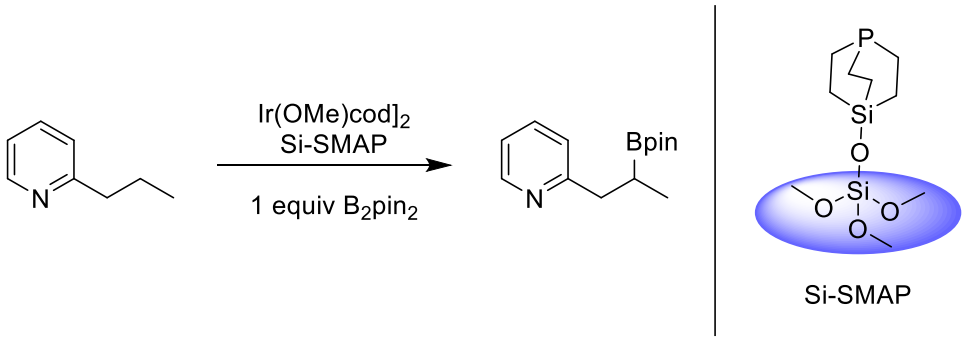

Other examples of catalysts exist in the literature for sp^3 borylation, but these systems operate based on either using activated substrates, relay-direction, or chelate-direction methods.

1.10 Conclusions

Organoboron compounds are incredibly versatile materials that have prominent use as intermediates for drug discovery in the pharmaceutical industry, late-stage functionalization of important complex molecules, and agrochemicals in the farming industry. C–H borylation reactions catalyzed by an iridium catalyst are the most atom economical way of producing organoboron reagents directly from hydrocarbon starting materials, cutting out the need of using prefunctionalized substrates. Iridium catalysts are adept at performing CHB chemistry and modifications and improvements to this system's efficiency and selectivity are still being presently explored.

REFERENCES

REFERENCES

(1) Chenier, P. J. *Basic Organic Chemicals*. In *Survey of Industrial Chemistry*; 3rd ed.; Kluwer Academic: New York, 2002, p 130.

(2) Mitscherlich, E. *Justus Liebigs Ann. Chem.* **1834**, *12*, 308.

(3) Holleman, A. F. Some Factors Influencing Substitution in the Benzene Ring. *Chem. Rev.* **1924**, *1*, 187–230.

(4) Brown, H. C.; Prasad, J. V. *J. Am. Chem. Soc.* **1986**, *108*, 2049.

(5) Miyaura, N.; Yanagi, T.; Suzuki, A. The Palladium-Catalyzed Cross-Coupling Reaction of Phenylboronic Acid with Haloarenes in the Presence of Bases. *Synth. Commun.* **1981**, *11*, 513–519.

(6) Ben Halima, T.; Zhang, W.; Yalaoui, I.; Hong, X.; Yang, Y.-F.; Houk, K. N.; Newman, S. G. Palladium-Catalyzed Suzuki-Miyaura Coupling of Aryl Esters. *J. Am. Chem. Soc.* **2017**, *139*, 1311–1318.

(7) Norberg, A. M.; Smith, M. R., 3rd; Maleczka, R. E., Jr. Practical One-Pot C-H Activation/borylation/oxidation: Preparation of 3-Bromo-5-Methylphenol on a Multigram Scale. *Synthesis* **2011**, *2011*, 857–859.

(8) Chan, D. M. T.; Monaco, K. L.; Wang, R.-P.; Winters, M. P. New N- and O-Arylations with Phenylboronic Acids and Cupric Acetate. *Tetrahedron Lett.* **1998**, *39*, 2933–2936.

(9) Hardouin Duparc, V.; Bano, G. L.; Schaper, F. Chan–Evans–Lam Couplings with Copper Iminoarylsulfonate Complexes: Scope and Mechanism. *ACS Catal.* **2018**, *8*, 7308–7325.

(10) Vints, I.; Gatenyo, J.; Rozen, S. Fluorination of Aryl Boronic Acids Using Acetyl Hypofluorite Made Directly from Diluted Fluorine. *J. Org. Chem.* **2013**, *78*, 11794–11797.

(11) Szumigala, R. H., Jr; Devine, P. N.; Gauthier, D. R., Jr; Volante, R. P. Facile Synthesis of 2-Bromo-3-Fluorobenzonitrile: An Application and Study of the Halodeboronation of Aryl Boronic Acids. *J. Org. Chem.* **2004**, *69*, 566–569.

(12) Dai, J.-J.; Zhang, W.-M.; Shu, Y.-J.; Sun, Y.-Y.; Xu, J.; Feng, Y.-S.; Xu, H.-J. Deboronative Cyanation of Potassium Alkyltrifluoroborates via Photoredox Catalysis. *Chem. Commun.* **2016**, *52*, 6793–6796.

(13) Zhu, Y.; Li, L.; Shen, Z. Cu-Catalyzed Cyanation of Arylboronic Acids with Acetonitrile: A Dual Role of TEMPO. *Chemistry* **2015**, *21*, 13246–13252.

(14) Nagaki, A.; Moriwaki, Y.; Yoshida, J.-I. Flow Synthesis of Arylboronic Esters Bearing Electrophilic Functional Groups and Space Integration with Suzuki-Miyaura Coupling without Intentionally Added Base. *Chem. Commun.* **2012**, *48*, 11211–11213.

(15) Cho, J.-Y.; Tse, M. K.; Holmes, D.; Maleczka, R. E., Jr; Smith, M. R., 3rd. Remarkably Selective Iridium Catalysts for the Elaboration of Aromatic C-H Bonds. *Science* **2002**, *295*, 305–308.

(16) Ishiyama, T.; Murata, M.; Miyaura, N. Palladium(0)-Catalyzed Cross-Coupling Reaction of Alkoxydiboron with Haloarenes: A Direct Procedure for Arylboronic Esters. *J. Org. Chem.* **1995**, *60*, 7508–7510.

(17) Rablen, P. R.; Hartwig, J. F.; Nolan, S. P. First Transition Metal-Boryl Bond Energy and Quantitation of Large Differences in Sequential Bond Dissociation Energies of Boranes. *J. Am. Chem. Soc.* **1994**, *116*, 4121–4122.

(18) Iverson, C. N.; Smith, M. R. Stoichiometric and Catalytic B−C Bond Formation from Unactivated Hydrocarbons and Boranes. *J. Am. Chem. Soc.* **1999**, *121*, 7696–7697.

(19) Pabst, T. P.; Obligacion, J. V.; Rochette, É.; Pappas, I.; Chirik, P. J. Cobalt-Catalyzed Borylation of Fluorinated Arenes: Thermodynamic Control of C(sp2)-H Oxidative Addition Results in Ortho-to-Fluorine Selectivity. *J. Am. Chem. Soc.* **2019**, *141*, 15378–15389.

(20) Obligacion, J. V.; Semproni, S. P.; Chirik, P. J. Cobalt-Catalyzed C-H Borylation. *J. Am. Chem. Soc.* **2014**, *136*, 4133–4136.

(21) Palmer, W. N.; Obligacion, J. V.; Pappas, I.; Chirik, P. J. Cobalt-Catalyzed Benzylic Borylation: Enabling Polyborylation and Functionalization of Remote, Unactivated C(sp3)–H Bonds. *J. Am. Chem. Soc.* **2016**, *138*, 766–769.

(22) He, J.; Jiang, H.; Takise, R.; Zhu, R.-Y.; Chen, G.; Dai, H.-X.; Dhar, T. G. M.; Shi, J.; Zhang, H.; Cheng, P. T. W.; Yu, J.-Q. Ligand-Promoted Borylation of C(sp(3))-H Bonds with Palladium(II) Catalysts. *Angew. Chem. Int. Ed Engl.* **2016**, *55*, 785–789.

(23) He, J.; Shao, Q.; Wu, Q.; Yu, J.-Q. Pd(II)-Catalyzed Enantioselective C(sp3)-H Borylation. *J. Am. Chem. Soc.* **2017**, *139*, 3344–3347.

(24) Esteruelas, M. A.; Oliván, M.; Vélez, A. POP–Rhodium-Promoted C–H and B–H Bond Activation and C–B Bond Formation. *Organometallics* **2015**, *34*, 1911–1924.

(25) Hatanaka, T.; Ohki, Y.; Tatsumi, K. C-H Bond Activation/borylation of Furans and Thiophenes Catalyzed by a Half-Sandwich Iron N-Heterocyclic Carbene Complex. *Chem. Asian J.* **2010**, *5*, 1657–1666.

(26) Yan, G.; Jiang, Y.; Kuang, C.; Wang, S.; Liu, H.; Zhang, Y.; Wang, J. Nano-Fe2O3-Catalyzed Direct Borylation of Arenes. *Chem. Commun.* **2010**, *46*, 3170–3172.

(27) Cho, J.-Y.; Iverson, C. N.; Smith, M. R. Steric and Chelate Directing Effects in Aromatic Borylation. *J. Am. Chem. Soc.* **2000**, *122*, 12868–12869.

(28) Ishiyama, T.; Takagi, J.; Ishida, K.; Miyaura, N.; Anastasi, N. R.; Hartwig, J. F. Mild Iridium-Catalyzed Borylation of Arenes. High Turnover Numbers, Room Temperature Reactions, and Isolation of a Potential Intermediate. *J. Am. Chem. Soc.* **2002**, *124*, 390–391.

(29) Tamura, H.; Yamazaki, H.; Sato, H.; Sakaki, S. Iridium-Catalyzed Borylation of Benzene with Diboron. Theoretical Elucidation of Catalytic Cycle Including Unusual Iridium(v) Intermediate. *J. Am. Chem. Soc.* **2003**, *125*, 16114–16126.

(30) Boebel, T. A.; Hartwig, J. F. Silyl-Directed, Iridium-Catalyzed Ortho-Borylation of Arenes. A One-Pot Ortho-Borylation of Phenols, Arylamines, and Alkylarenes. *J. Am. Chem. Soc.* **2008**, *130*, 7534–7535.

(31) Ishiyama, T.; Isou, H.; Kikuchi, T.; Miyaura, N. Ortho-C–H Borylation of Benzoate Esters with Bis(pinacolato)diboron Catalyzed by Iridium–phosphine Complexes. *Chem. Commun.* **2010**, *46*, 159–161.

(32) Ghaffari, B.; Preshlock, S. M.; Plattner, D. L.; Staples, R. J.; Maligres, P. E.; Krska, S. W.; Maleczka, R. E., Jr; Smith, M. R., 3rd. Silyl Phosphorus and Nitrogen Donor Chelates for Homogeneous Ortho Borylation Catalysis. *J. Am. Chem. Soc.* **2014**, *136*, 14345–14348.

(33) Ros, A.; Estepa, B.; López-Rodríguez, R.; Álvarez, E.; Fernández, R.; Lassaletta, J. M. Use of Hemilabile N,N Ligands in Nitrogen-Directed Iridium-Catalyzed Borylations of Arenes. *Angew. Chem. Int. Ed Engl.* **2011**, *50*, 11724–11728.

(34) Chattopadhyay, B.; Dannatt, J. E.; Andujar-De Sanctis, I. L.; Gore, K. A.; Maleczka, R. E., Jr; Singleton, D. A.; Smith, M. R., 3rd. Ir-Catalyzed Ortho-Borylation of Phenols Directed by Substrate-Ligand Electrostatic Interactions: A Combined Experimental/in Silico Strategy for Optimizing Weak Interactions. *J. Am. Chem. Soc.* **2017**, *139*, 7864–7871.

(35) Smith, M. R., 3rd; Bisht, R.; Haldar, C.; Pandey, G.; Dannatt, J. E.; Ghaffari, B.; Maleczka, R. E., Jr; Chattopadhyay, B. Achieving High Ortho Selectivity in Aniline C-H Borylations by Modifying Boron Substituents. *ACS Catal.* **2018**, *8*, 6216–6223.

(36) Li, H. L.; Kuninobu, Y.; Kanai, M. Lewis Acid-Base Interaction-Controlled Ortho-Selective C-H Borylation of Aryl Sulfides. *Angew. Chem. Int. Ed Engl.* **2017**, *56*, 1495–1499.

(37) Kuninobu, Y.; Ida, H.; Nishi, M.; Kanai, M. A Meta-Selective C–H Borylation Directed by a Secondary Interaction between Ligand and Substrate. *Nat. Chem.* **2015**, *7*, 712–717.

(38) Davis, H. J.; Genov, G. R.; Phipps, R. J. Meta -Selective C−H Borylation of Benzylamine-, Phenethylamine-, and Phenylpropylamine-Derived Amides Enabled by a Single Anionic Ligand. *Angew. Chem. Int. Ed.* **2017**, *56*, 13351–13355.

(39) Mihai, M. T.; Davis, H. J.; Genov, G. R.; Phipps, R. J. Ion Pair-Directed C–H Activation on Flexible Ammonium Salts: Meta-Selective Borylation of Quaternized Phenethylamines and Phenylpropylamines. *ACS Catal.* **2018**, *8*, 3764–3769.

(40) Davis, H. J.; Mihai, M. T.; Phipps, R. J. Ion Pair-Directed Regiocontrol in Transition-Metal Catalysis: A Meta-Selective C–H Borylation of Aromatic Quaternary Ammonium Salts. *J. Am. Chem. Soc.* **2016**, *138*, 12759–12762.

(41) Saito, Y.; Segawa, Y.; Itami, K. Para-C–H Borylation of Benzene Derivatives by a Bulky Iridium Catalyst. *J. Am. Chem. Soc.* **2015**, *137*, 5193–5198.

(42) Saito, Y.; Yamanoue, K.; Segawa, Y.; Itami, K. Selective Transformation of Strychnine and 1,2-Disubstituted Benzenes by C–H Borylation. *Chem* **2020**, *6*, 985–993.

(43) Mihai, M. T.; Williams, B. D.; Phipps, R. J. Para-Selective C-H Borylation of Common Arene Building Blocks Enabled by Ion-Pairing with a Bulky Countercation. *J. Am. Chem. Soc.* **2019**, *141*, 15477–15482.

(44) Montero Bastidas, J. R.; Oleskey, T. J.; Miller, S. L.; Smith, M. R., 3rd; Maleczka, R. E., Jr. Para-Selective, Iridium-Catalyzed C-H Borylations of Sulfated Phenols, Benzyl Alcohols, and Anilines Directed by Ion-Pair Electrostatic Interactions. *J. Am. Chem. Soc.* **2019**, *141*, 15483–15487.

(45) Hoque, M. E.; Bisht, R.; Haldar, C.; Chattopadhyay, B. Noncovalent Interactions in Ir-Catalyzed C-H Activation: L-Shaped Ligand for Para-Selective Borylation of Aromatic Esters. *J. Am. Chem. Soc.* **2017**, *139*, 7745–7748.

(46) Groll, M.; Berkers, C. R.; Ploegh, H. L.; Ovaa, H. Crystal Structure of the Boronic Acid-Based Proteasome Inhibitor Bortezomib in Complex with the Yeast 20S Proteasome. *Structure* **2006**, *14*, 451–456.

(47) Gentile, M.; Offidani, M.; Vigna, E.; Corvatta, L.; Recchia, A. G.; Morabito, L.; Morabito, F.; Gentili, S. *Expert Opin. Investig. Drugs* **2015**, *24*, 1287.

(48) Liskey, C. W.; Hartwig, J. F. Iridium-Catalyzed Borylation of Secondary C-H Bonds in Cyclic Ethers. *J. Am. Chem. Soc.* **2012**, *134*, 12422–12425.

(49) Cho, S. H.; Hartwig, J. F. Iridium-Catalyzed Diborylation of Benzylic C–H Bonds Directed by a Hydrosilyl Group: Synthesis of 1,1-Benzyldiboronate Esters. *Chem. Sci.* **2013**, *5*, 694–698.

(50) Larsen, M. A.; Cho, S. H.; Hartwig, J. Iridium-Catalyzed, Hydrosilyl-Directed Borylation of Unactivated Alkyl C-H Bonds. *J. Am. Chem. Soc.* **2016**, *138*, 762–765.

(51) Reyes, R. L.; Iwai, T.; Maeda, S.; Sawamura, M. Iridium-Catalyzed Asymmetric Borylation of Unactivated Methylene C(sp3)-H Bonds. *J. Am. Chem. Soc.* **2019**, *141*, 6817–6821.

Chapter 2. Readily-Accessible Phenylenediamine Pyridyl Ligands for Iridium Catalyzed Ortho-Directed C–H Borylation

2.1 Background to Nitrogen-Based Ligands for Iridium Catalyzed C–H Borylation

For catalyzed CHBs, iridium precatalysts paired with nitrogen-based ligands have been at the forefront as the catalyst system of choice. The catalysts generated from this metal and ligand combination are known for their high performance, broad functional group tolerance, and versatility in *ortho*,[1-5] *meta*,[6-8] and *para*[9-11] directed borylations of C(sp^2)–H aromatic substrates. They are also well-known for their use in the borylation C(sp^3)–H aliphatic substrates.[12-15] Initial usage of bipyridines (bpy) and phenanthrolines (phen) have been employed in CHBs since 2002 and yield products from functionalization at the least sterically hindered C–H bond of aromatic substrates.[16] These catalysts are proposed to have a single open coordination site where C–H bond functionalization occurs (Figure 2.1).

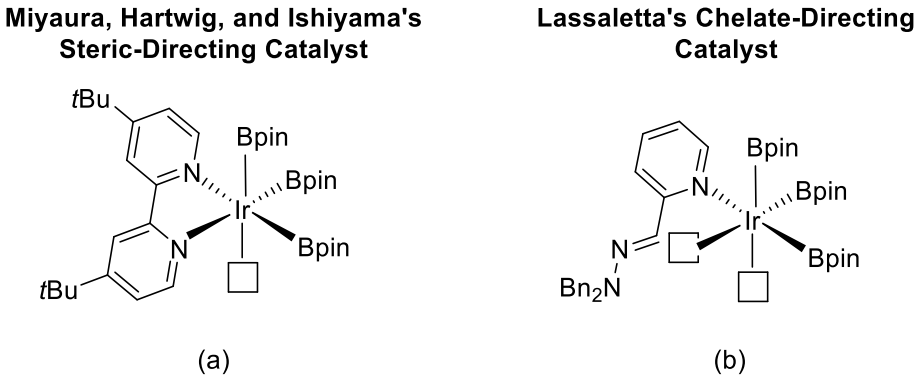

Figure 2.1 Proposed active catalyst structures for (a) steric-directed catalyst using dtbpy and (b) chelate-directed catalyst using a hemilabile ligand.

In the years following Miyaura, Hartwig, and Ishiyama's initial use of bipyridyl ligands, pyridyl-hydrazone and benzylic amine pyridyl ligands by Lassaletta[17-19] and Clark,[20-22] respectively, had been designed to perform *ortho* CHBs relative to nitrogen-

based directing groups like hydrazone or amine groups of the substrate. Those ligands were proposed to be 'hemilabile' and thus create an active catalyst with two vacant coordination sites by the process of the weaker imine donor atom dissociating from the metal center (Figure 2.1). This type of directed borylation is called chelate-directed borylation since the substrate will interact with the metal center directly via a directing group and position the adjacent C–H bond close to the metal for activation to occur.

However, a substrate scope limited to hydrazone, quinoline, or amine directing groups was observed. Functionalities such as esters and amides were not viable for these systems, and borylations of the substrates lead to low yields and selectivity. Not only that, but it is still unclear as to how this class of 'hemilabile' ligands work, which makes improvements upon their structures more elusive and challenging.

2.2 Other Ligand Types for Ortho-Directed C–H Borylation

Other ligand types have been developed for chelate-directed CHBs, like Sawamura's[23,24] solid-supported monodentate phosphine silicon ligand (Si-SMAP) and Li's[25,26] Si,B- and Si,S-chelating ligands (Figure 2.2). These ligands have good *ortho* selectivity for various directing groups and produce products in moderate to high yields.

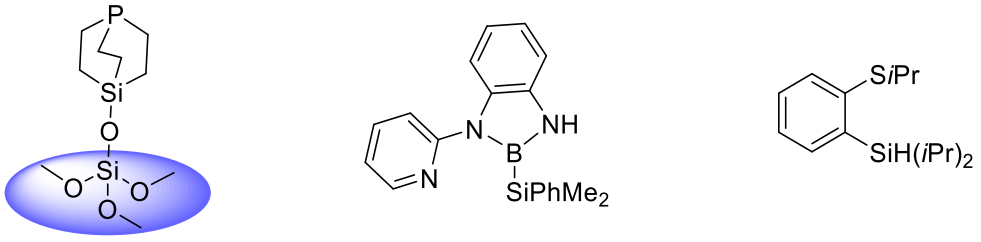

(a) (b) (c)

Figure 2.2 Ligand structures for Sawamura's (a) Si-SMAP monodentate ligand and Li's (b) silicon-boryl and (c) silicon-sulfur ligand.

Although these ligands function well and are efficient for CHB chemistry, they involve nontrivial, multistep air-sensitive syntheses and/or require stoichiometric amounts of lithium reagents to produce, making their use less appealing. Sawamura's Si-SMAP ligand requires an 11-step synthesis and involves multiple lithiations. Li's ligands are also multistep and need stoichiometric amounts of lithium as well. Given these downsides, chelate-directed CHB is less appealing for syntheses since the ligands are either not readily accessible, have poor air-stability, or difficult for further modifications.

2.3 Phenylenediamine Pyridyl Ligands Usage in C–H Borylations

In 2015, Li and coworkers developed a dimeric boryl ligand with a phenylenediamine backbone and pyridyl arm.[27] This ligand operated as a steric-directed ligand for CHB catalysis using $[Ir(OMe)cod]_2$, the same precatalyst used in the other systems. Based on the structures of previously designed ligands in Scheme 2.1, we wondered whether the pyridyl diamine precursor to Li's diboron boryl ligand synthon might also work for CHB since pyridines are privileged ligands in Ir-catalyzed CHBs and a present feature of many ligand systems.

Of the nitrogen-based ligands in Scheme 2.1, a limited substrate scope (Lassaletta's ligand), lack of regioselectivity (Hartwig's ligand), or air-sensitivity (Li's ligand) are the main drawbacks. Because of these limitations and pitfalls, a ligand family that is both trivial to synthesize and tune, while imparting high regioselectivities in CHBs, would be valuable to chemists. The phenylenediamine pyridyl precursor of Li's boryl dimer ligand is air and moisture stable, very tunable for both steric and electronic features, and its synthesis is trivial in that it can be synthesized in a single step starting with inexpensive starting materials with no need for stoichiometric amounts of metals. The precursor is also

easily purified by many means such as recrystallization, sublimation, flash column chromatography, or Soxhlet extraction. The design and investigation of these air-stable phenylenediamine pyridyls as CHB ligands is described.

Scheme 2.1 Ir-catalyzed C–H borylation of using nitrogen-based ligands.

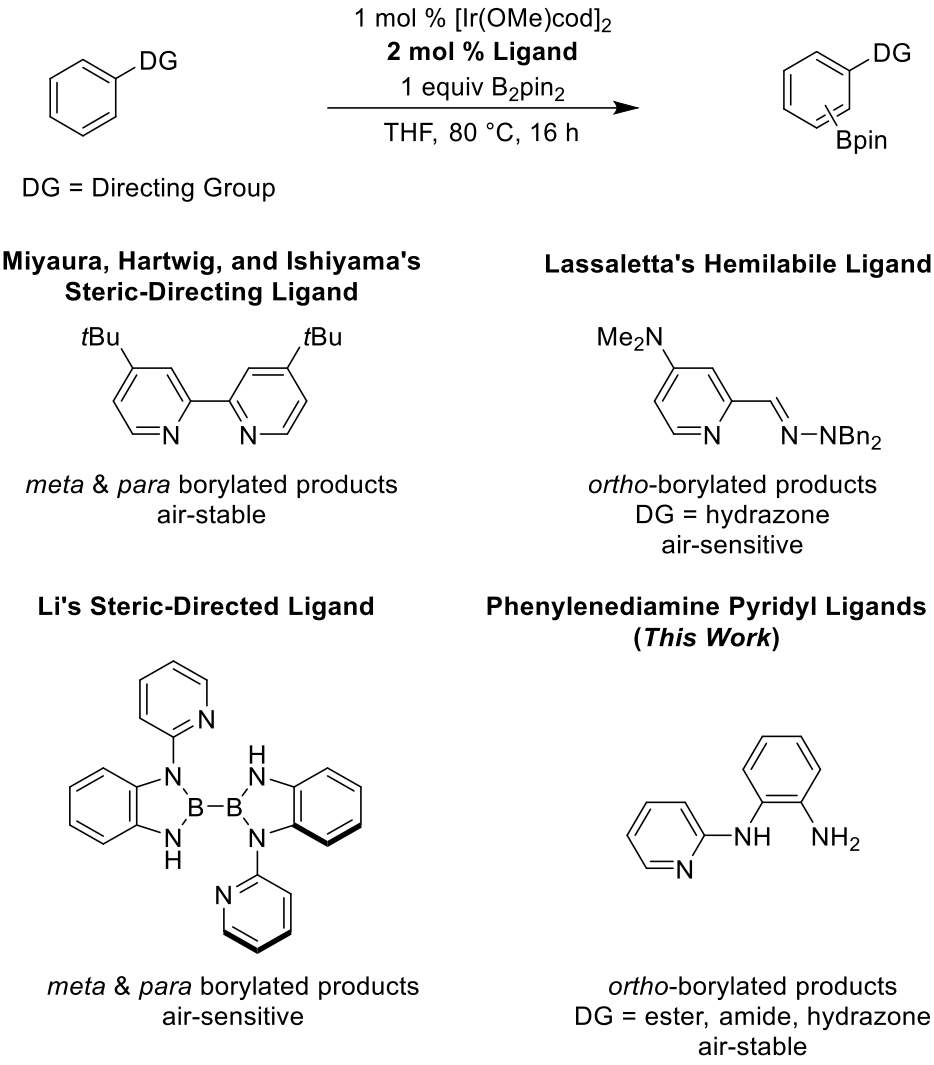

2.4 Analysis and Scope of Phenylenediamine Pyridyl Ligands–Amine Type, NMR Studies, and Electronic Effects

Starting with the initial phenylenediamine pyridyl ligand, **L1** (Scheme 2.2), and *tert*-butyl benzoate as the substrate, the borylation reaction exhibited high ortho selectivity.

While this ligand proved to be useful for *ortho*-directed CHB, the relevance of its structural features including the two amino groups substituted on the ligand was unclear.

Ligands **L2**-**L11** were designed to systematically investigate the structural features that contribute to the reactivity and selectivity of phenylenediamine pyridyl ligands. Their modular synthesis makes preparation of **L2**-**L7** straightforward since each ligand can be synthesized by reacting halogenated pyridines with phenylenediamine starting materials under neat conditions as shown in Scheme 2.3.

Scheme 2.3 General reaction for ligand synthesis.

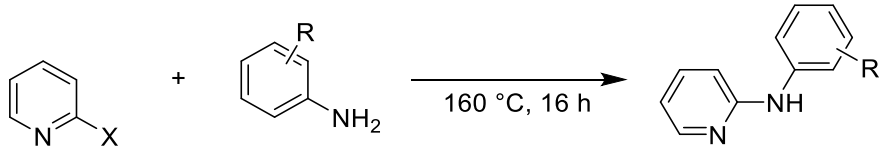

X = Cl, Br R = H, NH_2, NMe_2

Pure ligands were easily obtained from the crude mixtures by sublimation (**L1**), recrystallization (**L2**), or flash column chromatography (**L3** and **L6**). Synthesis of ligands **L4** and **L5** resulted in clean conversions that did not need further purification beyond workup and washing of the product. These ligands synthesized contained changes in the location, presence, and substitutions for the two amino groups. Ligands **L7**-**L11** were also used to test various structural components and smaller fragments of **L1**. These are shown in Scheme 2.3 along with their ability to perform CHB chemistry.

First, we tested the placement of the ortho substituted primary amine in the phenylenediamine **L1**. Ligands **L2** and **L3** were synthesized to place that amino group in the meta and para positions, respectively, of the phenyl ring. For both of these ligands, lower conversions were observed, however, there was no dramatic drop in selectivity. **L4**

lacks the primary amine group and borylations run under the same conditions of Scheme 2.2 show inferior conversion to product and a slight decrease in regioselectivity.

Scheme 2.2 Nitrogen-based ligand screen for *ortho*-directed CHB using *tert*-butyl benzoate as model substrate.

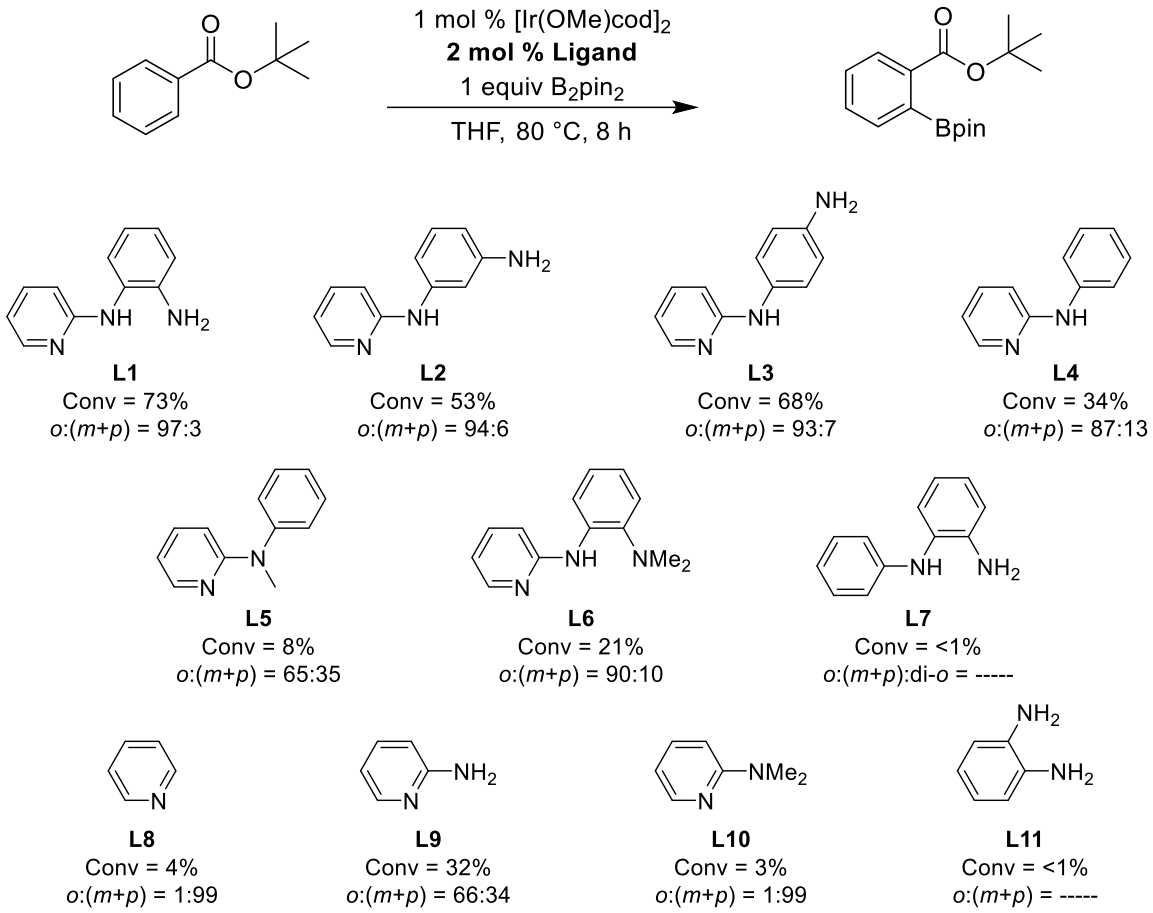

This suggests that the role of the primary amine group plays into the reactivity of the catalyst. Having shown that an ortho substituted amino group is beneficial for the ligand, we next tested the effects of N-substitution in the ortho-phenylenediamine fragment. The tertiary amine of **L5** significantly hindered *ortho* CHBs. Comparing this to **L1** and **L4** suggests that the secondary amine has a major role in these reactions.

Initially, since selectivity had plummeted when the secondary amino group had been changed to a tertiary amine, it was thought that a hydrogen-bonding effect was taking

place between the amino group and the directing group of the substrate. An ^{1}H NMR study revealed that hydrogen-bonding interactions between the secondary amine of **L1** and **L4**, and the carbonyl group of methyl benzoate was present. This was determined by collecting proton NMR of the ligand with methyl benzoate at varying concentrations. The extent of hydrogen bonding is affected by the solution concentration. A more concentrated sample will have more interaction between species and increase the amount of hydrogen bonding that occurs. This can be seen spectroscopically by the observance of the hydrogen that is involved in hydrogen bonding to be shifted more downfield due to it being deshielded. In this NMR experiment, concentration of the initial NMR sample was diluted by the addition of more solvent. Thus, as concentration decreases, the N–H bond of the secondary amine should be more upfield and show less of a hydrogen bonding effect.

However, doing these same studies with **L6** did not show any hydrogen bonding effect, yet the selectivity was still high. Thus, it was concluded that the added steric hindrance of the methyl group on the amine of **L5** was the inhibitor for higher *ortho* selectivity. These spectra are displayed in Figures 2.3-2.5.

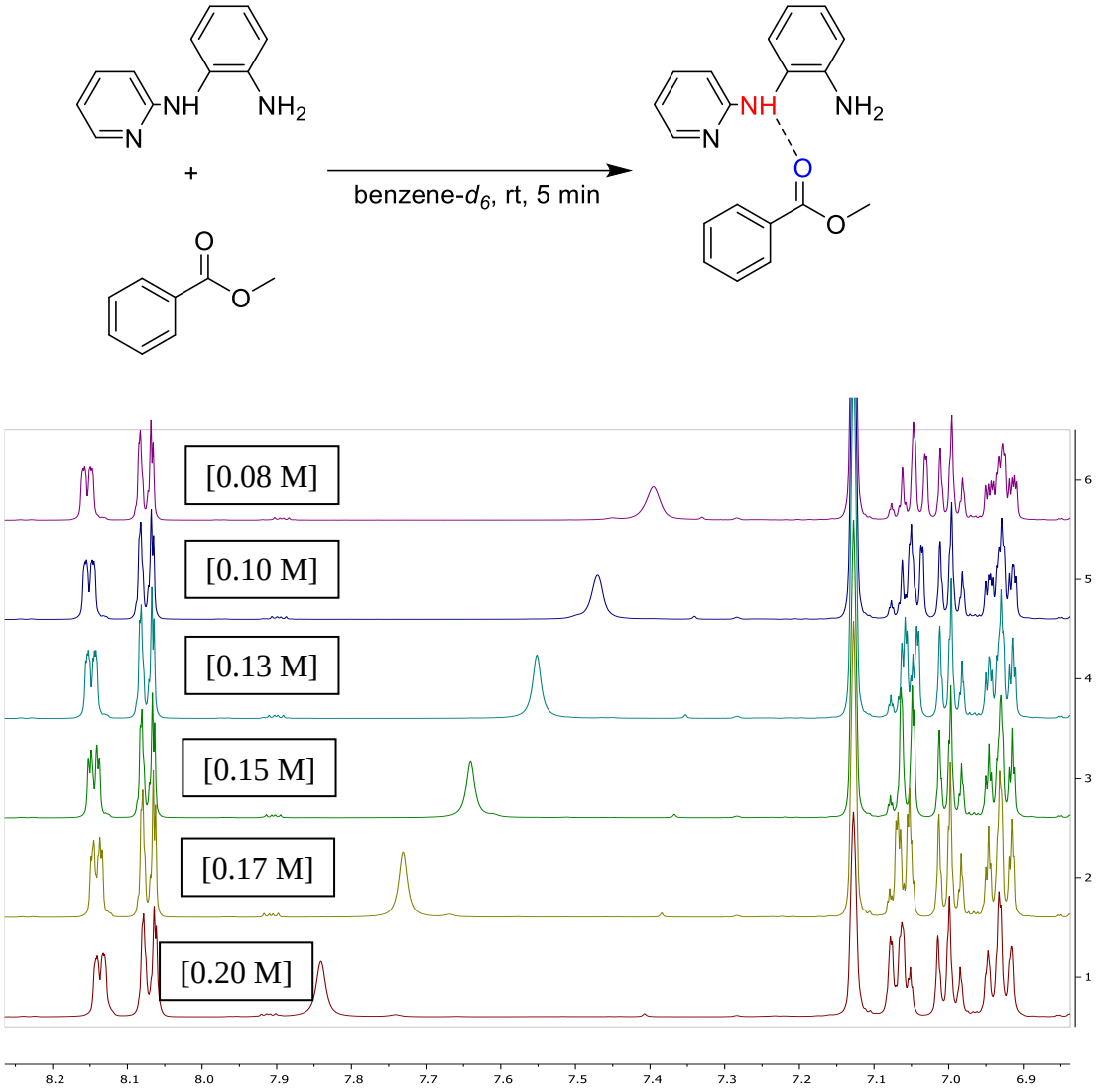

Figure 2.3 Hydrogen-Bonding Effect Between **L1** and Substrate.

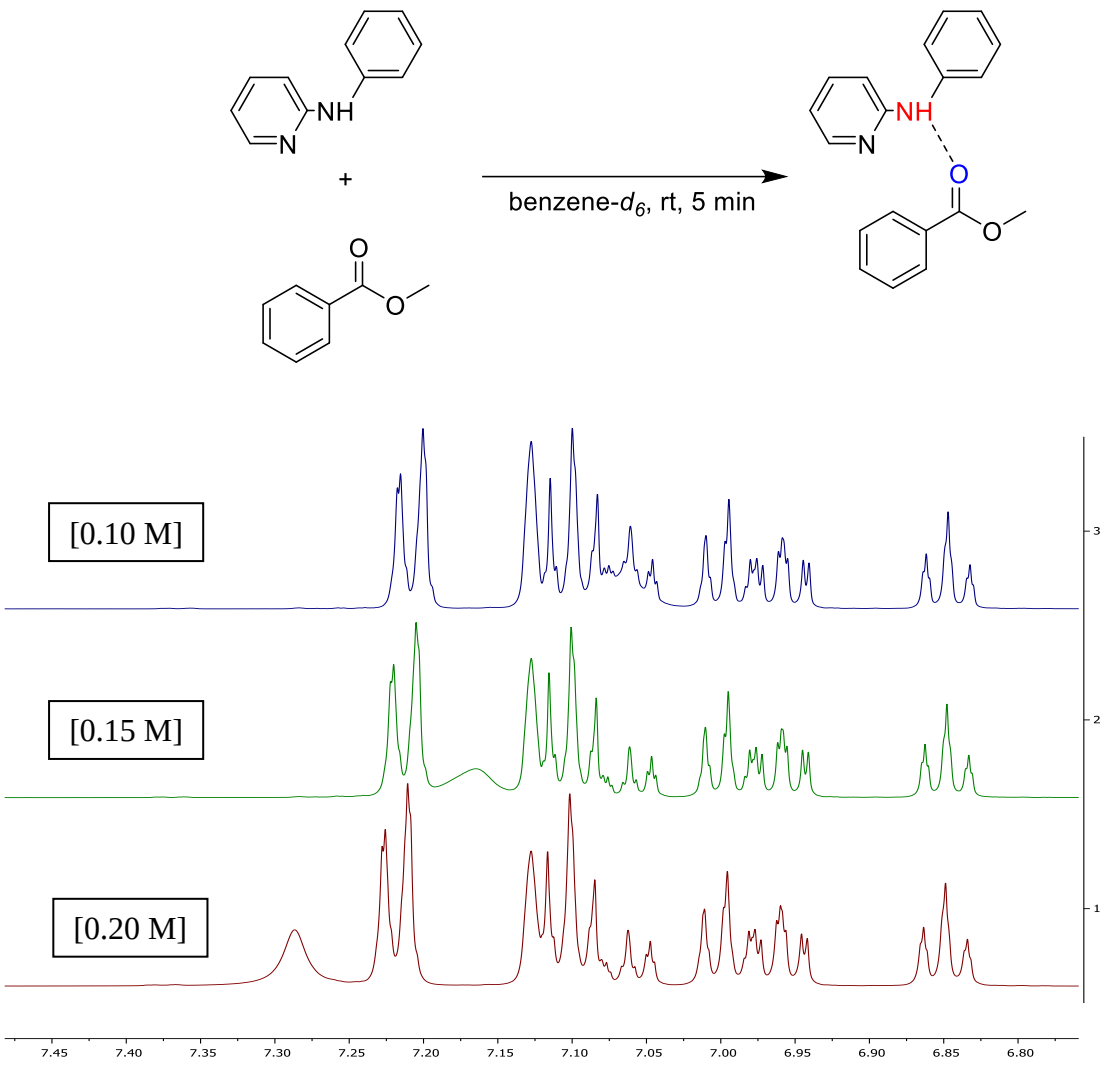

Figure 2.4 Hydrogen-Bonding Effect Between **L4** and Substrate.

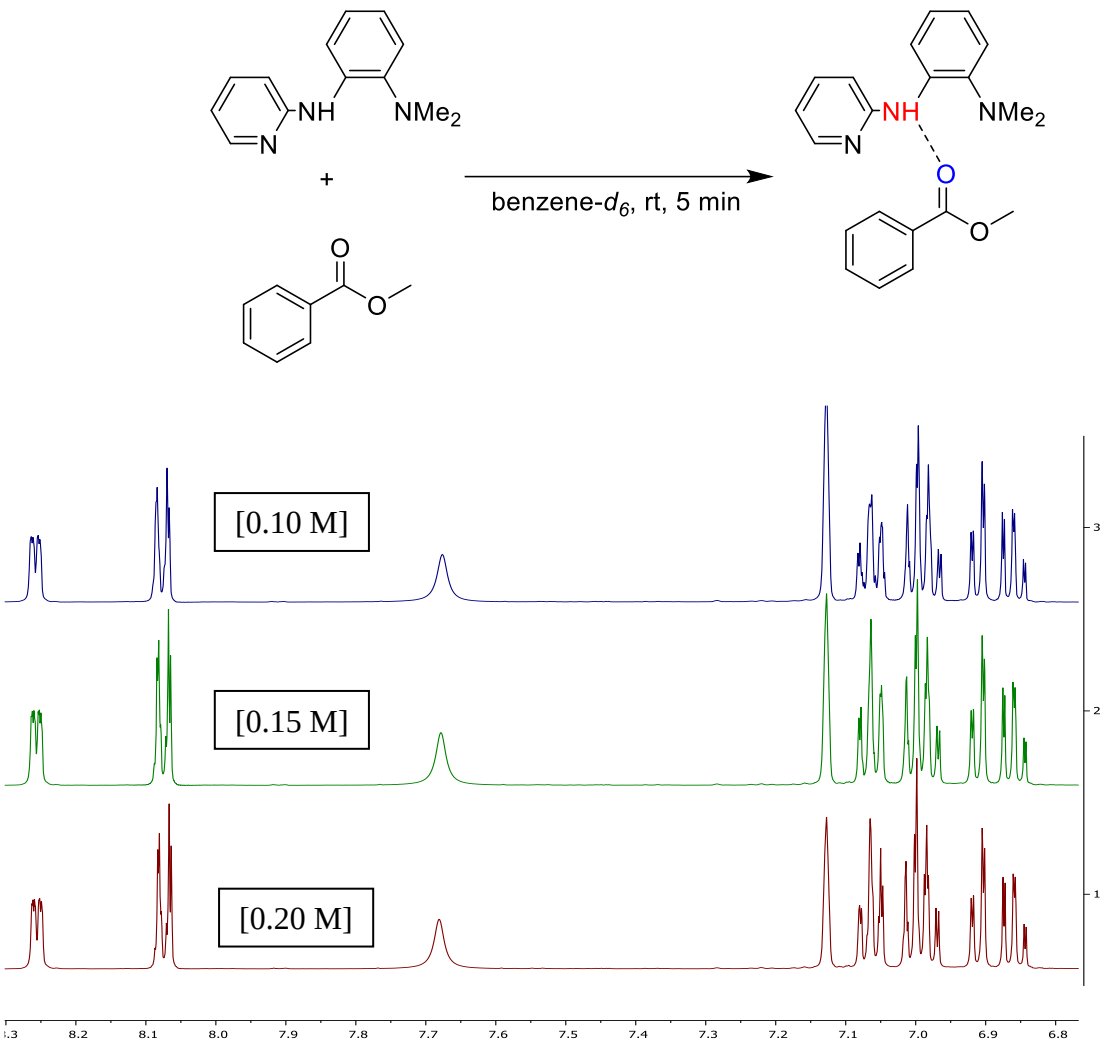

Figure 2.5 Hydrogen-Bonding Effect Between **L6** and Substrate.

Subjecting ligands **L1**-**L6** to 1.2 equivalents of HBpin at room temperature had shown N–B bonding between the primary amine and boryl group, as evidenced by the ^{11}B NMR showing a broadened peak at 24 ppm. No N–B bonding was seen for **L6** or **L4** indicating that the secondary amine is not responsible for the peak observed on NMR and that the interaction between the primary amine and boron source aids in catalysis. It has been proposed that the interaction between the ligand and boron source aids in preorganization of the ligand and better orients it to interact with the metal. [17] Also, the Smith and Maleczka groups have disclosed that the rigidity of the ligand can improve

coordination with the metal, evidenced by the more inflexible 3,4,7,8-tetramethyl-1,10-phenanthroline (tmphen) being a better ligand than 4,4'-di-*tert*-butyl-2,2'-bipyridyl (dtbpy).[28] Perhaps the coordination of **L1** with the boryl group also creates a similar effect.

Ligand to metal connectivity was hypothesized to be occurring between the pyridyl nitrogen atom based on the previous literature. Ligand **L7** was designed to test this hypothesis by replacing the pyridyl group with a phenyl group. When this ligand was used for CHB, it was shown to be unreactive. To confirm the ligand-metal connectivity, the reaction of $[Ir(Cl)cod]_2$ (1 equiv) and **L1** (2 equiv) was performed in hexanes at 65 °C for 3 hours. The proton NMR showed complete consumption of reagents and formation of a new compound. A crystal suitable for x-ray of the **L1** ligated iridium complex (**IrN**) was obtained by recrystallization using DCM/pentane. This structure (Figure 2.6) revealed an iridium complex ligated with 1,5-cyclooctadiene (cod), chlorine, and **L1** through the pyridyl nitrogen. The hydrogen of the secondary amine was measured to not be in close enough proximity to the metal center for hydrogen bonding to the metal or chlorine ligand. The **IrN** complex used for CHB reactions gave results consistent with the reactivity and selectivity of the catalyst generated *in situ*. For example, when using **IrN** to borylate methyl benzoate, a yield of 63% of product with an ortho selectivity of 80% was obtained. The *in situ* generated catalyst borylated methyl benzoate with a 65% yield with the same selectivity.

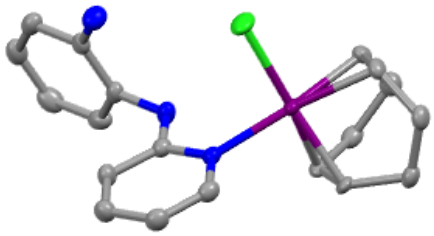

Figure 2.6 Crystal structure of **IrN** complex with hydrogen atoms omitted for clarity. Ir (purple); N (blue); Cl (green); C (gray).

To verify that both the pyridyl and phenylenediamine components of **L1** were crucial to the catalysis, ligands **L8**-**L11** were used for CHBs. Of these ligands, none of the substituted pyridines or diaminobenzene groups that make up **L1** had shown a high propensity for either selectivity or reactivity, indicating that both parts of the ligand are necessary for CHBs. Furthermore, when no ligand was used for catalysis, there was <5% conversion and selectivity was dominated by steric effects. If only **L1** was used without a precatalyst, no reaction took place.

Lastly, **L12** and **L13** were synthesized in similar fashion to Scheme 2.3 in a single step, demonstrating the ease of tuning the ligand with either electron donating or withdrawing substituents. Many combinations and locations are possible for modification; however, the 4-position of pyridine and backbone of the phenyl group are particularly attractive since these groups are in resonance with the pyridine sp^2-N and could increase reactivity of the system. Following the reaction setup in Scheme 2.4, it was found that both ligands were viable for *ortho* CHB and showed a modest increase in reactivity.

Scheme 2.4 Electronic effects of a modified **L1**.

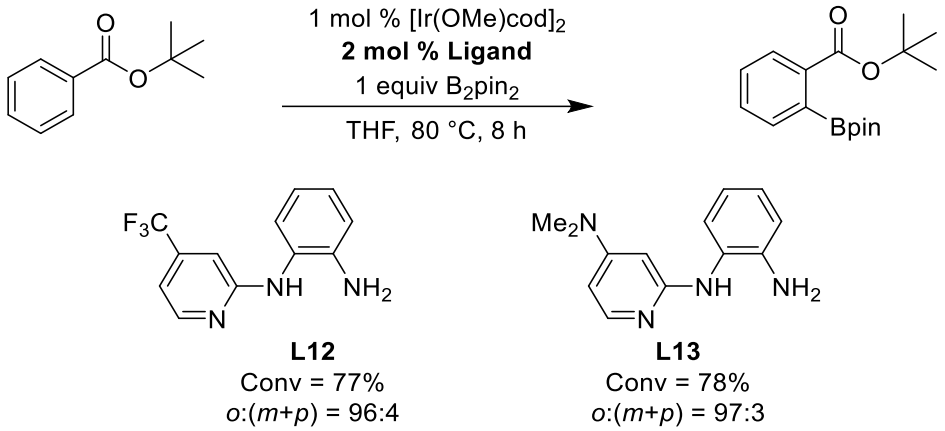

From these reactions, it can be seen that this ligand framework is versatile and easily modified for different electronic groups. With further modifications available, different possibilities exist for changing the structure and capabilities of the ligand.

2.5 Studies into the Catalyst System–Ligand Loading and Chloride Source

In order to glean information on the structure of the active catalyst, tests were performed to determine if multiple **L1** ligands could be binding onto the metal during catalysis. This phenomenon of bis-ligation of monodentate ligands is hypothesized to occur in Miyaura and Ishiyama's chelate-directing catalyst system. For this catalyst, monodentate, electron withdrawing ligands would dissociate from the metal center to free a second coordination site. However, it would be thermodynamically more favorable for the iridium center to be a pentacoordinate bis-ligated structure, which would decrease ortho selectivity, as shown in Scheme 2.5.[29,30]

Scheme 2.5 Mono- and bis-ligated iridium structures of Miyaura and Ishiyama's catalysts where L = $AsPh_3$ or tris[3,5-bis(trifluoromethyl)phenyl]phosphine.

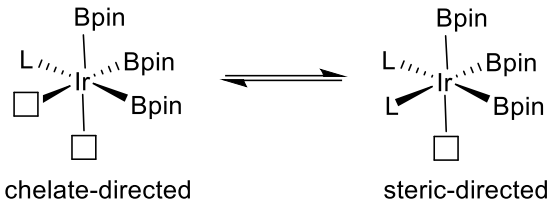

To test whether the active catalyst could be mono- or bis-ligated, similar conditions to Scheme 2.2 were performed using 2, 4, and 8 mol % ligand loadings of **L1**. Selectivity and reactivity dropped precipitously as more ligand was added (Table 2.1), suggesting that the catalyst has one **L1** ligand bound to the iridium.

Table 2.1 Effects of ligand loading on the catalyst system.

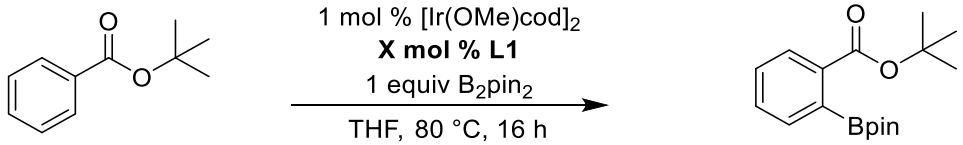

Entry	Ligand Loading (mol %)	Conversion (%)	*o*:(*m*+*p*) (%)
1	2	72	95:5
2	4	46	78:22
3	8	23	5:95

Reactions run on a 0.5 mmol scale of substrate, 0.5 mmol B_2pin_2, 1 mol % $[Ir(OMe)cod]_2$, and 2 mol % L1 in 1.0 mL THF for 16 h. Selectivity determined by ^1H NMR analysis of sample.

Continuing with these studies, another test was run to determine whether the chlorine ligand remains on the metal during catalysis. Following the setup in Table 2.2, it was seen that concentrations of a chloride source ($Et_4N^+Cl^-$) had an inverse relationship to both selectivity and conversion. Based on this, it can be reasoned that the chloride ligand is eliminated from the metal center before forming the active catalyst competent for CHB. The possibility of the chloride inhibiting catalysis is present as well.

Table 2.2 Effects of a chloride source on the catalyst system.

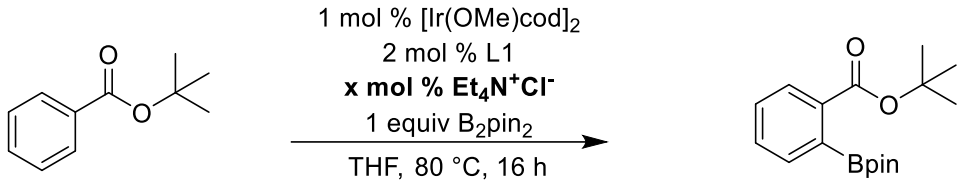

Entry	$Et_4N^+Cl^-$ (mol %)	Conversion (%)	*o*:(*m*+*p*) (%)
1	0	72	95:5
2	2	26	67:33
3	4	<1	---

Reactions run on a 0.5 mmol scale of substrate, 0.5 mmol B_2pin_2, 1 mol % $[Ir(OMe)cod]_2$, and 2 mol % L1 in 1.0 mL THF for 16 h. Selectivity determined by ^1H NMR analysis of sample.

From these studies, it is proposed that the active catalyst for this *ortho*-directing system has one **L1** ligand bound, no chloride ligand, and would likely be a trisboryl species based on what has already been disclosed about traditional Ir-catalyzed CHB systems.

2.6 Substrate Scope

To demonstrate the effectiveness of this catalyst system, a substrate scope was carried out on several substrates with varying functionalities and directing groups. The substrates of Table 2.3 contain ester, amide, or hydrazone functionalities, which were all shown to be effective directing groups for *ortho*-directed CHB. For these substrates (**1**-**7**), high *ortho* regioselectivity could be achieved (80-97%) and in moderate to high yields (65-82%). For monosubstituted substrate **1**, more diborylation in the *ortho* position occurred (**1a**), but when the methyl ester directing group was bulkier like in the case for substrates **2**, **6**, and **7**, there was no *ortho* diborylation seen. Likewise, for phenyl substrates substituted in the 3-position (**3**-**5**) no diborylation was observed.

Table 2.3 Substrate scope.

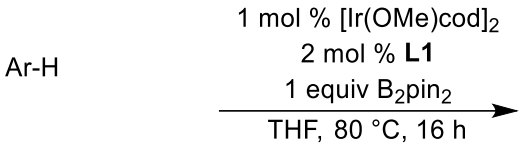

substrate	product	*o*:(*m*+*p*):di-*o*	% yield
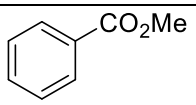 **1**	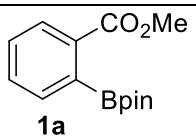 **1a**	80:8:12	65
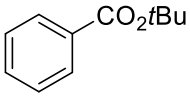 **2**	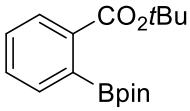 **2a**	91:9:0	77
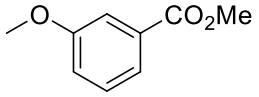 **3**	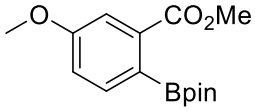	92:8:0	56
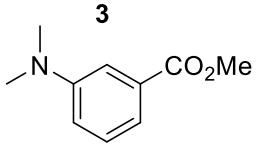 **4**	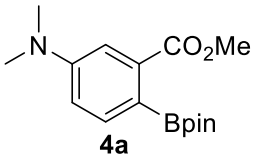 **4a**	97:3:0	54
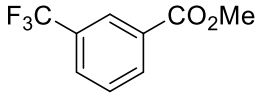 **5**	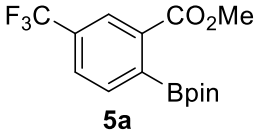 **5a**	83:17:0	82
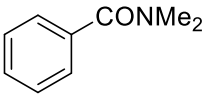 **6**	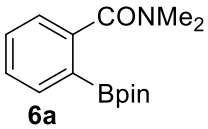 **6a**	95:5:0	82
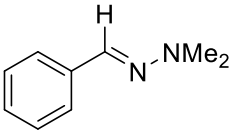 **7**	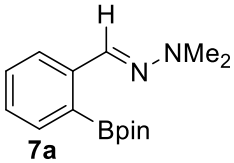 **7a**	84:16:0	74
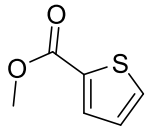 **8**	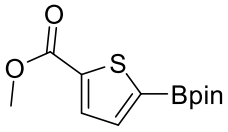 **8a**	3:(4+5) 1:99	95

Reactions run on a 0.5 mmol scale of substrate, 0.5 mmol B_2pin_2, 1 mol % $[Ir(OMe)cod]_2$, and 2 mol % L1 in 1.0 mL THF for 16 h. Selectivity determined by ^1H NMR analysis of sample.

For these same disubstituted arenes, both electron donating groups (methoxy and dimethyl amine) and electron withdrawing groups (trifluoromethyl) were shown to be borylated with high selectivity and moderate to high yields. High *ortho* selectivity was also observed with amide (**6**) and hydrazone (**7**) directing groups. Substrates with ketone (acetophenone) or aldehyde (benzaldehyde) functionalities were not viable as directing groups or CHB under the conditions of Table 2.3. These substrates had shown no conversion to borylated product by ^{1}H NMR. Testing for other possible directing groups, it was found that chlorine, fluorine, and methoxy groups were non-directing and selectivity of the borylations were determined by steric factors. The heterocycle methyl 2-thiophenecarboxylate was tested as well to see if the catalyst could borylate ortho to the ester group. Full conversion was achieved within 4 hours, but the product was borylated in the 5-position. The quinoline silyl ligand designed by the Smith and Maleczka group could borylate this challenging heterocycle adjacent to the ester, but this ligand required air-free conditions and stoichiometric amounts of lithium to synthesize.

2.7 Conclusions

In conclusion, phenylenediamine pyridyl ligands are capable of performing iridium catalyzed CHBs of arenes. Reactions yielded products borylated in the *ortho* position relative to an ester, amide, or hydrazone directing group of the substrate with various electron donating/withdrawing substituents. Ligand **L1** works as a monodentate ligand, bonded through the pyridyl nitrogen. Based on the experiments mentioned, the primary amine coordinates to the boron source, which helps aid in the formation of the active catalyst, and the sterics of the secondary amine influence selectivity. The ligands

synthesized are air-stable and easily modified. The starting materials for the ligand are inexpensive, making these ligands very accessible to use in CHB catalysis.

REFERENCES

REFERENCES

(1) Boebel, T. A.; Hartwig, J. F. Silyl-Directed, Iridium-Catalyzed Ortho-Borylation of Arenes. A One-Pot Ortho-Borylation of Phenols, Arylamines, and Alkylarenes. *J. Am. Chem. Soc.* **2008**, *130*, 7534–7535.

(2) Li, H. L.; Kuninobu, Y.; Kanai, M. Lewis Acid-Base Interaction-Controlled Ortho-Selective C-H Borylation of Aryl Sulfides. *Angew. Chem. Int. Ed Engl.* **2017**, *56*, 1495–1499.

(3) Roosen, P. C.; Kallepalli, V. A.; Chattopadhyay, B.; Singleton, D. A.; Maleczka, R. E., Jr; Smith, M. R., 3rd. Outer-Sphere Direction in Iridium C-H Borylation. *J. Am. Chem. Soc.* **2012**, *134*, 11350–11353.

(4) Kawamorita, S.; Ohmiya, H.; Hara, K.; Fukuoka, A.; Sawamura, M. Directed Ortho Borylation of Functionalized Arenes Catalyzed by a Silica-Supported Compact Phosphine-Iridium System. *J. Am. Chem. Soc.* **2009**, *131*, 5058–5089.

(5) Ghaffari, B.; Preshlock, S. M.; Plattner, D. L.; Staples, R. J.; Maligres, P. E.; Krska, S. W.; Maleczka, R. E., Jr; Smith, M. R., 3rd. Silyl Phosphorus and Nitrogen Donor Chelates for Homogeneous Ortho Borylation Catalysis. *J. Am. Chem. Soc.* **2014**, *136*, 14345–14348.

(6) Kuninobu, Y.; Ida, H.; Nishi, M.; Kanai, M. A Meta-Selective C–H Borylation Directed by a Secondary Interaction between Ligand and Substrate. *Nat. Chem.* **2015**, *7*, 712–717.

(7) Davis, H. J.; Genov, G. R.; Phipps, R. J. Meta -Selective C−H Borylation of Benzylamine-, Phenethylamine-, and Phenylpropylamine-Derived Amides Enabled by a Single Anionic Ligand. *Angew. Chem. Int. Ed.* **2017**, *56*, 13351–13355.

(8) Mihai, M. T.; Davis, H. J.; Genov, G. R.; Phipps, R. J. Ion Pair-Directed C–H Activation on Flexible Ammonium Salts: Meta-Selective Borylation of Quaternized Phenethylamines and Phenylpropylamines. *ACS Catal.* **2018**, *8*, 3764–3769.

(9) Saito, Y.; Segawa, Y.; Itami, K. Para-C–H Borylation of Benzene Derivatives by a Bulky Iridium Catalyst. *J. Am. Chem. Soc.* **2015**, *137*, 5193–5198.

(10) Mihai, M. T.; Williams, B. D.; Phipps, R. J. Para-Selective C-H Borylation of Common Arene Building Blocks Enabled by Ion-Pairing with a Bulky Countercation. *J. Am. Chem. Soc.* **2019**, *141*, 15477–15482.

(11) Montero Bastidas, J. R.; Oleskey, T. J.; Miller, S. L.; Smith, M. R., 3rd; Maleczka, R. E., Jr. Para-Selective, Iridium-Catalyzed C-H Borylations of Sulfated Phenols, Benzyl

Alcohols, and Anilines Directed by Ion-Pair Electrostatic Interactions. *J. Am. Chem. Soc.* **2019**, *141*, 15483–15487.
(12) Miyamura, S.; Araki, M.; Suzuki, T.; Yamaguchi, J.; Itami, K. Stereodivergent Synthesis of Arylcyclopropylamines by Sequential C-H Borylation and Suzuki-Miyaura Coupling. *Angew. Chem. Int. Ed Engl.* **2015**, *54*, 846–851.

(13) Ohmura, T.; Torigoe, T.; Suginome, M. Catalytic Functionalization of Methyl Group on Silicon: Iridium-Catalyzed C(sp3)-H Borylation of Methylchlorosilanes. *J. Am. Chem. Soc.* **2012**, *134*, 17416–17419.

(14) Liskey, C. W.; Hartwig, J. F. Iridium-Catalyzed Borylation of Secondary C-H Bonds in Cyclic Ethers. *J. Am. Chem. Soc.* **2012**, *134*, 12422–12425.

(15) Cho, S. H.; Hartwig, J. F. Iridium-Catalyzed Diborylation of Benzylic C–H Bonds Directed by a Hydrosilyl Group: Synthesis of 1,1-Benzyldiboronate Esters. *Chem. Sci.* **2013**, *5*, 694–698.

(16) Ishiyama, T.; Takagi, J.; Ishida, K.; Miyaura, N.; Anastasi, N. R.; Hartwig, J. F. Mild Iridium-Catalyzed Borylation of Arenes. High Turnover Numbers, Room Temperature Reactions, and Isolation of a Potential Intermediate. *J. Am. Chem. Soc.* **2002**, *124*, 390–391.

(17) Ros, A.; Estepa, B.; López-Rodríguez, R.; Álvarez, E.; Fernández, R.; Lassaletta, J. M. Use of Hemilabile N,N Ligands in Nitrogen-Directed Iridium-Catalyzed Borylations of Arenes. *Angew. Chem. Int. Ed Engl.* **2011**, *50*, 11724–11728.

(18) López-Rodríguez, R.; Ros, A.; Fernández, R.; Lassaletta, J. M. Pinacolborane as the Boron Source in Nitrogen-Directed Borylations of Aromatic N,N-Dimethylhydrazones. *J. Org. Chem.* **2012**, *77*, 9915–9920.

(19) Ros, A.; López-Rodríguez, R.; Estepa, B.; Álvarez, E.; Fernández, R.; Lassaletta, J. M. Hydrazone as the Directing Group for Ir-Catalyzed Arene Diborylations and Sequential Functionalizations. *J. Am. Chem. Soc.* **2012**, *134*, 4573–4576.

(20) Roering, A. J.; Hale, L. V. A.; Squier, P. A.; Ringgold, M. A.; Wiederspan, E. R.; Clark, T. B. Iridium-Catalyzed, Substrate-Directed C-H Borylation Reactions of Benzylic Amines. *Org. Lett.* **2012**, *14*, 3558–3561.

(21) Crawford, K. M.; Ramseyer, T. R.; Daley, C. J. A.; Clark, T. B. Phosphine-Directed C–H Borylation Reactions: Facile and Selective Access to Ambiphilic Phosphine Boronate Esters. *Angew. Chem. Int. Ed.* **2014**, *53*, 7589–7593.

(22) Hale, L. V. A.; McGarry, K. A.; Ringgold, M. A.; Clark, T. B. Role of Hemilabile Diamine Ligands in the Amine-Directed C–H Borylation of Arenes. *Organometallics* **2015**, *34*, 51–55.

(23) Sawamura, M. Air-Stable, Compact, Caged Trialkylphosphines (SMAPs): Synthesis, Properties and Applications to Homogeneous and Heterogeneous Catalysis. *J. Synth. Org. Chem Jpn.* **2009**, *67*, 1125–1135.

(24) Kawamorita, S.; Ohmiya, H.; Sawamura, M. Ester-Directed Regioselective Borylation of Heteroarenes Catalyzed by a Silica-Supported Iridium Complex. *J. Org. Chem.* **2010**, *75*, 3855–3858.

(25) Wang, G.; Liu, L.; Wang, H.; Ding, Y.-S.; Zhou, J.; Mao, S.; Li, P. N,B-Bidentate Boryl Ligand-Supported Iridium Catalyst for Efficient Functional-Group-Directed C-H Borylation. *J. Am. Chem. Soc.* **2017**, *139*, 91–94.

(26) Jiao, J.; Nie, W.; Song, P.; Li, P. A New Air-Stable Si,S-Chelating Ligand for Ir-Catalyzed Directed Ortho C-H Borylation. *Org. Biomol. Chem.* **2021**, *19*, 355–359.

(27) Wang, G.; Xu, L.; Li, P. Double N,B-Type Bidentate Boryl Ligands Enabling a Highly Active Iridium Catalyst for C-H Borylation. *J. Am. Chem. Soc.* **2015**, *137*, 8058–8061.

(28) Preshlock, S. M.; Ghaffari, B.; Maligres, P. E.; Krska, S. W.; Maleczka, R. E., Jr; Smith, M. R., 3rd. High-Throughput Optimization of Ir-Catalyzed C-H Borylation: A Tutorial for Practical Applications. *J. Am. Chem. Soc.* **2013**, *135*, 7572–7582.

(29) Ishiyama, T.; Isou, H.; Kikuchi, T.; Miyaura, N. Ortho-C–H Borylation of Benzoate Esters with Bis(pinacolato)diboron Catalyzed by Iridium–phosphine Complexes. *Chem. Commun.* **2010**, *46*, 159–161.

(30) Itoh, H.; Kikuchi, T.; Ishiyama, T.; Miyaura, N. Iridium-Catalyzed Ortho-C–H Borylation of Aryl Ketones with Bis(pinacolato)diboron. *Chem. Lett.* **2011**, *40*, 1007–1008.

Chapter 3. Modification of a Steric- to a Chelate-Directed Iridium Catalyst for C–H Borylation with a Dimeric Boryl Support Ligand

3.1 The Catalyst Cycle for Iridium Catalyzed C–H Borylation

Iridium precatalysts supported by nitrogen-based ligands like 4,4'-di-*tert*-butyl-2,2'-dipyridyl (dtbpy) or 3,4,7,8-tetramethyl-1,10-phenanthroline (tmphen) form active catalysts whose proposed active structure is an Ir(III) trisboryl complex.[1,2] The catalytic cycle using iridium and an L_2 ligand (bisphosphine) framework was first proposed by Smith and Maleczka as involving $Ir^{III/V}$.[3] Following this hypothesis, computational[4] and experimental data[2] were consistent with an $Ir^{III/V}$ cycle. The cycle begins with the Ir(III) trisboryl complex **A** and through oxidative addition of the substrate becomes an Ir(V) complex **B**. The organoboron product reductively eliminates leaving the catalyst as a monohydride, bisboryl Ir(III) complex **C**, which then undergoes a second oxidative addition of the boron source to replenish the lost boryl group, forming the Ir(V) complex **D**. Lastly, HBpin is expelled via reductive elimination to complete the cycle and return the iridium to the Ir(III) complex **A** (Scheme 3.1).

Scheme 3.1 Catalyst cycle for Ir-catalyzed CHBs.

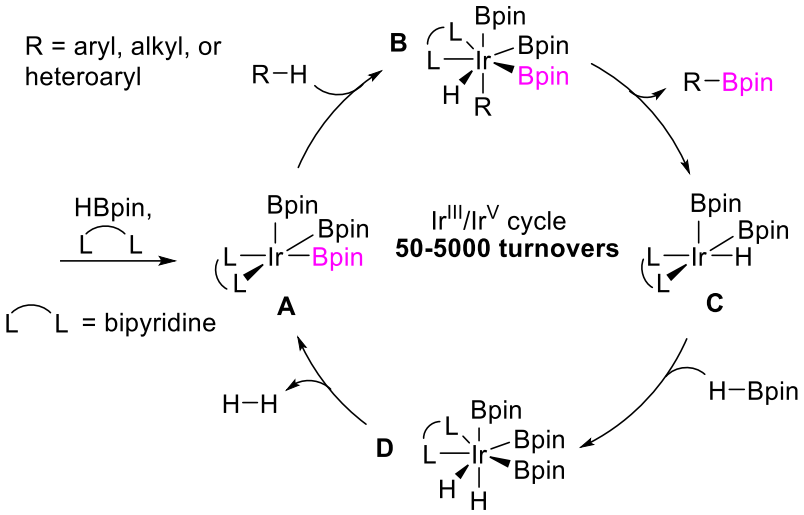

In this mechanism, the rate determining step is thought to be the initial oxidative addition of the C–H bond onto the metal. This is supported by the large primary kinetic isotope effect observed for the borylation of benzene versus benzene-d_6. Because of this, it can be reasoned that a more electron-rich and donating ligand to the metal center would be valuable since it could promote faster cleavage of the C–H bond, thus creating a more reactive catalyst system. Since the initial Ir(III) complex only requires one boryl ligand to form the boronic ester product, the Li group designed a catalyst where the other two boryl ligands are preinstalled as support ligands, taking greater advantage of boron's strong donor ability as a ligand.[5]

3.2 Boryl Ligands in Iridium Catalyzed C–H Borylation

For iridium-catalyzed CHBs, boryl ligands (like HBpin or B_2pin_2) typically act as active ligands, coming on and off the metal center during catalysis. These ligands are usually the boron source, pinacolborane (HBpin) or B_2pin_2, which oxidatively add to the metal and reductively eliminate to form the organoboron product. Because these ligands

are monodentate, have empty (or less filled) p-orbitals, and are reactive, they are more susceptible to being removed from the metal during catalysis.

In recent years, catalytic CHBs by Li and coworkers has shown that iridium catalysts with boron–nitrogen chelating ligands can operate well, like commonly employed bipyridine and phenanthroline ligated catalysts.[6] Some of these applications include borylating electron rich (hetero)arenes and sterically hindered substrates, which is particularly impressive since sterics have been shown to be one of the greatest obstacles for CHB that are ortho to large substituents.[7] The B,N-bidentate ligands were modeled after Yamashita and Nozaki's tridentate PBP boryl pincer ligands[8-10] and are sufficiently stable to maintain the boron-metal bond due to the chelate effect[11] and reducing the Lewis acidity of the boron atom with π-donating nitrogen substituents. Because of this increased stability, the ligands were less susceptible to being removed from the catalyst and can operate as support ligands for catalysis. Designs of these ligands are shown below in Figure 3.1. Previous work by Yamashita and Nozaki has shown that tridentate boryl ligands are quite versatile and tunable. Their uses in catalysis have been explored for hydrogenation,[12,13] cross-couplings,[14,15] and now CHBs.

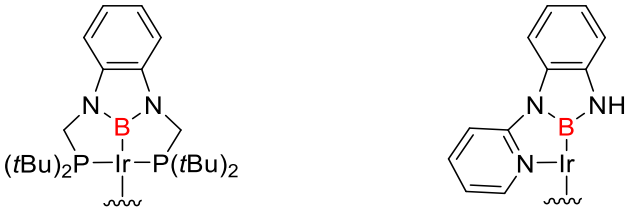

(a) (b)

Figure 3.1 Yamashita and Nozakis' (a) pincer PBP ligand and Li's bidentate (b) bidentate boryl ligand designs.

As can be seen by structures (a) and (b) of Figure 3.1, stabilization of the typically reactive boryl ligand was achieved by chelation and having nitrogen atoms bonded to the

boron atom, which can donate into the empty orbital of boron and reduce its susceptibility of being removed from the metal since the Lewis acidity of the boron is reduced. From this stabilization, an electron-rich ligand that has a strong propensity for σ-donation to the metal center was created.

3.3 Modification of Boryl Support Ligand Systems

The catalyst designed by Li that possesses two B,N-bidentate ligands (**IrBB**) works as a steric-directed catalyst whose synthesis is shown in Scheme 3.2. Based on **IrBB**'s structure, it was wondered whether this catalyst could be modified to yield chelate-directed products by removing one of the bidentate ligands. This would free a second coordination site and allow for *ortho* borylation of a substrate, relative to its directing group.

Scheme 3.2 Synthetic route to double B,N-bidentate complex (**IrBB**).

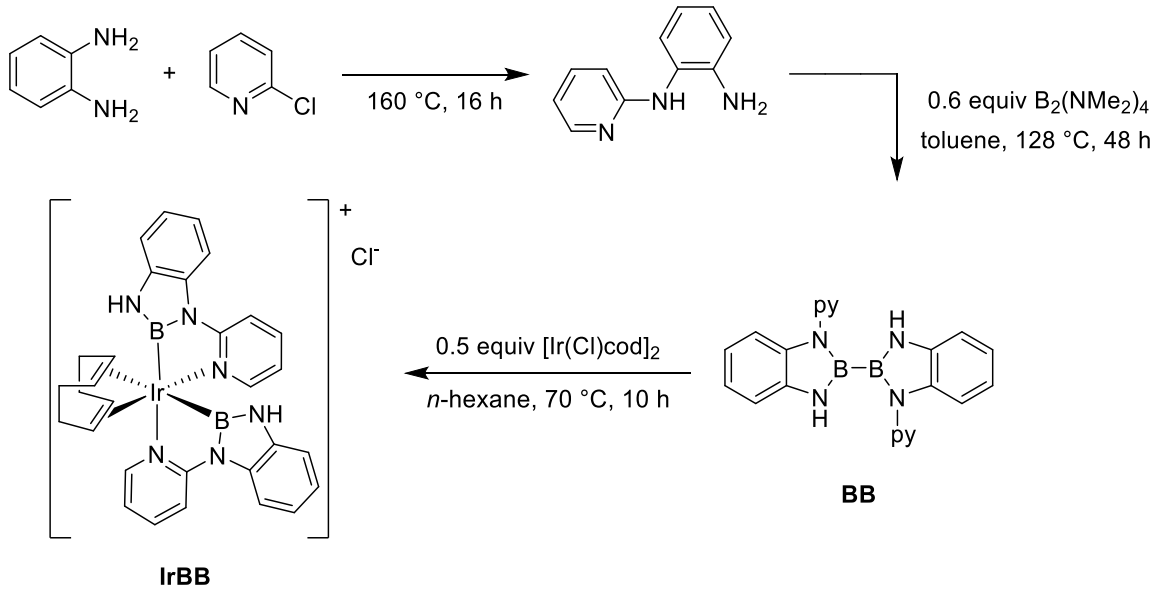

IrBB **BB**

The method for changing the regioselectivity of **IrBB** for *ortho* CHB was initially attempted by using a base additive, like KO-*t*-Bu, that could interact with one of boron's p orbitals and initiate cleavage of the bidentate ligand (Scheme 3.3). Similar reactions have precedent in the literature and our research group.[3,16]

Scheme 3.3 Removal of boryl ligand by base additive KO-*t*-Bu.

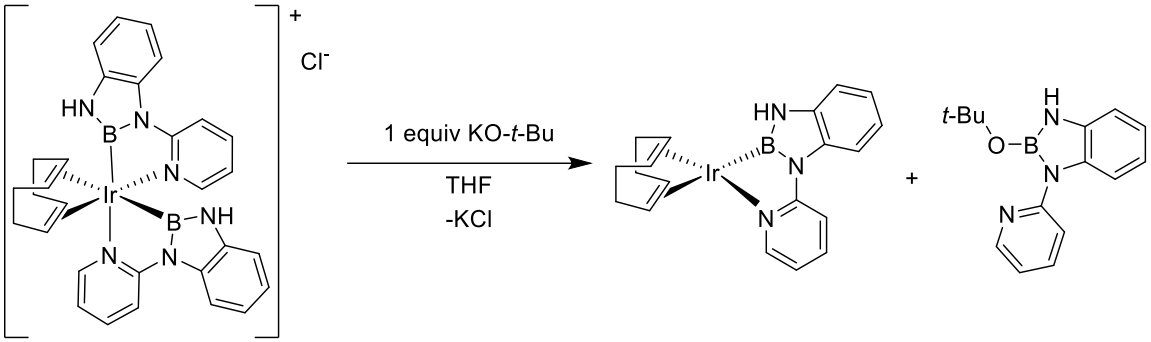

This method was not successful in accomplishing the desired outcome, and in fact, inhibited borylation proportional to the amount of KO-*t*-Bu used based on both conversion and *ortho* selectivity. All reactions using KO-*t*-Bu suffered from low conversion and selectivity based on steric factors (see Chapter 4 for details). In order to have an iridium center possessing only one chelating ligand, an environment where there is only one bidentate ligand per iridium metal would be needed.

In the original catalyst system, the B,N-bidentate compound (**BB**) was used in a 2:1 ratio to $[Ir(OMe)cod]_2$, where there are two bidentate ligands per iridium metal, and yielded products borylated in positions predominantly based on steric effects. However, it was found that by reducing the ligand loading to a 1:1 ratio a new catalyst is formed. This was evidenced by the dramatic changes in selectivity between the original system and the new system using the reduced loading of ligand, which gave products borylated in the *ortho* position to a directing group. Results demonstrating the differences in selectivity and ligand loading are shown in Table 3.1.

Table 3.1 Comparison of ligand loading and regioselectivity.

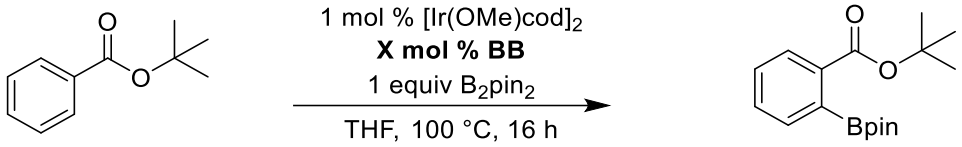

Entry	Ligand	Ligand Loading (mol %)	Conversion (%)	*o*:(*m**+*p*) (%)
1	BB	2	99	1:99
2	BB	1	80	60:40
3	BB	0.75	74	90:10
4	BB	0.50	67	95:5
5	dtbpy	2	99	1:99
6	dtbpy	0.50	74	1:99

Reactions run on 0.5 mmol scale of substrate, 0.5 mmol B_2pin_2, 1 mol % $[Ir(OMe)cod]_2$, and x mol % **BB** or dtbpy ligand in 1 mL THF. Conversions and selectivity determined by ^{1}H NMR analysis of sample. Meta selectivity (m*) includes dimeta-borylated products.

The results of Table 1 demonstrated that using the **BB** ligand in lower loadings resulted in higher *ortho* selectivity. In fact, as the loading decreases, the chelate product is formed in much higher ratios to the steric product. These results did not follow typical CHBs using iridium catalysts. Stoichiometrically, traditional catalyst systems, like Hartwig's $[Ir(OMe)cod]_2$/dtbpy system, require a 2:1 ratio of ligand and precatalyst. Previous work done in the Smith and Maleczka group on ligand to precatalyst ratio had shown that optimal catalytic activity results when the ligand is in slight excess of the precatalyst. Attempts using a 1:1 ligand to precatalyst ratio have been performed before using dtbpy or tmphen and $[Ir(OMe)cod]_2$, but resulted in lower catalyst activity.[17] This is due to one chelating ligand being needed per iridium metal. With a less than 2:1 ratio of ligand:precatalyst, a lower concentration of competent catalyst is generated. Entries 5 and 6 of Table 3.1 demonstrate this concept using a standard L_2 type bidentate ligand (dtbpy).

Under the same conditions of Table 3.1, CHBs were attempted using solely **BB** or iridium precatalyst and yielded no borylated products, indicating the need for both to

provide successful borylation. Borylations were also run using the preassembled catalyst **IrBB** (2 mol %) with an additional (2 mol %) $[Ir(Cl)cod]_2$ added to the reaction vessel. Interestingly, this setup gave products borylated in the *ortho* sites at similar conversions and selectivity as the conditions used in Table 3.1, entry 4.

Other iridium complexes like $[Ir(Cl)cod]_2$ and (Ind)Ir(cod) were also viable precatalyst options for *ortho*-directed CHBs. When using these precatalysts with lower ligand loading conditions, a high proclivity for the chelate-directed product was observed. Following the reaction conditions of Table 3.1, entry 4 with $[Ir(Cl)cod]_2$ yielded borylated products in a ratio of 95:5 for (*o*:(*m*+*p*)) at 83% conversion. Under the same conditions but using (Ind)Ir(cod) gave products in a ratio of 45:55 for (*o*:(*m*+*p*)) at 66% conversion from starting material to borylated product. Using increased ligand loadings for these two precatalysts (2:1 **BB**:[Ir]) had shown an increase in steric-directed products. Table 3.2 outlines these results.

Table 3.2 Comparison of iridium precatalyst and regioselectivity.

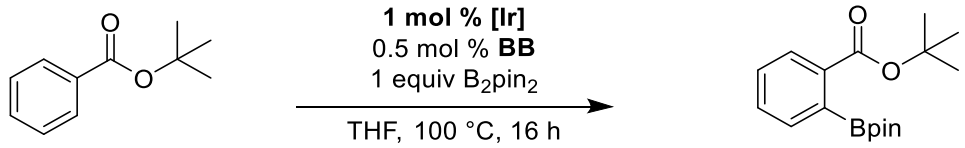

Entry	Precatalyst	Conversion (%)	*o*:(*m*+*p*) (%)
1	$[Ir(OMe)cod]_2$	85	92:8
2	$[Ir(Cl)cod]_2$	83	95:5
3	(Ind)Ir(cod)	66	45:55

Reactions run on 0.5 mmol scale of substrate, 0.5 mmol B_2pin_2, 1 mol % $[Ir(X)cod]_2$ or 0.5 mol % (Ind)Ir(cod) and 0.5 mol % **BB** in 1 mL THF. Conversions and selectivity determined by ^1H NMR analysis of sample.

3.4 Complexes for Steric- and Chelate-Directed Catalysis

Crystals were grown of the catalyst used for chelate-directed CHB (Figure 3.2) to determine the cause of contrast between the steric and chelate conditions. This was done by heating $[Ir(Cl)cod]_2$ and **BB** ligand in a 1:1 ratio in pentane at 70 °C for 3 hours. From the yellow solid that formed, crystals were grown via solvent displacement using DCM/hexanes. This iridium complex possessed the double B,N-bidentate ligands and was cationic, similar to **IrBB**. However, instead of having a chloride counter anion, **IrBB'** had a dichloro cyclooctadiene iridium (I) species as the counter anion.

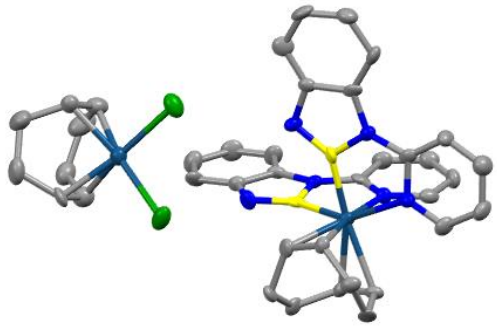

Figure 3.2 Crystal structure of complex **IrBB'** with hydrogen atoms omitted for clarity. Ir (dark blue); N (blue); boron (yellow); Cl (green); C (gray).

The **IrBB'** complex was used as catalyst for chelate-directed CHBs under standard reaction conditions, however, no borylated products were observed even after 24 h, which suggests that **IrBB'** may not be representative of the active catalyst.

The **IrBB** complex also required heating the system to 100 °C for meaningful reactivity to occur. At temperatures of 80 °C and below, the reaction was sluggish and gave minimum conversion to borylated products.

3.5 Comparison of a Boron Dimer Ligand and Silicon-Boryl Ligand

Shortly after the initial publication of CHB using the **BB** ligand, an asymmetric analog of **BB** consisting of a boron-silicon ligand were designed for chelate-directed CHB.

Reaction of the ligand and $[Ir(Cl)cod]_2$ precatalyst formed a complex with a single B,N-bidentate ligand and a silyl group that prevents the addition of another B,N group to the metal.[19] A comparison between the reduced ligand loading conditions with **BB** and the standard conditions with **SiB** ligand are shown in Table 3.3.

Based on the data presented, both **BB** and **SiB** ligands yield strikingly similar results in both conversion and selectivity. Although both can produce the chelate-directed products, the **BB** ligand at lower loadings would be more appealing to use for catalyzed CHBs. Its synthesis can be done in two steps starting from commercially available materials does not produce as large a waste stream as the **SiB** ligand, which uses an excess of lithium metal for its synthesis and is 4 steps to prepare.

Table 3.3 Comparison of **BB** and **SiB** ligands for chelate-directed CHB.

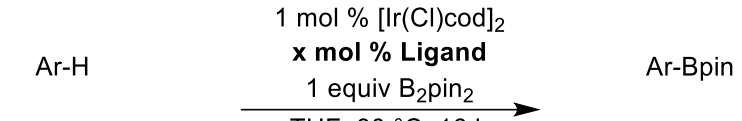

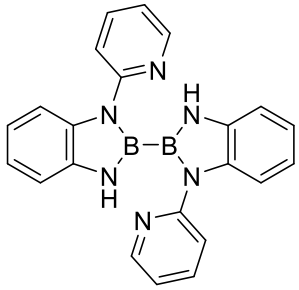

BB

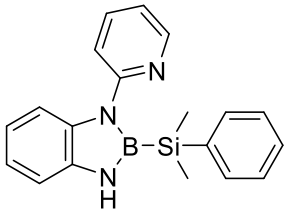

SiB

Entry	Substrate	Ligand	Conversion (%)	*o*:(*m*+*p*) (%)
1	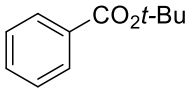	**BB**	78	93:7
		SiB	77	90:10
2	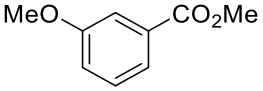	**BB**	75	93:7
		SiB	75	92:8

Reactions run on 0.5 mmol scale of substrate, 1 equiv B_2pin_2, and 1 mol % $[Ir(Cl)cod]_2$. For **BB** ligand, 0.50 mol % was used and for **SiB** ligand, 2 mol % was used. Conversion and selectivity determined by ^1H NMR.

3.6 Substrate Scope at Lower Ligand Loading Conditions

Based on the promising results in Table 3.1, entry 4, a substrate scope was carried out using these lowered ligand loading conditions for achieving ortho regioselectivity. To fully show the effects of ligand loading in the catalysis of the system, reactions were run in parallel using the original 2:1 ligand to precatalyst ratio alongside the varied ligand loading system (Table 3.4). Results with $[Ir(Cl)cod]_2$ are also shown in Chapter 4.

Table 3.4 CHBs of arenes using conditions for chelate- and steric-directed catalysis. Condition A (chelate conditions) yield Product A and Condition B (steric conditions) yield Product B.

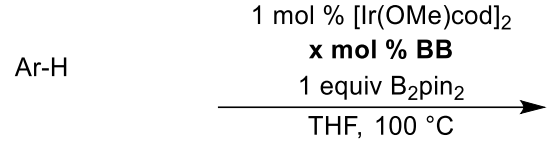

Entry	Substrate	Product A	Product B
1	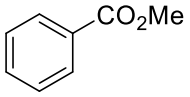	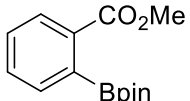 **1a** 73%	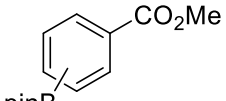 **1b** 95%
2	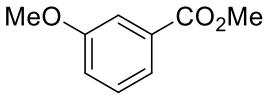	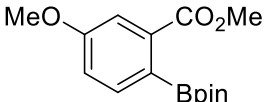 **2a** 62%	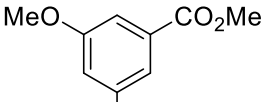 **2b** 76%
3	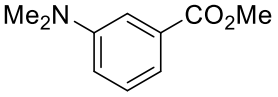	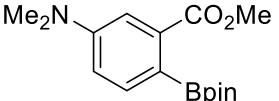 **3a** 65%	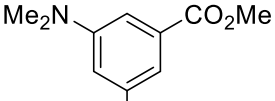 **3b** 80%
4	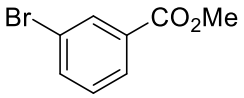	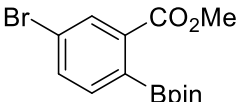 **4a** 77%	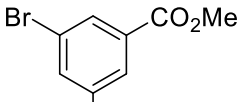 **4b** 92%
5	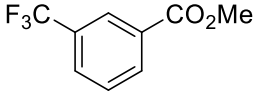	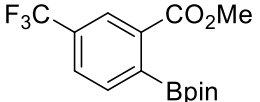 **5a** 72%	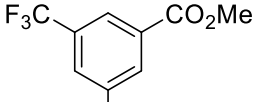 **5b** 88%
6	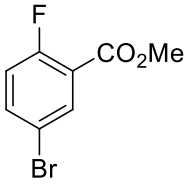	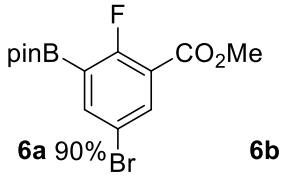 **6a** 90%	**6b** 93% 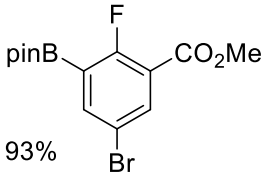
7	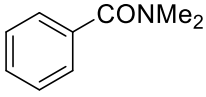	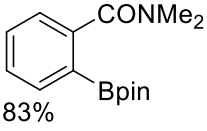 **7a** 83%	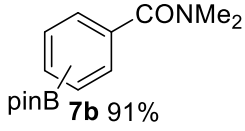 **7b** 91%

Reactions run on 0.5 mmol scale of substrate, 0.5 mmol B_2pin_2, 1 mol % $[Ir(OMe)cod]_2$, and 0.50 mol % **BB** ligand for condition A or 2 mol % for condition B, in 1.0 mL THF for 4-16 h. Selectivity determined by ^1H NMR analysis of sample.

From this scope, it was found that for most arenes tested, changing the ligand loading changes the regioselectivity. For substrates having an ester or amide functionality, particularly substrates **1**-**5** and **7**, significant *ortho*-selectivity was noted, ranging from 60-90%. Steric controlled conditions (Products B) gave almost exclusively the steric product (*meta* and *para*). To see the efficacy of the chelate-directed conditions, *ortho* borylation was attempted for substrate **6**, which has only one *ortho* site to the ester directing group and a bulky substituent in the position *meta* to that directing group. Borylation of this substrate was in the steric position for both Conditions A and B. This result was expected however since the substrate has never been ortho borylated before and has a bulky halogen greatly hindering the ortho site. For 1,3-disubstituted arenes (**2**-**5**), Conditions A yielded the chelate product in good yields and selectivity, while Conditions B yielded almost exclusively 1,3,5 substituted product, also in good yields. CHB reactions for both Conditions A and B were effective for a variety of functional groups with both electron withdrawing or donating substituents.

For heterocycles, Conditions A and B were run using 2-thiophenecarboxylate (entry 8) and 5-methyl-2-thiophenecarboxylate (entry 9) (Table 3.5). For entry 8, the thiophene was borylated in the more reactive 5-position of the substrate. By blocking the 5-position with a methyl group in entry 9, the heterocycle could be *ortho* borylated to an ester using Conditions A. Conditions B gave products borylated in the 4-position for the same substrate.

Table 3.5 CHBs of heteroarenes using conditions for chelate- and steric-directed catalysis. Conditions A (chelate conditions) yield Product A and Conditions B (steric conditions) yield Product B.

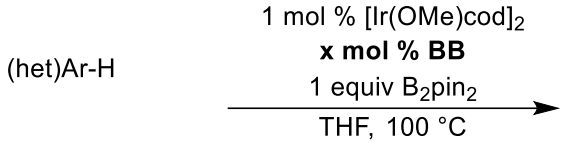

Entry	Substrate	Product A	Product B
8	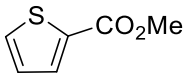	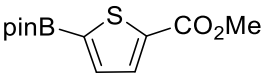 **8a** 90%	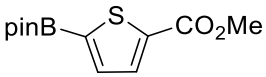 **8b** 99%
9	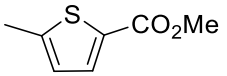	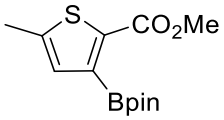 **9a** 55%	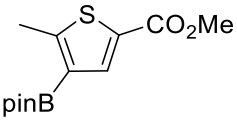 **9b** 93%

Reactions run on 0.5 mmol scale of substrate, 0.5 mmol B_2pin_2, 1 mol % $[Ir(OMe)cod]_2$, and 0.50 mol % **BB** ligand for condition A or 2 mol % for condition B, in 1.0 mL THF for 4-16 h. Selectivity determined by ^1H NMR analysis of sample.

Substrates of Entries 1-9 were also run using $[Ir(Cl)cod]_2$ as the precatalyst for Condition A. Using this precatalyst would give higher chelate-directed products and a higher degree of regioselectivity than when $[Ir(OMe)cod]_2$ was used. This difference in selectivity for chelate products was also observed in the **SiB** ligated systems as well although reason for this change is not known.

For Condition B, using substrates 1-9, borylations gave higher yields and almost solely the steric product as expected from what has already been seen in the literature.[5] Overall, from these studies, it was shown that for most substrates, regioselectivity could be flipped by altering the preligand loading of the **BB** dimeric boryl ligand. While usually a preligand can be used to change selectivity, this is the first case where selectivity can be changed without the need for a new preligand.

3.7 Applications of Boryl Support Ligands

Given that spectator boryl ligands have become a powerful and versatile ligand for CHBs of both C(sp^2)–H and C(sp^3)–H bonds, the insights on derivatives of **BB** may be valuable due to their unique capabilities.

Since the initial use of bidentate boryl ligands for homogeneous CHB catalysis, other boryl support ligands have appeared in the literature. These ligands are modeled after the asymmetric **SiB** ligand in that the boryl group is bonded to a silyl that can oxidatively add to the iridium precatalyst. Examples of these ligands and their capacity for CHB are shown below in Figure 3.3.[6,19-22]

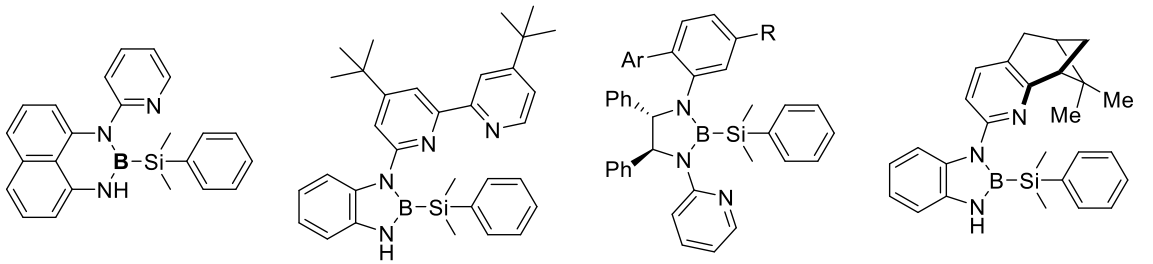

Figure 3.3 Boryl support ligands for CHB catalysis.

From the beginnings of Ir catalyzed CHBs,[23] boron has typically been an actor ligand, but through new developments has shown to be a promising support ligand that can be tuned for different selectivities and capabilities.

3.8 Conclusions

In conclusion, a catalyst system was modified from steric- to chelate-directed by changing the ligand loading so that there was a 1:2 ratio of bidentate ligand BB to iridium dimer precatalyst. This system works well for *ortho* CHB using esters and amides as directing groups and for (hetero)arenes. Although it is not fully understood what causes the

shift in regioselectivity, it was found that the iridium counteranion is necessary for the chelate-directed products to form since the chloride counteranion gave steric CHB products. More work on reaction mechanism and conditions with other boryl ligands are currently being carried out.

REFERENCES

REFERENCES

(1) Ishiyama, T.; Takagi, J.; Ishida, K.; Miyaura, N.; Anastasi, N. R.; Hartwig, J. F. Mild Iridium-Catalyzed Borylation of Arenes. High Turnover Numbers, Room Temperature Reactions, and Isolation of a Potential Intermediate. *J. Am. Chem. Soc.* **2002**, *124*, 390–391.

(2) Boller, T. M.; Murphy, J. M.; Hapke, M.; Ishiyama, T.; Miyaura, N.; Hartwig, J. F. Mechanism of the Mild Functionalization of Arenes by Diboron Reagents Catalyzed by Iridium Complexes. Intermediacy and Chemistry of Bipyridine-Ligated Iridium Trisboryl Complexes. *J. Am. Chem. Soc.* **2005**, *127*, 14263–14278.

(3) Cho, J.-Y.; Tse, M. K.; Holmes, D.; Maleczka, R. E., Jr; Smith, M. R., 3rd. Remarkably Selective Iridium Catalysts for the Elaboration of Aromatic C-H Bonds. *Science* **2002**, *295*, 305–308.

(4) Tamura, H.; Yamazaki, H.; Sato, H.; Sakaki, S. Iridium-Catalyzed Borylation of Benzene with Diboron. Theoretical Elucidation of Catalytic Cycle Including Unusual Iridium(v) Intermediate. *J. Am. Chem. Soc.* **2003**, *125*, 16114–16126.

(5) Wang, G.; Xu, L.; Li, P. Double N,B-Type Bidentate Boryl Ligands Enabling a Highly Active Iridium Catalyst for C-H Borylation. *J. Am. Chem. Soc.* **2015**, *137*, 8058–8061.

(6) Ding, S.; Wang, L.; Miao, Z.; Li, P. NNB-Type Tridentate Boryl Ligands Enabling a Highly Active Iridium Catalyst for C⁻H Borylation. *Molecules* **2019**, *24*, 2407-1434.

(7) Furukawa, T.; Tobisu, M.; Chatani, N. C-H Functionalization at Sterically Congested Positions by the Platinum-Catalyzed Borylation of Arenes. *J. Am. Chem. Soc.* **2015**, *137*, 12211–12214.

(8) Segawa, Y.; Yamashita, M.; Nozaki, K. Syntheses of PBP Pincer Iridium Complexes: A Supporting Boryl Ligand. *J. Am. Chem. Soc.* **2009**, *131*, 9201–9203.

(9) Yamashita, M.; Suzuki, Y.; Segawa, Y.; Nozaki, K. Synthesis, Structure of Borylmagnesium, and Its Reaction with Benzaldehyde to Form Benzoylborane. *J. Am. Chem. Soc.* **2007**, *129*, 9570–9571.

(10) Segawa, Y.; Yamashita, M.; Nozaki, K. Boryl Anion Attacks Transition-Metal Chlorides to Form Boryl Complexes: Syntheses, Spectroscopic, and Structural Studies on Group 11 Borylmetal Complexes. *Angew. Chem. Int. Ed Engl.* **2007**, *46*, 6710–6713.

(11) Hancock, R. D.; Martell, A. E. Chelate Ring Geometry, and the Metal Ion Selectivity of Macrocyclic Ligands. Some Recent Developments. *Supramol. Chem.* **1996**, *6*, 401–407.

(12) Lin, T.-P.; Peters, J. C. Boryl-Mediated Reversible H2 Activation at Cobalt: Catalytic Hydrogenation, Dehydrogenation, and Transfer Hydrogenation. *J. Am. Chem. Soc.* **2013**, *135*, 15310–15313.

(13) Harman, W. H.; Peters, J. C. Reversible H2 Addition across a Nickel-Borane Unit as a Promising Strategy for Catalysis. *J. Am. Chem. Soc.* **2012**, *134*, 5080–5082.

(14) Ben Halima, T.; Zhang, W.; Yalaoui, I.; Hong, X.; Yang, Y.-F.; Houk, K. N.; Newman, S. G. Palladium-Catalyzed Suzuki-Miyaura Coupling of Aryl Esters. *J. Am. Chem. Soc.* **2017**, *139*, 1311–1318.

(15) Miyaura, N.; Yanagi, T.; Suzuki, A. The Palladium-Catalyzed Cross-Coupling Reaction of Phenylboronic Acid with Haloarenes in the Presence of Bases. *Synth. Commun.* **1981**, *11*, 513–519.

(16) Cho, J. Y. Ph.D. dissertation, Michigan State University, **2002**.

(17) Preshlock, S. M.; Ghaffari, B.; Maligres, P. E.; Krska, S. W.; Maleczka, R. E., Jr; Smith, M. R., 3rd. High-Throughput Optimization of Ir-Catalyzed C-H Borylation: A Tutorial for Practical Applications. *J. Am. Chem. Soc.* **2013**, *135*, 7572–7582.

(18) Weng, W.; Guo, C.; Moura, C.; Yang, L.; Foxman, B. M.; Ozerov, O. V. Competitive Activation of N−C and C−H Bonds of the PNP Framework by Monovalent Rhodium and Iridium. *Organometallics* **2005**, *24*, 3487–3499.

(19) Wang, G.; Liu, L.; Wang, H.; Ding, Y.-S.; Zhou, J.; Mao, S.; Li, P. N,B-Bidentate Boryl Ligand-Supported Iridium Catalyst for Efficient Functional-Group-Directed C-H Borylation. *J. Am. Chem. Soc.* **2017**, *139*, 91–94.

(20) Shi, Y.; Gao, Q.; Xu, S. Chiral Bidentate Boryl Ligand Enabled Iridium-Catalyzed Enantioselective C(sp3)-H Borylation of Cyclopropanes. *J. Am. Chem. Soc.* **2019**. https://doi.org/10.1021/jacs.9b04549.

(21) Zou, X.; Zhao, H.; Li, Y.; Gao, Q.; Ke, Z.; Xu, S. Chiral Bidentate Boryl Ligand Enabled Iridium-Catalyzed Asymmetric C(sp2)-H Borylation of Diarylmethylamines. *J. Am. Chem. Soc.* **2019**. https://doi.org/10.1021/jacs.8b13756.

(22) Song, P.; Hu, L.; Yu, T.; Jiao, J.; He, Y.; Xu, L.; Li, P. Development of a Tunable Chiral Pyridine Ligand Unit for Enantioselective Iridium-Catalyzed C–H Borylation. *ACS Catal.* **2021**, *11*, 7339–7349.

(23) Iverson, C. N.; Smith, M. R. Stoichiometric and Catalytic B−C Bond Formation from Unactivated Hydrocarbons and Boranes. *J. Am. Chem. Soc.* **1999**, *121*, 7696–7697.

Chapter 4. Experimental

4.1 Chapter 2 Experimental Procedures and Details

General Information

All reactions were carried out in oven-dried glassware under an inert atmosphere. Solvents used came from wet stills and commercially available chemicals were used as received unless otherwise noted. Proton NMR spectra were recorded on a Varian 500 MHz instrument. Carbon NMR and Boron NMR were recorded on 126 MHz and 160 MHz instruments, respectively. Borylation reactions were conducted using stock solutions of the ligand and precatalyst in a nitrogen-filled glovebox.

High-resolution mass spectra (HRMS) were obtained at the Michigan State University Mass Spectrometry Service Center using electrospray ionization (ESI+ or ESI-) on quadrupole time-of-flight (Q-TOF) instruments. Melting points were measured in a capillary melting point apparatus and are uncorrected.

Synthesis of *N*^{1}-(pyridin-2-yl)benzene-1,2-diamine (L1)

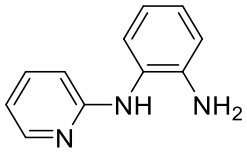

1,2-Diaminobenzene (1.0 g, 9.26 mmol, 2.0 equiv) along with 2-chloropyridine (0.42 mL, 4.63 mmol, 1.0 equiv) were added to a 100 mL round bottom flask containing a magnetic stir bar. A condenser was attached, the system was purged with N_2, and the contents were heated at 160 °C for 16 hours while under nitrogen. The black solid that formed was cooled to room temperature, after which the reaction flask was opened to air. Water and acetone were then added in equal amounts to the solid until it completely dissolved. The pH of the solution was adjusted to 10 by adding a saturated Na_2CO_3 solution.

Brine was then added, and the crude product was extracted with ethyl acetate. Organic layers were combined, dried over Na_2SO_4, filtered, and concentrated under reduced pressure. The residue was washed with hexanes (3 x 10 mL) on a filter frit. The solids were then transferred to a Soxhlet thimble, and a Soxhlet extraction was performed with DCM for 20 hours. Solvent was removed from the filtrate by rotary evaporation, yielding the product as a pale violet solid (528 mg, 62%). ^{1}H NMR (500 MHz, $CDCl_3$) δ 8.16 (ddd, *J* = 5.1, 1.9, 0.9 Hz, 1H), 7.44 (ddd, *J* = 8.6, 7.2, 1.9 Hz, 1H), 7.20 (dd, *J* = 7.8, 1.5 Hz, 1H), 7.10 (td, *J* = 7.7, 1.5 Hz, 1H), 6.83 (dd, *J* = 8.0, 1.4 Hz, 1H), 6.78 (td, *J* = 7.6, 1.4 Hz, 1H), 6.69 (ddd, *J* = 7.1, 5.0, 0.9 Hz, 1H), 6.42 (dt, *J* = 8.4, 0.9 Hz, 1H), 6.27 – 6.12 (s, 1H), 3.88 (s, 2H); ^{13}C NMR (126 MHz, $CDCl_3$) δ 157.7, 148.3, 143.0, 137.9, 127.2, 127.0, 125.8, 118.9, 116.2, 114.4, 107.2.[1]

Synthesis of *N*^{1}-(pyridin-2-yl)benzene-1,3-diamine (L2)

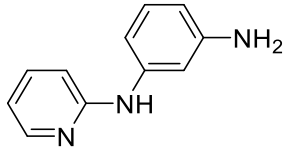

1,3-Diaminobenzene (1.0 g, 9.26 mmol, 2.0 equiv) along with 2-chloropyridine (0.42 mL, 4.63 mmol, 1.0 equiv) were added to a 100 mL round bottom flask containing a magnetic stir bar in open air. A condenser was attached, the system was purged with N_2, and the contents were heated at 160 °C for 16 hours while under nitrogen. The black solid that formed was cooled to room temperature, after which the reaction flask was opened to air. Water and acetone were added in equal amounts to the solid until it completely dissolved. The pH of the solution was adjusted to 10 by adding a saturated Na_2CO_3 solution. Brine was then added, and the crude product was extracted with ethyl acetate. Organic layers were combined, dried over Na_2SO_4, filtered, and concentrated under

reduced pressure. The residue was purified via hexanes wash (3 x 10 mL) followed by flash column chromatography with 100% EtOAc to give the product as a tan solid (357 mg, 43%), m.p. = 127-130 °C. ^{1}H NMR (500 MHz, $CDCl_3$) δ 8.19 (ddd, *J* = 5.0, 2.0, 0.9 Hz, 1H), 7.47 (ddd, *J* = 8.8, 7.2, 2.0 Hz, 1H), 7.09 (t, *J* = 7.9 Hz, 1H), 6.91 (dd, *J* = 8.4, 0.9 Hz, 1H), 6.79 (s, 1H), 6.75 – 6.68 (m, 2H), 6.66 (ddd, *J* = 8.0, 2.2, 0.9 Hz, 1H), 6.38 (ddd, *J* = 8.0, 2.3, 0.9 Hz, 1H), 3.70 (s, 3H); ^{13}C NMR (126 MHz, $CDCl_3$) δ 156.0, 148.4, 147.4, 141.5, 137.6, 130.0, 114.9, 110.5, 109.8, 108.5, 106.7. HRMS (ESI) (*m*+1)/*z* calc for $C_{11}H_{11}N_3$ 186.0952, found 186.1017.[2]

Synthesis of *N*^{1}-(pyridin-2-yl)benzene-1,4-diamine (L3)

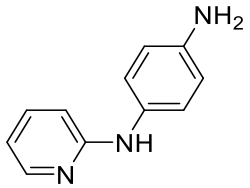

1,4-Diaminobenzene (1.0 g, 9.26 mmol, 2.0 equiv) along with 2-chloropyridine (0.42 mL, 4.63 mmol, 1.0 equiv) were added to a 100 mL round bottom flask containing a magnetic stir bar in open air. A condenser was attached, the system was purged with N_2, and the contents were heated at 160 °C for 16 hours while under nitrogen. The black solid that formed was cooled to room temperature, after which the reaction flask was opened to air. Water and acetone were added in equal amounts to the solid until it completely dissolved. The pH of the solution was adjusted to 10 by adding a saturated Na_2CO_3 solution. Brine was then added, and the crude product was extracted with ethyl acetate. Organic layers were combined, dried over Na_2SO_4, filtered, and concentrated under reduced pressure. The residue was purified via hexanes wash (3 x 10 mL) followed by flash chromatography using 100% EtOAc to give the product as an off-white solid (611 mg,

74%), m.p. = 118-120 °C. ^{1}H NMR (500 MHz, $CDCl_3$) δ 8.12 (dd, *J* = 5.4, 2.0 Hz, 1H), 7.40 (td, *J* = 8.5, 2.0 Hz, 1H), 7.10 (d, *J* = 8.20, 2H), 6.70 (d, *J* = 8.20, 2H), 6.64 (m, 2H), 6.58 (bs, 1H) 3.65 (bs, 2H); ^{13}C NMR (126 MHz, C_6D_6) δ 158.3, 148.5, 143.4, 136.8, 131.1, 124.6, 115.1, 113.3, 106.6. HRMS (ESI) (*m*+1)/*z* calc for $C_{11}H_{11}N_3$ 185.0952, found 185.1068.[3]

Synthesis of *N*-phenylpyridin-2-amine (L4)

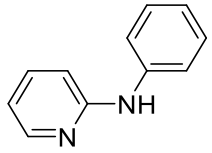

Aniline (1.4 g, 15.0 mmol, 1.0 equiv) along with 2-chloropyridine (1.42 mL, 15.0 mmol, 1.0 equiv) were added to a 100 mL round bottom flask containing a magnetic stir bar in open air. A condenser was attached, the system was purged with N_2, and the contents were heated at 160 °C for 16 hours while under nitrogen. The black solid that formed was cooled to room temperature, after which the reaction flask was opened to air. Water and acetone were added in equal amounts to the solid until it completely dissolved. The pH of the solution was adjusted to 10 by adding a saturated Na_2CO_3 solution. Brine was then added, and the crude product was extracted with ethyl acetate. Organic layers were combined, dried over Na_2SO_4, filtered, and concentrated under reduced pressure. The residue was washed with hexanes (3 x 10 mL) and dried under reduced pressure to give the product as a deep purple solid (2.248 g, 81%), m.p. = 100-102 °C. ^{1}H NMR (500 MHz, $CDCl_3$) δ 8.22 (ddd, *J* = 5.01, 1.95, 0.93 Hz, 1H), 7.50 (ddd, *J* = 8.35, 7.17, 1.94 Hz, 1H), 7.34 (m, 4H), 7.05 (ddd, *J* = 8.7, 5.0, 3.7 Hz, 1H), 6.89 (dd, *J* = 8.3, 1.0 Hz, 1H), 6.86 (s, 1H), 6.73 (ddd, *J* = 7.1, 5.0, 0.9 Hz, 1H); ^{13}C NMR (126 MHz, $CDCl_3$) δ 156.0, 148.4,

140.5, 137.7, 129.3, 122.8, 120.3, 115.0, 108.1. HRMS (ESI) (*m*+1)*/z* calc for $C_{11}H_{10}N_2$ 171.0843, found 171.0912.[4]

Synthesis of *N*-methyl-*N*-phenylpyridin-2-amine (L5)

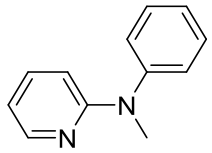

N-Methylaniline (1.76 g, 16.4 mmol, 1.0 equiv) along with 2-chloropyridine (1.55 mL, 16.4 mmol, 1.0 equiv) were added to a 100 mL round bottom flask containing a magnetic stir bar in open air. A condenser was attached, the system was purged with N_2, and the contents were heated at 160 °C for 16 hours while under nitrogen. The black solid that formed was cooled to room temperature, after which the reaction flask was opened to air. Water and acetone were added in equal amounts to the solid until it completely dissolved. The pH of the solution was adjusted to 10 by adding a saturated Na_2CO_3 solution. Brine was then added, and the crude product was extracted with ethyl acetate. Organic layers were combined, dried over Na_2SO_4, filtered, and concentrated under reduced pressure. The residue was washed with hexanes (3 x 10 mL) and dried under reduced pressure to give the product as a white crystalline solid (871 mg, 29%), m.p. = 187-190 °C. ^{1}H NMR (500 MHz, $CDCl_3$) δ 8.29 (d, *J* = 5.0 Hz, 1H), 7.64 (ddd, *J* = 9.00, 6.98, 1.80 Hz, 1H), 7.54 (t, *J* = 2.0 Hz, 2H), 7.49 – 7.42 (m, 1H), 7.26 – 7.21 (m, 2H), 6.87 (ddd, *J* = 7.11, 6.34, 1.02 Hz, 1H), 6.54 (dt, *J* = 9.19, 0.92 Hz, 1H), 3.86 (s, 3H); ^{13}C NMR (126 MHz, $CDCl_3$) δ 152.5, 142.5, 142.3, 137.7, 131.1, 129.2, 126.6, 112.9, 112.6, 42.3. HRMS (ESI) (*m*+1)*/z* calc for $C_{12}H_{12}N_2$ 185.1000, found 185.1068.[5]

Synthesis of N^1-N^1-dimethyl-N^2-(pyridin-2-yl)benzene-1,2-diamine (L6)

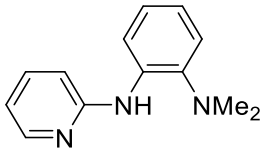

Method A: 1,2-Diaminobenzene (0.0216 g, 0.2 mmol, 2.0 equiv) along with 2-bromopyridine (0.0158 g, 0.1 mmol, 1.0 equiv) were added to a 100 mL round bottom flask containing a magnetic stir bar in open air. A condenser was attached, the system was purged with N_2, and the contents were heated at 160 °C for 16 hours while under nitrogen. The black solid that formed was cooled to room temperature, after which the reaction flask was opened to air. Water and acetone were added in equal amounts to the solid until it completely dissolved. The pH of the solution was adjusted to 10 by adding a saturated Na_2CO_3 solution. Brine was then added, and the crude product was extracted with ethyl acetate. Organic layers were combined, dried over Na_2SO_4, filtered, and concentrated under reduced pressure. The residue was purified via hexanes wash (3 x 10 mL) followed by flash chromatography using 100% ACN to give the product as tan solid (4.8 mg, 23%). ^{1}H NMR (500 MHz, $CDCl_3$) δ 8.25 (ddd, *J* = 5.1, 2.0, 0.9 Hz, 1H), 8.00 (dd, *J* = 8.1, 1.5 Hz, 1H), 7.51 (ddd, *J* = 8.4, 7.2, 2.0 Hz, 2H), 7.14 (dd, *J* = 7.8, 1.5 Hz, 1H), 7.08 (td, *J* = 7.7, 1.6 Hz, 1H), 6.95 (td, *J* = 7.6, 1.5 Hz, 1H), 6.91 (dt, *J* = 8.3, 0.9 Hz, 1H), 6.73 (ddd, *J* = 7.1, 5.0, 0.9 Hz, 1H), 2.67 (s, 6H); ^{13}C NMR (126 MHz, $CDCl_3$) δ 155.7, 148.3, 143.1, 137.4, 135.6, 124.3, 121.4, 119.7, 117.6, 114.8, 109.6, 44.4. HRMS (ESI) (*m*+1)/*z* calc for $C_{13}H_{15}N_3$ 213.1265, found 213.1755.

Method B[6]: In a 25 mL three-neck flask equipped with a stir bar, 2-aminopyridine(0.4887 g, 4 mmol, 2.0 equiv), sodium *tert*-butoxide (0.3844 g, 4 mmol, 2 equiv), (dibenzylideneacetone)dipalladium(0) (0.03 mmol, 3 mol % Pd), and BINAP (0.06

mmol, 6 mol %) were added under a stream of nitrogen. The flask was sealed and dry toluene (10 mL) was added to the flask via syringe. A water condenser was added to the flask while under nitrogen. The contents were allowed to stir for ten minutes at rt before adding 2-bromo-*N*,*N*-aniline (0.29 mL, 2 mmol, 1 equiv) to the flask. The flask stirred at 80 °C for 20 h and before being cooled to rt. The solution was then taken up in ethyl acetate, filtered, and concentrated. Crude residue was purified via hexanes wash (3 x 10 mL) followed by flash chromatography using 100% ACN to give the product as an off-white solid (123 mg, 58%).

Synthesis of N^1-(4-(trifluoromethyl)pyridin-2-yl)benzene-1,2-diamine (L12)

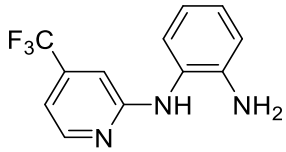

1,2-Diaminobenzene (1.0 g, 9.26 mmol, 2.0 equiv) along with 2-chloro-4-(trifluoromethyl)pyridine (0.60 mL, 4.63 mmol, 1.0 equiv) were added to a 100 mL round bottom flask containing a magnetic stir bar in open air. A condenser was attached, the system was purged with N_2, and the contents were heated at 160 °C for 16 hours while under nitrogen. The black solid that formed was cooled to room temperature, after which the reaction flask was opened to air. Water and acetone were added in equal amounts to the solid until it completely dissolved. The pH of the solution was adjusted to 10 by adding a saturated Na_2CO_3 solution. Brine was then added, and the crude product was extracted with ethyl acetate. Organic layers were combined, dried over Na_2SO_4, filtered, and concentrated under reduced pressure. The residue was purified via hexanes wash (3 x 10 mL) followed by flash chromatography using 100% EtOAc to give the product as an off-white solid (862 mg, 73%), m.p. = 135-137 °C. ^{1}H NMR (500 MHz, $CDCl_3$) δ 8.30 (d, *J* =

5.22 Hz, 1H), 7.19 (dd, *J* = 7.84, 1.41 Hz, 1H), 7.15 (td, *J* = 7.70, 1.47 Hz, 1H), 6.87 (m, 2H), 6.82 (td, *J* = 7.55, 1.42 Hz, 1H), 6.60 (d, *J* = 1.6 Hz, 1H), 6.43 (bs, 1H), 3.85 (bs, 2H); ^{13}C NMR (126 MHz, $CDCl_3$) δ 158.4, 149.5, 143.0, 140.2, 127.8, 127.1, 124.5, 121.8, 119.1, 116.4, 109.6, 102.9. HRMS (ESI) (*m*+1)/*z* calc for $C_{12}H_{10}N_3F_3$ 254.0826, found 254.0894.

Synthesis of *N*^{1}-(4-(dimethylamino)pyridin-2-yl)benzene-1,2-diamine (L13)

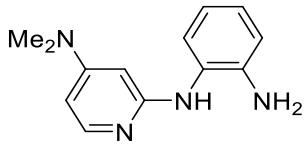

Method A: 1,2-Diaminobenzene (0.4320 g, 0.004 mol, 2.0 equiv) along with 2-bromo-4-(dimethylamino)pyridine (0.4021 g, 0.002 mol, 0.1 equiv) were added to a 100 mL round bottom flask containing a magnetic stir bar in open air. A condenser was attached, the system was purged with N_2, and the contents were heated at 160 °C for 16 hours while under nitrogen. The black solid that formed was cooled to room temperature, after which the reaction flask was opened to air. Water and acetone were added in equal amounts to the solid until it completely dissolved. The pH of the solution was adjusted to 10 by adding a saturated Na_2CO_3 solution. Brine was then added, and the crude product was extracted with ethyl acetate. Organic layers were combined, dried over Na_2SO_4, and concentrated under reduced pressure. The residue was purified via hexanes wash (3 x 10 mL) followed by flash chromatography using 100% ACN to give the product as an off-white solid (251 mg, 51%). ^{1}H NMR (500 MHz, $CDCl_3$) 7.85 (d, *J* = 6.1 Hz, 1H), 7.20 (dd, *J* = 7.8, 1.5 Hz, 1H), 7.05 (ddd, *J* = 7.9, 7.3, 1.5 Hz, 1H), 6.80 (dd, *J* = 7.9, 1.4 Hz, 1H), 6.75 (td, *J* = 7.5, 1.5 Hz, 1H), 6.07 (dd, *J* = 6.1, 2.3 Hz, 1H), 5.60 (d, *J* = 2.3 Hz, 1H), 3.89 (s, 2H), 2.88 (s, 7H); ^{13}C NMR (126 MHz, $CDCl_3$) δ 158.4, 156.2, 148.3, 142.9, 126.8, 126.6, 126.5, 118.8,

116.0, 100.0, 88.1, 39.1. HRMS (ESI) (*m*+1)/*z* calc for $C_{13}H_{16}N_4$ 229.1374, found 229.1430.

Method B: In a 25 mL three-neck flask equipped with a stir bar, 1,2-diaminobenzene (0.4320 g, 0.004 mol, 2.0 equiv), sodium *tert*-butoxide (0.3844 g, 0.004 mol, 2 equiv), (dibenzylideneacetone)dipalladium(0) (0.03 mmol, 1.5 mol % Pd), and BINAP (0.06 mmol, 3 mol %) were added under a stream of nitrogen. The flask was sealed and dry toluene (10 mL) was added to the flask via syringe. A water condenser was added to the flask while under nitrogen. The contents were allowed to stir for ten minutes at rt before adding 2-bromo-4-(dimethylamino)pyridine (0.4021 g, 0.002 mol, 0.1 equiv) to the flask. The flask stirred at 80 °C for 20 h and before being cooled to rt. The solution was then taken up in ethyl acetate, filtered, and concentrated. Crude residue was purified via hexanes wash (3 x 10 mL) followed by flash chromatography using 100% ACN to give the product as an off-white solid (301 mg, 66 %).[6]

Synthesis of IrN Complex

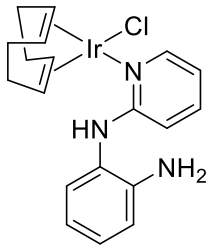

In a 10 mL Schlenk flask equipped with stir bar, $[Ir(Cl)cod]_2$ (26.8 mg, 0.04 mmol, 1 equiv) was added. **L1** (14.8 mg, 0.08 mmol, 2 equiv) and *n*-hexane (2.0 mL) were added. The flask was sealed and the mixture stirred at 70 °C for 3 hours, producing a yellow solution. The contents of the flask were cooled to room temperature, and volatiles were removed under reduced pressure, leaving a yellow solid (41.6 mg, quantitative yield). ^{1}H

NMR (500 MHz, C_6D_6) δ 8.29 (s, 1H), 7.70 (d, *J* = 5.00 Hz, 1H), 7.01 (dd, *J* = 7.75, 1.48 Hz, 1H), 6.94 (td, *J* = 7.74, 1.55 Hz, 1H), 6.58 (td, *J* = 7.58, 1.48 Hz, 1H), 6.53 (t, *J* = 5.00 Hz, 1H), 6.31 (dd, *J* = 8.03, 1.40 Hz, 1H), 5.94 (t, *J* = 5.00 Hz, 1H), 4.81 (s, 2H), 4.18 (s, 2H), 3.24 (s, 2H), 2.06 (s, 4H), 1.52 – 1.27 (m, 4H). ^{13}C NMR spectrum was not obtainable.

Single Crystal X-ray Diffraction Data for IrN Complex

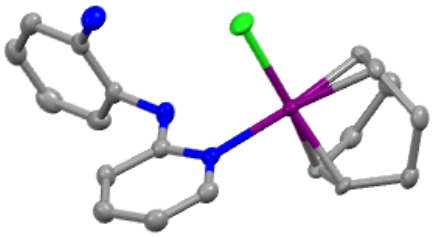

Crystals suitable for x-ray analysis were developed via solvent diffusion of DCM and pentane. IrN complex was dissolved in minimal DCM inside a test tube. The test tube was then placed in a larger vessel containing pentane and sealed in a nitrogen-filled glovebox. Golden crystals formed after 1 week. The crystal structure of IrN (with hydrogen atoms omitted for clarity) had a square planar Ir complex ligated with **L1** through the pyridyl nitrogen, bidentate cod, and chlorine atom. Ir (purple); N (blue); Cl (green); C (gray). No hydrogen-bonding between either of the primary and secondary amine protons with iridium was observed based on H–Ir distance.

Crystal data and structure refinement for AlexOIrN1prime.

Identification code	AlexOIrN1prime
Empirical formula	$C_{19}H_{23}ClIrN_3$
Formula weight	521.05
Temperature/K	173(2)
Crystal system	monoclinic

Space group	P21/c
a/Å	11.0305(2)
b/Å	7.76740(10)
c/Å	20.9114(3)
α/°	90
β/°	98.9910(10)
γ/°	90
Volume/Å^3	1769.64(5)
Z	4
ρcalcg/cm3	1.956
μ/mm-1	16.022
F(000)	1008.0
Crystal size/mm3	0.262 × 0.184 × 0.114
Radiation	CuKα (λ = 1.54178)
2Θ range for data collection/°	8.114 to 144.384
Index ranges	-13 ≤ h ≤ 13, -9 ≤ k ≤ 9, -25 ≤ l ≤ 24
Reflections collected	33562
Independent reflections	3502 [Rint = 0.0450, Rsigma = 0.0236]
Data/restraints/parameters	3502/0/218
Goodness-of-fit on F2	1.074
Final R indexes [I>=2σ (I)]	R1 = 0.0202, wR2 = 0.0480
Final R indexes [all data]	R1 = 0.0215, wR2 = 0.0487
Largest diff. peak/hole / e Å-3	0.69/-0.66

Fractional Atomic Coordinates ($\times 10^4$) and Equivalent Isotropic Displacement Parameters ($Å^2 \times 10^3$) for AlexOIrN1prime. U_{eq} is defined as 1/3 of the trace of the orthogonalised U_{IJ} tensor.

Atom	*x*	*y*	*z*	U(eq)
Ir01	2825.1(2)	1644.0(2)	6898.0(2)	18.82(6)
Cl02	1741.4(9)	-397.7(11)	6199.8(4)	38.1(2)
N003	3886(2)	2115(3)	6165.4(12)	20.6(5)
N004	1087(3)	1652(3)	4629.7(15)	30.8(6)
C005	4111(3)	2791(4)	7622.3(13)	20.9(6)
C006	3293(3)	4064(4)	7314.6(14)	22.5(6)
N007	2360(2)	3813(4)	5591.8(13)	25.1(5)
C008	1467(3)	1776(4)	7519.0(15)	22.8(6)
C009	1706(3)	6282(4)	4909.5(17)	27.0(7)
C00A	2271(3)	405(4)	7709.0(14)	23.3(6)
C00B	4998(3)	1326(4)	6211.5(15)	24.5(6)
C00C	5255(3)	2270(4)	5165.0(16)	27.2(7)
C00D	1706(3)	4524(4)	5005.7(14)	21.5(6)
C00E	1046(3)	3432(4)	4543.8(15)	21.6(6)
C00F	3308(3)	433(4)	8275.4(14)	25.2(6)
C00G	3456(3)	2998(4)	5619.2(14)	21.1(6)
C00H	4143(3)	3081(4)	5109.1(15)	25.2(6)
C00I	1478(3)	3482(4)	7883.5(16)	27.2(7)
C00J	395(3)	4178(4)	3983.3(15)	26.4(7)

C00K	5704(3)	1364(4)	5732.5(17)	27.5(7)
C00L	2242(3)	4845(4)	7594.9(15)	27.0(6)
C00M	422(3)	5920(5)	3886.4(17)	30.0(7)
C00N	1068(3)	7004(4)	4345.4(19)	31.7(7)
C00O	4069(3)	2083(4)	8299.1(14)	24.7(6)

Anisotropic Displacement Parameters ($Å^2×10^3$) for AlexOIrN1prime. The Anisotropic displacement factor exponent takes the form: $-2\pi^2[h^2a^*2U_{11}+2hka^*b^*U_{12}+\ldots]$.

Atom	U_{11}	U_{22}	U_{33}	U_{23}	U_{13}	U_{12}
Ir01	21.29(8)	19.73(8)	14.33(8)	-0.33(4)	-0.64(5)	-4.96(4)
Cl02	48.8(5)	35.4(4)	27.4(4)	-7.7(3)	-2.1(3)	-20.5(4)
N003	21.1(12)	22.9(12)	16.8(11)	-0.4(10)	-0.1(9)	-2.8(10)
N004	36.4(16)	23.5(14)	30.3(15)	0.3(11)	-1.0(12)	-0.4(11)
C005	22.2(14)	26.4(15)	12.5(13)	-3.5(11)	-2.7(10)	-6.2(12)
C006	29.4(16)	17.7(14)	19.1(14)	-2.3(11)	-0.5(12)	-8.8(12)
N007	23.1(13)	34.2(14)	17.8(12)	1.7(11)	2.4(10)	4.2(11)
C008	20.2(14)	26.3(15)	22.3(14)	3.1(12)	4.7(11)	-5.9(11)
C009	23.6(16)	26.6(15)	31.6(17)	-7.6(13)	6.4(13)	-2.7(12)
C00A	30.0(16)	20.9(14)	19.7(14)	3.1(11)	6.2(12)	-4.6(12)
C00B	25.1(16)	22.4(14)	24.1(15)	1.1(12)	-2.2(12)	1.3(12)
C00C	24.0(16)	32.1(16)	26.3(16)	1.3(13)	6.1(12)	0.7(13)
C00D	19.8(14)	27.8(15)	17.0(13)	1.0(12)	3.4(11)	4.5(11)
C00E	21.4(15)	25.3(15)	19.6(14)	-0.9(11)	7.6(12)	3.0(11)

C00F	32.3(17)	24.5(15)	18.6(14)	5.9(12)	3.1(12)	3.9(12)
C00G	22.4(14)	20.8(13)	19.1(14)	-1.4(12)	0.3(11)	-1.4(12)
C00H	25.5(16)	30.2(16)	19.9(14)	4.6(12)	3.4(12)	1.4(12)
C00I	27.2(16)	26.5(16)	27.9(16)	2.3(13)	4.6(13)	5.7(12)
C00J	21.9(15)	33.9(17)	22.5(15)	-2.4(13)	0.5(12)	4.2(13)
C00K	22.9(16)	28.6(16)	29.9(17)	0.6(13)	0.9(13)	4.1(12)
C00L	33.6(17)	20.8(14)	24.3(15)	-0.4(12)	-2.3(12)	-1.1(13)
C00M	26.0(16)	37.0(18)	27.6(16)	10.6(14)	6.0(13)	9.9(14)
C00N	31.3(17)	21.8(15)	44(2)	6.9(14)	12.6(15)	6.9(13)
C00O	26.8(16)	29.7(16)	16.3(14)	-0.2(12)	-1.1(11)	2.6(13)

Bond Lengths for AlexOIrN1prime.

Atom	Atom	Length/Å	Atom	Atom	Length/Å
Ir01	Cl02	2.3517(8)	C008	C00I	1.528(4)
Ir01	N003	2.100(2)	C009	C00D	1.381(5)
Ir01	C005	2.104(3)	C009	C00N	1.393(5)
Ir01	C006	2.102(3)	C00A	C00F	1.512(4)
Ir01	C008	2.133(3)	C00B	C00K	1.362(5)
Ir01	C00A	2.121(3)	C00C	C00H	1.368(5)
N003	C00B	1.361(4)	C00C	C00K	1.402(5)
N003	C00G	1.353(4)	C00D	C00E	1.400(4)
N004	C00E	1.394(4)	C00E	C00J	1.401(4)
C005	C006	1.423(4)	C00F	C00O	1.529(5)
C005	C00O	1.526(4)	C00G	C00H	1.403(4)

C006	C00L	1.506(5)	C00I	C00L	1.534(5)
N007	C00D	1.432(4)	C00J	C00M	1.369(5)
N007	C00G	1.358(4)	C00M	C00N	1.387(5)
C008	C00A	1.403(4)			

Bond Angles for AlexOIrN1prime.

Atom	Atom	Atom	Angle/˚	Atom	Atom	Atom	Angle/˚
N003	Ir01	Cl02	87.23(7)	C00A	C008	C00I	124.2(3)
N003	Ir01	C005	93.53(11)	C00I	C008	Ir01	113.2(2)
N003	Ir01	C006	91.01(11)	C00D	C009	C00N	120.7(3)
N003	Ir01	C008	163.78(11)	C008	C00A	Ir01	71.19(17)
N003	Ir01	C00A	157.70(11)	C008	C00A	C00F	125.3(3)
C005	Ir01	Cl02	162.26(9)	C00F	C00A	Ir01	110.0(2)
C005	Ir01	C008	90.00(12)	N003	C00B	C00K	123.4(3)
C005	Ir01	C00A	82.10(12)	C00H	C00C	C00K	119.8(3)
C006	Ir01	Cl02	158.20(9)	C009	C00D	N007	119.6(3)
C006	Ir01	C005	39.54(12)	C009	C00D	C00E	120.7(3)
C006	Ir01	C008	81.67(12)	C00E	C00D	N007	119.7(3)
C006	Ir01	C00A	99.06(12)	N004	C00E	C00D	120.6(3)
C008	Ir01	Cl02	94.20(9)	N004	C00E	C00J	121.3(3)
C00A	Ir01	Cl02	90.48(9)	C00D	C00E	C00J	118.0(3)
C00A	Ir01	C008	38.52(12)	C00A	C00F	C00O	112.4(2)
C00B	N003	Ir01	117.9(2)	N003	C00G	N007	117.7(3)
C00G	N003	Ir01	122.8(2)	N003	C00G	C00H	120.4(3)

C00G	N003	C00B	118.8(3)	N007	C00G	C00H	122.0(3)
C006	C005	Ir01	70.16(16)	C00C	C00H	C00G	119.8(3)
C006	C005	C00O	124.1(3)	C008	C00I	C00L	111.4(3)
C00O	C005	Ir01	113.6(2)	C00M	C00J	C00E	120.8(3)
C005	C006	Ir01	70.30(16)	C00B	C00K	C00C	117.8(3)
C005	C006	C00L	125.2(3)	C006	C00L	C00I	112.3(3)
C00L	C006	Ir01	111.5(2)	C00J	C00M	C00N	121.2(3)
C00G	N007	C00D	122.8(3)	C00M	C00N	C009	118.6(3)
C00A	C008	Ir01	70.29(17)	C005	C00O	C00F	111.6(2)

Torsion Angles for AlexOIrN1prime.

A	B	C	D	Angle/˚	A	B	C	D	Angle/˚
Ir01	N003	C00B	C00K	172.0(3)	C00A	C008	C00I	C00L	95.1(4)
Ir01	N003	C00G	N007	9.6(4)	C00A	C00F	C00O	C005	-31.5(4)
Ir01	N003	C00G	C00H	-171.6(2)	C00B	N003	C00G	N007	-178.3(3)
Ir01	C005	C006	C00L	103.0(3)	C00B	N003	C00G	C00H	0.5(4)
Ir01	C005	C00O	C00F	12.8(3)	C00D	N007	C00G	N003	-168.5(3)
Ir01	C006	C00L	C00I	34.7(3)	C00D	N007	C00G	C00H	12.7(5)
Ir01	C008	C00A	C00F	101.7(3)	C00D	C009	C00N	C00M	0.7(5)
Ir01	C008	C00I	C00L	13.9(3)	C00D	C00E	C00J	C00M	1.1(5)
Ir01	C00A	C00F	C00O	35.1(3)	C00E	C00J	C00M	C00N	-1.6(5)
N003	C00B	C00K	C00C	0.2(5)	C00G	N003	C00B	C00K	-0.5(5)
N003	C00G	C00H	C00C	-0.2(5)	C00G	N007	C00D	C009	-104.2(4)
N004	C00E	C00J	C00M	-176.0(3)	C00G	N007	C00D	C00E	77.5(4)

C005	C006	C00L	C00I	-45.8(4)	C00H	C00C	C00K	C00B	0.2(5)
C006	C005	C00O	C00F	94.1(4)	C00I	C008	C00A	Ir01	-105.2(3)
N007	C00D	C00E	N004	-4.3(4)	C00I	C008	C00A	C00F	-3.6(5)
N007	C00D	C00E	C00J	178.6(3)	C00J	C00M	C00N	C009	0.7(5)
N007	C00G	C00H	C00C	178.5(3)	C00K	C00C	C00H	C00G	-0.2(5)
C008	C00A	C00F	C00O	-45.6(4)	C00N	C009	C00D	N007	-179.5(3)
C008	C00I	C00L	C006	-31.5(4)	C00N	C009	C00D	C00E	-1.2(5)
C009	C00D	C00E	N004	177.4(3)	C00O	C005	C006	Ir01	-105.7(3)
C009	C00D	C00E	C00J	0.3(4)	C00O	C005	C006	C00L	-2.7(5)

Hydrogen Atom Coordinates (Å×10^4) and Isotropic Displacement Parameters (Å^2×10^3) for AlexOIrN1prime.

Atom	*x*	*y*	*z*	U(eq)
H00A	1205.33	1411.16	5045.96	37
H00B	388.16	1198.48	4444.91	37
H005	4957.55	2863.35	7509.6	25
H006	3675.29	4862.75	7028.04	27
H007	2037.63	3908.85	5949.56	30
H008	631.17	1405.54	7308.19	27
H009	2144.88	7006.89	5231.16	32
H00C	1899.67	-758.83	7611.8	28
H00D	5297.02	717.47	6598.04	29
H00E	5721.61	2321.35	4820.17	33
H00F	3849.6	-569.81	8244.19	30

H00G	2962.48	323.21	8682.93	30
H00H	3836.03	3699.32	4725.89	30
H00I	1823.75	3296.89	8344.34	33
H00J	625.72	3903.23	7862.99	33
H00K	-71.19	3466.68	3666.36	32
H00L	6475.73	794.45	5781.28	33
H00M	1705.52	5482.76	7250.94	32
H00N	2569.87	5678.36	7936.8	32
H00O	-9.06	6395.12	3497.66	36
H00P	1075.69	8212.75	4276.66	38
H00Q	3710.35	2961	8557.39	30
H00R	4915.56	1842.98	8516.26	30

Crystal structure determination of [AlexOIrN1prime]

Crystal Data for $C_{19}H_{23}ClIrN_3$ (M =521.05 g/mol): monoclinic, space group P21/c (no. 14), a = 11.0305(2) Å, b = 7.76740(10) Å, c = 20.9114(3) Å, β = 98.9910(10)°, V = 1769.64(5) Å3, Z = 4, T = 173(2) K, μ(CuKα) = 16.022 mm-1, Dcalc = 1.956 g/cm3, 33562 reflections measured (8.114° ≤ 2Θ ≤ 144.384°), 3502 unique (Rint = 0.0450, Rsigma = 0.0236) which were used in all calculations. The final R1 was 0.0202 (I > 2σ(I)) and wR2 was 0.0487 (all data).

Hydrogen-Bonding Effect Between L1 and Substrate

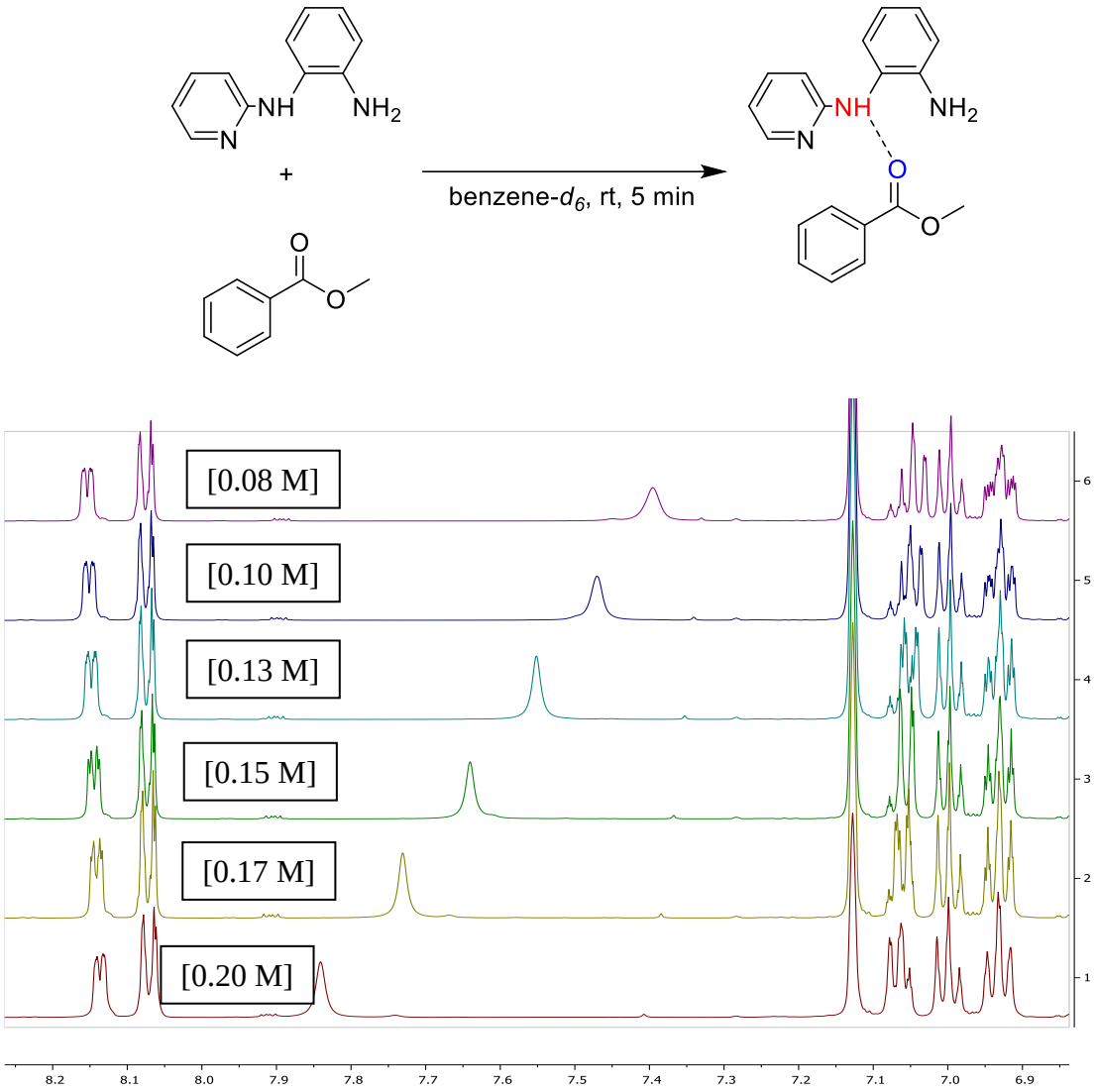

Inside a nitrogen-filled glovebox, a 0.20 M solution of **L1** (19.0 mg, 0.103 mmol) in benzene-d_6 (0.60 mL) was made inside a J-Young NMR tube. To this NMR tube, methyl benzoate (6.4 uL, 0.05 mmol) was added. The tube was sealed and ^{1}H NMR was acquired. Following the initial NMR taken, five subsequent additions of benzene-d_6 were added via syringe to this same NMR tube producing 0.20 M, 0.17 M, 0.15 M, 0.13 M, 0.10 M, and 0.08 M concentrations of the **L1** solution. The spectra above show the proton spectrum acquired from lower to higher concentrations of **L1** solution (from top to bottom). As seen

from the spectra, there is hydrogen-bonding between the secondary amine of **L1** and methyl benzoate substrate. The secondary amine of **L1** was unaffected by changes in concentration and showed little to no hydrogen-bonding with the substrate.

Hydrogen-Bonding Effect Between L4 and Substrate

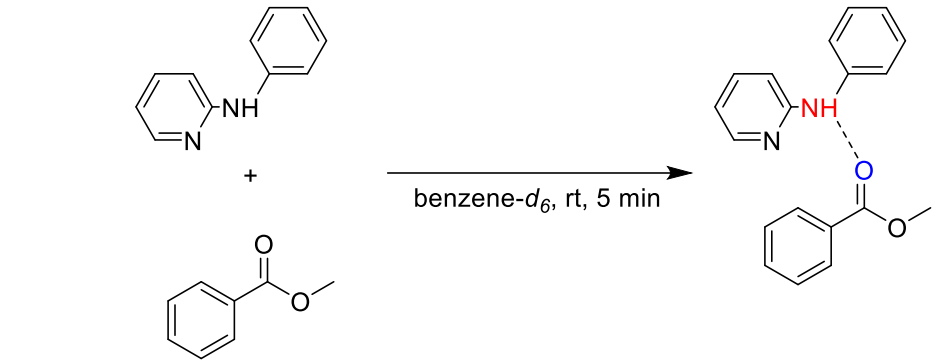

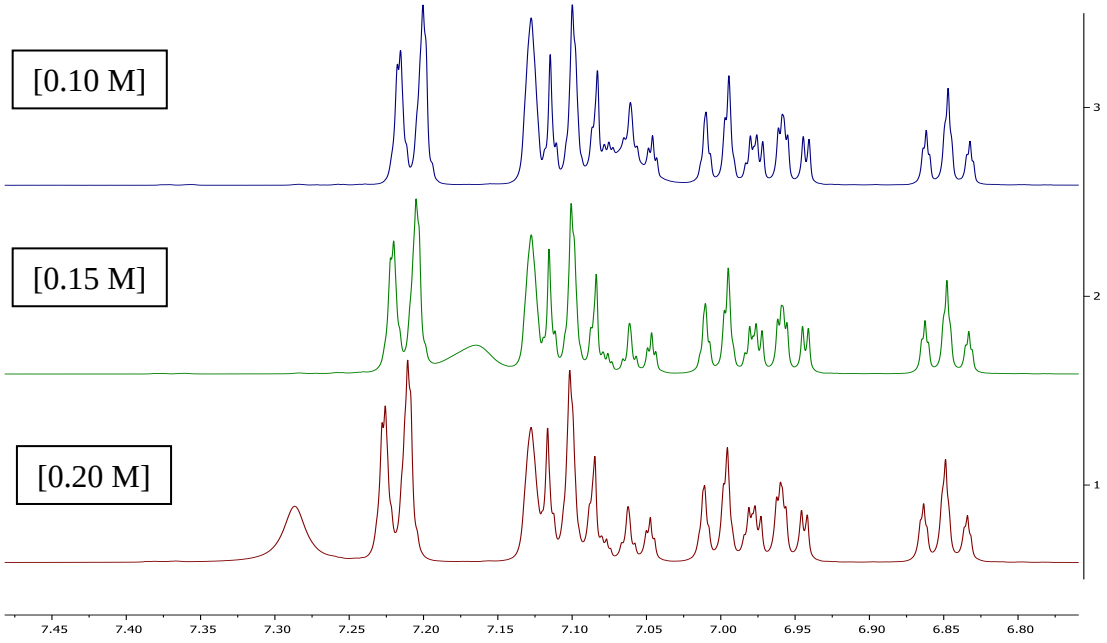

Inside a nitrogen-filled glovebox, a 0.20 M solution of **L4** (17.5 mg, 0.103 mmol) in benzene-d_6 (0.60 mL) was made inside a J-Young NMR tube. To this NMR tube, methyl benzoate (6.4 uL, 0.05 mmol) was added. The tube was sealed and ^{1}H NMR was acquired. Following the initial NMR taken, five subsequent additions of benzene-d_6 were added via syringe to this same NMR tube producing 0.10 M, 0.15 M, and 0.20 M concentrations of

the **L4** solution. The spectra above show the proton spectrum acquired from lower to higher concentrations of **L4** solution (from top to bottom). As seen from the spectra, there is hydrogen-bonding between the secondary amine of **L4** and methyl benzoate substrate.

Hydrogen-Bonding Effect Between L6 and Substrate

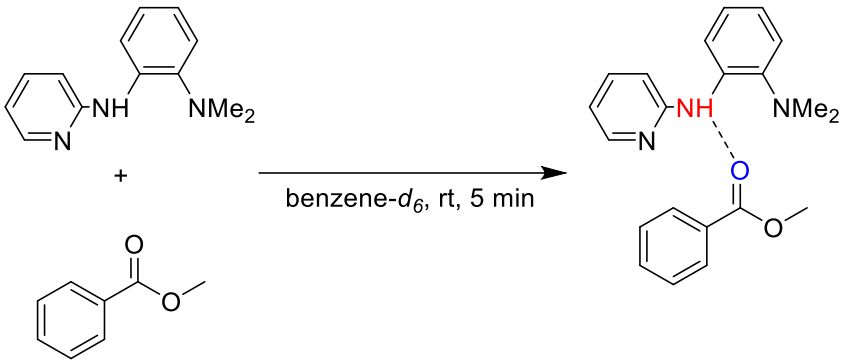

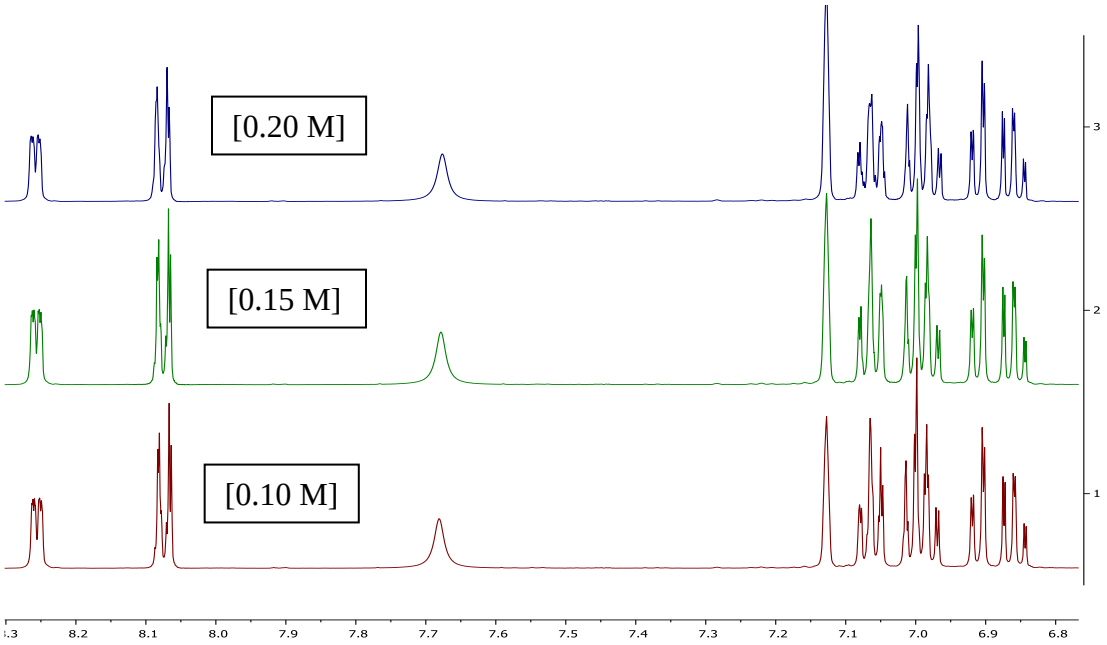

Inside a nitrogen-filled glovebox, a 0.20 M solution of **L6** (22.0 mg, 0.103 mmol) in benzene-d6 (0.60 mL) was made inside a J-Young NMR tube. To this NMR tube, methyl benzoate (6.4 uL, 0.05 mmol) was added. The tube was sealed and ^{1}H NMR was acquired. Following the initial NMR taken, five subsequent additions of benzene-d6 were added via syringe to this same NMR tube producing 0.10 M, 0.15 M, and 0.20 M concentrations of

the **L6** solution. The spectra above show the proton spectrum acquired from lower to higher concentrations of **L6** solution (from top to bottom). As seen from the spectra, there is hydrogen-bonding between the secondary amine of **L6** and methyl benzoate substrate. The secondary amine of **L6** was unaffected by changes in concentration and showed no hydrogen-bonding with the substrate.

Effects of Ligand Loading on *ortho*-Directed C–H Borylations

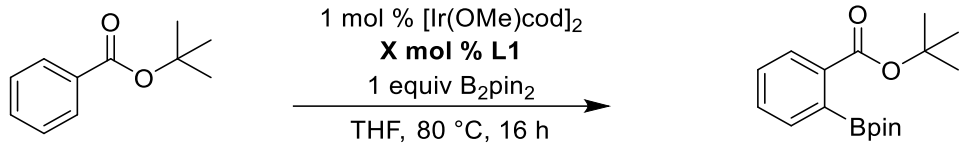

Entry	Ligand Loading (mol %)	Conversion (%)	*o*:(*m*+*p*) (%)
1	2	72	95:5
2	4	46	78:22
3	8	23	5:95

Inside a nitrogen-filled glove box, B_2pin_2 (127 mg, 0.500 mmol, 1 equiv) and 1 mol % $[Ir(OMe)cod]_2$ (3.3 mg, 0.005 mmol) were added to 2.5 mL reaction vial equipped with stir bar in THF (0.50 mL). Following these additions, either a 1, 2, 4, or 8 mol % stock solution of **L1** were added, bringing the total volume of THF solvent to 1 mL. Arene substrate (0.500 mmol, 1 equiv) was then added to the vial and sealed with a screw valve cap. The contents of the vial stirred at 80 °C for 16 hours. Conversion and selectivity were determined by proton NMR.

Effects of an Added Chloride Source on *ortho*-Directed C–H Borylations

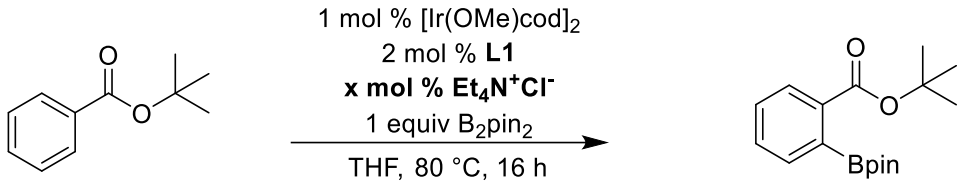

Entry	$Et_4N^+Cl^-$ (mol %)	Conversion (%)	*o*:(*m*+*p*) (%)
1	0	72	95:5
2	2	26	67:33
3	4	<1	---

Inside a nitrogen-filled glove box, B_2pin_2 (127 mg, 0.500 mmol, 1 equiv) and 1 mol % $[Ir(OMe)cod]_2$ (3.3 mg, 0.005 mmol), and 2 mol % **L1** (1.8 mg, 0.010 mmol) were added to 2.5 mL reaction vial equipped with stir bar in THF (1 mL). Following these additions, either 0, 2, or 4 mol% loading of $Et_4N^+Cl^-$ was added. Arene substrate (0.500 mmol, 1 equiv) was then added to the vial and sealed with a screw valve cap. The contents of the vial stirred at 80 °C for 16 hours. Conversion and selectivity were determined by ^1H NMR.

Effect of Precatalysts on *ortho*-Directed C–H Borylations

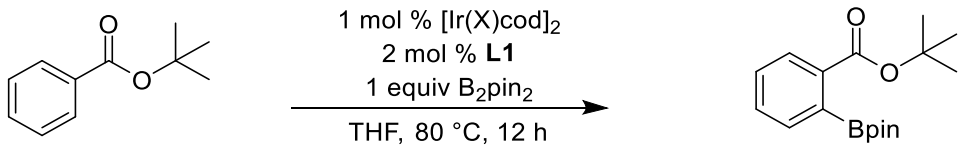

Entry	Precatalyst	Conversion (%)	*o*:(*m*+*p*) (%)
1	$[Ir(OMe)cod]_2$	54	90:10
2	$[Ir(Cl)cod]_2$	48	91:9

Inside a nitrogen-filled glove box, B_2pin_2 (0.1270 g, 0.500 mmol, 1 equiv) and 1 mol % $[Ir(OMe)cod]_2$ (3.3 mg, 0.005 mmol); (X = OMe or Cl), and 2 mol % **L1** (1.8 mg, 0.010 mmol) were added to 2.5 mL reaction vial equipped with stir bar in THF (1 mL). Arene substrate (0.500 mmol, 1 equiv) was then added to the vial and sealed with a screw

cap. The contents of the vial stirred at 80 °C for 8 hours. Conversion and selectivity were determined by ^{1}H NMR.

Evidence for N–B Bonding Between Ligands and Boron Source (HBpin)

To a J-Young NMR tube, **L1** (0.0092 g, 0.05 mmol, 1 equiv) and HBpin (0.0128 g, 0.10 mmol, 2 equiv) was added in benzene-d_6 (0.60 mL). The tube was sealed and ^{11}B NMR was taken. This same protocol was followed for **L2-L5**, using the same equivalents of ligand and boron source. The spectra for **L1-L3** had shown a broad singlet at 24.3 which is indicative of N–B bonding. HBpin as a sharp singlet (28.5 ppm) and a borates peak (21.8 ppm) were present as well. No N–B bonding appeared to be present for **L4** or **L5**. The stacked spectra below start at the top from **L1** and go sequentially to **L5** spectrum on the bottom.

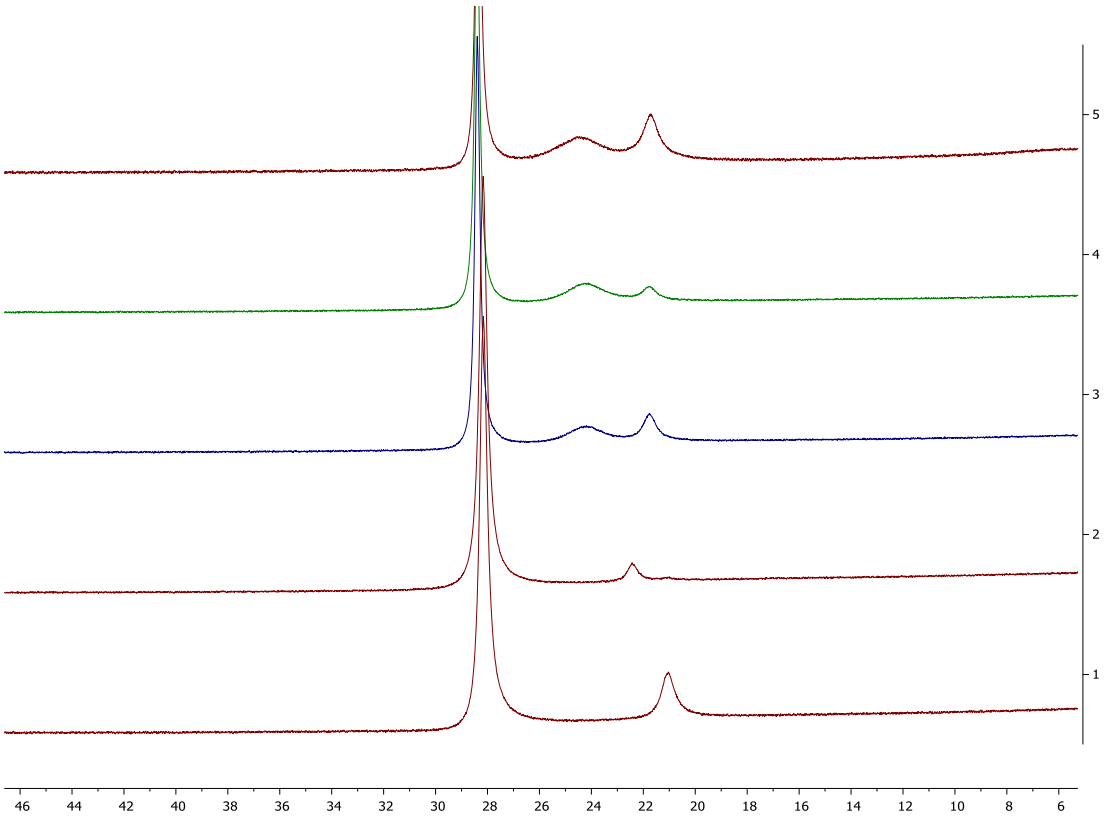

Borylation of Aromatic Substrates with L1

General conditions for *ortho*-directed C–H borylation:

Inside a nitrogen-filled glove box, B_2pin_2 (0.1270 g, 0.500 mmol, 1 equiv), 1 mol % $[Ir(OMe)cod]_2$ (3.3 mg, 0.005 mmol), and 2 mol % **L1** (1.8 mg, 0.010 mmol) were added to a 2.5 mL reaction vial equipped with stir bar and dissolved in THF (1 mL). Arene substrate (0.500 mmol, 1 equiv) was added to the vial which was then sealed with a screw valve cap. The contents of the vial were stirred at 80 °C for 16 hours. Contents were cooled to room temperature and volatiles were removed by rotary evaporation. The crude compound was then run through a small plug of silica gel with DCM as eluent. Collected material was dried under vacuum.

Methyl 2-(4,4,5,5-tetramethyl)-1,3,2-dioxaborolan-2-yl)benzoate (1a)

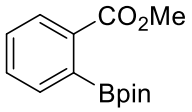

Following the general procedure, B_2pin_2 (0.1270 g, 0.50 mmol, 1 equiv), 1 mol % $[Ir(OMe)cod]_2$ (3.3 mg, 0.005 mmol), and 2 mol % **L1** (1.8 mg, 0.010 mmol) were added to a reaction vial equipped with a magnetic stir bar in THF (1 mL). Methyl benzoate (63 µL, 68 mg, 0.50 mmol) was added and the vial was sealed with a screw cap. The reaction mixture was stirred at 80 °C for 16 h. Starting material converted to 70% borylated products in the ratio of *o*:(*m*+*p*):di-*o* = 80:8:12 borylated products. Crude material was passed through a short plug of silica using DCM as eluent and dried to give **1a** as a colorless oil (0.085 g, 65%). ^{1}H NMR (500 MHz, $CDCl_3$) δ 7.95 (dt, *J* = 7.8, 0.9 Hz, 1H), 7.54 – 7.50 (ddd, *J* = 7.8, 6.2, 2.6 Hz, 1H), 7.44 – 7.40 (m, 1H), 3.92 (s, 3H), 1.43 (s, 12H). ^{11}B NMR (160 MHz, $CDCl_3$) δ 31.5 (s). Spectral data were in accordance with literature.[7]

***tert*-Butyl 2-(4,4,5,5-tetramethyl)-1,3,2-dioxaborolan-2-yl)benzoate (2a)**

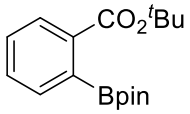

Following the general procedure, B_2pin_2 (0.1270 g, 0.50 mmol, 1 equiv), 1 mol % $[Ir(OMe)cod]_2$ (3.3 mg, 0.005 mmol), and 2 mol % **L1** (1.8 mg, 0.010 mmol) were added to a reaction vial equipped with a magnetic stir bar in THF (1 mL). *tert*-Butyl benzoate (89 µL, 89 mg, 0.50 mmol) was added and the vial was sealed with a screw cap. The reaction mixture was stirred at 80 °C for 16 h. Starting material converted to 80% borylated products in the ratio of *o*:(*m*+*p*):di-*o* = 91:9:0 borylated products. Crude material was passed through a short plug of silica using DCM as eluent and dried to give **2a** as a white solid (0.122 g, 77%). ^{1}H NMR (500 MHz, $CDCl_3$) δ 7.82 (dt, *J* = 7.7, 0.9 Hz, 1H), 7.49 – 7.45 (m, 2H), 7.39 – 7.34 (ddd, *J* = 7.7, 6.0, 2.8 Hz, 1H), 1.59 (s, 3H), 1.42 (s, 12H). ^{11}B NMR (160 MHz, $CDCl_3$) δ 31.2 (s). Spectral data were in accordance with literature.[8]

Methyl 3-methoxy-6-(4,4,5,5-tetramethyl)-1,3,2-dioxaborolan-2-yl)benzoate (3a)

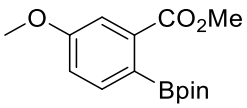

Following the general procedure, B_2pin_2 (0.1270 g, 0.50 mmol, 1 equiv), 1 mol % $[Ir(OMe)cod]_2$ (3.3 mg, 0.005 mmol), and 2 mol % **L1** (1.8 mg, 0.010 mmol) were added to a reaction vial equipped with a magnetic stir bar in THF (1 mL). Methyl 3-methoxybenzoate (73 µL, 83 mg, 0.50 mmol) was added and the vial was sealed with a screw cap. The reaction mixture was stirred at 80 °C for 16 h. Starting material converted to 63% borylated products in the ratio of (*6 position:5 position*) = 92:8 borylated products. Crude material was passed through a short plug of silica using DCM as eluent and dried to

give **3a** as a colorless oil (0.082 g, 56%). ^{1}H NMR (500 MHz, $CDCl_3$) δ 7.43 (s, 1H), 7.42 (d, *J* = 2.4 Hz, 1H), 7.03 (dd, *J* = 8.1, 2.6 Hz, 1H), 3.91 (s, 3H), 3.84 (s, 3H), 1.40 (s, 12H). ^{11}B NMR (160 MHz, $CDCl_3$) δ 30.9 (s). Spectral data were in accordance with literature.[8]

Methyl 3-dimethylamino-6-(4,4,5,5-tetramethyl)-1,3,2-dioxaborolan-2-yl)benzoate (4a)

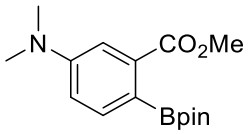

Following the general procedure, B_2pin_2 (0.1270 g, 0.50 mmol, 1 equiv), 1 mol % $[Ir(OMe)cod]_2$ (3.3 mg, 0.005 mmol), and 2 mol % **L1** (1.8 mg, 0.010 mmol) were added to a reaction vial equipped with a magnetic stir bar in THF (1 mL). Methyl 3-(dimethylamino)benzoate (81 µL, 90 mg, 0.50 mmol) was added and the vial was sealed with a screw cap. The reaction mixture was stirred at 80 °C for 16 h. Starting material converted to 54% borylated products in the ratio of (*6 position:5 position*) = 97:3 borylated products. Crude material was passed through a short plug of silica using DCM as eluent and dried to give **4a** as a colorless oil (0.082 g, 54%). ^{1}H NMR (500 MHz, $CDCl_3$) δ 7.42 (d, *J* = 8.3 Hz, 1H), 7.18 (d, *J* = 2.6 Hz, 1H), 6.79 (dd, *J* = 8.3, 2.6 Hz, 1H), 3.87 (s, 3H), 2.97 (s, 6H), 1.36 (s, 12H). ^{11}B NMR (160 MHz, $CDCl_3$) δ 31.8 (s). Spectral data were in accordance to literature.[9]

Methyl 3-trifluoromethyl-6-(4,4,5,5-tetramethyl)-1,3,2-dioxaborolan-2-yl)benzoate (5a)

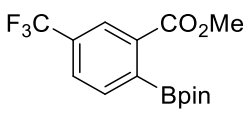

Following the general procedure, B_2pin_2 (0.1270 g, 0.50 mmol, 1 equiv), 1 mol % $[Ir(OMe)cod]_2$ (3.3 mg, 0.005 mmol), and 2 mol % **L1** (1.8 mg, 0.010 mmol) were added to a reaction vial equipped with a magnetic stir bar in THF (1 mL). Methyl 3-(trifluoromethyl)benzoate (79 µL, 102 mg, 0.50 mmol) was added and the vial was sealed with a screw cap. The reaction mixture was stirred at 80 °C for 16 h. Starting material converted to 89% borylated products in the ratio of (*6 position:5 position*) = 83:17 borylated products. Crude material was passed through a short plug of silica using DCM as eluent and dried to give **5a** as a white solid (0.135 g, 82%). ^{1}H NMR (500 MHz, $CDCl_3$) δ 8.21 (dt, *J* = 1.6, 0.8 Hz, 1H), 7.77 (dtd, *J* = 7.70, 1.42, 0.69 Hz, 1H), 7.63 (dt, *J* = 7.72, 0.75 HZ, 1H), 3.96 (s, 3H), 1.44 (s, 12H). ^{11}B NMR (160 MHz, $CDCl_3$) δ 31.3 (s). Spectral data were in accordance to literature.[8]

***N*,*N*-dimethyl-2-(4,4,5,5-tetramethyl-1,3,2-dioxaborolan-2-yl)benzamide (6a)**

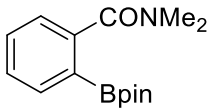

Following the general procedure, B_2pin_2 (0.1270 g, 0.50 mmol, 1 equiv), 1 mol % $[Ir(OMe)cod]_2$ (3.3 mg, 0.005 mmol), and 2 mol % **L1** (1.8 mg, 0.010 mmol) were added to a reaction vial equipped with a magnetic stir bar in THF (1 mL). *N*,*N*-Dimethylbenzamide (74 mg, 0.50 mmol) was added and the vial was sealed with a screw cap. The reaction mixture was stirred at 80 °C for 16 h. Starting material converted to 92% borylated products in the ratio of *o*:(*m*+*p*):di-*o* = 95:5:0 borylated products. Crude material was passed through a short plug of silica using DCM as eluent and dried to give **6a** as a white solid (0.113 g, 82%). ^{1}H NMR (500 MHz, $CDCl_3$) δ 7.81 (ddd, *J* = 7.5, 1.4, 0.6 Hz, 1H), 7.46 (td, *J* = 7.5, 1.4 Hz, 1H), 7.37 (td, *J* = 7.5, 1.2 Hz, 1H), 7.30 (ddd, *J* = 7.6, 1.3,

0.7 Hz, 1H), 3.06 (s, 3H), 2.89 (s, 3H), 1.30 (s, 12H). ^{11}B NMR (160 MHz, $CDCl_3$) δ 29.4 (s). Spectral data were in accordance to literature.[8]

1,1-dimethyl-2-(2-(4,4,5,5-tetramethyl-1,3,2-dioxaborolan-2-yl)benzylidene) hydrazine (7a)

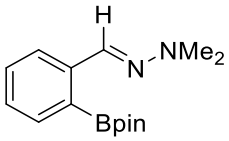

Following the general procedure, B_2pin_2 (0.1270 g, 0.50 mmol, 1 equiv), 1 mol % $[Ir(OMe)cod]_2$ (3.3 mg, 0.005 mmol), and 2 mol % **L1** (1.8 mg, 0.010 mmol) were added to a reaction vial equipped with a magnetic stir bar in THF (1 mL). 2-Benzylidene-1,1-dimethylhydrazine (75 µL, 74 mg, 0.50 mmol) was added and the vial was sealed with a screw cap. The reaction mixture was stirred at 80 °C for 16 h. Starting material converted to 92% borylated products in the ratio of *o*:(*m*+*p*):di-*o* = borylated products. Crude material was passed through a short plug of silica using DCM as eluent and dried to give **7a** as a (0.102 g, 74%). ^{1}H NMR (500 MHz, $CDCl_3$) δ 8.12 (s, 1H), 7.77 (dd, *J* = 7.5, 1.5 Hz, 1H), 7.64 (d, *J* = 7.3 Hz, 1H), 7.20 (td, *J* = 7.4, 1.4 Hz, 1H), 2.98 (s, 6H), 1.36 (s, 12H). ^{11}B NMR (160 MHz, $CDCl_3$) δ 31.1 (s). Spectral data were in accordance to literature.[10]

2-(3-chloro-5-fluorophenyl)-4,4,5,5-tetramethyl-1,3,2-dioxaborolane (8a)

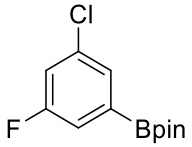

Following the general procedure, B_2pin_2 (0.1270 g, 0.50 mmol, 1 equiv), 1 mol % $[Ir(OMe)cod]_2$ (3.3 mg, 0.005 mmol), and 2 mol % **L1** (1.8 mg, 0.010 mmol) were added to a reaction vial equipped with a magnetic stir bar in THF (1 mL). 1-chloro-3-

fluorobenzene (54 µL, 65 mg, 0.50 mmol) was added and the vial was sealed with a screw cap. The reaction mixture was stirred at 80 °C for 16 h. Starting material converted to 32% borylated products in the ratio of *o*:*m* (relative to F) = 52:48 borylated products. Crude material was passed through a short plug of silica using DCM as eluent and dried to give **8a** as a clear oil (0.019 g, 29%). ^{1}H NMR (500 MHz, $CDCl_3$) δ 7.64 (dd, *J* = 8.0, 6.8 Hz, 1H), 7.14 (dd, *J* = 7.9, 1.7 Hz, 1H), 7.05 (dd, *J* = 7.9, 1.7 Hz, 1H), 1.34 (s, 12H). ^{11}B NMR (160 MHz, $CDCl_3$) δ 30.6 (s). Spectral data were in accordance to literature.[11]

Methyl5-(4,4,5,5-tetramethyl-1,3,2-dioxaborolan-2-yl)thiophene-2-carboxylate (9a)

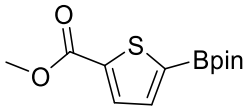

Following the general procedure, B_2pin_2 (0.1270 g, 0.50 mmol, 1 equiv), 1 mol % $[Ir(OMe)cod]_2$ (3.3 mg, 0.005 mmol), and 2 mol % **L1** (1.8 mg, 0.010 mmol) were added to a reaction vial equipped with a magnetic stir bar in THF (1 mL). 2-thiophenecarboxylate (75 µL, 71 mg, 0.50 mmol) was added and the vial was sealed with a screw cap. The reaction mixture was stirred at 80 °C for 16 h. Starting material converted to 99% borylated products in the ratio of *3*:*5* = 0:100 borylated products. Crude material was passed through a short plug of silica using DCM as eluent and dried to give **9a** as a white solid (0.121 g, 90%). ^{1}H NMR (500 MHz, $CDCl_3$) δ 7.80 (d, *J* = 3.7 Hz, 1H), 7.55 (d, *J* = 3.7 Hz, 1H), 3.88 (s, 3H), 1.34 (s, 12H). ^{11}B NMR (160 MHz, $CDCl_3$) δ 28.9 (bs). Spectral data were in accordance to literature.[12]

4.2 Chapter 3 Experimental Procedures and Details

General Information

All reactions were carried out in oven-dried glassware under an inert atmosphere. Solvents used came from wet stills and commercially available chemicals were used as received unless otherwise noted. Proton NMR spectra were recorded on a Varian 500 MHz instrument. Carbon NMR and Boron NMR were recorded on 126 MHz and 160 MHz instruments, respectively. Borylation reactions were conducted using stock solutions of the ligand and precatalyst in a nitrogen-filled glovebox.

High-resolution mass spectra (HRMS) were obtained at the Michigan State University Mass Spectrometry Service Center using electrospray ionization (ESI+ or ESI-) on quadrupole time-of-flight (Q-TOF) instruments. Melting points were measured in a capillary melting point apparatus and are uncorrected.

Synthesis of *N*^{1}-(pyridin-2-yl)benzene-1,2-diamine (L1)

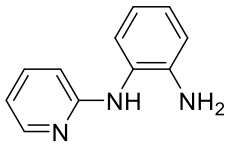

1,2-Diaminobenzene (1.0 g, 9.26 mmol, 2.0 equiv) along with 2-chloropyridine (0.42 mL, 4.63 mmol, 1.0 equiv) were added to a 100 mL round bottom flask containing a magnetic stir bar. A condenser was attached, the system was purged with N_2, and the contents were heated at 160 °C for 16 hours while under nitrogen. After the allotted time, the black solid formed was cooled to room temperature, after which the reaction flask was opened to air. Water and acetone were then added in equal amounts to the solid until it completely dissolved. The pH of the solution was adjusted to 10 by adding a saturated Na_2CO_3 solution. Brine was then added, and the crude product was extracted with ethyl

acetate. Organic layers were combined, dried over Na_2SO_4, filtered, and concentrated under reduced pressure. The residue was washed with hexanes (3 x 10 mL) on a filter frit. The solids were then transferred to a Soxhlet thimble, and a Soxhlet extraction was performed with DCM for 20 hours. Solvent was removed from the filtrate by rotary evaporation, yielding the product as a pale violet solid (528 mg, 62%). ^{1}H NMR (500 MHz, $CDCl_3$) δ 8.16 (ddd, *J* = 5.1, 1.9, 0.9 Hz, 1H), 7.44 (ddd, *J* = 8.6, 7.2, 1.9 Hz, 1H), 7.20 (dd, *J* = 7.8, 1.5 Hz, 1H), 7.10 (td, *J* = 7.7, 1.5 Hz, 1H), 6.83 (dd, *J* = 8.0, 1.4 Hz, 1H), 6.78 (td, *J* = 7.6, 1.4 Hz, 1H), 6.69 (ddd, *J* = 7.1, 5.0, 0.9 Hz, 1H), 6.42 (dt, *J* = 8.4, 0.9 Hz, 1H), 6.27 – 6.12 (s, 1H), 3.88 (s, 2H); ^{13}C NMR (126 MHz, $CDCl_3$) δ 157.7, 148.3, 143.0, 137.9, 127.2, 125.8, 118.9, 116.2, 114.4, 107.2.[1]

Synthesis 1,1'-Di(Pyridin-2-yl)-1,1',3,3'-tetrahydro-2,2'-bibenzo[d][1,3,2]diazaborole (BB)

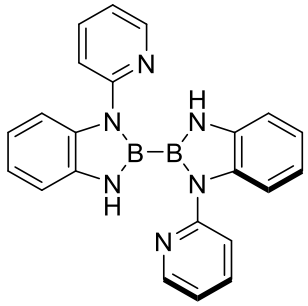

Inside a glovebox, **L1** (0.3700 g, 2 mmol, 1 equiv) was added to a 10 mL Schlenk flask equipped with a magnetic stir bar. Tetrakis(dimethylamino)diboron (0.24 mL, 1.2 mmol, 0.6 equiv) was added, along with 5 mL of toluene via syringes. The flask was then sealed and taken outside of the glovebox. Next, under a positive flow of nitrogen, a water condenser was attached to the flask. Contents were stirred and heated at 128 °C for 48 hours while under nitrogen. After 48 hours, volatiles were removed, and a light tan solid was obtained (0.390 g, 99%). ^{1}H NMR (500 MHz, $CDCl_3$) δ 8.53 (d, *J* = 4.9 Hz, 1H), 7.64

– 7.56 (m, 2H), 7.50 (bs, 1H), 7.30 (d, *J* = 8.0 Hz, 1H), 7.15 (dd, *J* = 7.5, 1.5 Hz, 1H), 7.10 (ddd, *J* = 7.3, 4.9, 1.0 Hz, 1H), 7.03 (dtd, *J* = 22.0, 7.4, 1.3 Hz, 2H); ^{13}C NMR (126 MHz, $CDCl_3$) δ 155.1, 148.7, 137.9, 137.3, 135.8, 120.6, 120.3, 119.5, 118.6, 111.5; ^{11}B NMR (160 MHz, CDCl3) δ 29.1 (bs).[1]

Synthesis of Double B,N-Bidenate Catalyst (IrBB)

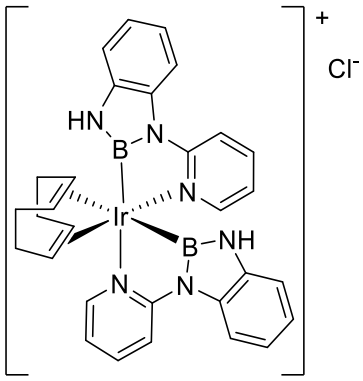

In a 10 mL Schlenk flask with stir bar, $[Ir(Cl)cod]_2$ (26.8 mg, 0.04 mmol, 1 equiv) was added. **BB** (31.2 mg, 0.08 mmol, 2 equiv) and n-hexane (1.0 mL) were added. The flask stirred at 70 °C for 12 hours, producing a yellow mixture. Once the contents cooled to room temperature, volatiles were removed via reduced pressure, leaving a light-yellow solid that was catalyst IrBB (0.023 g, 80%). ^{1}H NMR (500 MHz, DMSO-d_6) δ 9.63 (s, 1H), 9.44 (d, *J* = 5.6 Hz, 1H), 8.34 (t, *J* = 5.6 Hz, 1H), 8.15 (d, *J* = 8.4 Hz, 1H), 8.07 (d, *J* = 4.2 Hz, 1H), 8.05 (s, 1H), 7.90 (t, *J* = 8.7 Hz, 1H), 7.86 (t, *J* = 8.0 Hz, 2H), 7.75 (d, *J* = 8.1 Hz, 2H), 7.56 (t, *J* = 6.4 Hz, 1H), 7.39 (d, *J* = 7.8 Hz, 1H), 7.17 (t, *J* = 7.5 Hz, 1H), 7.07 (d, *J* = 8.7 Hz, 1H), 7.01 (t, *J* = 7.8 Hz, 1H), 6.92 – 6.82 (m, 3H), 4.84 – 4.78 (m, 1H), 4.74 – 4.68 (m, 1H), 4.29 (t, *J* = 8.6 Hz, 1H), 3.40 (t, *J* = 8.5 Hz, 1H), 3.00 (q, *J* = 11.6 Hz, 1H), 2.55 – 2.35 (m, 3H), 2.26 – 1.99 (m, 1H), 2.09 – 1.99 (m, 1H). Spectra were in accordance with the literature.[1]

Synthesis of B,N-Double Bidentate Iridium Complex (IrBB')

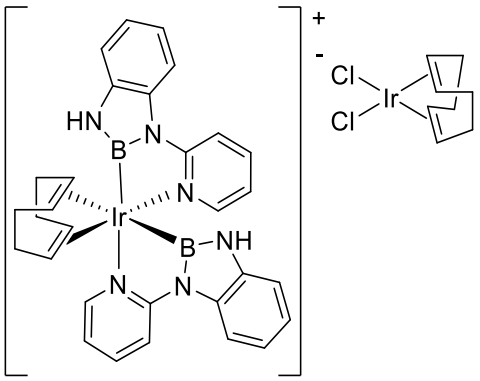

$[Ir(Cl)cod]_2$ (0.0375 g, 0.056 mmol, 1 equiv) and **BB** (0.0205 g, 0.053 mmol, 1 equiv) were added to a Schlenk flask containing a magnetic stir bar. The contents were dissolved in pentane. Contents were stirred at 36 °C for 3 hours, then the reaction was allowed to cool to room temperature before removing solvent by reduced pressure. A bright yellow solid was obtained (mass recovery 58 mg) that was catalyst (**IrBB'**). ^{1}H NMR (500 MHz, DMSO-d_6) δ 9.63 (s, 1H), 9.44 (d, *J* = 5.6 Hz, 1H), 8.34 (t, *J* = 5.6 Hz, 1H), 8.15 (d, *J* = 8.4 Hz, 1H), 8.07 (d, *J* = 4.2 Hz, 1H), 8.05 (s, 1H), 7.90 (t, *J* = 8.7 Hz, 1H), 7.86 (t, *J* = 8.0 Hz, 2H), 7.75 (d, *J* = 8.1 Hz, 2H), 7.56 (t, *J* = 6.4 Hz, 1H), 7.39 (d, *J* = 7.8 Hz, 1H), 7.17 (t, *J* = 7.5 Hz, 1H), 7.07 (d, *J* = 8.7 Hz, 1H), 7.01 (t, *J* = 7.8 Hz, 1H), 6.92 – 6.82 (m, 3H), 4.84 – 4.78 (m, 1H), 4.74 – 4.68 (m, 1H), 4.29 (t, *J* = 8.6 Hz, 1H), 3.97 (S, 4H), 3.40 (t, *J* = 8.5 Hz, 1H), 3.00 (q, *J* = 11.6 Hz, 1H), 2.55 – 2.35 (m, 3H), 2.26 – 1.99 (m, 1H), 2.16 (m, 4H), 2.09 – 1.99 (m, 1H), 1.57 (m, 4H).

Single Crystal X-ray Diffraction Data for Complex 2

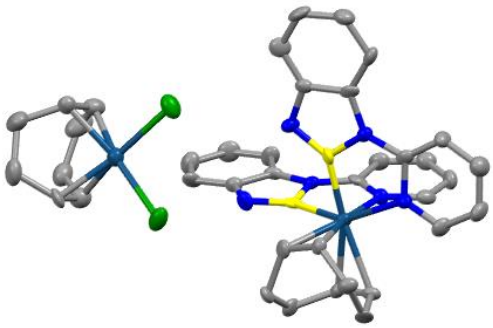

Crystals suitable for x-ray analysis were made via solvent diffusion. Complex 2 was dissolved in minimal DCM inside a 20 mL vial. The vial was then placed in a larger vessel containing pentane and sealed in a nitrogen-filled glovebox. Golden sheet-like crystals formed from this method.

Crystal data and structure refinement for IrBB'.

Identification code	IrBB'
Empirical formula	$C_{19}H_{21}BClIrN_3$
Formula weight	529.85
Temperature/K	173.15
Crystal system	monoclinic
Space group	P21/n
a/Å	16.7801(14)
b/Å	15.1131(12)
c/Å	17.9229(15)
α/°	90
β/°	112.8850(10)
γ/°	90

Volume/Å^3	4187.5(6)
Z	8
ρcalcg/cm3	1.681
μ/mm-1	6.510
F(000)	2040.0
Crystal size/mm3	0.22 × 0.16 × 0.085
Radiation	MoKα (λ = 0.71073)
2Θ range for data collection/°	3.654 to 50.844
Index ranges	-20 ≤ h ≤ 20, -18 ≤ k ≤ 18, -21 ≤ l ≤ 21
Reflections collected	33637
Independent reflections	7716 [Rint = 0.1098, Rsigma = 0.0967]
Data/restraints/parameters	7716/0/451
Goodness-of-fit on F2	0.944
Final R indexes [I>=2σ (I)]	R1 = 0.0487, wR2 = 0.1049
Final R indexes [all data]	R1 = 0.0817, wR2 = 0.1178
Largest diff. peak/hole / e Å-3	2.40/-1.35

Fractional Atomic Coordinates (×10^4) and Equivalent Isotropic Displacement Parameters (Å^2×10^3) for AlexOBN. U_{eq} is defined as 1/3 of the trace of the orthogonalized U_{IJ} tensor.

Atom	*x*	*y*	*z*	U(eq)
Ir01	7236.2(2)	4353.3(2)	7400.9(2)	23.04(12)
Ir02	7449.5(3)	1692.4(3)	4318.2(2)	29.32(13)
Cl1	6366.7(18)	1446.9(18)	4833.8(17)	41.7(7)

Cl2	8411.8(18)	2135.4(18)	5632.1(16)	44.2(7)
N007	6358(5)	5418(5)	6967(4)	20.6(17)
N008	6394(5)	5064(5)	5747(4)	22.4(18)
N009	6723(5)	4211(5)	8369(5)	26.2(19)
N00A	5822(5)	3226(5)	7472(5)	24.1(18)
N00B	6004(5)	2741(5)	6333(4)	27.1(19)
N00C	7262(5)	3969(5)	5599(5)	28.1(19)
C00D	5343(6)	2237(6)	6429(5)	23(2)
C00E	6051(6)	5606(6)	6161(6)	27(2)
C00F	6322(5)	5060(6)	4926(5)	22(2)
C00G	8116(6)	3332(6)	8082(5)	23(2)
C00H	6021(6)	3666(6)	8201(6)	24(2)
C00I	6798(6)	921(7)	3288(6)	35(3)
C00J	8495(7)	1457(7)	3987(7)	35(3)
C00K	5230(6)	2533(6)	7124(6)	28(2)
C00L	8337(6)	5349(6)	7512(6)	28(2)
C00M	5480(6)	6584(6)	7134(6)	30(2)
B00N	7040(6)	4394(6)	6199(7)	21(2)
C00O	9052(6)	3927(6)	7336(6)	27(2)
C00P	5428(6)	6258(6)	5814(6)	33(2)
C00Q	8996(6)	4642(6)	8903(5)	29(2)
C00R	8345(6)	5221(6)	8271(6)	26(2)
C00S	8939(6)	4929(6)	7185(5)	31(2)

C00T	5846(6)	5571(6)	4242(6)	34(3)
C00U	4596(6)	2129(6)	7336(6)	30(2)
C00V	4849(6)	1566(6)	5960(6)	33(3)
C00W	4249(7)	1173(6)	6157(6)	37(3)
C00X	8249(6)	3449(6)	7371(6)	27(2)
C00Y	6857(6)	4380(6)	4860(6)	24(2)
C00Z	6087(6)	5927(6)	7427(6)	28(2)
C010	5585(7)	3593(7)	8710(6)	33(2)
C011	6936(6)	4217(7)	4137(5)	33(3)
B012	6308(7)	3391(7)	6963(7)	24(2)
C013	8177(7)	2302(7)	3769(7)	43(3)
C014	6503(7)	1799(7)	3150(7)	42(3)
C015	8712(6)	3667(6)	8905(6)	30(2)
C016	5141(6)	6740(6)	6315(6)	31(2)
C017	6458(7)	4727(6)	3484(6)	37(3)
C018	5926(7)	5398(7)	3540(6)	38(3)
C019	4104(7)	1439(7)	6832(7)	38(3)
C01A	6602(7)	4586(7)	9627(6)	39(3)
C01B	7000(7)	4654(7)	9088(6)	33(2)
C01C	6724(8)	2451(8)	2635(7)	57(4)
C01D	8338(8)	698(7)	3389(7)	51(3)
C01E	5876(7)	4047(7)	9426(7)	44(3)
C01F	7683(8)	2598(8)	2890(7)	47(3)

C01G	7382(7)	540(8)	2882(8)	58(4)

Anisotropic Displacement Parameters ($Å^2×10^3$) for AlexOBN. The Anisotropic displacement factor exponent takes the form: $-2\pi^2[h^2a^*2U_{11}+2hka^*b^*U_{12}+…]$.

Atom	U_{11}	U_{22}	U_{33}	U_{23}	U_{13}	U_{12}
Ir01	20.0(2)	24.7(2)	18.7(2)	0.33(17)	1.34(15)	0.24(16)
Ir02	31.5(2)	31.3(2)	24.8(2)	1.21(18)	10.61(18)	3.82(18)
Cl1	44.5(17)	46.8(16)	41.1(16)	14.2(13)	24.8(14)	11.9(13)
Cl2	46.9(17)	47.0(16)	26.8(14)	-6.0(13)	1.3(13)	15.7(14)

N007	23(4)	20(4)	18(4)	6(3)	7(4)	5(3)
N008	18(4)	21(4)	22(4)	-2(3)	2(3)	-1(3)
N009	23(4)	23(4)	33(5)	-5(4)	11(4)	-1(4)
N00A	22(4)	26(4)	21(4)	-3(3)	4(4)	1(4)
N00B	26(5)	34(5)	18(4)	-1(4)	5(4)	-8(4)
N00C	26(5)	28(4)	30(5)	6(4)	10(4)	15(4)
C00D	16(5)	24(5)	24(5)	4(4)	3(4)	2(4)
C00E	13(5)	33(6)	36(6)	0(5)	10(4)	-8(4)
C00F	13(5)	24(5)	24(5)	7(4)	1(4)	0(4)
C00G	26(5)	19(5)	21(5)	0(4)	6(4)	5(4)
C00H	18(5)	21(5)	24(5)	1(4)	-3(4)	5(4)
C00I	27(6)	45(6)	28(6)	-3(5)	6(5)	3(5)
C00J	27(6)	44(7)	43(7)	-5(5)	25(5)	6(5)
C00K	13(5)	24(5)	33(6)	-2(4)	-5(4)	4(4)
C00L	28(6)	29(5)	22(5)	-7(4)	3(5)	-2(5)

C00M	32(6)	29(6)	34(6)	-4(5)	17(5)	6(5)
B00N	12(5)	15(5)	29(6)	10(5)	2(5)	-3(4)
C00O	21(5)	45(6)	22(5)	-2(5)	14(4)	2(5)
C00P	27(6)	33(6)	29(6)	4(5)	1(5)	5(5)
C00Q	10(5)	51(6)	14(5)	-3(5)	-7(4)	1(4)
C00R	15(5)	28(5)	28(6)	3(4)	2(4)	0(4)
C00S	36(6)	42(6)	12(5)	-6(4)	6(4)	-5(5)
C00T	29(6)	36(6)	25(6)	0(5)	-2(5)	15(5)
C00U	33(6)	31(6)	21(5)	-11(4)	4(5)	5(5)
C00V	32(6)	33(6)	27(6)	14(5)	3(5)	8(5)
C00W	33(6)	29(6)	33(6)	-10(5)	-3(5)	-10(5)
C00X	29(6)	21(5)	30(6)	-2(4)	10(5)	12(4)
C00Y	20(5)	25(5)	24(5)	1(4)	3(4)	2(4)
C00Z	22(5)	38(6)	22(5)	5(5)	6(4)	-6(5)
C010	31(6)	43(6)	30(6)	-9(5)	18(5)	-12(5)
C011	16(5)	64(7)	14(5)	0(5)	-1(4)	0(5)
B012	21(6)	28(6)	26(6)	-3(5)	13(5)	8(5)
C013	40(7)	50(7)	35(7)	0(6)	11(5)	-2(6)
C014	30(6)	54(7)	37(7)	-1(6)	9(5)	-8(5)
C015	25(6)	30(5)	26(6)	2(4)	0(5)	-1(4)
C016	30(6)	31(6)	30(6)	7(5)	7(5)	2(5)
C017	44(7)	34(6)	28(6)	1(5)	8(5)	10(5)
C018	38(7)	40(6)	26(6)	13(5)	1(5)	9(5)

C019	26(6)	40(6)	46(7)	-2(5)	13(5)	-7(5)
C01A	49(7)	47(7)	23(6)	-12(5)	15(5)	-12(6)
C01B	36(6)	39(6)	17(5)	-1(5)	2(5)	0(5)
C01C	72(9)	52(8)	37(7)	0(6)	10(7)	-20(7)
C01D	60(8)	52(7)	43(7)	-7(6)	24(6)	18(6)
C01E	40(7)	58(7)	36(7)	-5(6)	17(6)	-4(6)
C01F	60(8)	45(7)	40(7)	-7(6)	24(6)	-6(6)
C01G	46(8)	61(8)	58(9)	-29(7)	12(7)	-8(6)

Bond Lengths for AlexOBN.

Atom	Atom	Length/Å	Atom	Atom	Length/Å
Ir01	N007	2.115(7)	C00F	C00Y	1.400(12)
Ir01	N009	2.226(8)	C00G	C00X	1.388(13)
Ir01	C00G	2.156(8)	C00G	C015	1.512(12)
Ir01	C00L	2.330(9)	C00H	C010	1.378(13)
Ir01	B00N	2.050(11)	C00I	C014	1.405(14)
Ir01	C00R	2.314(9)	C00I	C01G	1.540(15)
Ir01	C00X	2.198(9)	C00J	C013	1.380(14)
Ir01	B012	2.051(11)	C00J	C01D	1.522(14)
Ir02	Cl1	2.366(3)	C00K	C00U	1.402(13)
Ir02	Cl2	2.376(3)	C00L	C00R	1.368(13)
Ir02	C00I	2.097(10)	C00L	C00S	1.493(13)
Ir02	C00J	2.090(9)	C00M	C00Z	1.372(13)
Ir02	C013	2.060(11)	C00M	C016	1.372(13)

Ir02	C014	2.085(11)	C00O	C00S	1.538(13)
N007	C00E	1.361(12)	C00O	C00X	1.551(13)
N007	C00Z	1.330(12)	C00P	C016	1.383(14)
N008	C00E	1.373(11)	C00Q	C00R	1.509(12)
N008	C00F	1.429(11)	C00Q	C015	1.550(13)
N008	B00N	1.474(12)	C00T	C018	1.344(14)
N009	C00H	1.372(11)	C00U	C019	1.416(13)
N009	C01B	1.364(12)	C00V	C00W	1.330(14)
N00A	C00H	1.386(11)	C00W	C019	1.383(14)
N00A	C00K	1.410(11)	C00Y	C011	1.375(13)
N00A	B012	1.461(13)	C010	C01E	1.367(14)
N00B	C00D	1.410(11)	C011	C017	1.370(13)
N00B	B012	1.432(12)	C013	C01F	1.535(15)
N00C	B00N	1.421(13)	C014	C01C	1.492(15)
N00C	C00Y	1.379(11)	C017	C018	1.380(13)
C00D	C00K	1.404(13)	C01A	C01B	1.375(14)
C00D	C00V	1.370(13)	C01A	C01E	1.392(14)
C00E	C00P	1.395(13)	C01C	C01F	1.509(16)
C00F	C00T	1.405(12)	C01D	C01G	1.524(16)

Bond Angles for AlexOBN.

Atom	Atom	Atom	Angle/˚	Atom	Atom	Atom	Angle/˚
N007	Ir01	N009	86.3(3)	C00Y	C00F	C00T	119.8(9)
N007	Ir01	C00G	168.1(3)	C00X	C00G	Ir01	73.1(5)

N007	Ir01	C00L	87.5(3)	C00X	C00G	C015	124.9(9)
N007	Ir01	C00R	94.6(3)	C015	C00G	Ir01	111.1(6)
N007	Ir01	C00X	154.0(3)	N009	C00H	N00A	111.5(8)
N009	Ir01	C00L	122.0(3)	N009	C00H	C010	122.3(9)
N009	Ir01	C00R	89.0(3)	C010	C00H	N00A	126.2(9)
C00G	Ir01	N009	82.9(3)	C014	C00I	Ir02	69.9(6)
C00G	Ir01	C00L	93.9(3)	C014	C00I	C01G	121.0(10)
C00G	Ir01	C00R	80.2(3)	C01G	C00I	Ir02	114.5(7)
C00G	Ir01	C00X	37.1(3)	C013	C00J	Ir02	69.4(6)
B00N	Ir01	N007	77.7(3)	C013	C00J	C01D	123.9(10)
B00N	Ir01	N009	150.4(3)	C01D	C00J	Ir02	113.2(7)
B00N	Ir01	C00G	114.3(4)	C00D	C00K	N00A	108.3(8)
B00N	Ir01	C00L	82.4(4)	C00U	C00K	N00A	133.0(9)
B00N	Ir01	C00R	116.7(4)	C00U	C00K	C00D	118.7(8)
B00N	Ir01	C00X	78.6(4)	C00R	C00L	Ir01	72.2(6)
B00N	Ir01	B012	80.3(4)	C00R	C00L	C00S	125.7(9)
C00R	Ir01	C00L	34.3(3)	C00S	C00L	Ir01	109.0(6)
C00X	Ir01	N009	119.7(3)	C016	C00M	C00Z	118.1(9)
C00X	Ir01	C00L	79.0(3)	N008	B00N	Ir01	112.4(7)
C00X	Ir01	C00R	86.7(3)	N00C	B00N	Ir01	143.1(7)
B012	Ir01	N007	94.7(4)	N00C	B00N	N008	104.3(8)
B012	Ir01	N009	76.3(4)	C00S	C00O	C00X	114.5(8)
B012	Ir01	C00G	87.7(4)	C016	C00P	C00E	118.2(9)

B012	Ir01	C00L	161.7(4)	C00R	C00Q	C015	114.8(7)
B012	Ir01	C00R	162.1(4)	C00L	C00R	Ir01	73.5(5)
B012	Ir01	C00X	91.7(4)	C00L	C00R	C00Q	123.5(9)
Cl1	Ir02	Cl2	89.21(10)	C00Q	C00R	Ir01	109.6(6)
C00I	Ir02	Cl1	92.3(3)	C00L	C00S	C00O	114.0(8)
C00I	Ir02	Cl2	161.9(3)	C018	C00T	C00F	118.6(9)
C00J	Ir02	Cl1	160.3(3)	C00K	C00U	C019	117.6(9)
C00J	Ir02	Cl2	90.4(3)	C00W	C00V	C00D	120.5(10)
C00J	Ir02	C00I	82.1(4)	C00V	C00W	C019	120.7(10)
C013	Ir02	Cl1	160.8(3)	C00G	C00X	Ir01	69.8(5)
C013	Ir02	Cl2	92.7(3)	C00G	C00X	C00O	123.2(9)
C013	Ir02	C00I	91.7(4)	C00O	C00X	Ir01	113.8(6)
C013	Ir02	C00J	38.8(4)	N00C	C00Y	C00F	110.0(8)
C013	Ir02	C014	81.2(4)	C011	C00Y	N00C	129.2(9)
C014	Ir02	Cl1	90.2(3)	C011	C00Y	C00F	120.7(9)
C014	Ir02	Cl2	158.8(3)	N007	C00Z	C00M	124.3(9)
C014	Ir02	C00I	39.3(4)	C01E	C010	C00H	119.6(10)
C014	Ir02	C00J	97.1(4)	C017	C011	C00Y	117.7(10)
C00E	N007	Ir01	118.1(6)	N00A	B012	Ir01	114.0(7)
C00Z	N007	Ir01	124.7(6)	N00B	B012	Ir01	140.6(8)
C00Z	N007	C00E	117.2(8)	N00B	B012	N00A	105.1(8)
C00E	N008	C00F	132.4(8)	C00J	C013	Ir02	71.8(6)
C00E	N008	B00N	119.0(8)	C00J	C013	C01F	123.7(10)

C00F	N008	B00N	108.2(7)	C01F	C013	Ir02	116.0(8)
C00H	N009	Ir01	116.5(6)	C00I	C014	Ir02	70.8(6)
C01B	N009	Ir01	126.6(6)	C00I	C014	C01C	125.2(11)
C01B	N009	C00H	116.7(8)	C01C	C014	Ir02	113.4(7)
C00H	N00A	C00K	130.0(8)	C00G	C015	C00Q	113.7(8)
C00H	N00A	B012	121.2(8)	C00M	C016	C00P	120.0(9)
C00K	N00A	B012	108.6(8)	C011	C017	C018	122.1(10)
C00D	N00B	B012	109.3(8)	C00T	C018	C017	121.1(9)
C00Y	N00C	B00N	110.3(7)	C00W	C019	C00U	121.0(10)
C00K	C00D	N00B	108.6(8)	C01B	C01A	C01E	118.5(10)
C00V	C00D	N00B	129.9(9)	N009	C01B	C01A	123.2(10)
C00V	C00D	C00K	121.5(9)	C014	C01C	C01F	113.8(10)
N007	C00E	N008	112.6(8)	C00J	C01D	C01G	113.0(9)
N007	C00E	C00P	122.0(9)	C010	C01E	C01A	119.6(10)
N008	C00E	C00P	125.3(9)	C01C	C01F	C013	110.7(9)
C00T	C00F	N008	133.4(8)	C01D	C01G	C00I	112.1(9)
C00Y	C00F	N008	106.8(7)				

Hydrogen Atom Coordinates (Å×10^4) and Isotropic Displacement Parameters (Å^2×10^3) for AlexOBN.

Atom	*x*	*y*	*z*	U(eq)
H00B	5862	2960	5843	33
H00C	7608	3509	5686	34
H00G	7824	2762	8102	27

H00J	6374	490	3347	42
H00K	9068	1434	4453	42
H00L	8125	5947	7280	34
H00M	5300	6921	7488	36
H00A	9550	3826	7855	33
H00D	9195	3656	6901	33
H00P	5208	6367	5247	39
H00E	9116	4901	9443	35
H00F	9543	4651	8815	35
H00R	8146	5743	8496	31
H00H	9512	5217	7434	37
H00I	8718	5038	6594	37
H00T	5474	6030	4276	41
H00U	4500	2311	7801	36
H00V	4936	1381	5491	40
H00W	3915	705	5830	44
H00X	8029	2952	6975	33
H00Z	6329	5829	7995	34
H010	5086	3229	8564	39
H011	7309	3766	4092	40
H013	8569	2771	4114	51
H014	5906	1877	3137	50
H01A	9235	3288	9110	36

H01B	8416	3609	9284	36
H016	4709	7180	6094	38
H017	6494	4615	2976	45
H018	5613	5742	3074	46
H019	3668	1154	6959	45
H01C	6819	4900	10126	47
H01D	7492	5027	9223	40
H01F	6445	3023	2653	68
H01G	6481	2240	2067	68
H01H	8592	150	3692	61
H01I	8639	826	3023	61
H01E	5583	3996	9784	53
H01J	7795	3234	2837	56
H01K	7893	2261	2528	56
H01L	7276	-103	2799	69
H01M	7229	819	2344	69

Crystal structure determination of [AlexOBN]

Crystal Data for $C_{19}H_{21}BClIrN_3$ (M =529.85 g/mol): monoclinic, space group P21/n (no. 14), a = 16.7801(14) Å, b = 15.1131(12) Å, c = 17.9229(15) Å, β = 112.8850(10)°, V = 4187.5(6) Å3, Z = 8, T = 173.15 K, μ(MoKα) = 6.510 mm-1, Dcalc = 1.681 g/cm3, 33637 reflections measured (3.654° ≤ 2Θ ≤ 50.844°), 7716 unique (Rint = 0.1098, Rsigma = 0.0967) which were used in all calculations. The final R1 was 0.0487 (I > 2σ(I)) and wR2 was 0.1178 (all data).

Synthesis of 2-(dimethyl(phenyl)silyl)-1-(pyridin-2-yl)-2,3-dihydro-1H-benzo[d][1,3,2]diazaborole (SiB)

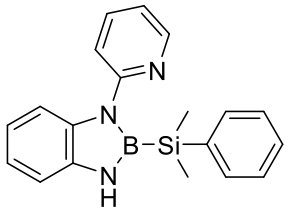

a) Synthesis of Chlorobis(diisopropylamino)borane ($BClN_2$)

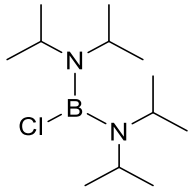

In a 250 mL three-neck flask with magnetic stir bar and condenser, diisopropylamine (9.1 g, 12.6 mL, 90 mmol, 4.5 equiv) and toluene (20 mL) were added under nitrogen flow. 1.0 M solution of boron trichloride in heptane (20 mL, 20 mmol, 1 equiv) was added dropwise over 5 minutes at room temperature via syringe. Once the boron reagent was added, the temperature was kept at 40 °C for 7 hours. After this, the reaction was cooled to room temperature and solids were filtered off and rinsed with cyclohexane (2 x 20 mL). The filtrate was concentrated, and the resulting crude oil was distilled (33 °C, 0.008 mmHg) to yield 1.82 g (37%) as a milky white oil. ^{1}H NMR (500 MHz, $CDCl_3$) δ 3.47 (septet, J = 6.8 Hz, 2H), 1.21 (d, J = 1.2 Hz, 12H); ^{11}B NMR (160 MHz, $CDCl_3$) δ 30.2 (s).[13]

b) Synthesis of Dimethylphenylsilyllithium Solution (LiSi)

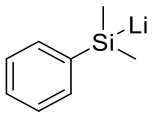

In a 50 mL Schlenk flask equipped with a magnetic stir bar, granular lithium (1.11 g, 160 mmol, 10 equiv) was added under a flow of argon gas. Under continuous argon flow, THF (17.6 mL) was added followed by chloro(dimethyl)phenylsilane (2.72 g, 16 mmol, 1 equiv) dropwise via syringe. The contents were allowed to stir for 16 hours at room temperature yielding a dark brown silyl-lithium solution (0.8 M in THF, 20 mL).[13]

c) Synthesis of Dimethylphenylsilylbis(diisopropylamino)borane Preligand (SiBP)

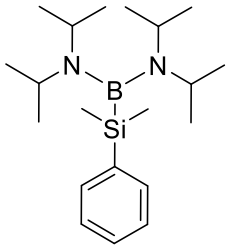

To a 50 mL Schlenk flask with stir bar, **$BClN_2$** (2.96 g, 12 mmol, 1 equiv) was added via syringe under a flow of argon gas. 12 mL of n-hexane was added to this same flask followed by **LiSi** solution (15 mL, 12 mmol, 1 equiv) dropwise. The solution was stirred at room temperature until the contents went from dark brown to a light tan color. The solid precipitate that formed was filtered off and THF (3 x 5 mL) was passed through the same filter. The oil that resulted was concentrated and distilled (115 °C, 0.007 mmHg) to give a colorless oil (2.25 g, 54%). ^{1}H NMR (500 MHz, $CDCl_3$) δ 7.54 (m, 2H), 7.30 (m, 3H), 3.82 (m, 4H), 1.18 (dd, *J* = 26.7, 6.9 Hz, 24H), 0.34 (d, *J* = 0.32 Hz, 6H); ^{11}B NMR (160 MHz, $CDCl_3$) δ 41.5 (s).[13]

d) Synthesis of (SiB)

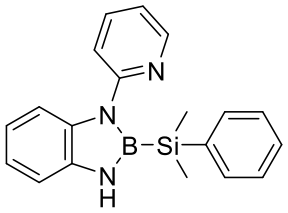

In a 10 mL Schlenk flask equipped with a magnetic stir bar, with **L1** (0.185 g, 1 mmol, 1 equiv) was added along with **SiBP** (0.450 g, 1.3 mmol, 1.3 equiv). Next, 2 mL of toluene was added to the flask. The flask was sealed and stirred at 125 °C for 36 hours. After this time, volatiles were removed, and the crude solid was washed with cyclohexane (3 x 5 mL). A pale lavender solid was obtained (0.253 g, 77%). ^{1}H NMR (500 MHz, $CDCl_3$) δ 8.52 (ddd, *J* = 4.9, 2.0, 0.9 Hz, 1H), 7.72 – 7.68 (ddd, *J* = 8.0, 7.4, 2.0 Hz, 1H), 7.54 – 7.51 (m, 2H), 7.47 (dd, *J* = 7.5, 1.6 Hz, 1H), 7.34 – 7.30 (m, 4H), 7.29 (t, *J* = 0.9Hz, 1H), 7.16 (ddd, *J* = 7.4, 4.9, 1.0 Hz, 1H), 7.13 – 7.10 (m, 1H), 7.05 – 6.98 (m, 2H) 6.93 (bs, 1H), 0.34 (s, 6H); ^{13}C NMR (126 MHz, $CDCl_3$) δ 154.8, 148.9, 140.4, 137.9, 137.1, 136.0, 134.0, 128.4, 127.8, 120.6, 119.8, 118.5, 111.5, 111.3, -2.47; ^{11}B NMR (160 MHz, $CDCl_3$) δ 31.1 (bs).[13]

Optimization Screen for ortho C—H Borylation—potassium *tert*-butoxide additive.

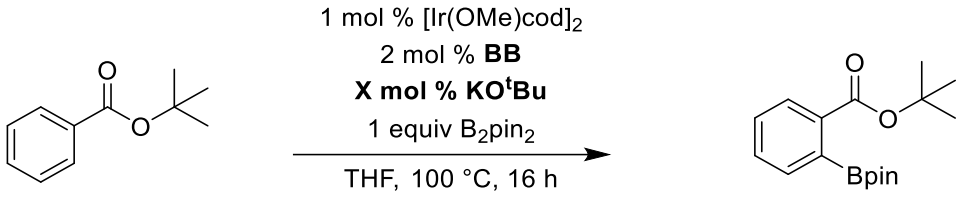

Entry	KO^{t}Bu Loading (mol %)	Conversion (%)	*o*:(*m*+*p*) (%)
1	1	80	1:99
2	2	65	1:99
3	5	16	1:99
4	10	---	---

Reactions run on 0.5 mmol scale of substrate, 0.5 mmol B_2pin_2, 1 mol % $[Ir(OMe)cod]_2$, and 2 mol % **BB** ligand in 1 mL THF. Conversions and selectivity determined by ^{1}H NMR analysis of sample.

Optimization Screen for ortho C—H Borylation

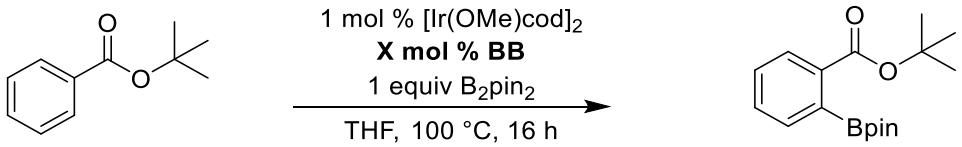

Entry	Ligand Loading (mol %)	Conversion (%)	*o*:(*m**+*p*) (%)
1	2	99	1:99
2	1	80	60:40
3	0.75	74	90:10
4	0.50	67	95:5

Reactions run on 0.5 mmol scale of substrate, 0.5 mmol B_2pin_2, 1 mol % $[Ir(OMe)cod]_2$, and x mol % **BB** ligand in 1 mL THF. Conversions and selectivity determined by ^{1}H NMR analysis of sample. Meta selectivity (m*) includes dimeta-borylated products.

Compound Characterizations for Steric- and Chelate-Directed Products

Condition A (for *ortho* borylation):

Inside a nitrogen-filled glove box, B_2pin_2 (127 mg, 0.50 mmol, 1 equiv), 1 mol % $[Ir(X)cod]_2$ (0.005 mmol) (X = OMe or Cl), 0.50 mol % **BB** ligand (0.0025 mmol), in 1 mL THF to a reaction vial equipped with a stir bar. (Hetero)Arene substrate (0.5 mmol, 1 equiv) was added and the vial was sealed with a screw cap. Heat the vial while stirring for 4-16 hours. Allow contents to cool to room temperature, remove volatiles, run compound through a small plug of silica gel with DCM as eluent. Concentrate collected material and dry under vacuum.

Condition B (for steric borylation):

Inside a nitrogen-filled glove box, B_2pin_2 (127 mg, 0.50 mmol, 1 equiv), 1 mol % $[Ir(OMe)cod]_2$ (0.005 mmol), 2 mol % **BB** ligand (0.010 mmol), in 1 mL THF to a reaction vial equipped with a stir bar. (Hetero)Arene substrate (0.5 mmol, 1 equiv) was added and the vial was sealed with a screw cap. Heat the vial while stirring for 4-8 hours. Allow contents to cool to room temperature, remove volatiles, run compound through a small plug of silica gel with DCM as eluent. Concentrate collected material and dry under vacuum.

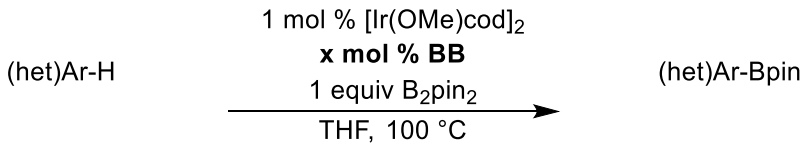

Methyl 2-(4,4,5,5-tetramethyl)-1,3,2-dioxaborolan-2-yl)benzoate (1a)

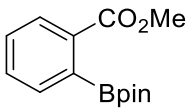

Following general procedure A, B_2pin_2 (127 mg, 0.50 mmol, 1 equiv), 1 mol % $[Ir(Cl)cod]_2$ (0.005 mmol), 0.50 mol % **BB** ligand (0.0025 mmol), and THF (1 mL) were added to a reaction vial equipped with a stir bar. Methyl benzoate (63 µL, 68 mg, 0.50 mmol) was added, and the vial was sealed with a screw cap. The reaction mixture was stirred at 100 °C for 16 h. Starting material converted to 80% (*o*:(*m*+*p*):di-*o*) = 76:6:2:14) borylated products. **1a** was obtained as a colorless oil (96 mg, 73%) after passing crude material through a short plug of silica using DCM as eluent. ^{1}H NMR (500 MHz, $CDCl_3$) δ 7.95 (dt, *J* = 7.8, 0.9 Hz, 1H), 7.54 – 7.50 (m, 2H), 7.44 – 7.40 (ddd, *J* = 7.8, 6.2, 2.6 Hz, 1H), 3.92 (s, 3H), 1.43 (s, 12H); ^{11}B NMR (160 MHz, $CDCl_3$) δ 31.6 (s). Using $[Ir(Cl)cod]_2$ as the precatalyst yielded 111 mg (85%) borylated products in the ratio (*o*:(*m*+*p*):di-*o*) = 76:6:2:14). Spectral data were in accordance to literature.[7]

Methyl 3,5-(4,4,5,5-tetramethyl)-1,3,2-dioxaborolan-2-yl)benzoate (1b)

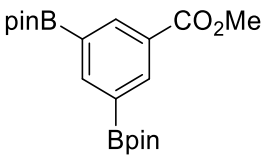

Following general procedure B, B_2pin_2 (127 mg, 0.50 mmol, 1 equiv), 1 mol % $[Ir(OMe)cod]_2$ (0.005 mmol), 2 mol % **BB** ligand (0.010 mmol), and THF (1 mL) were added to a reaction vial equipped with a stir bar. Methyl benzoate (63 µL, 68 mg, 0.50 mmol) was added, and the vial was sealed with a screw cap. The reaction mixture was stirred at 100 °C for 8 h. Starting material converted to 99% (*o*:(*m*+di-*m*):*p*) = (0:70:30)

borylated products. **1b** was obtained as a colorless oil (124 mg, 95%) after passing crude material through a short plug of silica using DCM as eluent. ^{1}H NMR (500 MHz, $CDCl_3$) δ 8.56 (d, *J* = 1.3 Hz, 1H), 8.44 (t, *J* = 1.3 Hz, 1H), 4.00 – 3.81 (m, 3H), 1.36 (d, *J* = 4.2 Hz, 12H); ^{11}B NMR (160 MHz, $CDCl_3$) δ 31.4 (s). Spectral data were in accordance to literature.[15]

***tert*-Butyl 2-(4,4,5,5-tetramethyl)-1,3,2-dioxaborolan-2-yl)benzoate (2a)**

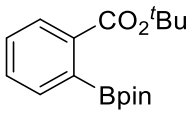

Following general procedure A, B_2pin_2 (127 mg, 0.50 mmol, 1 equiv), 1 mol % $[Ir(OMe)cod]_2$ (0.005 mmol), 0.50 mol % **BB** ligand (0.0025 mmol), and THF (1 mL) were added to a reaction vial equipped with a stir bar. *tert*-Butyl benzoate (89 µL, 89 mg, 0.50 mmol) was added, and the vial was sealed with a screw cap. The reaction mixture was stirred at 100 °C for 16 h. Starting material converted to 67% (*o*:(*m*+*p*) = 95:5) borylated products. **2a** was obtained as a white solid (99 mg, 63%) after passing crude material through a short plug of silica using DCM as eluent. ^{1}H NMR (500 MHz, $CDCl_3$) δ 7.82 (dt, *J* = 7.7, 0.9 Hz, 1H), 7.49 – 7.45 (m, 2H), 7.39 – 7.34 (ddd, *J* = 7.7, 6.0, 2.8 Hz, 1H), 1.59 (s, 3H), 1.42 (s, 12H); ^{11}B NMR (160 MHz, $CDCl_3$) δ 31.4 (s). Using $[Ir(Cl)cod]_2$ as the precatalyst yielded 126 mg (83%) borylated products in the ratio (*o*:(*m*+*p*) = 96:4). Spectral data were in accordance to literature.[8]

***tert*-Butyl 3,5-(4,4,5,5-tetramethyl)-1,3,2-dioxaborolan-2-yl)benzoate (2b)**

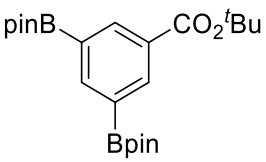

Following general procedure B, B_2pin_2 (127 mg, 0.50 mmol, 1 equiv), 1 mol % $[Ir(OMe)cod]_2$ (0.005 mmol), 2 mol % **BB** ligand (0.010 mmol), and THF (1 mL) were added to a reaction vial equipped with a stir bar. *tert*-Butyl benzoate (89 µL, 89 mg, 0.5 mmol) was added, and the vial was sealed with a screw cap. The reaction mixture was stirred at 100 °C for 8 h. Starting material converted to 90% (*o*:(*m*+di-*m*):*p* = 0:65:35) products. **2b** was obtained as a colorless oil (225 mg, 66%) after passing crude material through a short plug of silica using DCM as eluent. ^{1}H NMR (500 MHz, $CDCl_3$) δ 8.40 (dt, *J* = 2.8, 1.5 Hz, 1H), 8.31 (dt, *J* = 7.8, 1.6 Hz, 1H), (d, *J* = 1.4 Hz, 9H), 1.18 (d, *J* = 2.6 Hz, 12H); ^{11}B NMR (160 MHz, $CDCl_3$) δ 30.2 (bs). Spectral data were in accordance to literature.[13]

Methyl 3-methoxy-6-(4,4,5,5-tetramethyl)-1,3,2-dioxaborolan-2-yl)benzoate (3a)

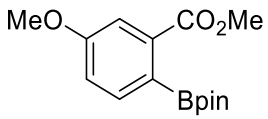

Following general procedure A, B_2pin_2 (127 mg, 0.50 mmol, 1 equiv), 1 mol % $[Ir(OMe)cod]_2$ (0.005 mmol), 0.50 mol % **BB** ligand (0.0025 mmol), and THF (1 mL) were added to a reaction vial equipped with a stir bar. Methyl 3-methoxybenzoate (73 µL, 83 mg, 0.50 mmol) was added, and the vial was sealed with a screw cap. The reaction mixture was stirred at 100 °C for 16 h. Starting material converted to 65% (*6 position:5 position* = 92:8) borylated products. **3a** was obtained as a colorless oil (83 mg, 62%) after passing crude material through a short plug of silica using DCM as eluent. ^{1}H NMR (500 MHz, $CDCl_3$) δ 7.43 (s, 1H), 7.42 (d, *J* = 2.4 Hz, 1H), 7.03 (dd, *J* = 8.1, 2.6 Hz, 1H), 3.91 (d, *J* = 1.3 Hz, 4H), 3.84 (s, 3H), 1.41 (s, 12H).; ^{11}B NMR (160 MHz, $CDCl_3$) δ 31.1 (bs). Using

[Ir(Cl)cod]$_2$ as the precatalyst yielded 104 mg (78%) borylated products in the ratio (*6 position:5 position* = 93:7). Spectral data were in accordance to literature.[8]

Methyl 3-methoxy-5-(4,4,5,5-tetramethyl)-1,3,2-dioxaborolan-2-yl)benzoate (3b)

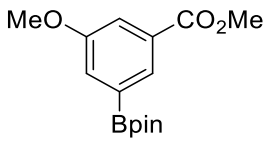

Following general procedure B, B_2pin_2 (127 mg, 0.50 mmol, 1 equiv), 1 mol % [Ir(OMe)cod]$_2$ (0.005 mmol), 2 mol % **BB** ligand (0.010 mmol), and THF (1 mL) were added to a reaction vial equipped with a stir bar. Methyl 3-methoxybenzoate (73 µL, 83 mg, 0.50 mmol) was added, and the vial was sealed with a screw cap. The reaction mixture was stirred at 100 °C for 8 h. Starting material converted to 85% (*6 position:5 position* = 5:95) borylated products. **3b** was obtained as a colorless oil (112 mg, 76%) after passing crude material through a short plug of silica using DCM as eluent. ^{1}H NMR (500 MHz, $CDCl_3$) δ 8.07 (dd, *J* = 1.5, 0.9 Hz, 1H), 7.66 (dd, *J* = 2.7, 1.5 Hz, 1H), 7.52 (dd, *J* = 2.8, 0.9 Hz, 1H), 3.92 (s, 3H), 3.87 (s, 3H), 1.36 (s, 12H); ^{11}B NMR (160 MHz, $CDCl_3$) δ 30.8 (s). Spectral data were in accordance to literature.[16]

Methyl 3-dimethylamino-6-(4,4,5,5-tetramethyl)-1,3,2-dioxaborolan-2-yl)benzoate (4a)

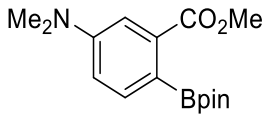

Following general procedure A, B_2pin_2 (127 mg, 0.50 mmol, 1 equiv), 1 mol % [Ir(OMe)cod]$_2$ (0.005 mmol), 0.50 mol % **BB** ligand (0.0025 mmol), and THF (1 mL) were added to a reaction vial equipped with a stir bar. Methyl 3-(dimethylamino)benzoate (81

μL, 90 mg, 0.50 mmol) was added, and the vial was sealed with a screw cap. The reaction mixture was stirred at 100 °C for 16 h. Starting material converted to 76% (*6 position:5 position* = 84:16) products. **4a** was obtained as a colorless oil (90 mg, 62%) after passing crude material through a short plug of silica using DCM as eluent. ^{1}H NMR (500 MHz, $CDCl_3$) δ 7.44 (d, *J* = 8.3 Hz, 1H), 7.20 (d, *J* = 2.6 Hz, 1H), 6.81 (dd, *J* = 8.3, 2.6 Hz, 1H), 3.89 (s, 3H), 2.99 (s, 6H), 1.38 (s, 12H). ^{11}B NMR (160 MHz, $CDCl_3$) δ 31.9 (bs). Using $[Ir(Cl)cod]_2$ as the precatalyst yielded 110 mg (72%) borylated products in the ratio (*6 position:5 position* = 91:9). Spectral data were in accordance to literature.[9]

Methyl 3-dimethylamino-5-(4,4,5,5-tetramethyl)-1,3,2-dioxaborolan-2-yl)benzoate (4b)

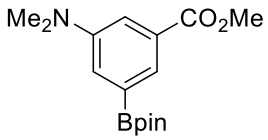

Following general procedure B, B_2pin_2 (127 mg, 0.50 mmol, 1 equiv), 1 mol % $[Ir(OMe)cod]_2$ (0.005 mmol), 2 mol % **BB** ligand (0.010 mmol), and THF (1 mL) were added to a reaction vial equipped with a stir bar. Methyl 3-(dimethylamino)benzoate (81 μL, 90 mg, 0.50 mmol) was added, and the vial was sealed with a screw valve cap. The reaction mixture was stirred at 100 °C for 8 h. Starting material converted to 94% (*6 position:5 position* = 1:99) products. 4b was obtained as a colorless oil (122 mg, 80%) after passing crude material through a short plug of silica using DCM as eluent. ^{1}H NMR (500 MHz, $CDCl_3$) δ 7.82 (dd, *J* = 1.5, 0.9 Hz, 1H), 7.49 (dd, *J* = 2.9, 1.5 Hz, 1H), 7.34 (dd, *J* = 2.9, 0.9 Hz, 1H), 3.89 (s, 3H), 3.01 (s, 6H), 1.35 (s, 12H);); ^{11}B NMR (160 MHz, $CDCl_3$) δ 31.1 (bs). Spectral data were in accordance to literature.[4]

Methyl 3-bromo-6-(4,4,5,5-tetramethyl)-1,3,2-dioxaborolan-2-yl)benzoate (5a)

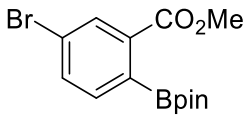

Following general procedure A, B_2pin_2 (127 mg, 0.50 mmol, 1 equiv), 1 mol % $[Ir(OMe)cod]_2$ (0.005 mmol), 0.50 mol % **BB** ligand (0.0025 mmol), and THF (1 mL) were added to a reaction vial equipped with a stir bar. Methyl 3-bromobenzoate (108 mg, 0.5 mmol) was added, and the vial was sealed with a screw cap. The reaction mixture was stirred at 100 °C for 16 h. Starting material converted to 80% (*6 position:5 position* = 80:20) products. **5a** was obtained as a colorless oil (132 mg, 77%) after passing crude material through a short plug of silica using DCM as eluent. ^{1}H NMR (500 MHz, $CDCl_3$) δ 8.09 (dd, *J* = 2.0, 0.5 Hz, 1H), 7.62 (dd, *J* = 7.9, 1.9 Hz, 1H), 7.35 (d, *J* = 7.9 Hz, 1H), 3.93 (s, 3H), 1.42 (s, 12H); ^{11}B NMR (160 MHz, $CDCl_3$) δ 30.9 (bs). Using $[Ir(Cl)cod]_2$ as the precatalyst yielded 138 mg (96%) borylated products in the ratio (*6 position:5 position* = 77:33). Spectral data were in accordance to literature.[4]

Methyl 3-bromo-5-(4,4,5,5-tetramethyl)-1,3,2-dioxaborolan-2-yl)benzoate (5b)

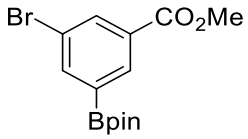

Following general procedure B, B_2pin_2 (127 mg, 0.50 mmol, 1 equiv), 1 mol % $[Ir(OMe)cod]_2$ (0.005 mmol), 2 mol % **BB** ligand (0.010 mmol), and THF (1 mL) were added to a reaction vial equipped with a stir bar. Methyl 3-bromobenzoate (108 mg, 0.50 mmol) was added, and the vial was sealed with a screw cap. The reaction mixture was stirred at 100 °C for 8 h. Starting material converted to 98% (*6 position:5 position* = 1:99)

products. **5b** was obtained as a colorless oil (159 mg, 93%) after passing crude material through a short plug of silica using DCM as eluent. ^{1}H NMR (500 MHz, $CDCl_3$) δ 8.37 (t, *J* = 1.3 Hz, 1H), 8.25 (t, *J* = 1.9 Hz, 1H), 8.10 (dd, *J* = 2.1, 1.0 Hz, 1H), 3.92 (s 3H), 1.35 (s, 12H); ^{11}B NMR (160 MHz, $CDCl_3$) δ 30.4 (bs). Spectral data were in accordance to literature.[17]

Methyl 3-trifluoromethyl-6-(4,4,5,5-tetramethyl)-1,3,2-dioxaborolan-2-yl)benzoate (6a)

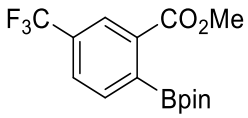

Following general procedure A, B_2pin_2 (127 mg, 0.500 mmol, 1 equiv), 1 mol % $[Ir(OMe)cod]_2$ (0.005 mmol), 0.50 mol % **BB** ligand (0.0025 mmol), and THF (1 mL) were added to a reaction vial equipped with a stir bar. Methyl 3-(trifluoromethyl)benzoate (79 µL, 102 mg, 0.50 mmol) was added and the vial was sealed with a screw cap. The reaction mixture was stirred at 100 °C for 16 h. Starting material converted to 85% (*6 position:5 position* = 73:27) products. **6a** was obtained as a colorless oil (117 mg, 72%) after passing crude material through a short plug of silica using DCM as eluent. ^{1}H NMR (500 MHz, $CDCl_3$) δ 8.21 (dt, *J* = 1.6, 0.8 Hz, 1H), 7.77 (ddt, *J* = 7.8, 1.8, 0.8 Hz, 1H), 7.63 (dt, *J* = 7.7, 0.7 Hz, 1H), 3.94 (s, 3H), 1.41 (s, 12H); ^{11}B NMR (160 MHz, $CDCl_3$) δ 29.6 (bs). Using $[Ir(Cl)cod]_2$ as the precatalyst yielded 134 mg (82%) borylated products in the ratio (*6 position:5 position* = 83:17). Spectral data were in accordance to literature.[8]

Methyl 3-trifluoromethyl-5-(4,4,5,5-tetramethyl)-1,3,2-dioxaborolan-2-yl)benzoate (6b)

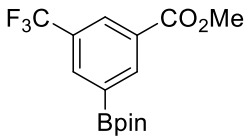

Following general procedure B, B_2pin_2 (127 mg, 0.50 mmol, 1 equiv), 1 mol % $[Ir(OMe)cod]_2$ (0.005 mmol), 0.50 mol % **BB** ligand (0.010 mmol), and THF (1 mL) were added to a reaction vial equipped with a stir bar. Methyl 3-(trifluoromethyl)benzoate (79 µL, 102 mg, 0.50 mmol) was added and the vial was sealed with a screw cap. The reaction mixture was stirred at 100 °C for 8 h. Starting material converted to 93% (*6 position:5 position* = 1:99) products. **6b** was obtained as a colorless oil (145 mg, 88%) after passing crude material through a short plug of silica using DCM as eluent. ^{1}H NMR (500 MHz, $CDCl_3$) δ 8.62 (ddd, *J* = 1.7, 1.2, 0.6 Hz, 1H), 8.37 (tq, *J* = 1.2, 0.6 Hz, 1H), 8.23 (dq, *J* = 1.9, 0.9 Hz, 1H)., 3.95 (s, 3H), 1.36 (s, 12H); ^{11}B NMR (160 MHz, $CDCl_3$) δ 30.5 (bs). Spectral data were in accordance to literature.[16]

Methyl 5-bromo-2-fluoro-3-(4,4,5,5-tetramethyl-1,3,2-dioxaborolan-2-yl)benzoate (7a)

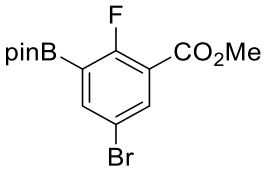

Following general procedure A, B_2pin_2 (127 mg, 0.500 mmol, 1 equiv), 1 mol % $[Ir(OMe)cod]_2$ (0.005 mmol), 0.50 mol % **BB** ligand (0.0025 mmol), and THF (1 mL) were added to a reaction vial equipped with a stir bar. Methyl 5-bromo-2-fluorobenzoate (116 mg, 0.50 mmol) was added, and the vial was sealed with a screw cap. The reaction mixture

was stirred at 100 °C for 16 h. Starting material converted to 94% (*3 position* = 100) products. **7a** was obtained as a colorless oil (116 mg, 65%) after passing crude material through a short plug of silica using DCM as eluent. ^{1}H NMR (500 MHz, $CDCl_3$) δ 8.12 (dd, *J* = 6.2, 2.7, 1H), 7.99 (dd, *J* = 4.4, 2.8 Hz, 1H), 3.91 (s, 3H), 1.35 (s, 12H); ^{11}B NMR (160 MHz, $CDCl_3$) δ 28.2 (bs). Using $[Ir(Cl)cod]_2$ as the precatalyst yielded 153 mg (90%) borylated products in the ratio (*3 position* = 1:99). Spectral data were in accordance to literature.[4]

Methyl 5-bromo-2-fluoro-3-(4,4,5,5-tetramethyl-1,3,2-dioxaborolan-2-yl)benzoate (7b)

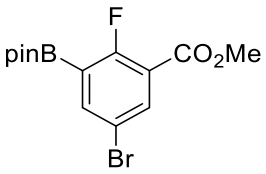

Following general procedure B, B_2pin_2 (127 mg, 0.50 mmol, 1 equiv), 1 mol % $[Ir(OMe)cod]_2$ (0.005 mmol), 2 mol % **BB** ligand (0.010 mmol), and THF (1 mL) were added to a reaction vial equipped with a stir bar. Methyl 5-bromo-2-fluorobenzoate (116 mg, 0.50 mmol) was added, and the vial was sealed with a screw cap. The reaction mixture was stirred at 100 °C for 8 h. Starting material converted to 98% (*3 position* = 1:99) products. **7b** was obtained as a colorless oil (167 mg, 93%) after passing crude material through a short plug of silica using DCM as eluent. ^{1}H NMR (500 MHz, $CDCl_3$) δ 8.12 (dd, *J* = 6.2, 2.7, 1H), 7.99 (dd, *J* = 4.4, 2.8 Hz, 1H), 3.91 (s, 3H), 1.35 (s, 12H). ^{11}B NMR (160 MHz, $CDCl_3$) δ 29.9 (bs). Spectral data were in accordance to literature.[4]

***N*,*N*-dimethyl-2-(4,4,5,5-tetramethyl-1,3,2-dioxaborolan-2-yl)benzamide (9a)**

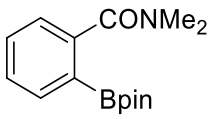

Following general procedure A, B_2pin_2 (127 mg, 0.50 mmol, 1 equiv), 1 mol % $[Ir(OMe)cod]_2$ (0.005 mmol), 0.50 mol % **BB** ligand (0.0025 mmol), and THF (1 mL) were added to a reaction vial equipped with a stir bar. *N*,*N*-Dimethylbenzamide (74 mg, 0.50 mmol) was added, and the vial was sealed with a screw cap. The reaction mixture was stirred at 100 °C for 16 h. Starting material converted to 95% (*o*:(*m*+*p*) = 95:5) products. **9a** was obtained as a colorless oil (114 mg, 83%) after passing crude material through a short plug of silica using DCM as eluent. ^{1}H NMR (500 MHz, $CDCl_3$) δ 7.81 (ddd, *J* = 7.5, 1.4, 0.6 Hz, 1H), 7.46 (td, *J* = 7.5, 1.4 Hz, 1H), 7.37 (td, *J* = 7.5, 1.2 Hz, 1H), 7.30 (ddd, *J* = 7.6, 1.3, 0.7 Hz, 1H), 3.06 (s, 3H), 2.89 (s, 3H), 1.30 (s, 12H); ^{11}B NMR (160 MHz, $CDCl_3$) δ 29.4 (bs). Using $[Ir(Cl)cod]_2$ as the precatalyst yielded 123 mg (89%) borylated products in the ratio (*o*:(*m*+*p*) = 96:4). Spectral data were in accordance to literature.[8]

***N*,*N*-dimethyl-3,5-(4,4,5,5-tetramethyl-1,3,2-dioxaborolan-2-yl)benzamide (9b)**

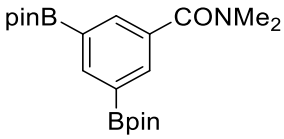

Following general procedure B, B_2pin_2 (127 mg, 0.50 mmol, 1 equiv), 1 mol % $[Ir(OMe)cod]_2$ (0.005 mmol), 2 mol % **BB** ligand (0.010 mmol), and THF (1 mL) were added to a reaction vial equipped with a stir bar. *N*,*N*-Dimethylbenzamide (75 mg, 0.50 mmol) was added, and the vial was sealed with a screw cap. The reaction mixture was stirred at 100 °C for 8 h. Starting material converted to 99% (*o*:(*m*+di-*m*):*p* = 1:77:22)

products. **9b** was obtained as a colorless oil (119 mg, 91%) after passing crude material through a short plug of silica using DCM as eluent. ^{1}H NMR (500 MHz, $CDCl_3$) δ 8.29 (d, *J* = 1.5 Hz, 1H), 7.93 (d, *J* = 1.2 Hz, 2H), 3.10 (s, 3H), 2.95 (s, 3H), 1.34 (s, 24H); ^{11}B NMR (160 MHz, $CDCl_3$) δ 29.0 (bs). Spectral data were in accordance to literature.[18]

Methyl 5-(4,4,5,5-tetramethyl-1,3,2-dioxaborolan-2-yl)thiophene-2-carboxylate (11a)

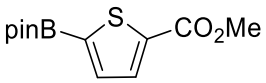

Following general procedure A, B_2pin_2 (127 mg, 0.50 mmol, 1 equiv), 1 mol % $[Ir(OMe)cod]_2$ (0.005 mmol), 0.50 mol % **BB** ligand (0.0025 mmol), and THF (1 mL) were added to a reaction vial equipped with a stir bar. Methyl thiophene-2-carboxylate (58 µL, 71 mg, 0.50 mmol) was added, and the vial was sealed with a screw cap. The reaction mixture was stirred at 100 °C for 16 h. Starting material converted to 99% (3:5 = 1:99) products. **11a** was obtained as a colorless oil (118 mg, 90%) after passing crude material through a short plug of silica using DCM as eluent. ^{1}H NMR (500 Hz, $CDCl_3$) δ 7.80 (d, *J* = 3.7 Hz, 1H), 7.55 (d, *J* = 3.7 Hz, 1H), 3.88 (s, 3H), 1.34 (s, 12H). ^{11}B NMR (160 MHz, $CDCl_3$) δ 28.9 (bs). Using $[Ir(Cl)cod]_2$ as the precatalyst yielded 124 mg (85%) borylated products in the ratio (3:5 = 1:99).[13]

Methyl 5-(4,4,5,5-tetramethyl-1,3,2-dioxaborolan-2-yl)thiophene-2-carboxylate (11b)

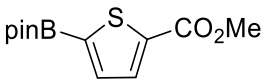

Following general procedure B, B_2pin_2 (127 mg, 0.50 mmol, 1 equiv), 1 mol % $[Ir(OMe)cod]_2$ (0.005 mmol), 2 mol % **BB** ligand (0.010 mmol), and THF (1 mL) were added to a reaction vial equipped with a stir bar. Methyl thiophene-2-carboxylate (58 µL, 71 mg, 0.50 mmol) was added, and the vial was sealed with a screw cap. The reaction

mixture was stirred at 100 °C for 4 h. Starting material converted to 99% (3-position:5-position = 1:99) products. **11b** was obtained as a colorless oil (156 mg, 99%) after passing crude material through a short plug of silica using DCM as eluent. ^{1}H NMR (500 MHz, $CDCl_3$) δ 7.82 (d, *J* = 3.8 Hz, 1H), 7.56 (d, *J* = 3.7 Hz, 1H), 3.90 (s, 3H), 1.36 (s, 12H); ^{11}B NMR (160 MHz, $CDCl_3$) δ 28.9 (bs). Spectral data were in accordance to literature.[13]

Methyl-5-methyl-3-(4,4,5,5-tetramethyl-1,3,2-dioxaborolan-2-yl)thiophene-2-carboxylate (12a)

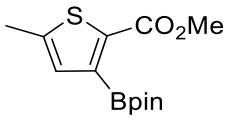

Following general procedure A, B_2pin_2 (127 mg, 0.50 mmol, 1 equiv), 1 mol % $[Ir(OMe)cod]_2$ (0.005 mmol), 0.50 mol % **BB** ligand (0.0025 mmol), and THF (1 mL) were added to a reaction vial equipped with a stir bar. Methyl 5-methylthiophene-2-carboxylate (66 μL, 78 mg, 0.50 mmol) was added, and the vial was sealed with a screw cap. The reaction mixture was stirred at 100 °C for 4 h. Starting material converted to 88% (3:4 = 80:20) products. **12a** was obtained as a colorless oil (78 mg, 55%) after passing crude material through a short plug of silica using DCM as eluent. ^{1}H NMR (500 MHz, $CDCl_3$) δ 6.86 (q, *J* = 1.0 Hz, 1H), 3.93 (s, 3H), 2.53 (d, *J* = 1.0 Hz, 3H), 1.40 (s, 12H); ^{11}B NMR (160 MHz, $CDCl_3$) δ 28.8 (bs). Using $[Ir(Cl)cod]_2$ as the precatalyst yielded 120 mg (85%) borylated products in the ratio (3:4 = 86:14).[14]

Methyl-4-methyl-3-(4,4,5,5-tetramethyl-1,3,2-dioxaborolan-2-yl)thiophene-2-carboxylate (12b)

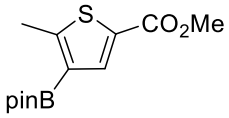

Following general procedure B, B_2pin_2 (127 mg, 0.50 mmol, 1 equiv), 1 mol % $[Ir(OMe)cod]_2$ (0.005 mmol), 2 mol % **BB** ligand (0.010 mmol), and THF (1 mL) were added to a reaction vial equipped with a stir bar. Methyl 5-methylthiophene-2-carboxylate (66 μL, 78 mg, 0.50 mmol) was added, and the vial was sealed with a screw cap. The reaction mixture was stirred at 100 °C for 4 h. Starting material converted to 99% (3:4 = 1:99) products. **12b** was obtained as a colorless oil (131 mg, 93%) after passing crude material through a short plug of silica using DCM as eluent. ^{1}H NMR (500 MHz, $CDCl_3$) δ 7.93 (s, 1H), 3.83 (s, 3H), 2.69 (s, 3H), 1.30 (s, 12H); ^{11}B NMR (160 MHz, $CDCl_3$) δ 31.0 (bs).[14]

4.3 Spectral Data

Proton NMR spectra were recorded on a Varian 500 MHz instrument. Carbon NMR and Boron NMR were recorded on 126 MHz and 160 MHz instruments, respectively. The following pages show the spectral data for chapters 2 and 3.

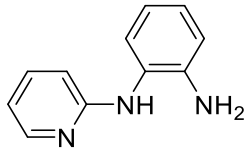

^{1}H NMR
(500 MHz, $CDCl_3$)

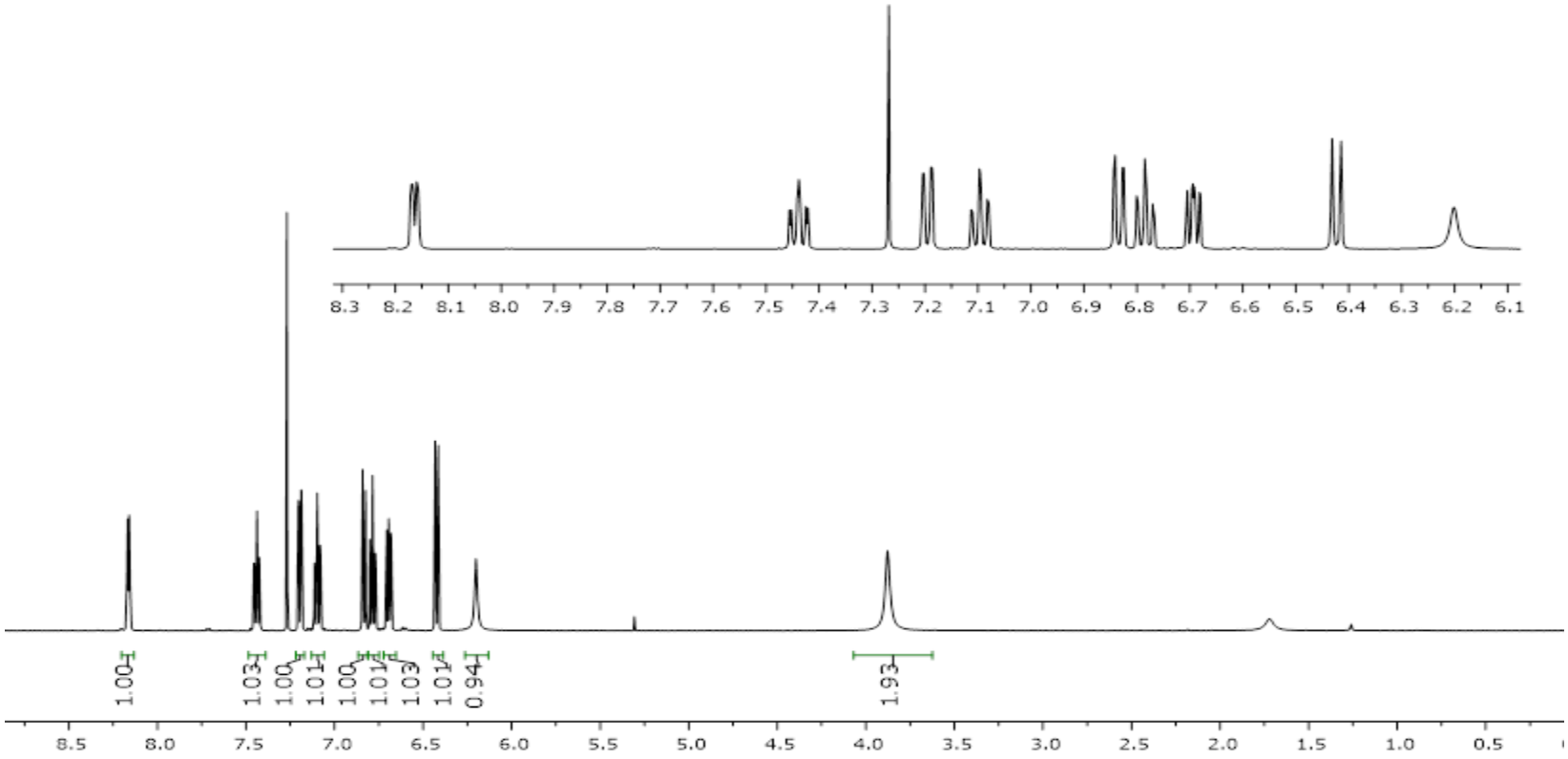

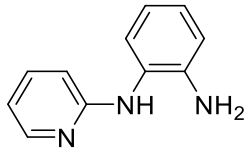

^{13}C NMR
(126 MHz, $CDCl_3$)

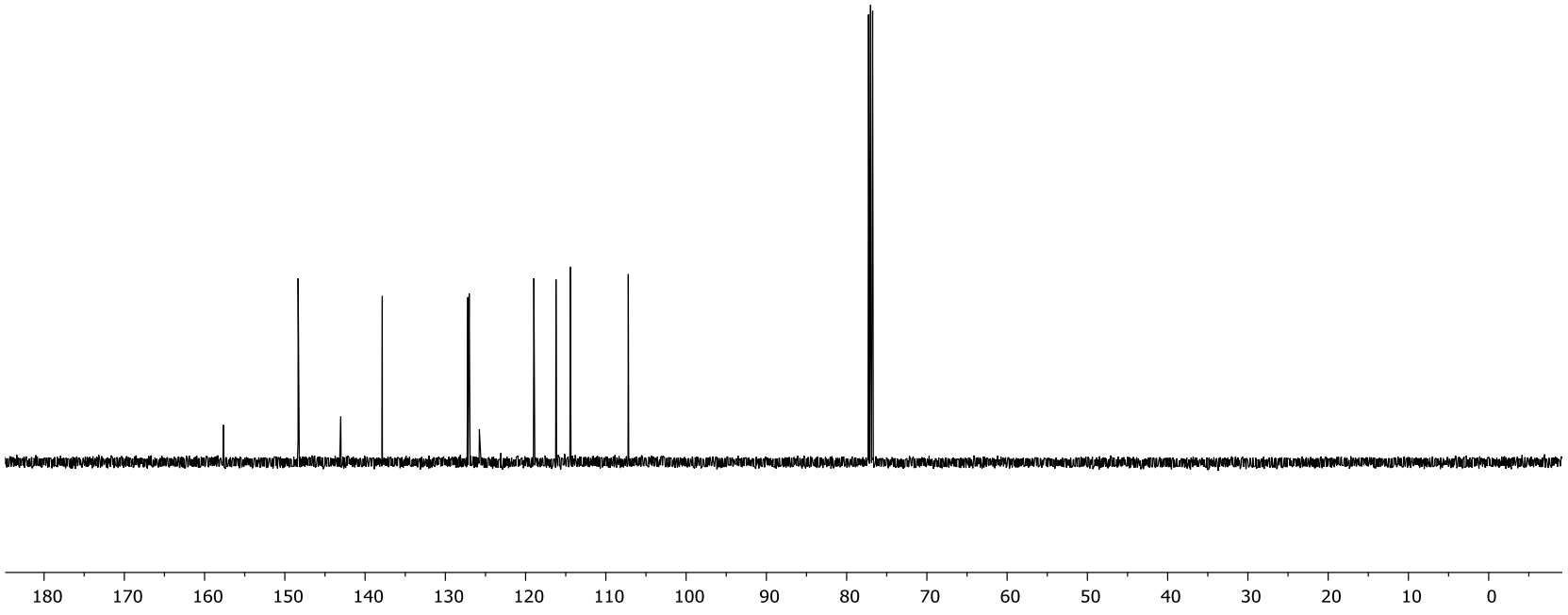

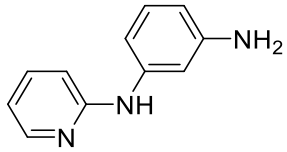

^{1}H NMR
(500 MHz, $CDCl_3$)

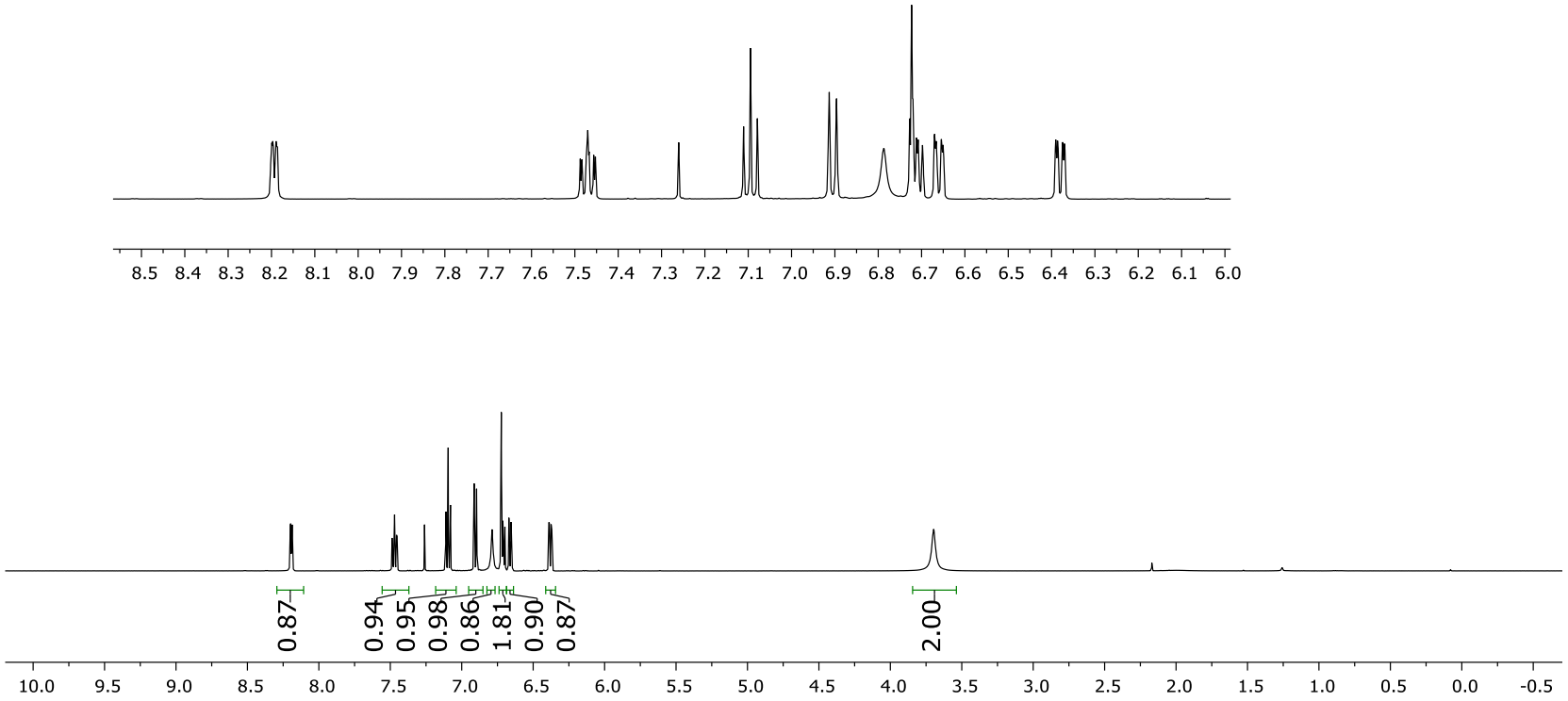

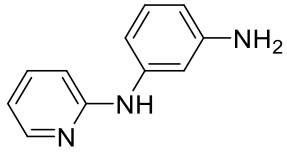

^{13}C NMR
(126 MHz, $CDCl_3$)

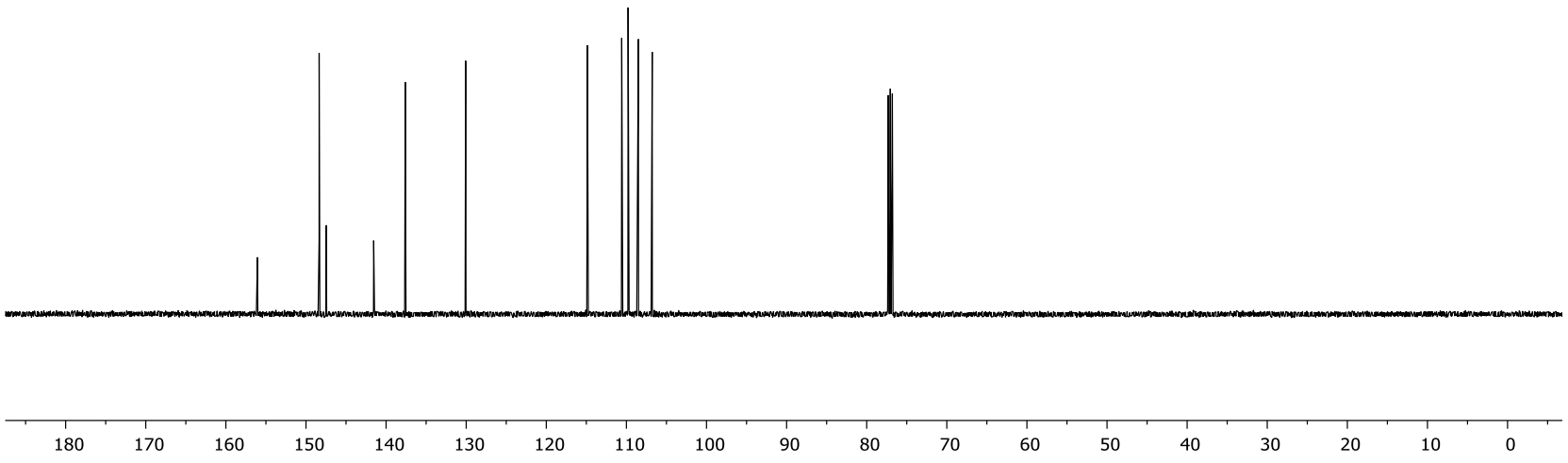

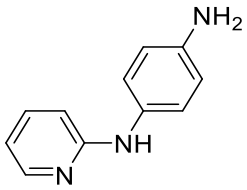

^{1}H NMR
(500 MHz, $CDCl_3$)

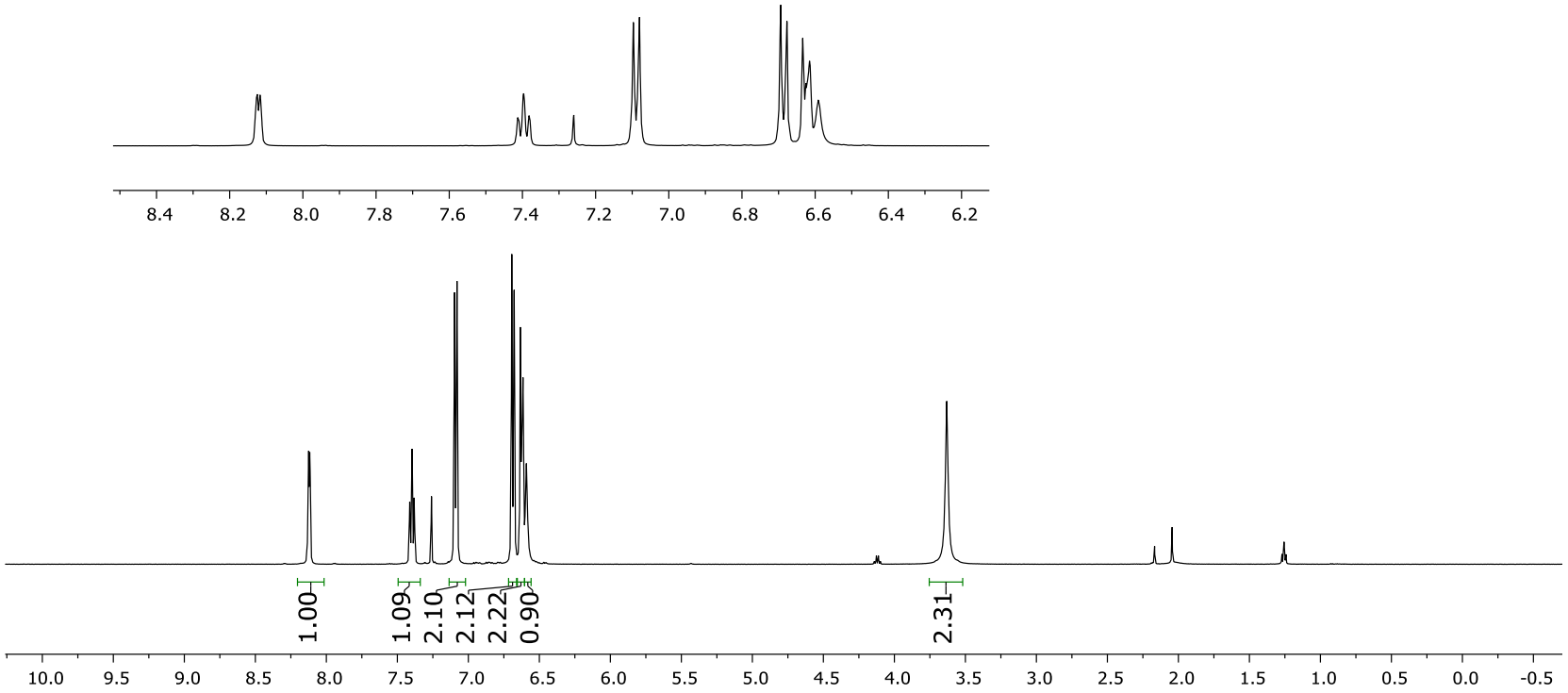

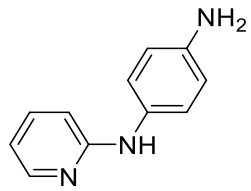

^{13}C NMR
(126 MHz, $CDCl_3$)

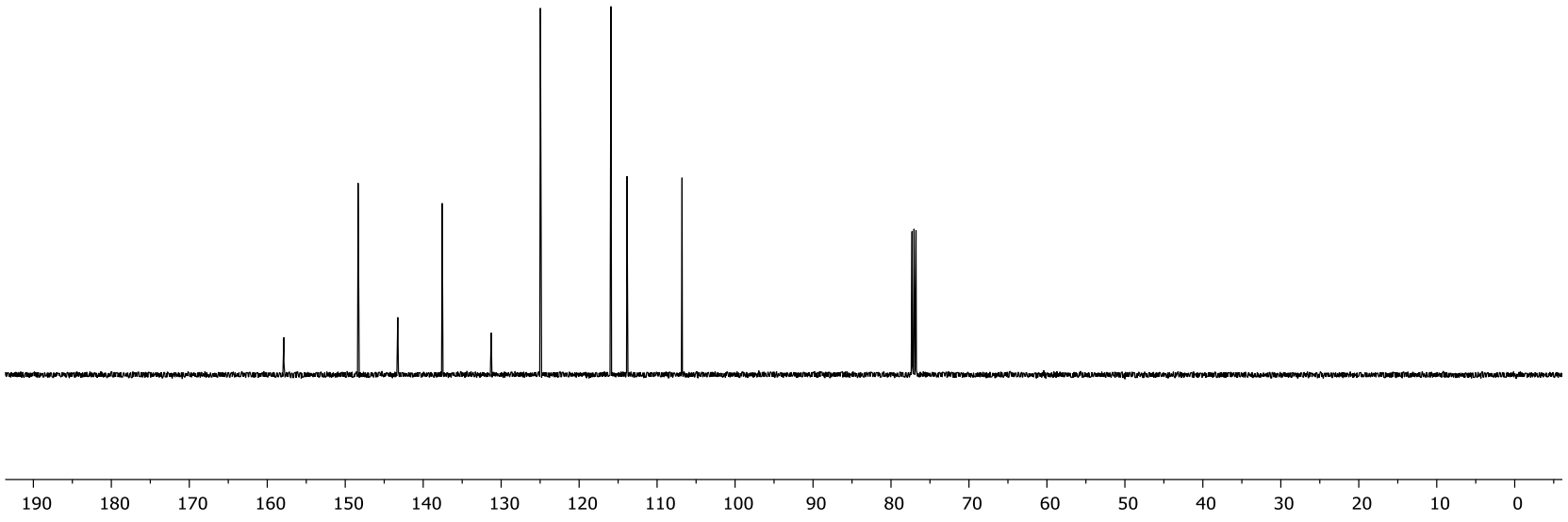

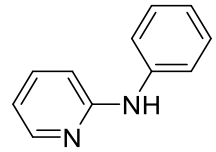

^{1}H NMR
(500 MHz, $CDCl_3$)

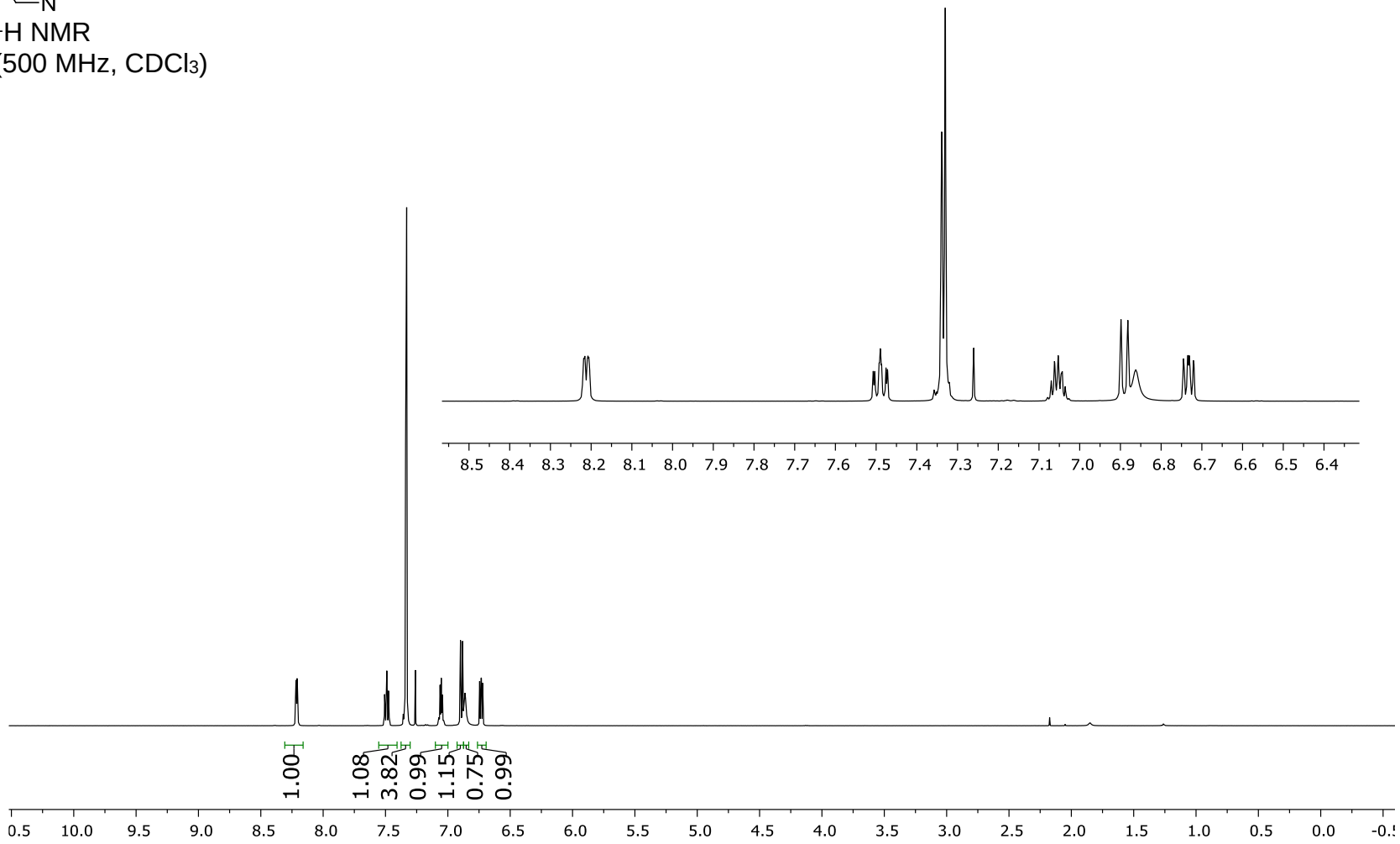

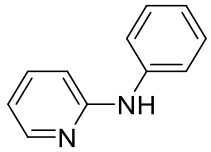

^{13}C NMR
(126 MHz, $CDCl_3$)

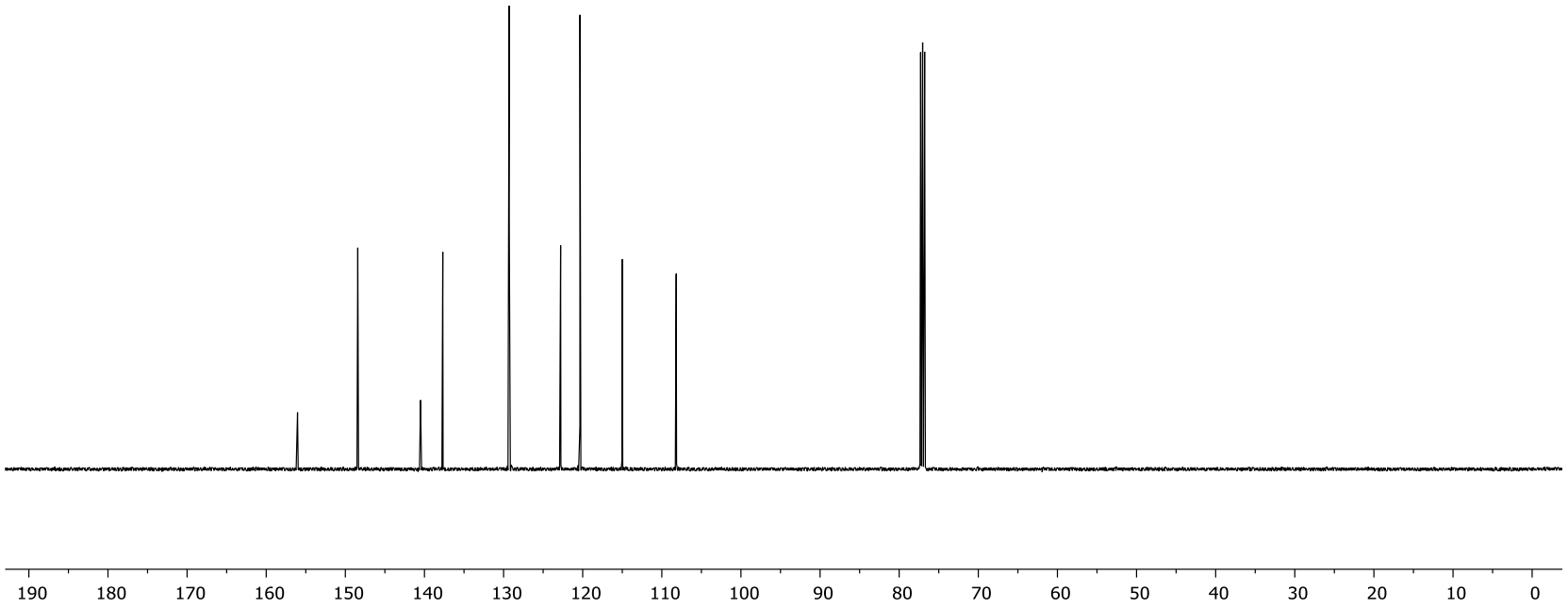

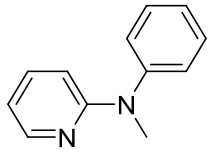

^{1}H NMR
(500 MHz, $CDCl_3$)

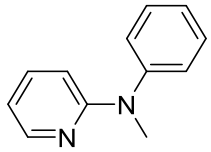

^{13}C NMR
(126 MHz, $CDCl_3$)

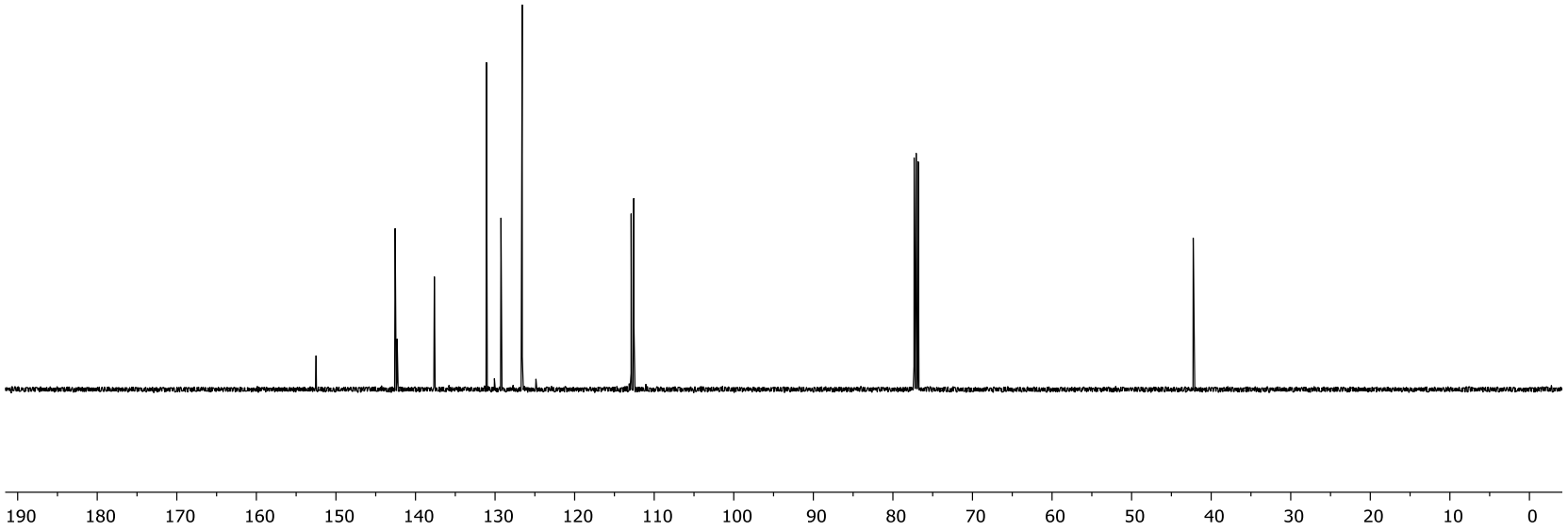

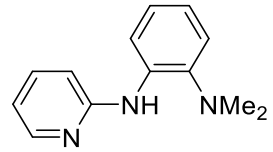

^{1}H NMR
(500 MHz, $CDCl_3$)

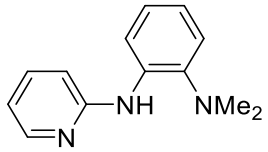

^{13}C NMR
(126 MHz, $CDCl_3$)

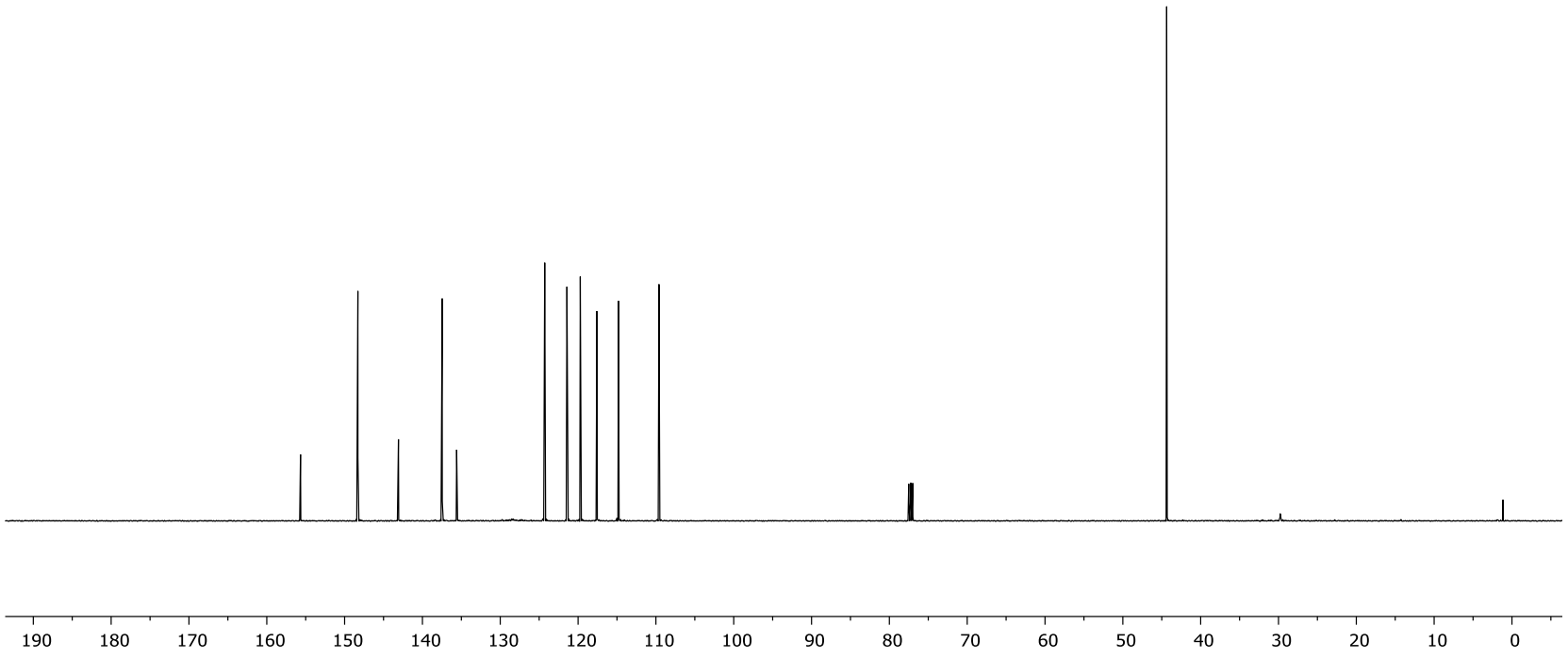

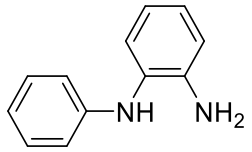

^{1}H NMR
(500 MHz, $CDCl_3$)

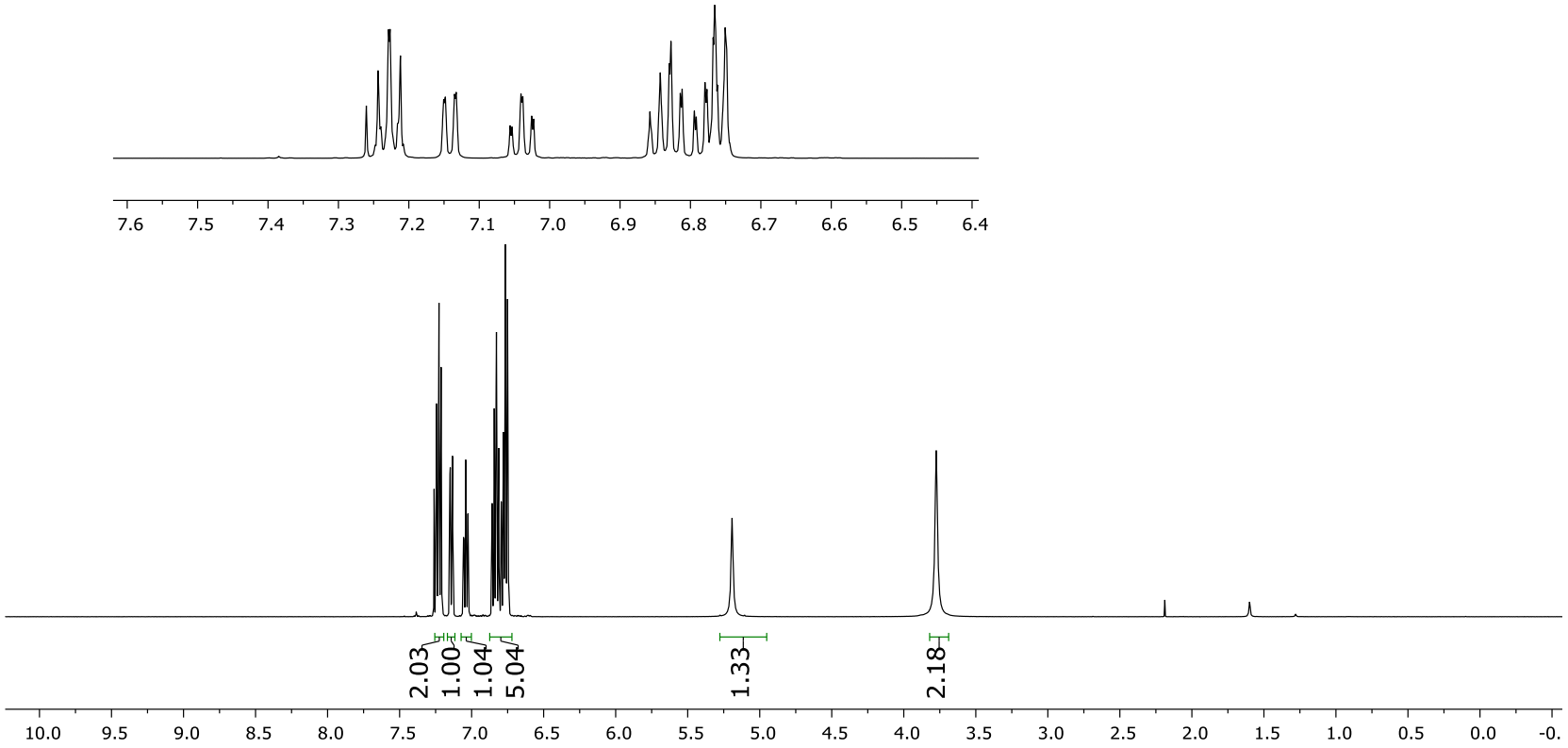

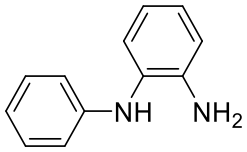

^{13}C NMR
(126 MHz, $CDCl_3$)

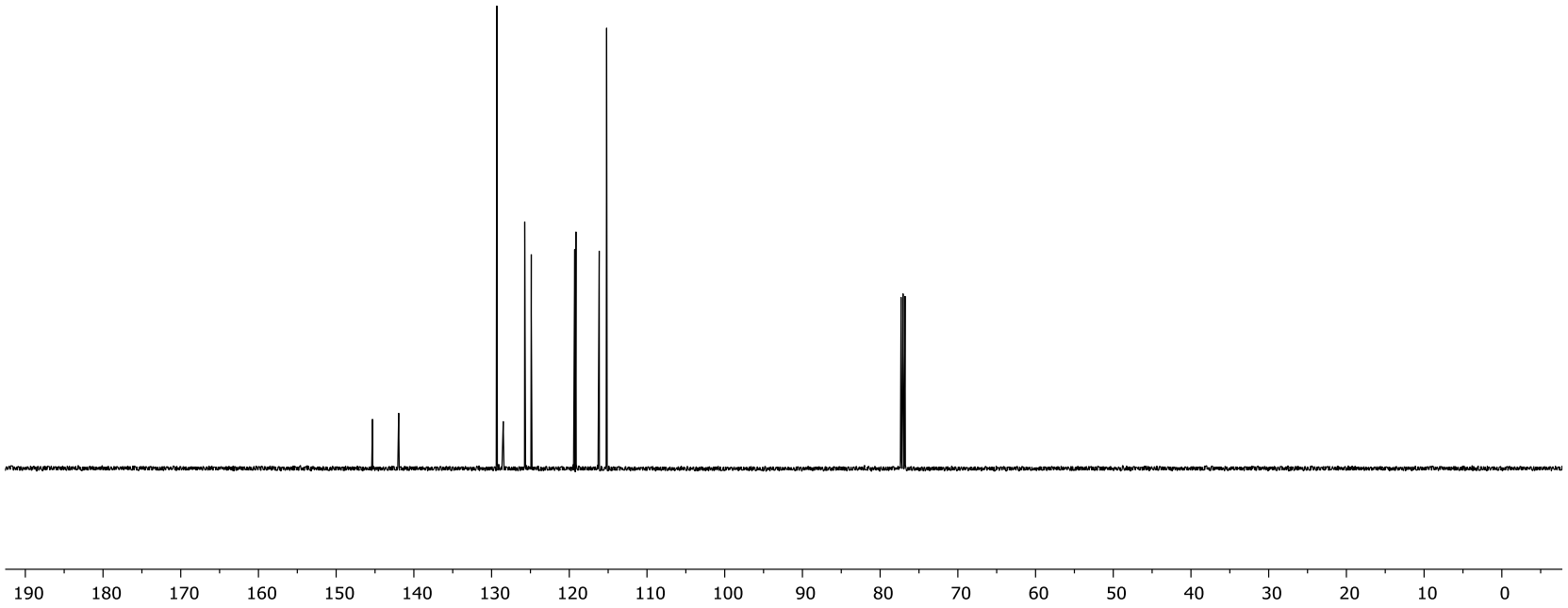

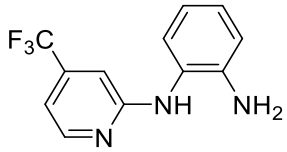

^{1}H NMR
(500 MHz, $CDCl_3$)

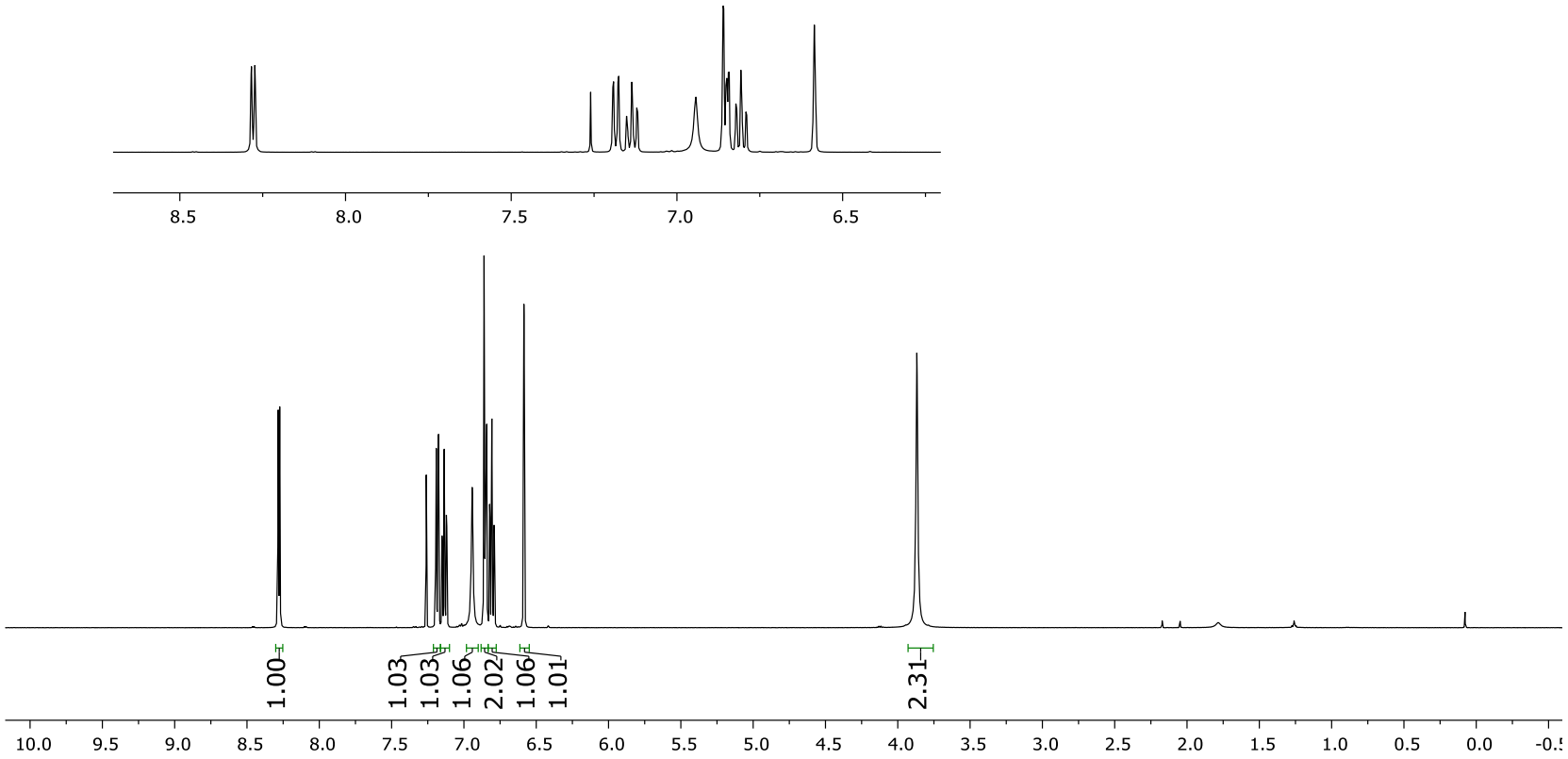

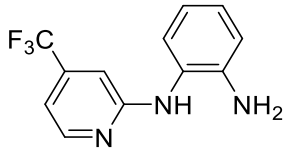

^{13}C NMR
(126 MHz, $CDCl_3$)

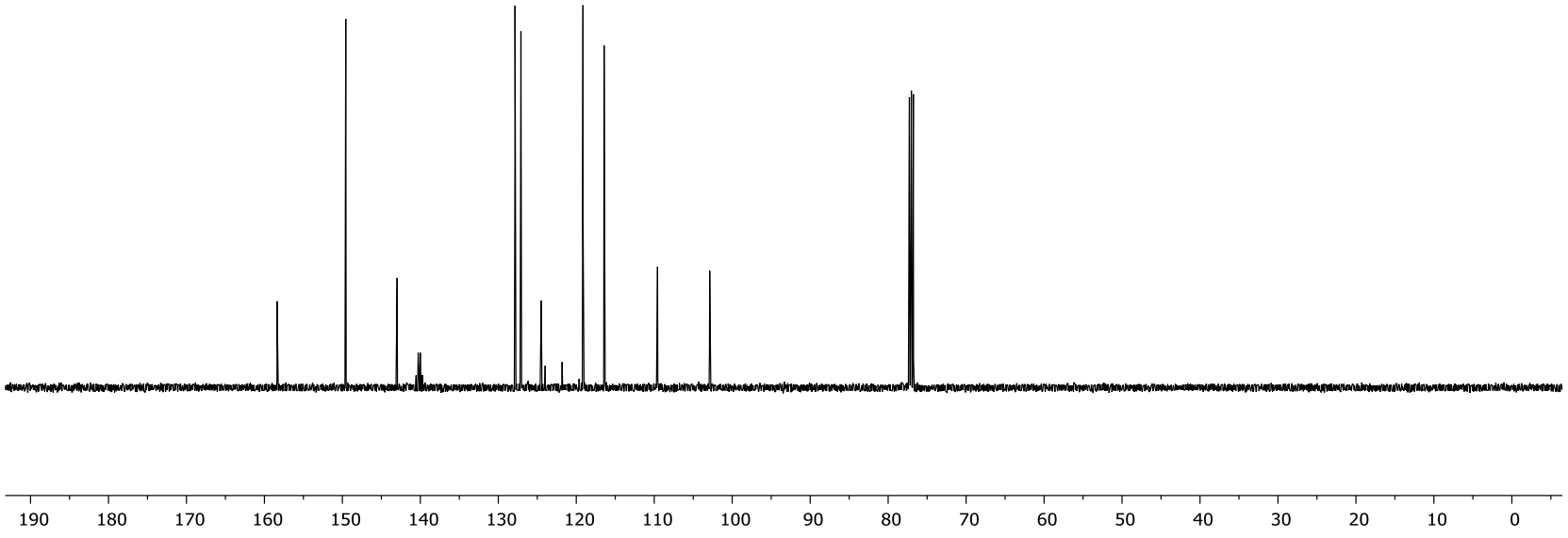

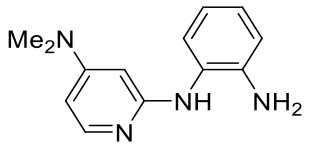

^{1}H NMR
(500 MHz, $CDCl_3$)

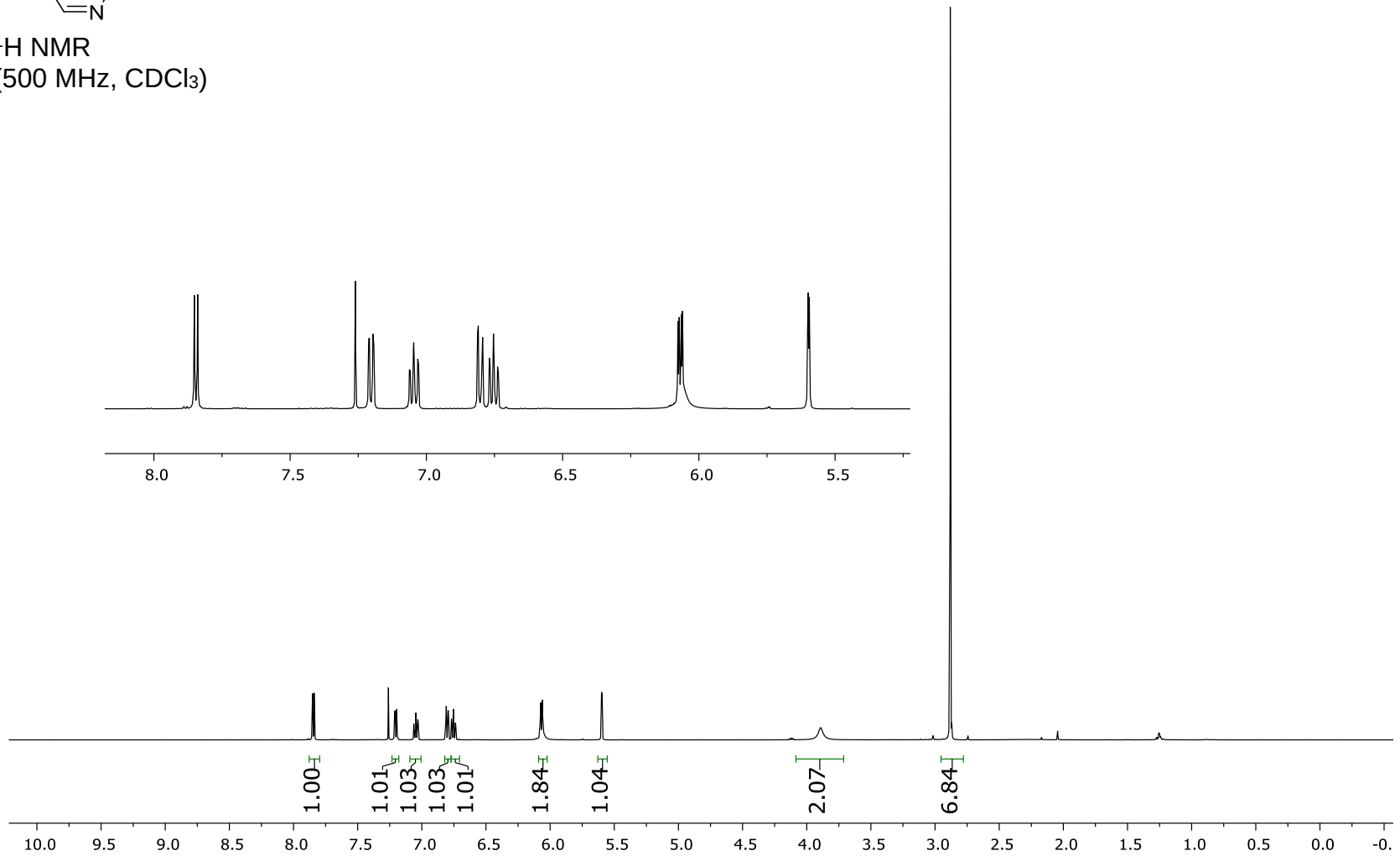

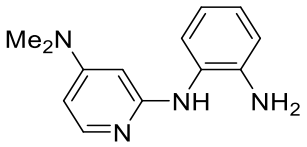

^{13}C NMR
(126 MHz, $CDCl_3$)

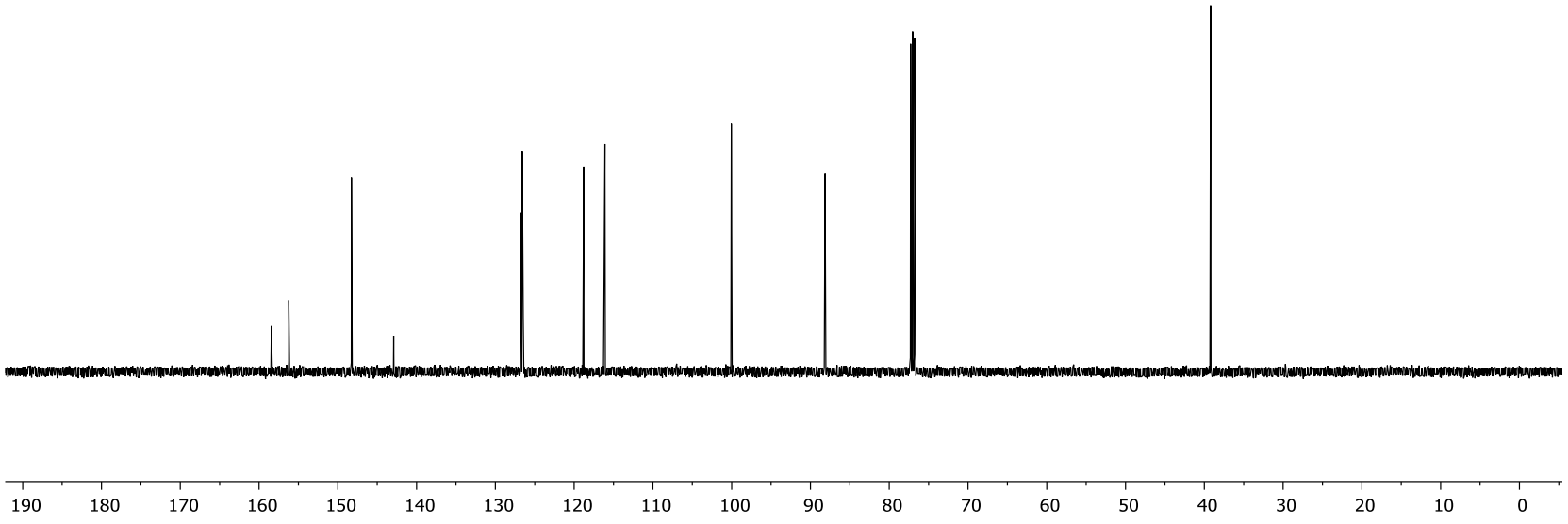

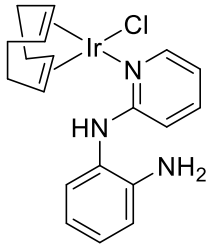

^{1}H NMR
(500 MHz, $CDCl_3$)

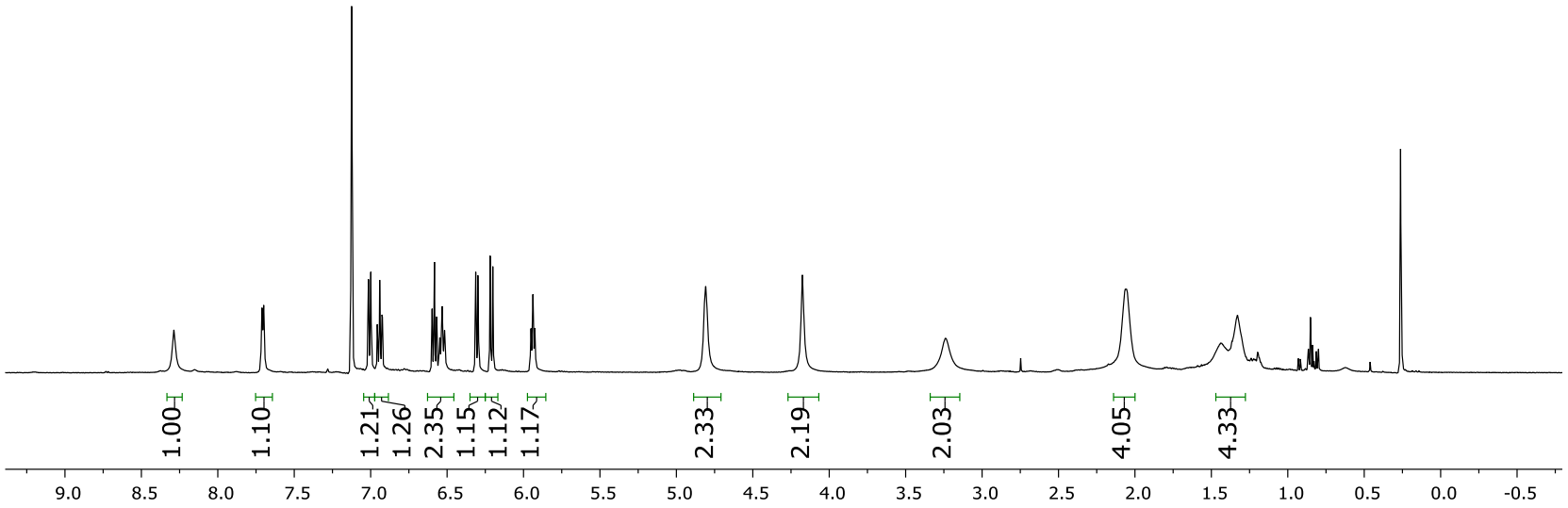

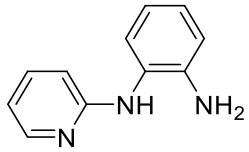

^{1}H NMR
(500 MHz, $CDCl_3$)

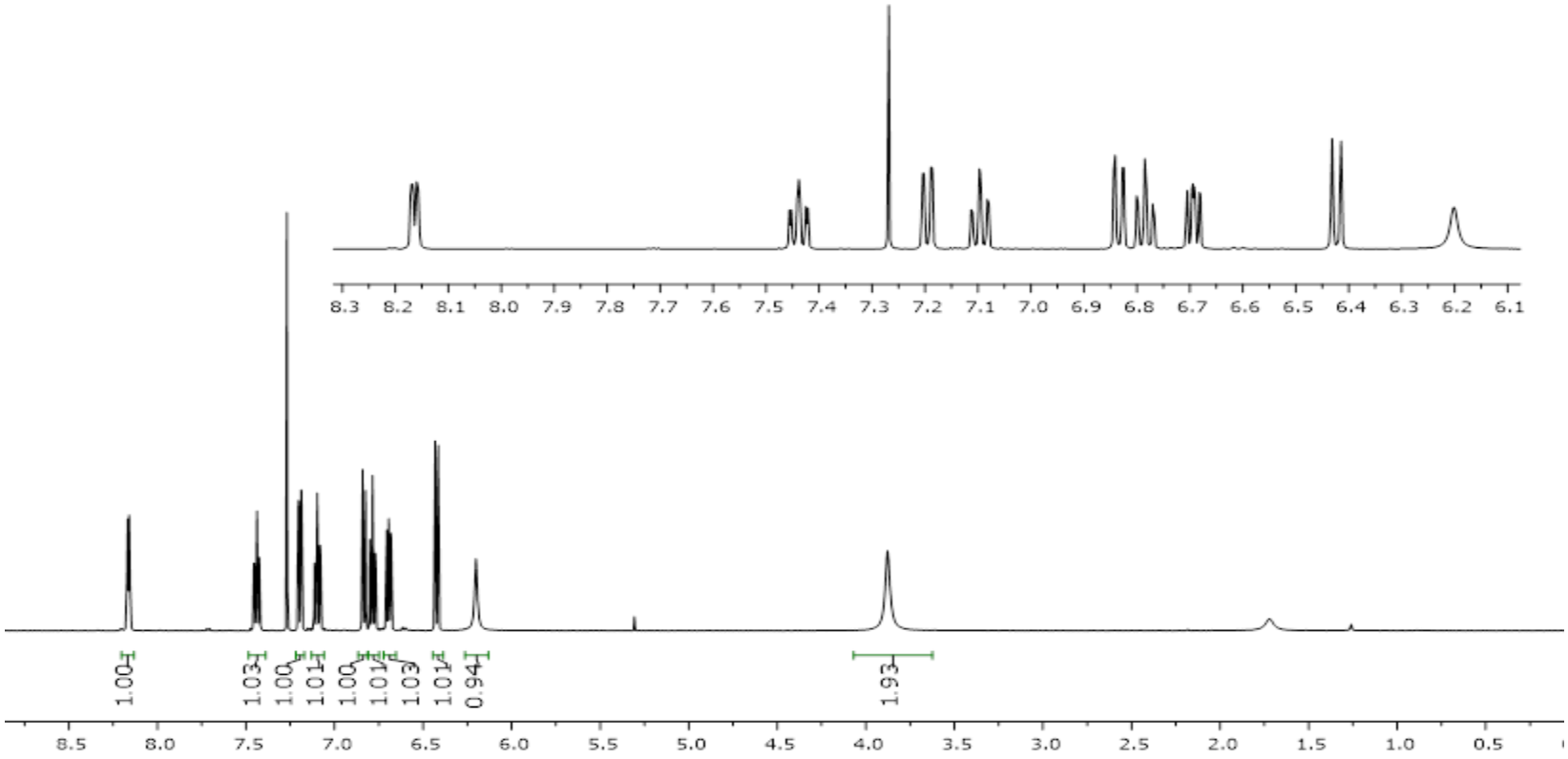

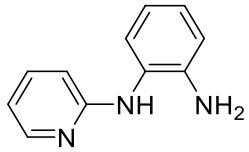

^{13}C NMR
(126 MHz, $CDCl_3$)

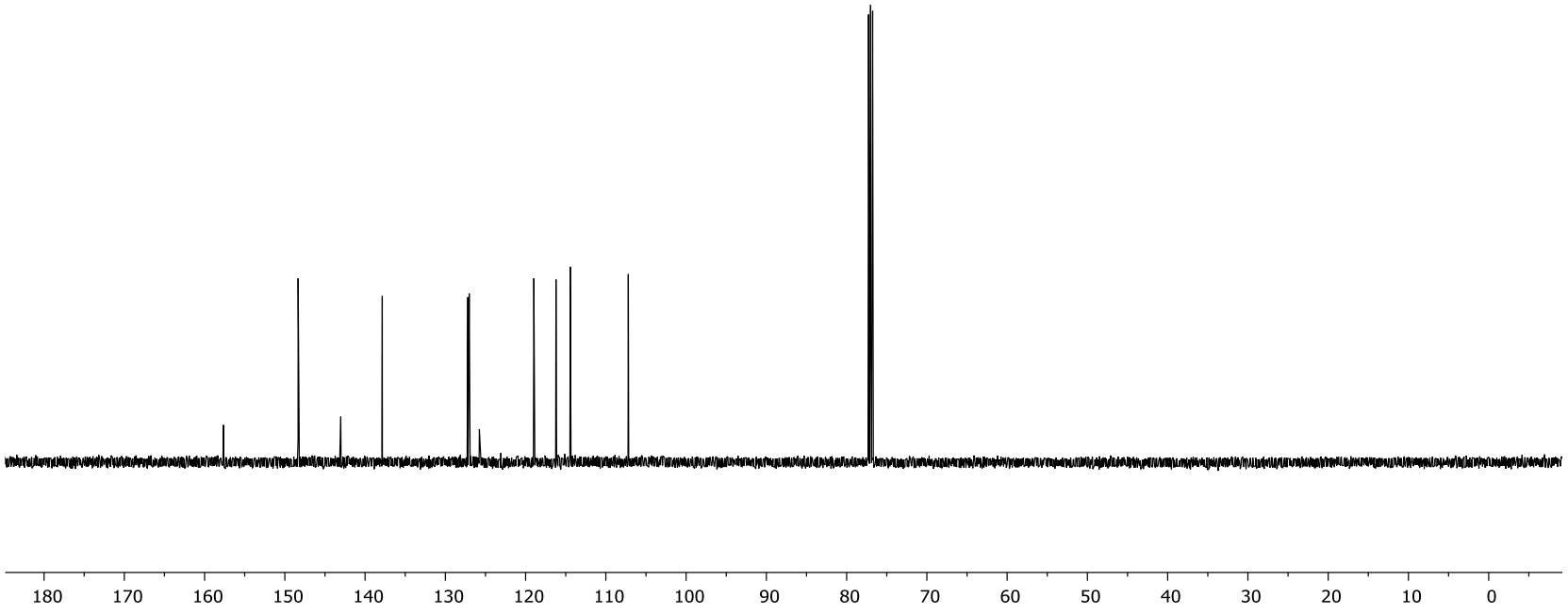

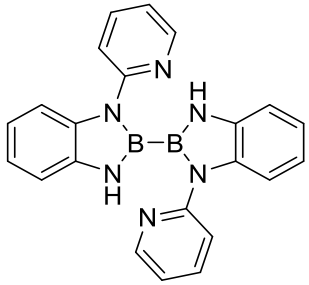

^{1}H NMR
(500 MHz, $CDCl_3$)

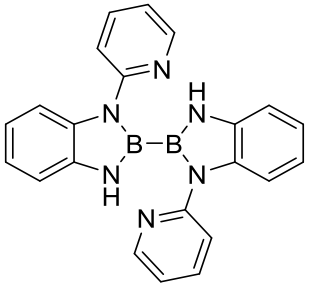

^{13}C NMR
(126 MHz, $CDCl_3$)

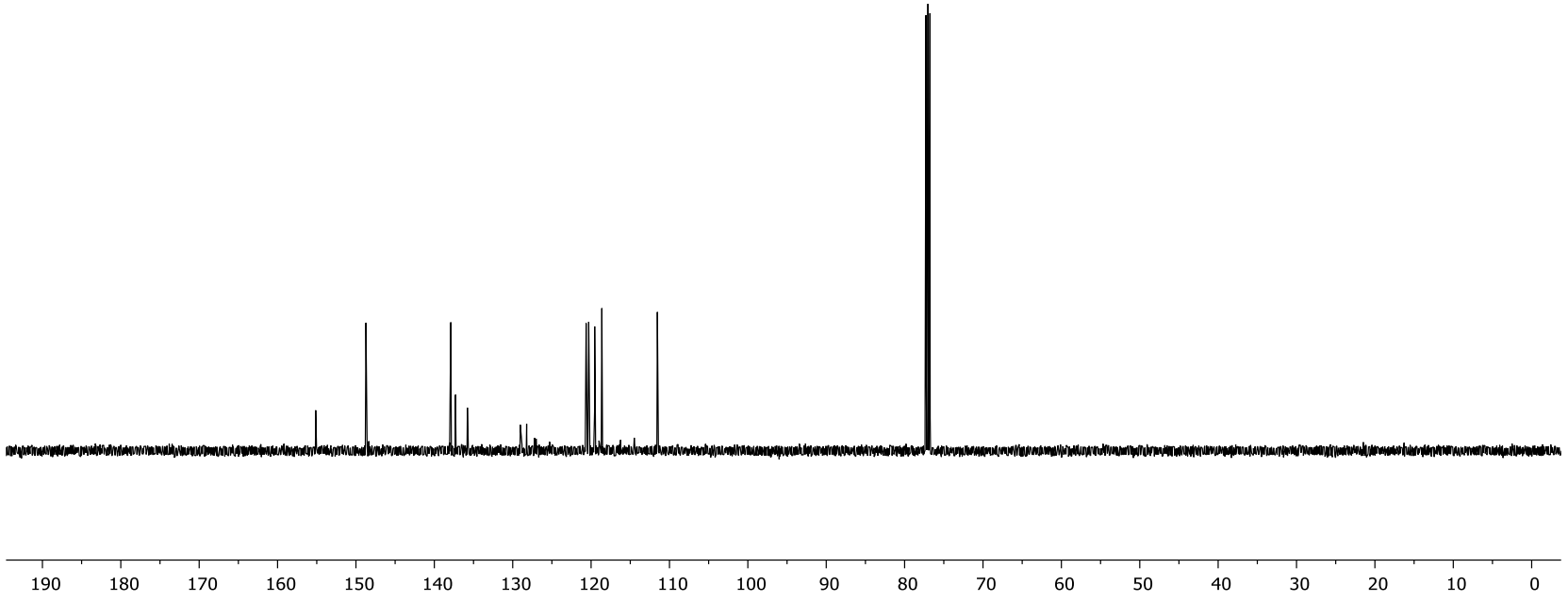

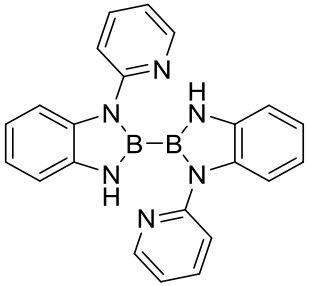

^{11}B NMR
(160 MHz, $CDCl_3$)

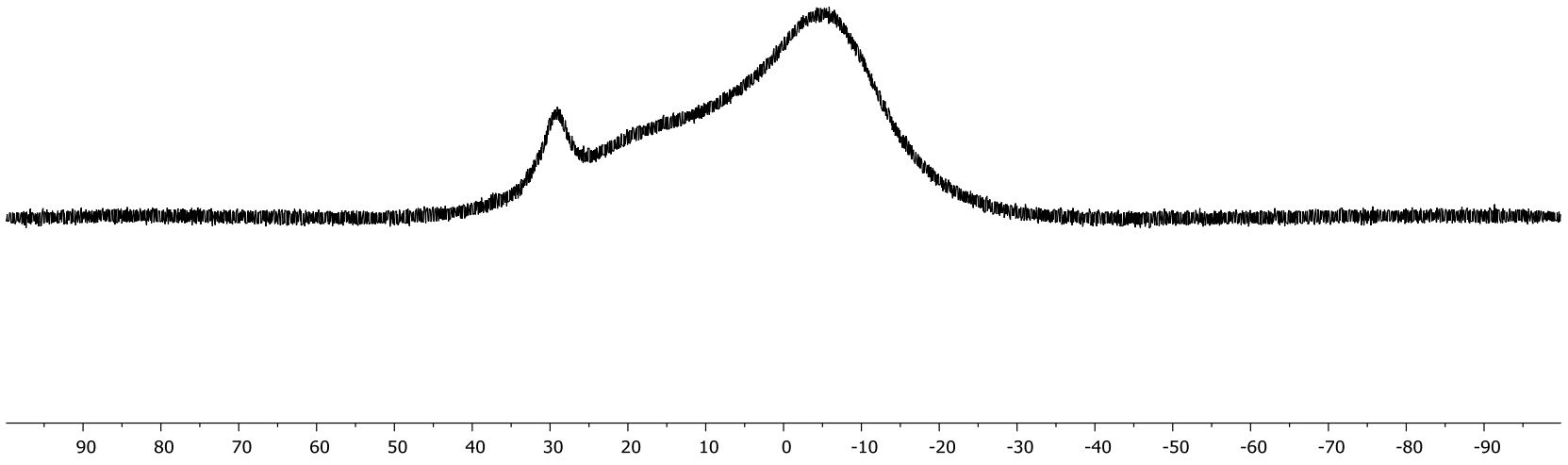

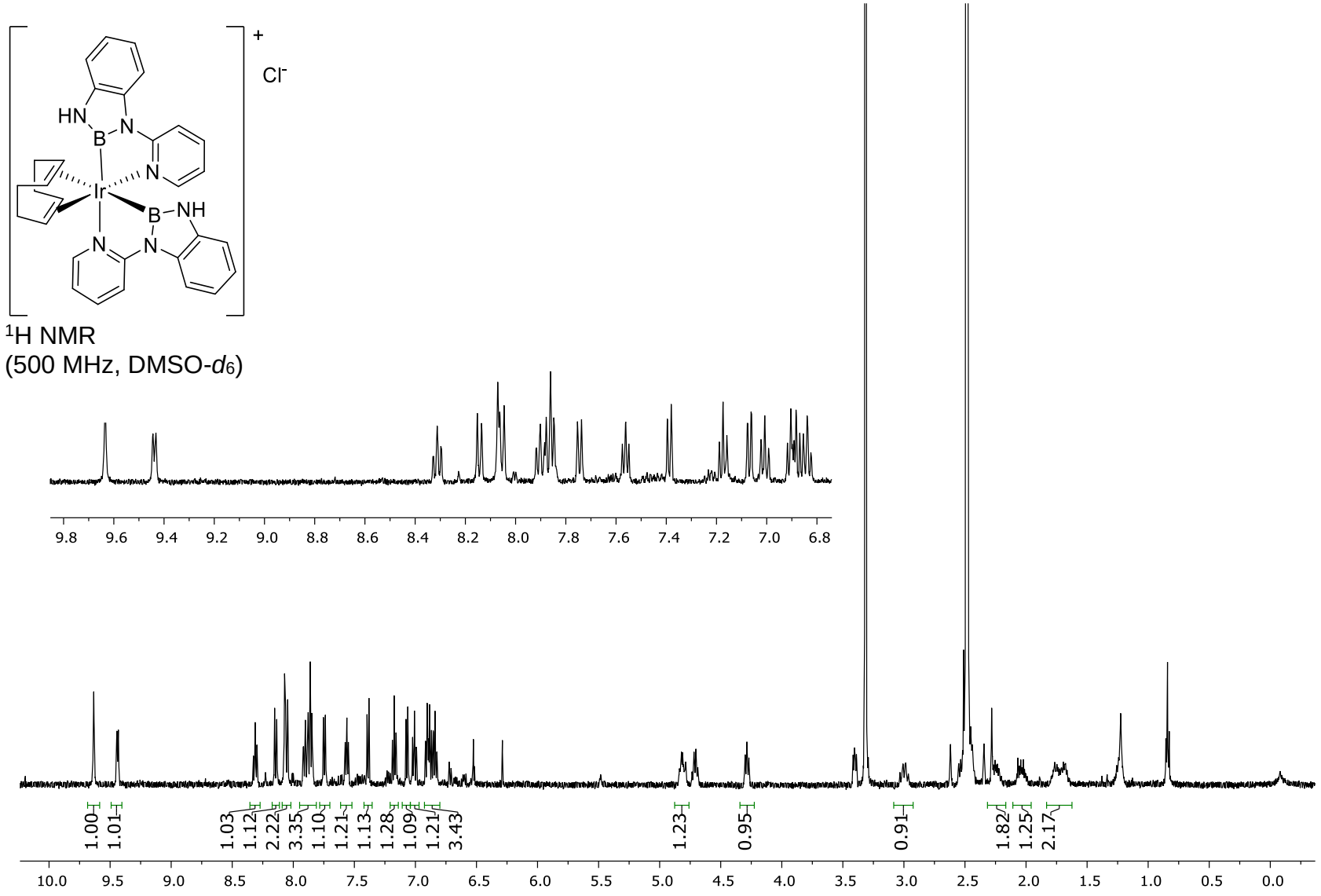
HN
B
N
N
Ir
B
NH
N
N
+
Cl-
1H NMR
(500 MHz, DMSO-d6)
9.8 9.6 9.4 9.2 9.0 8.8 8.6 8.4 8.2 8.0 7.8 7.6 7.4 7.2 7.0 6.8
1.00 1.01 1.03 1.12 2.22 3.35 1.10 1.21 1.13 1.28 1.09 1.21 3.43 1.23 0.95 0.91 1.82 1.25 2.17
10.0 9.5 9.0 8.5 8.0 7.5 7.0 6.5 6.0 5.5 5.0 4.5 4.0 3.5 3.0 2.5 2.0 1.5 1.0 0.5 0.0

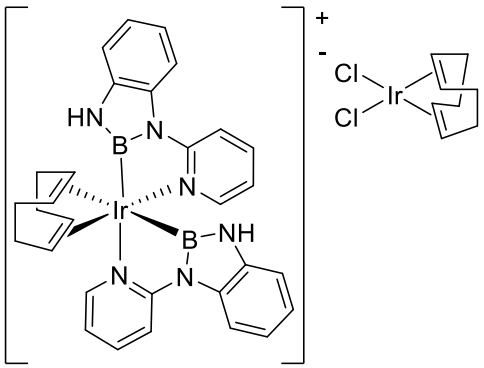

^{1}H NMR
(500 MHz, DMSO-d_6)

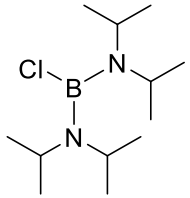

^{1}H NMR
(500 MHz, $CDCl_3$)

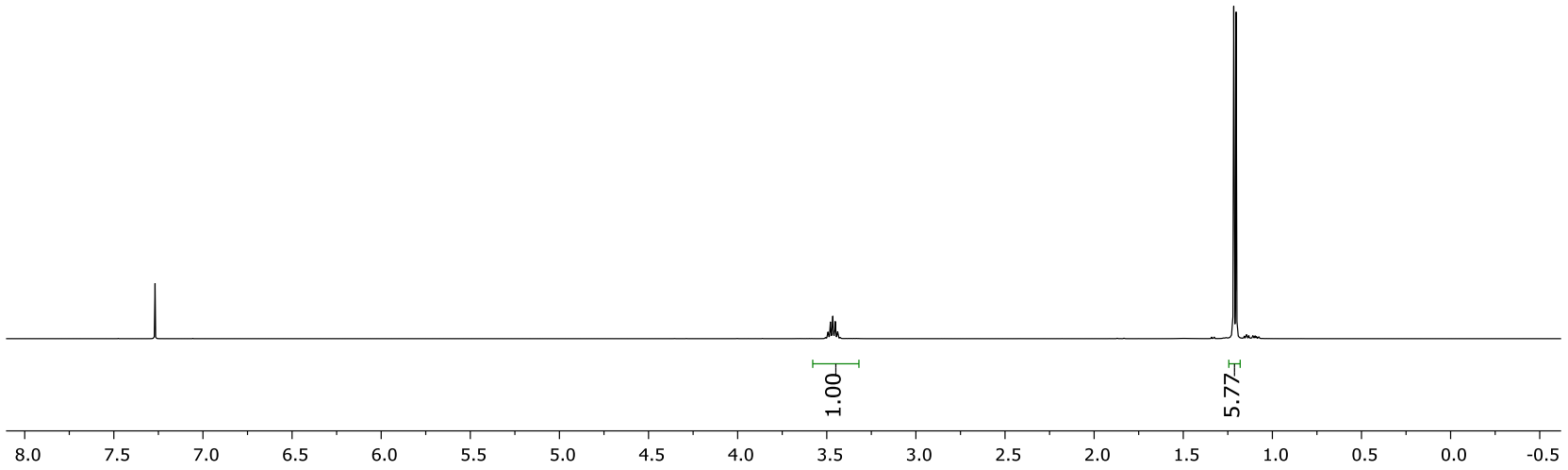

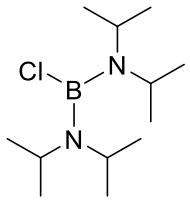

^{11}B NMR
(160 MHz, $CDCl_3$)

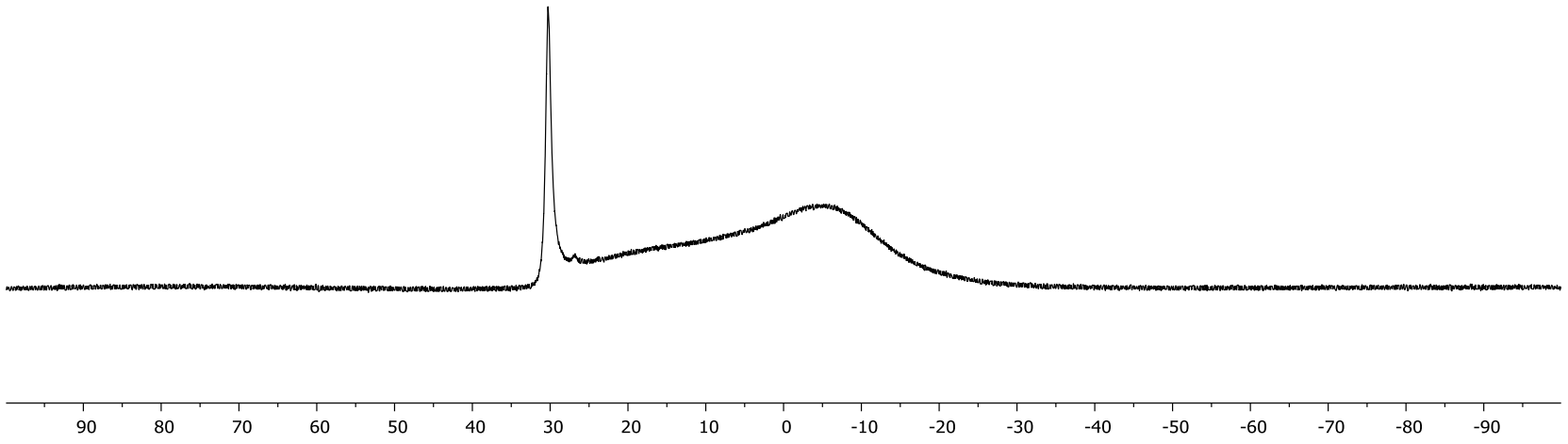

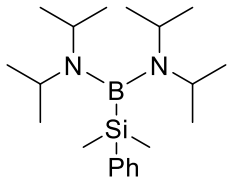

^{1}H NMR
(500 MHz, $CDCl_3$)

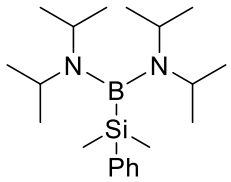

^{11}B NMR
(160 MHz, $CDCl_3$)

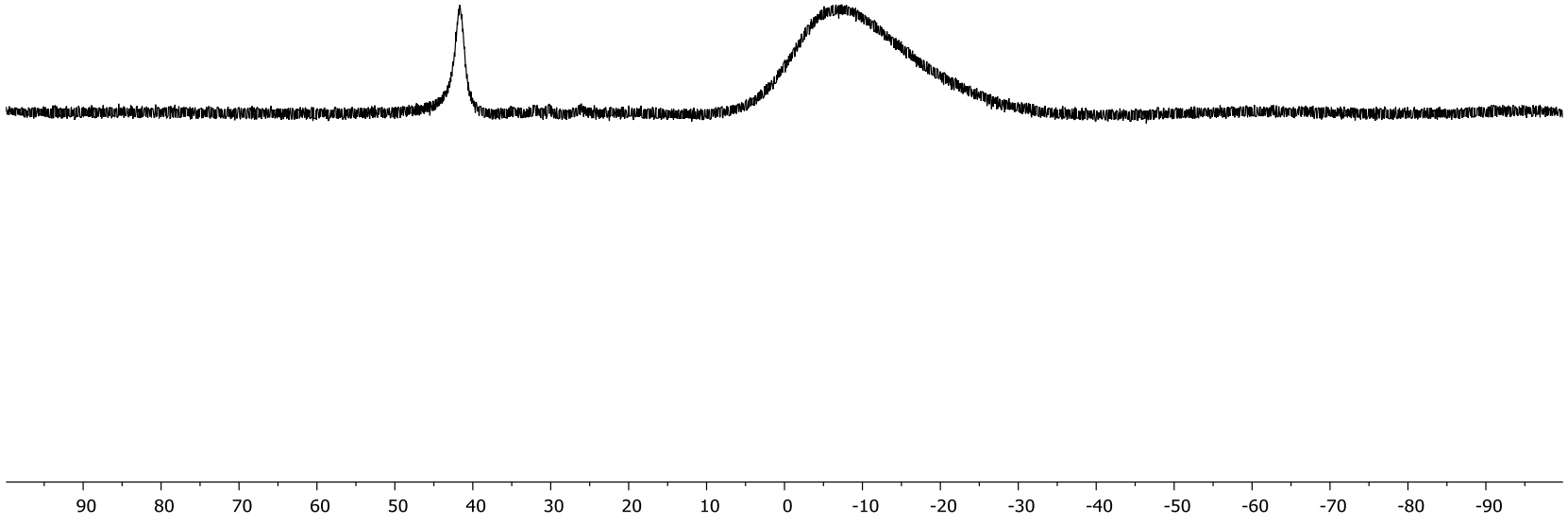

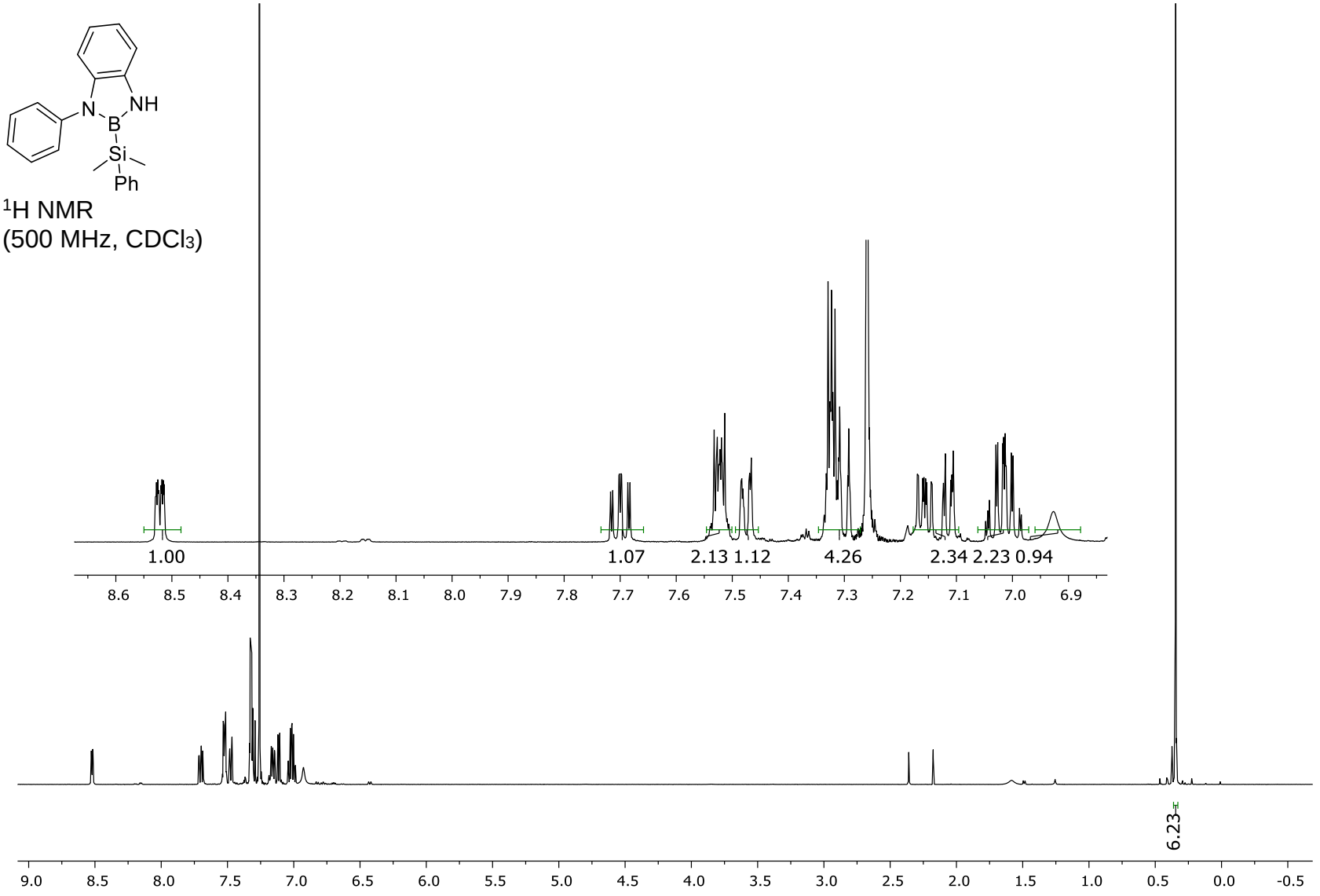
N
NH
B
Si
Ph
1H NMR
(500 MHz, CDCl3)
1.00
1.07
2.13 1.12
4.26
2.34 2.23 0.94
6.23

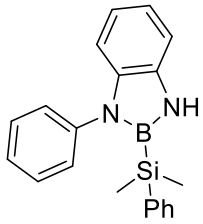

^{13}C NMR
(126 MHz, $CDCl_3$)

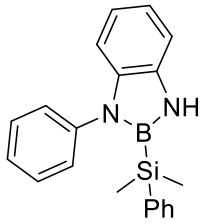

^{11}B NMR
(160 MHz, $CDCl_3$)

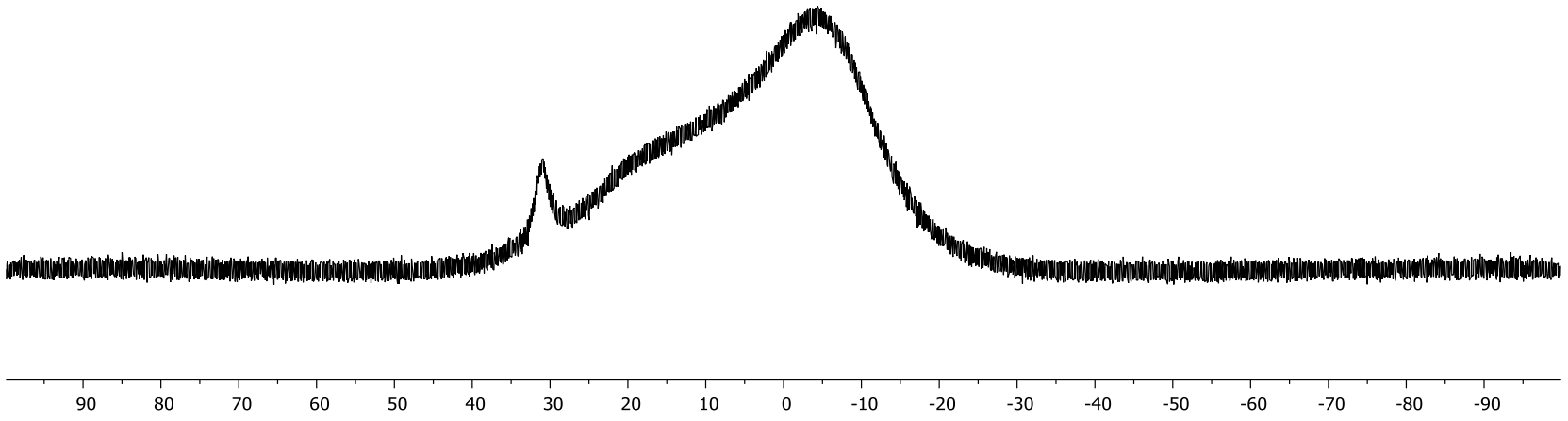

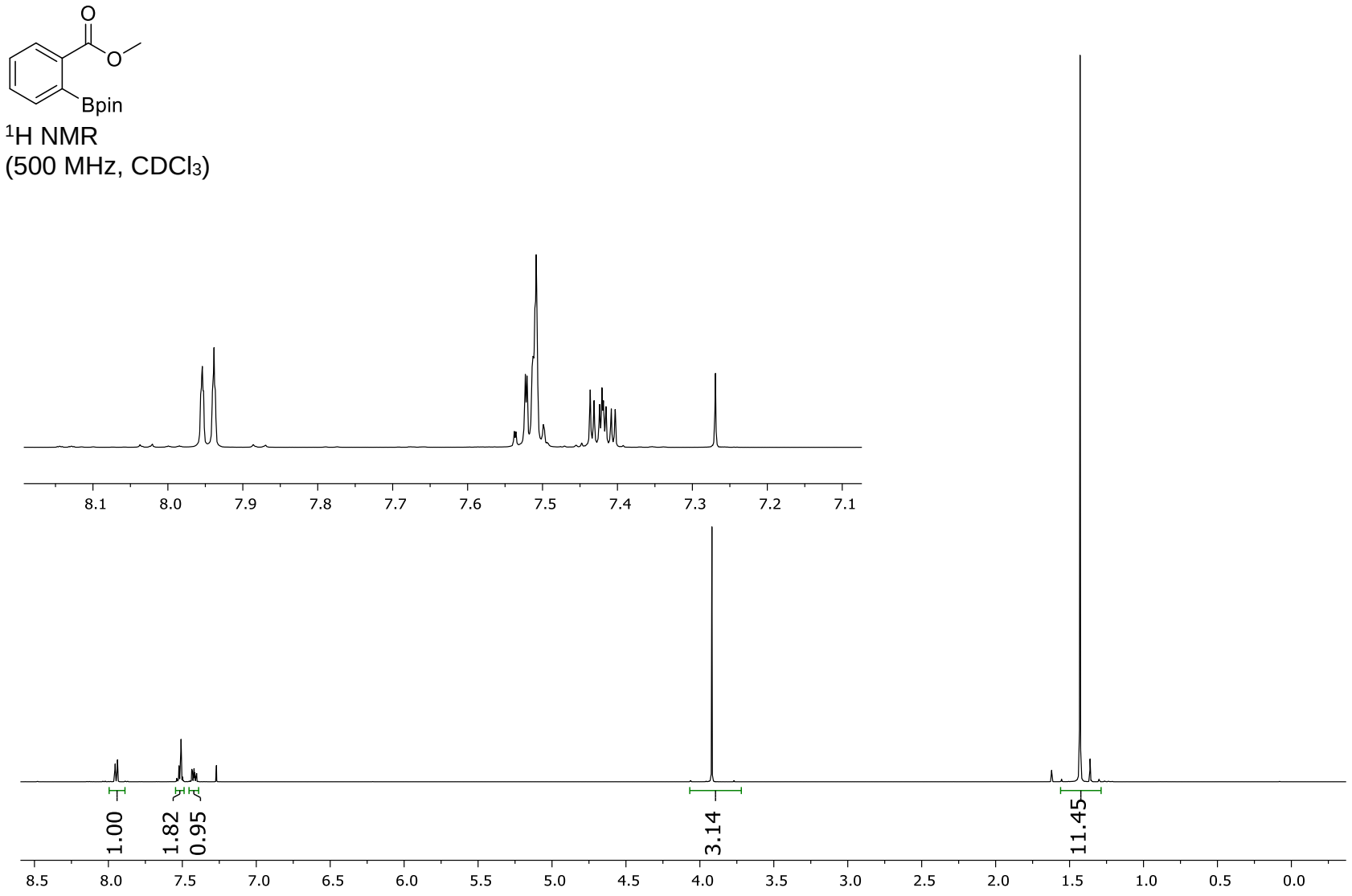
O
O
Bpin
1H NMR
(500 MHz, CDCl3)
8.1
8.0
7.9
7.8
7.7
7.6
7.5
7.4
7.3
7.2
7.1
1.00
1.82
0.95
3.14
11.45
8.5
8.0
7.5
7.0
6.5
6.0
5.5
5.0
4.5
4.0
3.5
3.0
2.5
2.0
1.5
1.0
0.5
0.0

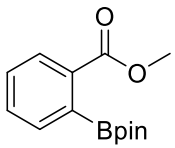

^{11}B NMR
(160 MHz, $CDCl_3$)

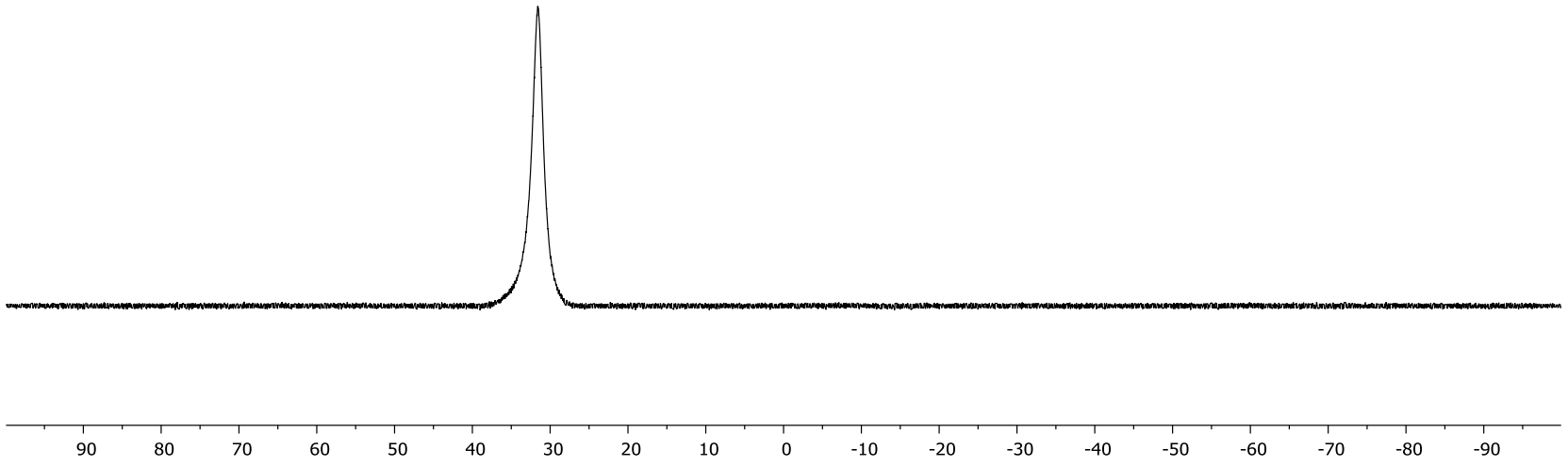

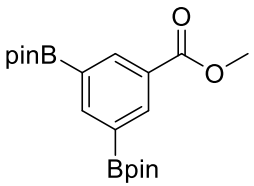

^{1}H NMR
(500 MHz, $CDCl_3$)

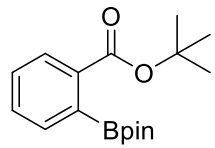

^{1}H NMR
(500 MHz, $CDCl_3$)

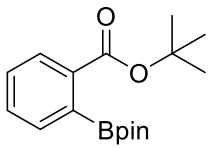

^{11}B NMR
(160 MHz, $CDCl_3$)

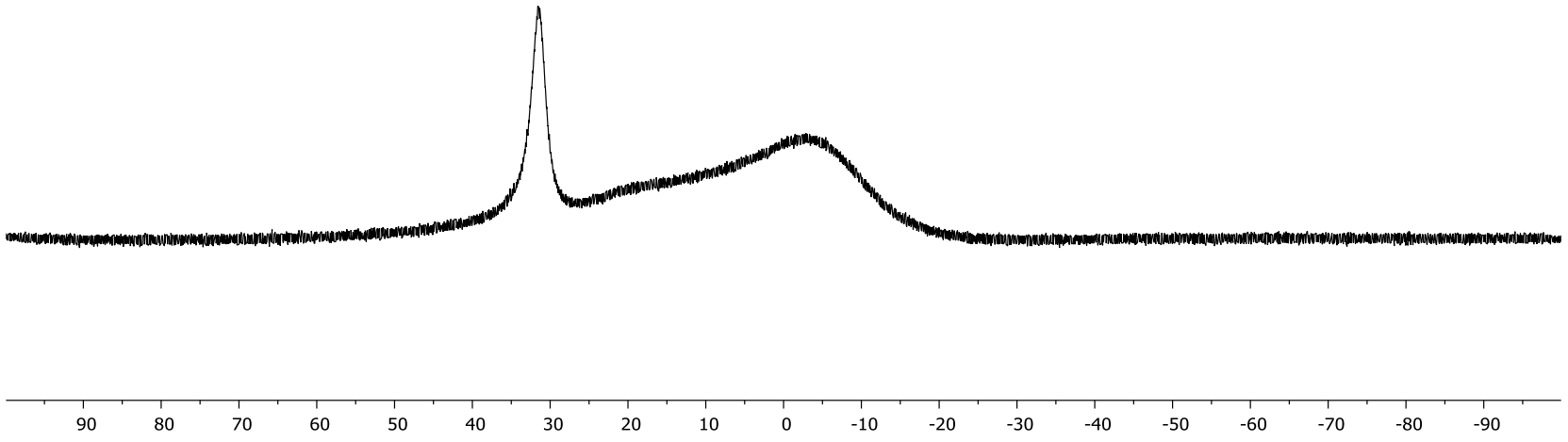

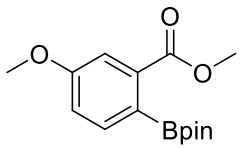

^{1}H NMR
(500 MHz, $CDCl_3$)

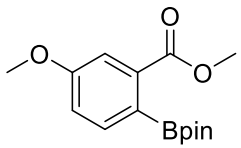

^{11}B NMR
(160 MHz, $CDCl_3$)

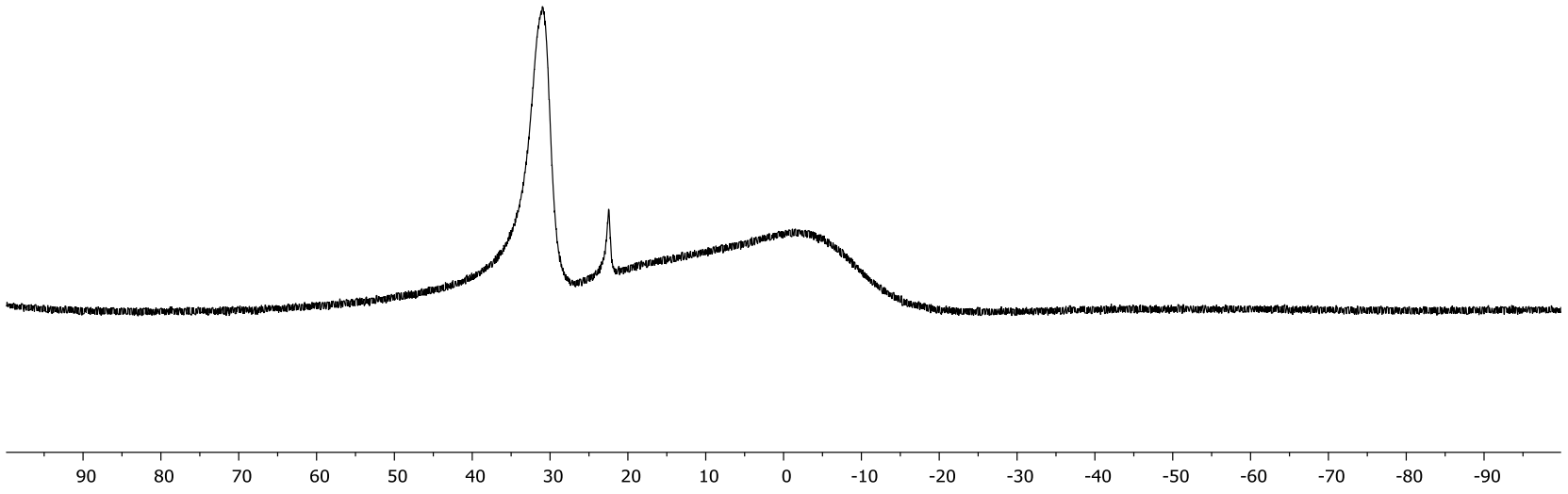

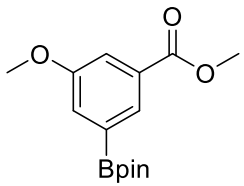

^{1}H NMR
(500 MHz, $CDCl_3$)

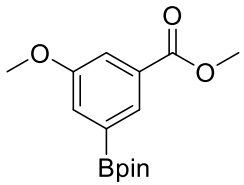

^{11}B NMR
(60 MHz, $CDCl_3$)

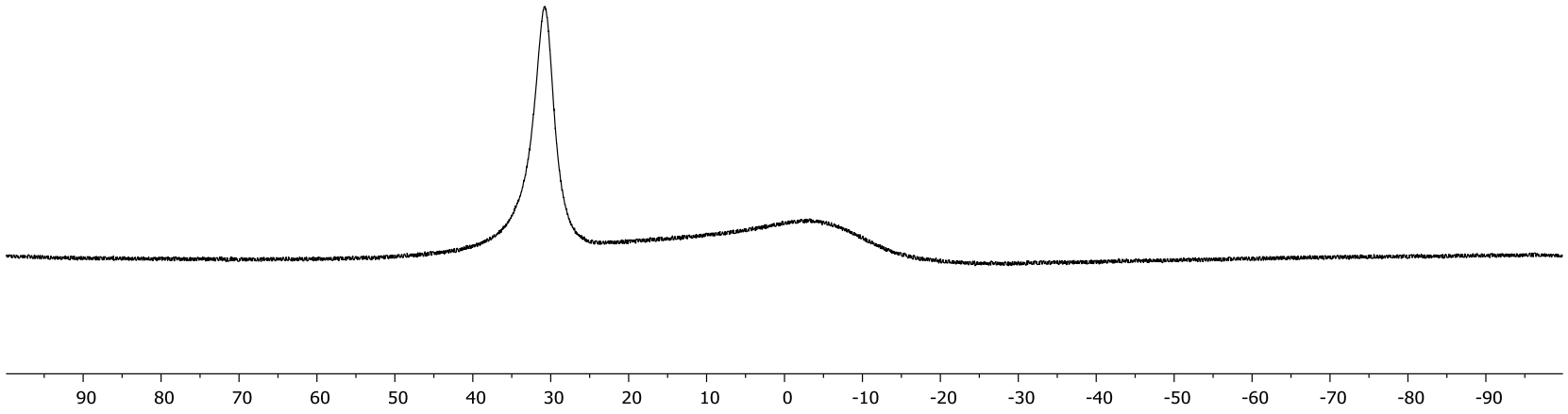

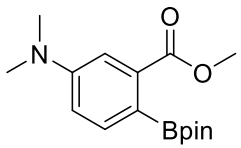

^{1}H NMR
(500 MHz, $CDCl_3$)

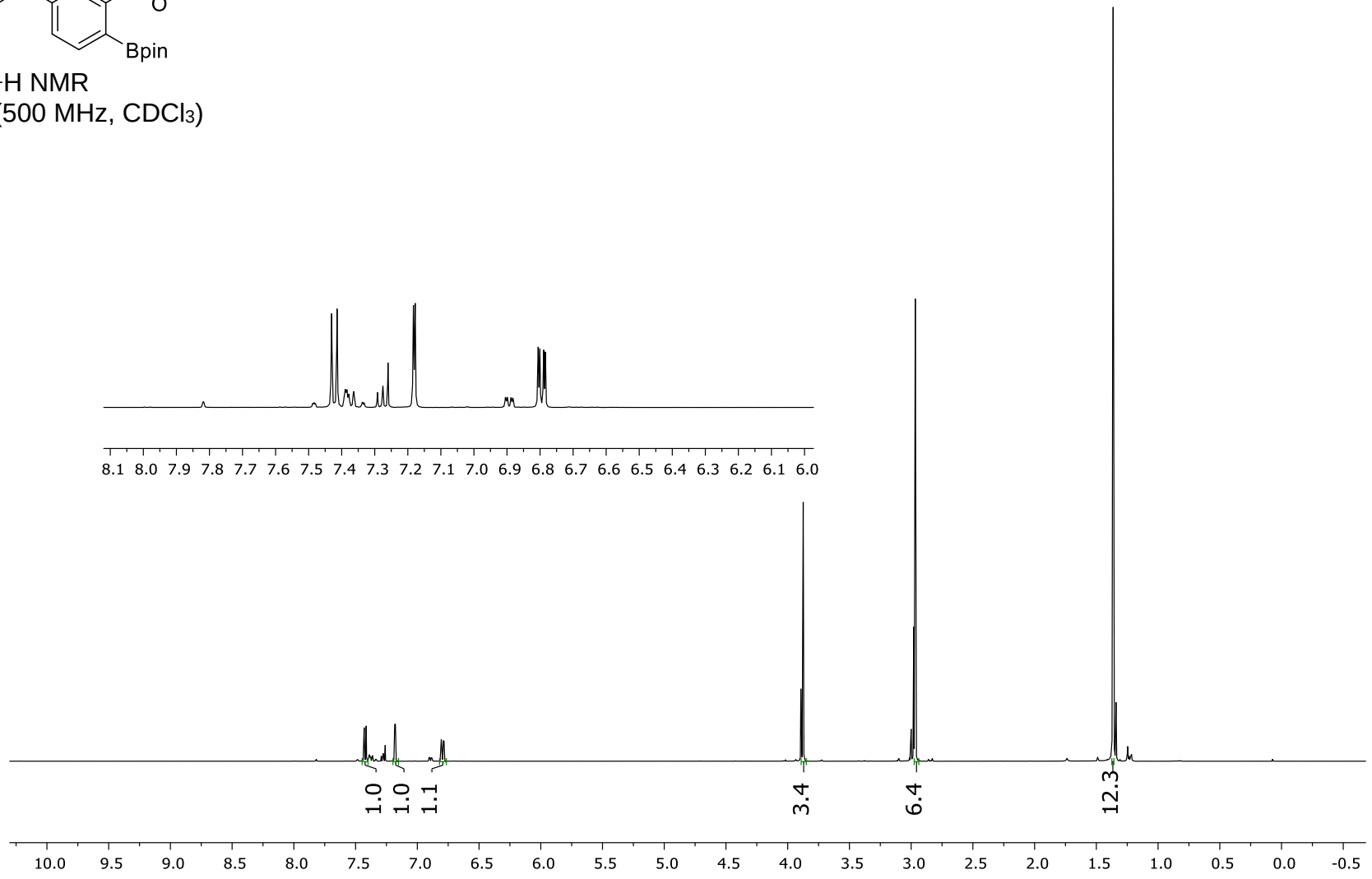

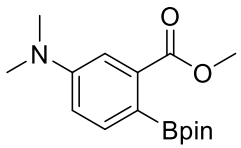

^{11}B NMR
(160 MHz, $CDCl_3$)

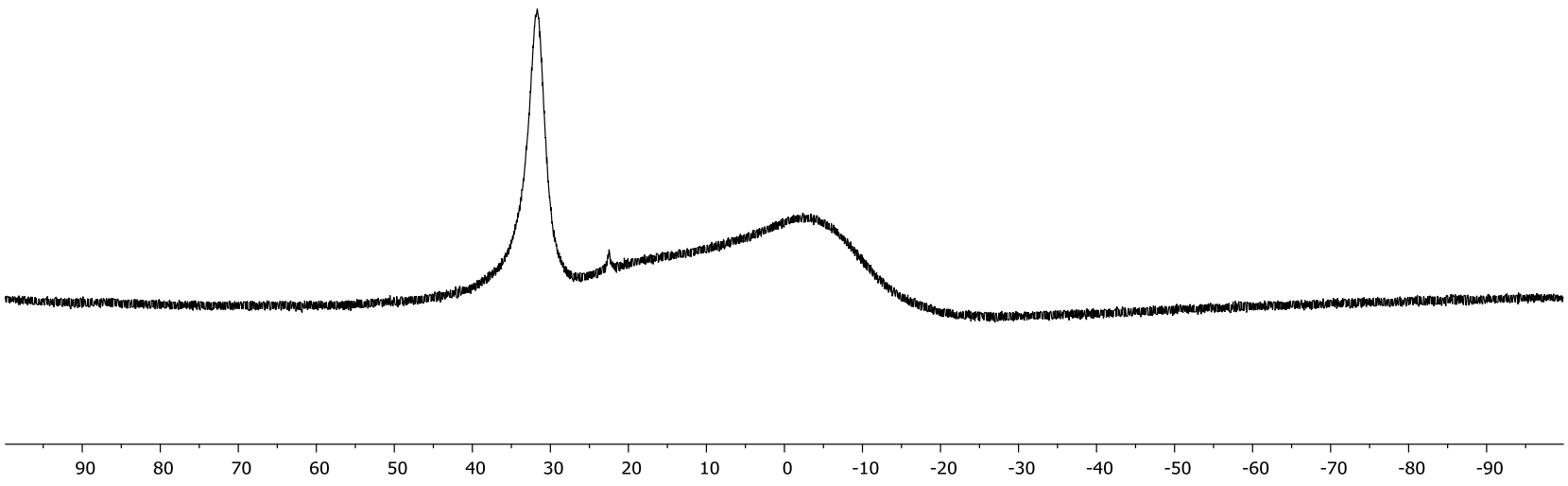

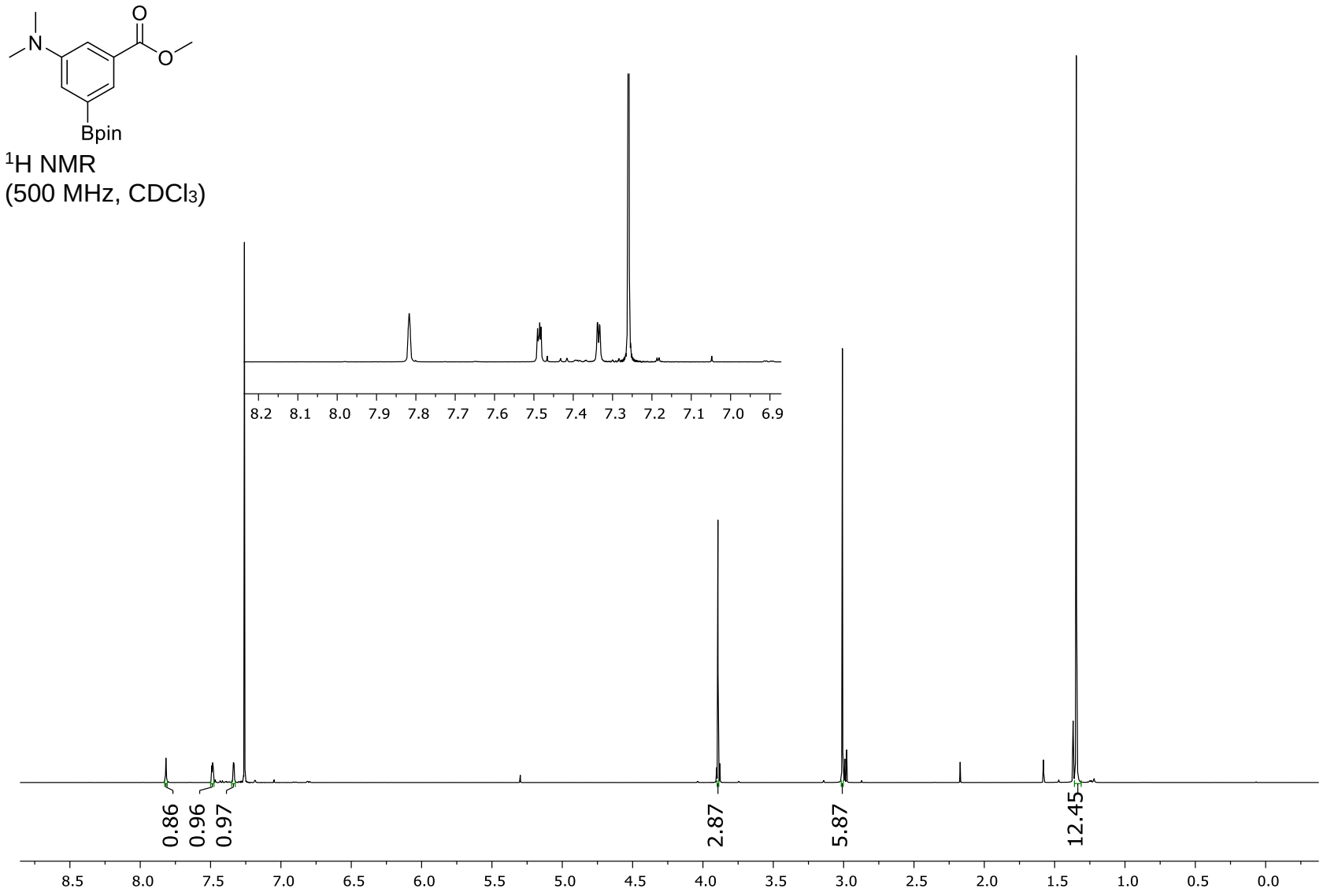
O
N
O
Bpin
^{1}H NMR
(500 MHz, CDCl$_3$)
8.2 8.1 8.0 7.9 7.8 7.7 7.6 7.5 7.4 7.3 7.2 7.1 7.0 6.9
0.86
0.96
0.97
2.87
5.87
12.45
8.5 8.0 7.5 7.0 6.5 6.0 5.5 5.0 4.5 4.0 3.5 3.0 2.5 2.0 1.5 1.0 0.5 0.0

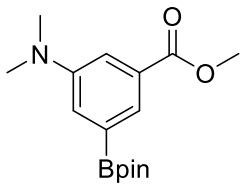

^{11}B NMR
(60 MHz, $CDCl_3$)

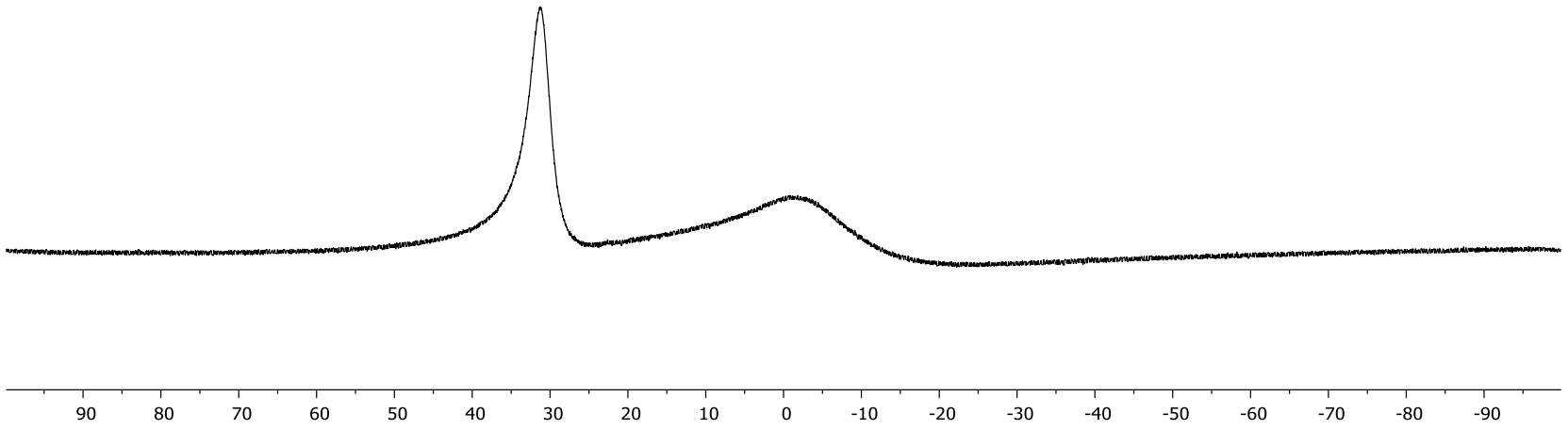

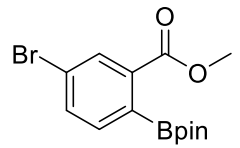

^{1}H NMR
(500 MHz, $CDCl_3$)

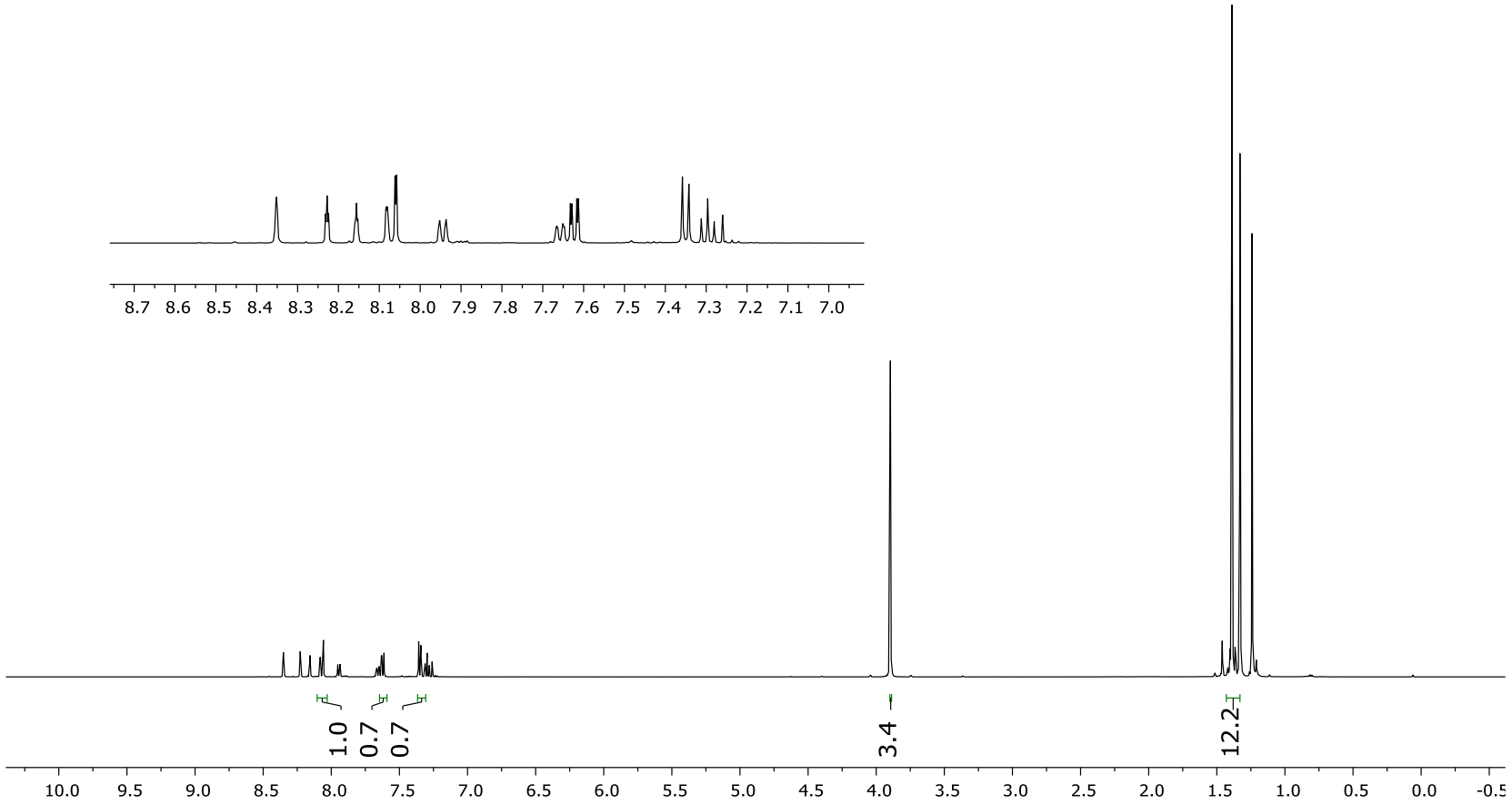

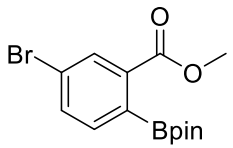

^{11}B NMR
(160 MHz, $CDCl_3$)

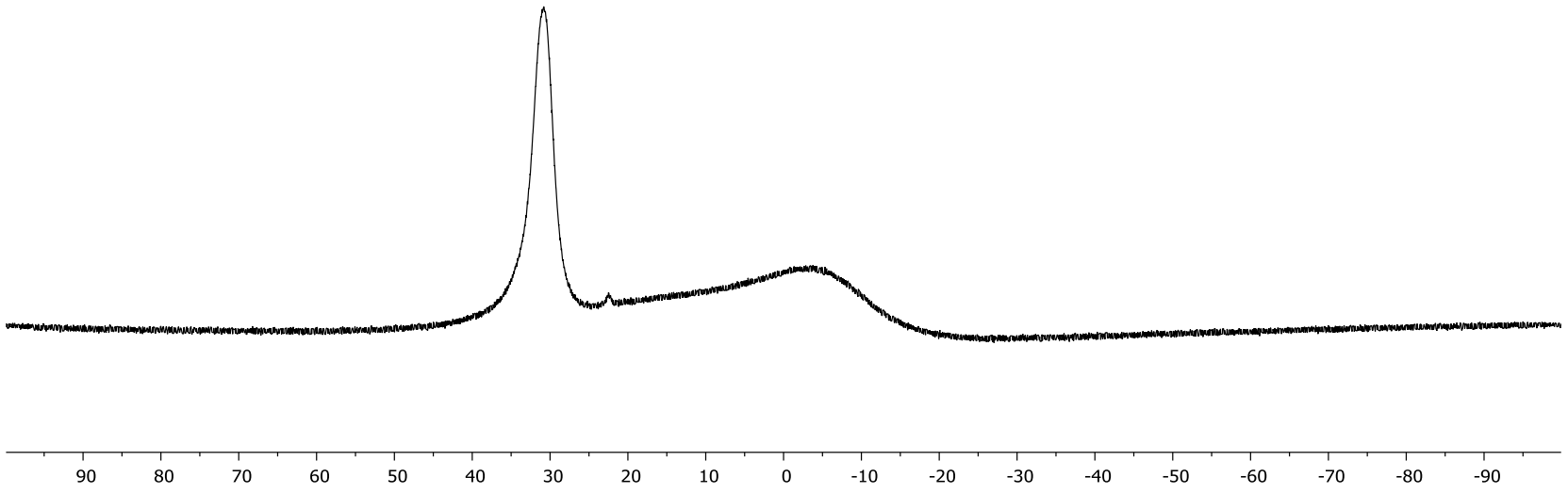

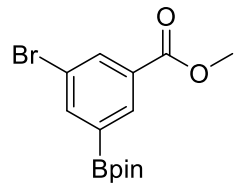

^{1}H NMR
(500 MHz, $CDCl_3$)

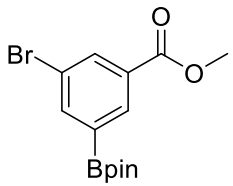

^{11}B NMR
(60 MHz, $CDCl_3$)

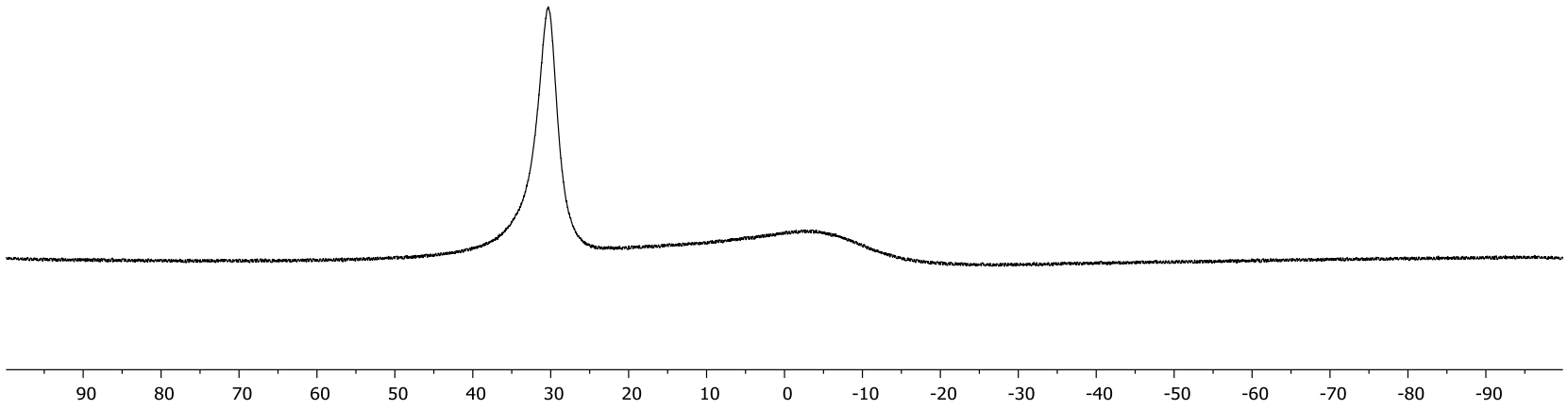

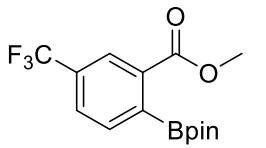

^{1}H NMR
(500 MHz, $CDCl_3$)

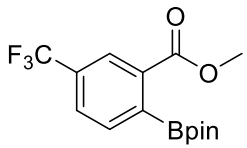

^{11}B NMR
(160 MHz, $CDCl_3$)

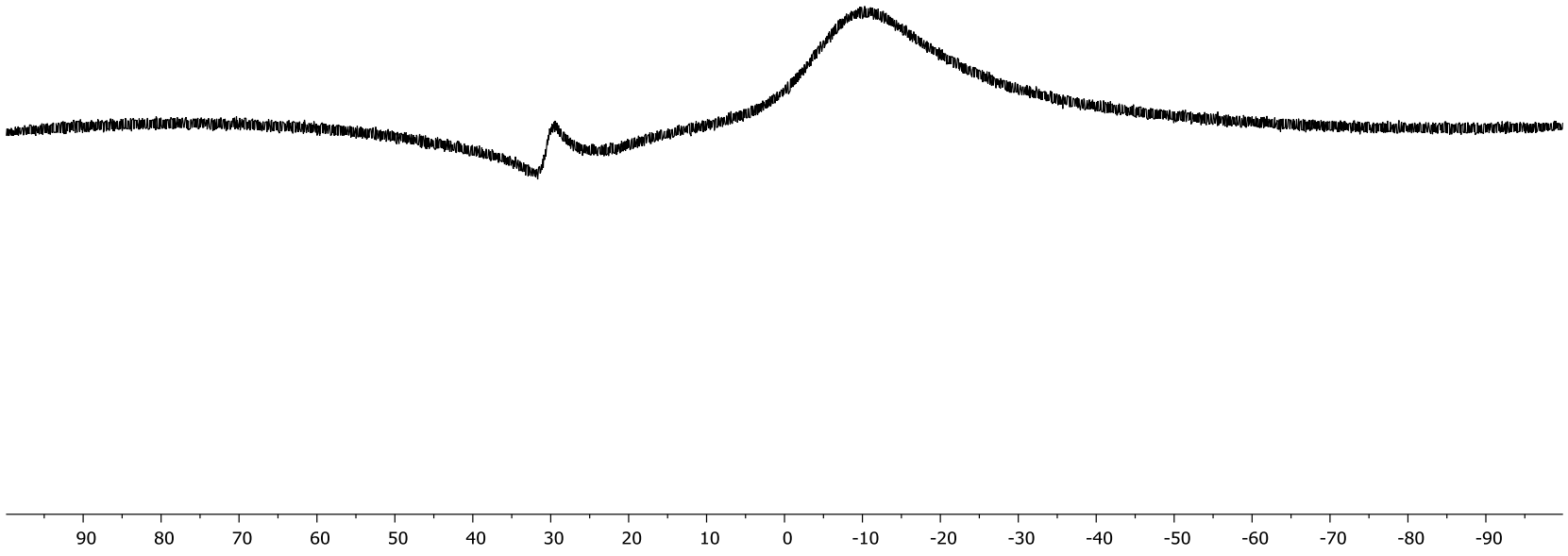

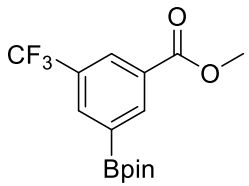

^{1}H NMR
(500 MHz, $CDCl_3$)

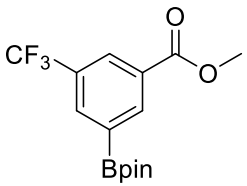

^{11}B NMR
(60 MHz, $CDCl_3$)

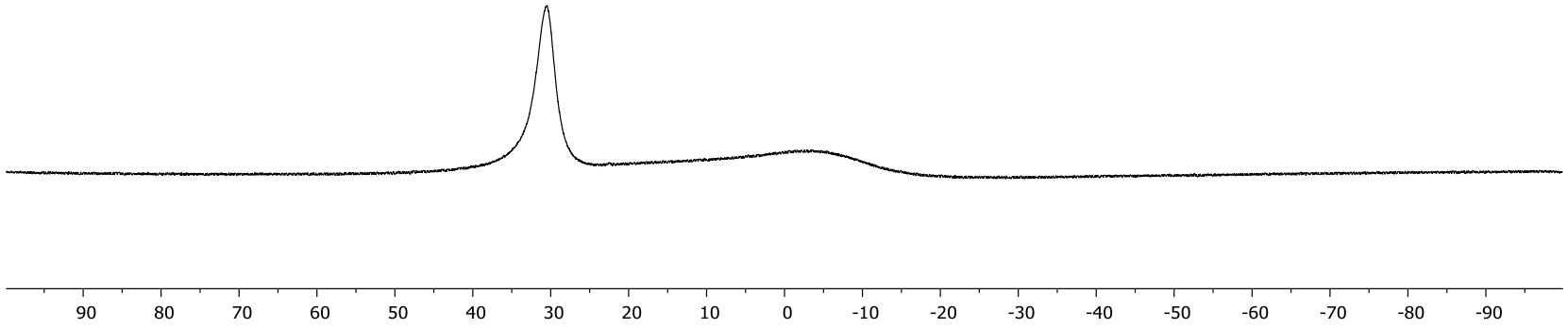

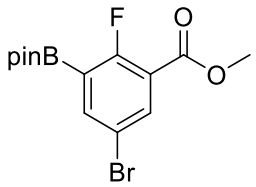

^{1}H NMR
(500 MHz, $CDCl_3$)

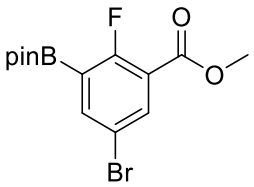

^{11}B NMR
(60 MHz, $CDCl_3$)

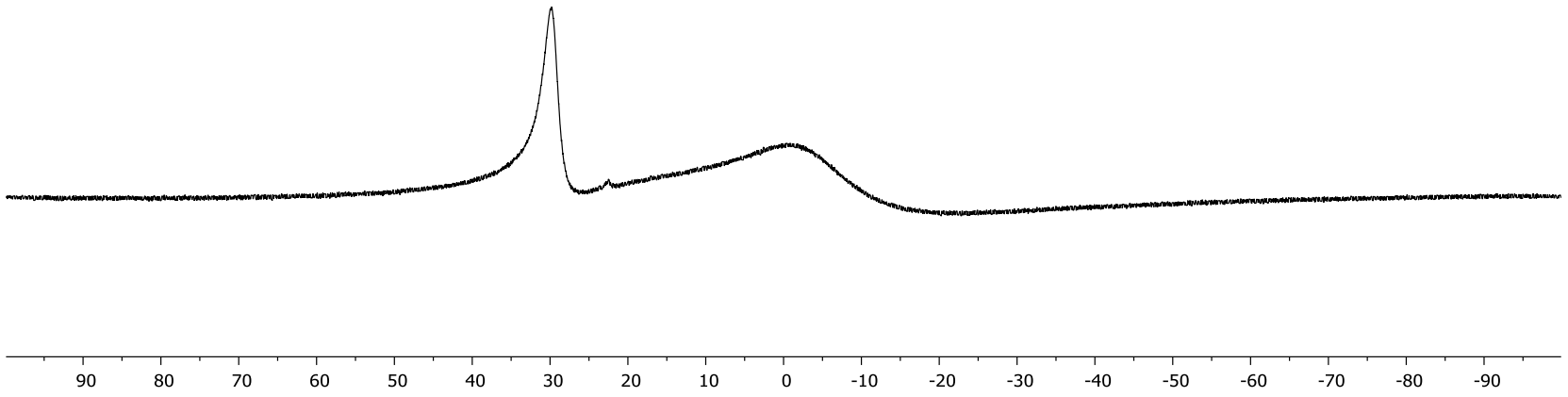

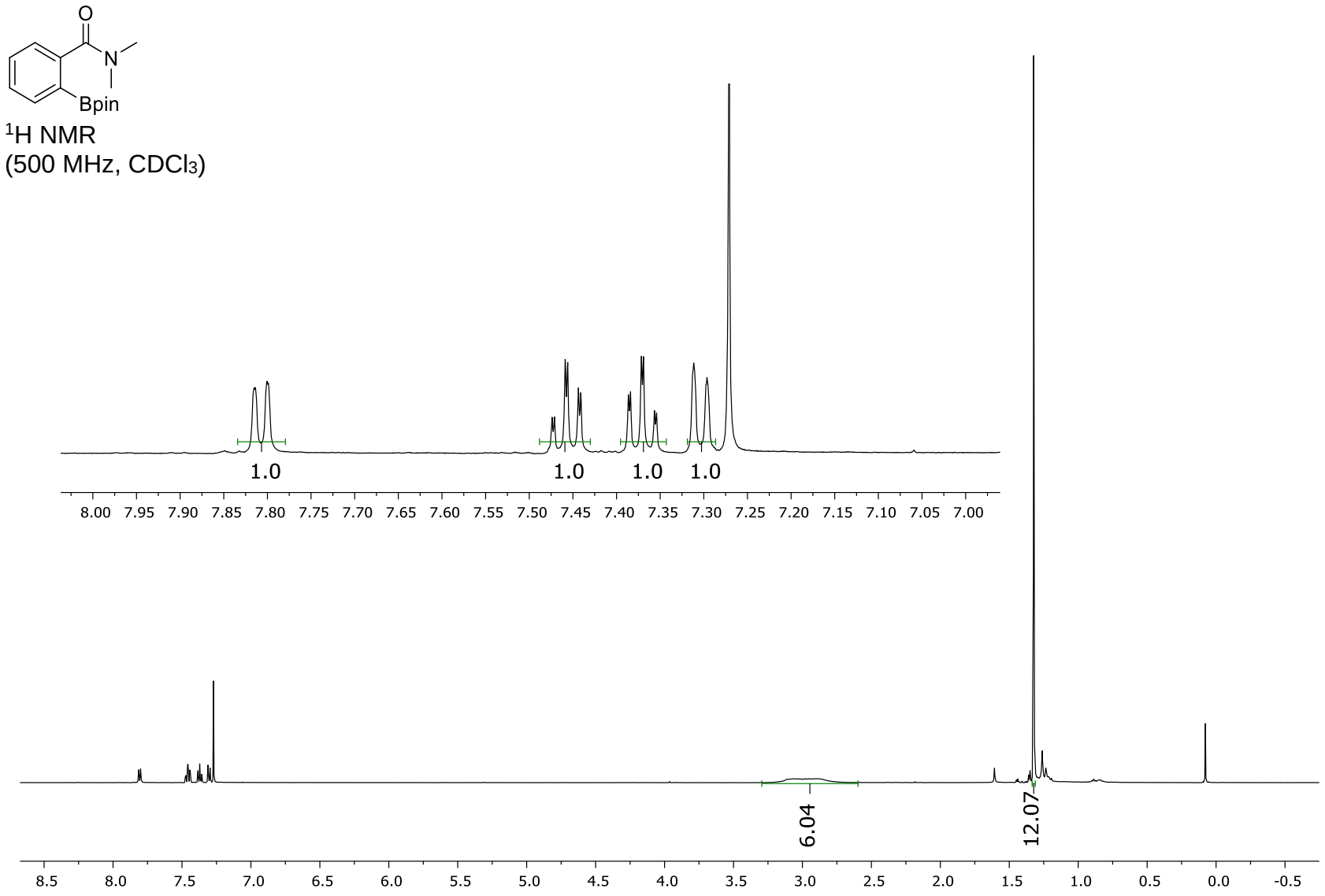
O
N
Bpin
1H NMR
(500 MHz, CDCl3)
1.0
1.0
1.0
1.0
8.00 7.95 7.90 7.85 7.80 7.75 7.70 7.65 7.60 7.55 7.50 7.45 7.40 7.35 7.30 7.25 7.20 7.15 7.10 7.05 7.00
6.04
12.07
8.5 8.0 7.5 7.0 6.5 6.0 5.5 5.0 4.5 4.0 3.5 3.0 2.5 2.0 1.5 1.0 0.5 0.0 -0.5

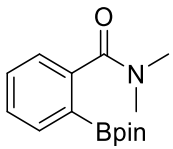

^{11}B NMR
(160 MHz, $CDCl_3$)

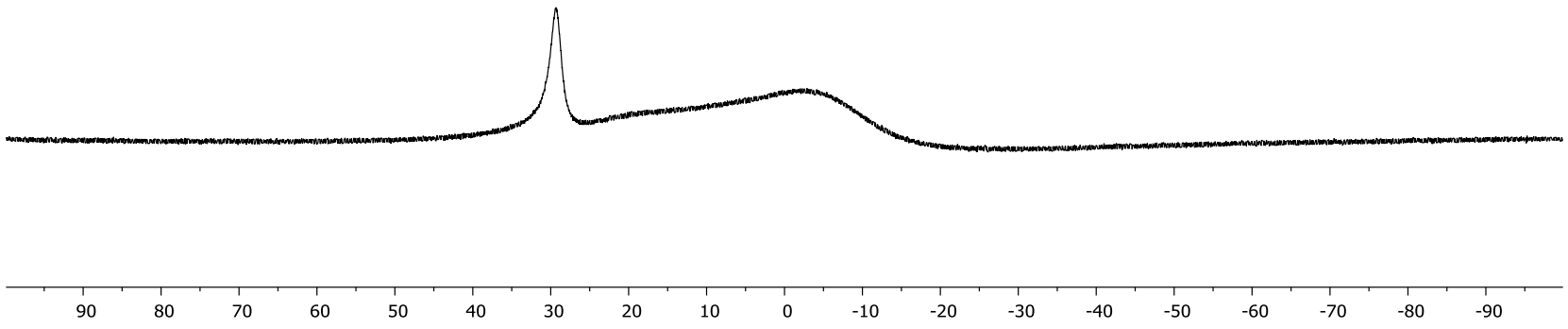

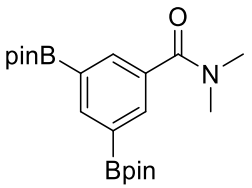

^{1}H NMR
(500 MHz, $CDCl_3$)

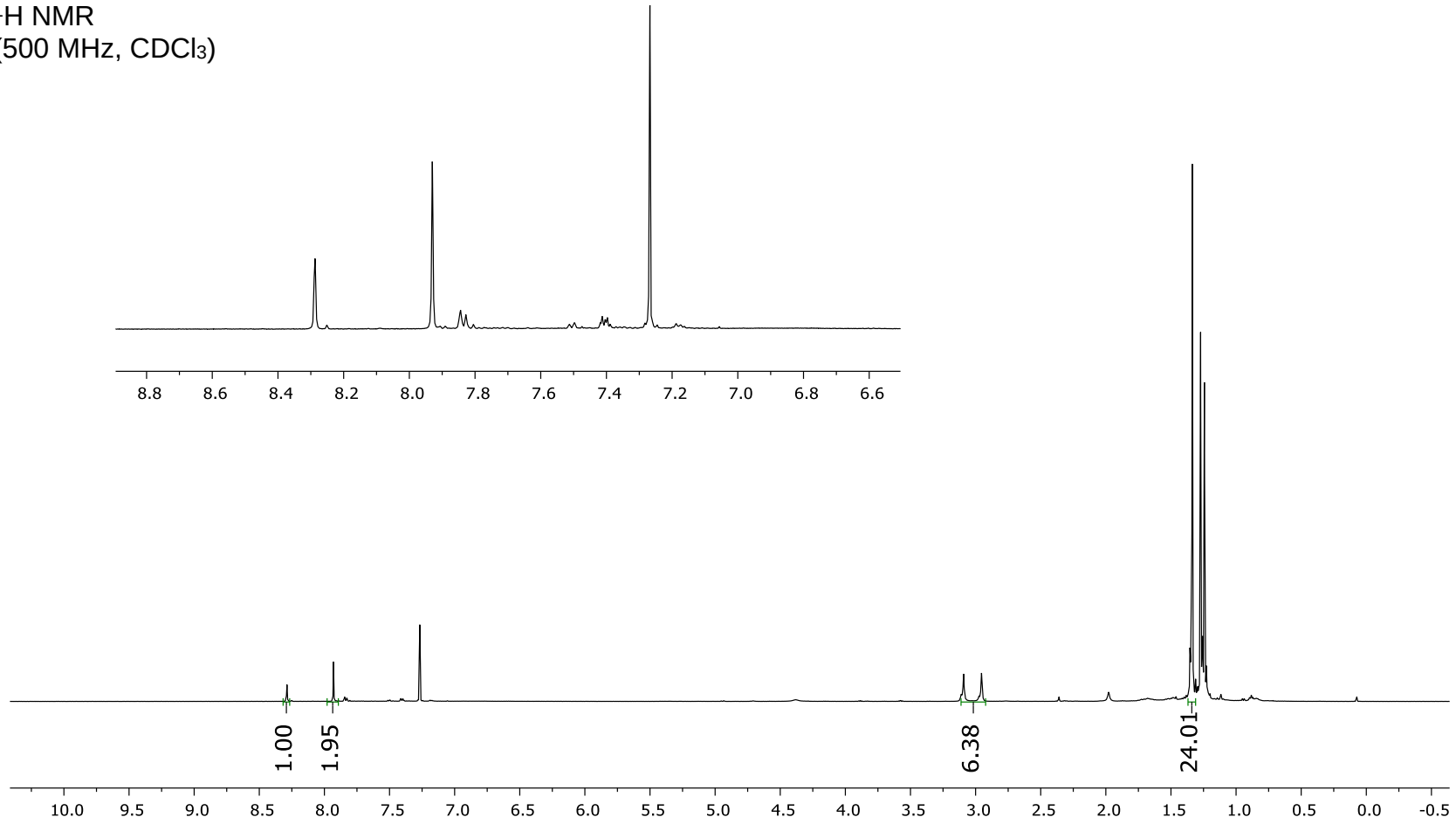

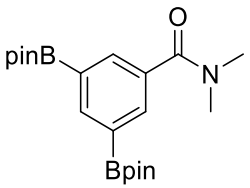

^{11}B NMR
(60 MHz, $CDCl_3$)

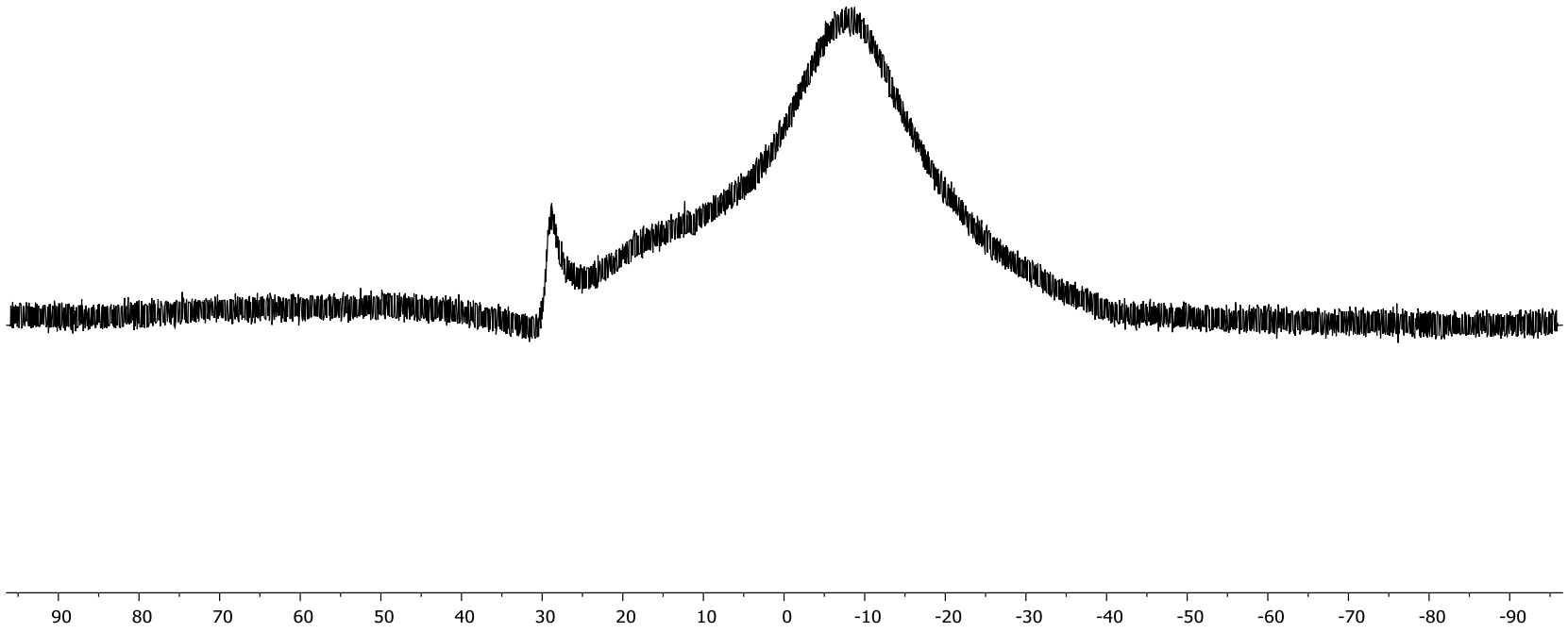

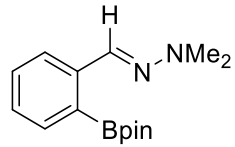

^{1}H NMR
(500 MHz, $CDCl_3$)

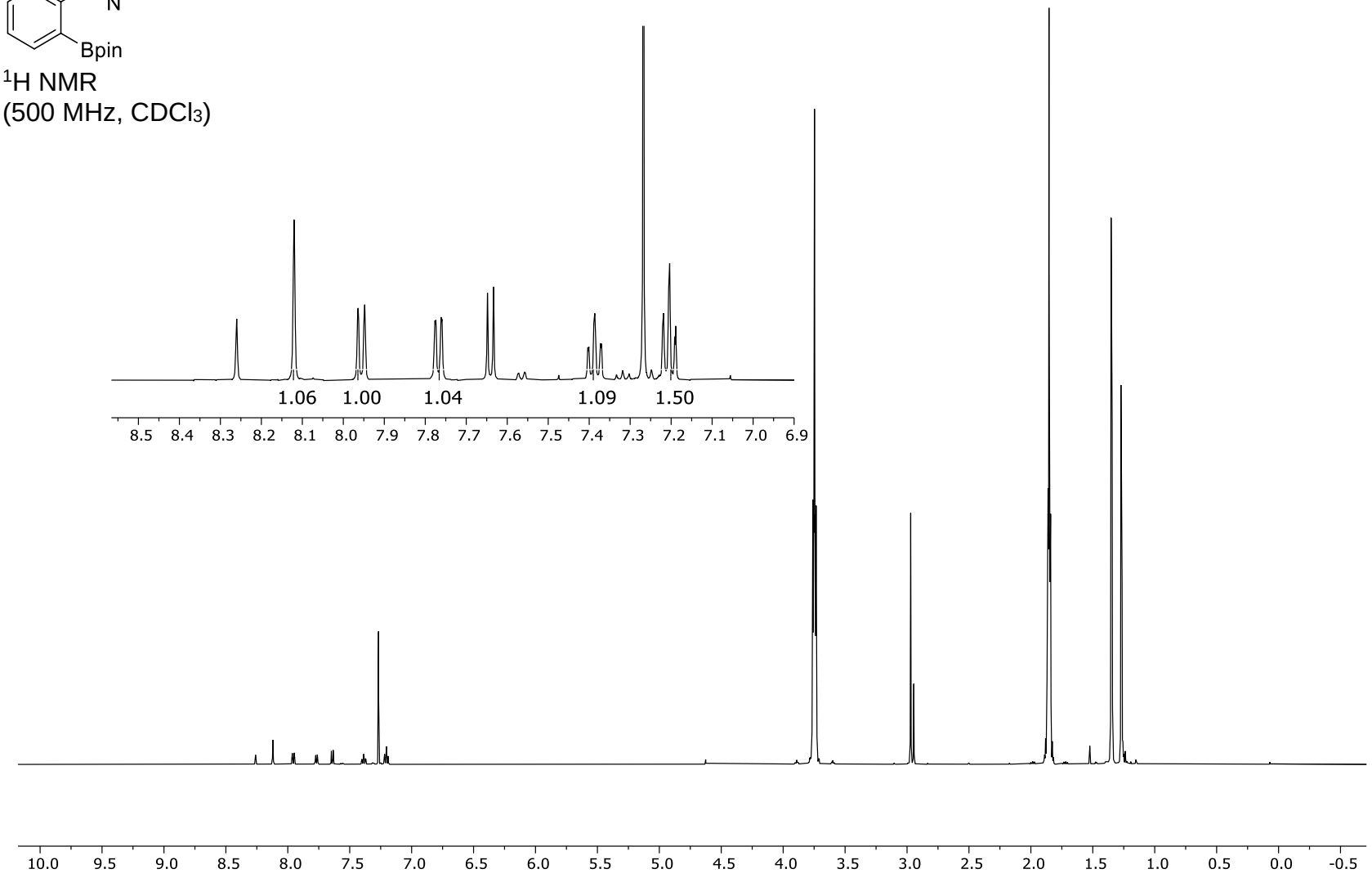

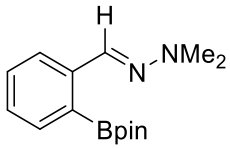

^{11}B NMR
(60 MHz, $CDCl_3$)

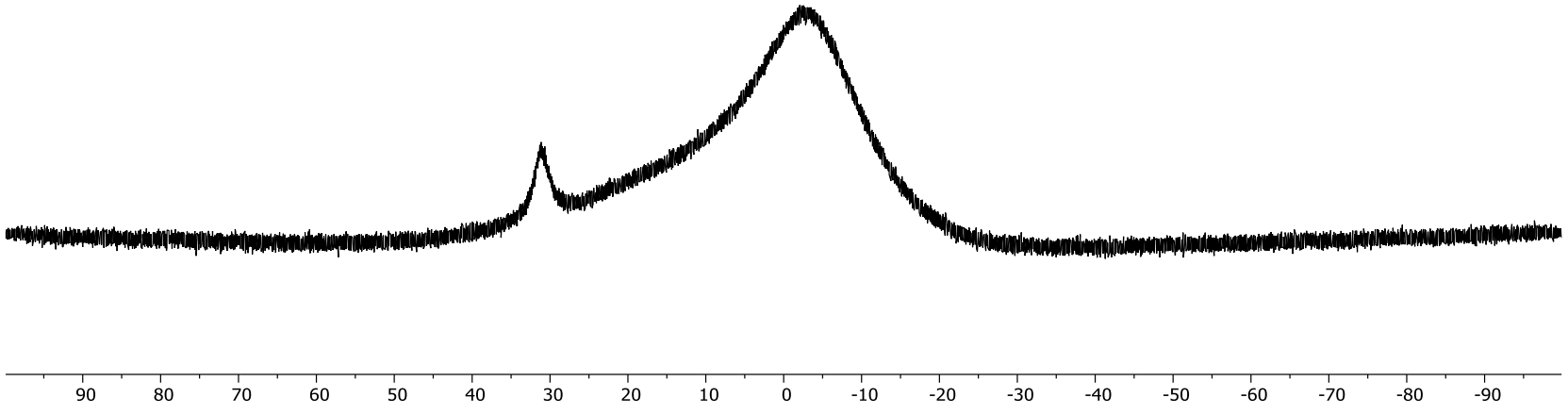

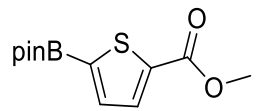

^{1}H NMR
(500 MHz, $CDCl_3$)

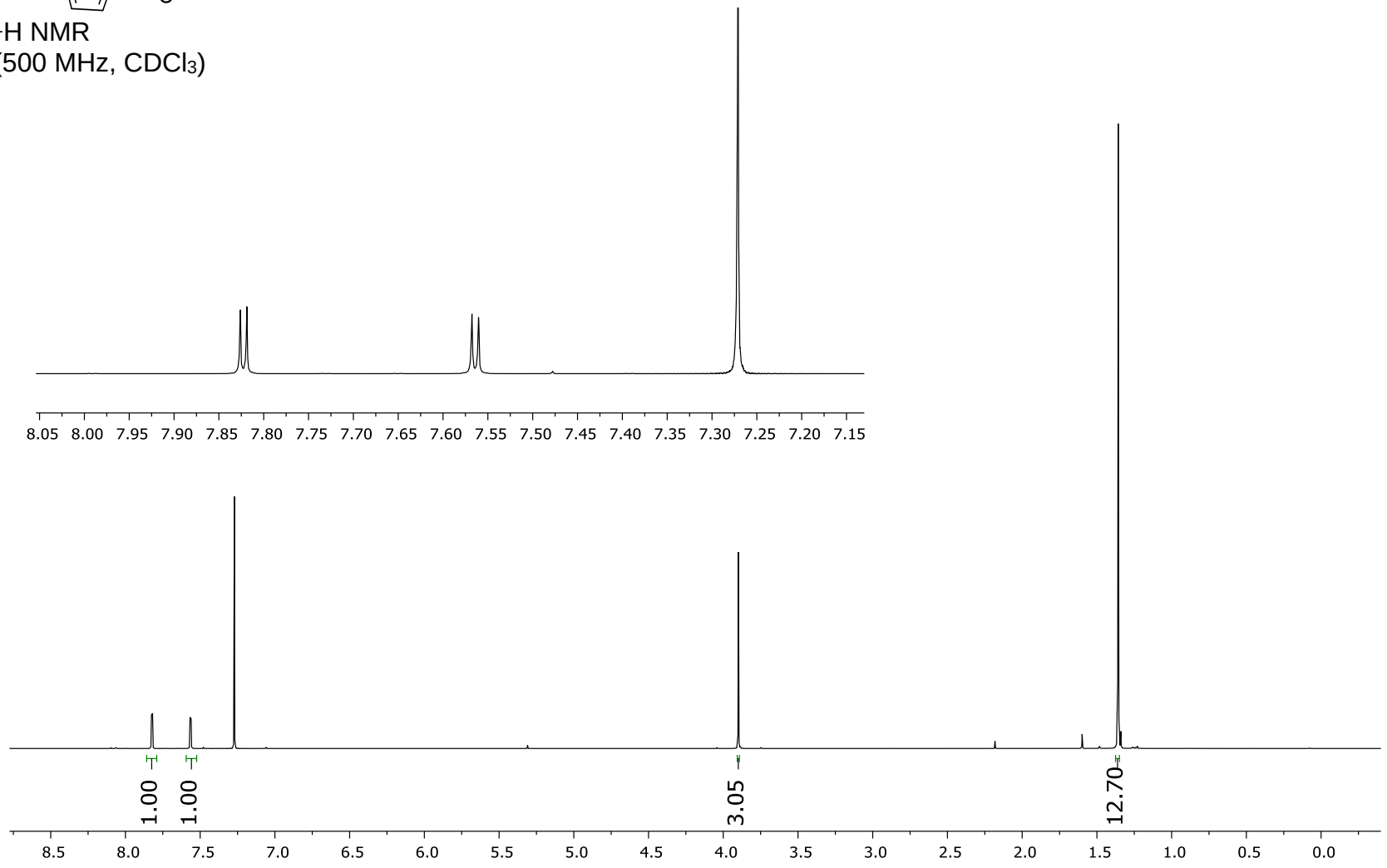

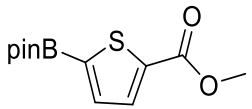

^{11}B NMR
(160 MHz, $CDCl_3$)

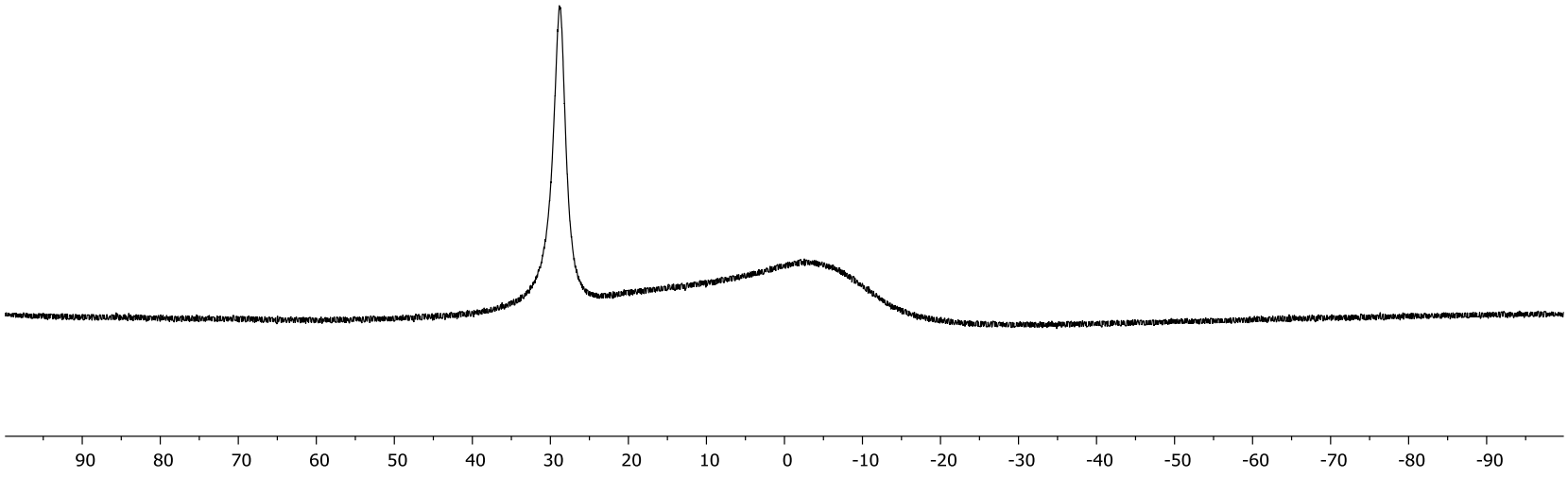

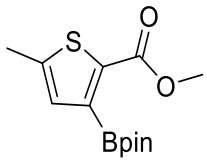

^{1}H NMR
(500 MHz, $CDCl_3$)

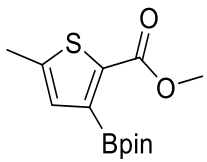

^{11}B NMR
(160 MHz, $CDCl_3$)

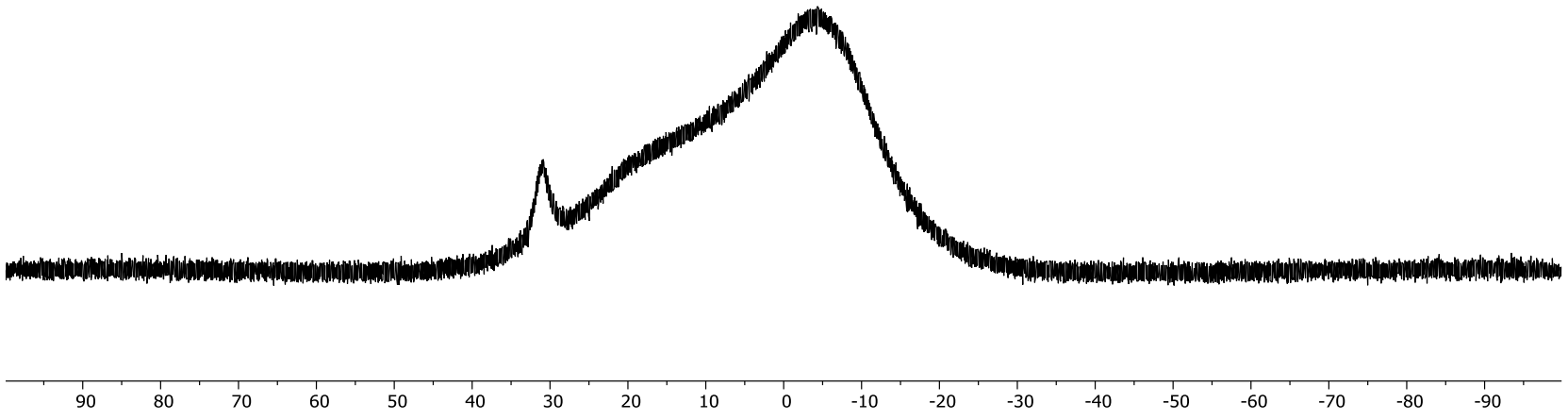

REFERENCES

REFERENCES

(1) Wang, G.; Xu, L.; Li, P. Double N,B-Type Bidentate Boryl Ligands Enabling a Highly Active Iridium Catalyst for C-H Borylation. *J. Am. Chem. Soc.* **2015**, *137*, 8058–8061.

(2) Meini, S.; Gado, F.; Stevenson, L. A.; Digiacomo, M.; Saba, A.; Codini, S.; Macchia, M.; Pertwee, R. G.; Bertini, S.; Manera, C. PSNCBAM-1 Analogs: Structural Evolutions and Allosteric Properties at Cannabinoid CB1 Receptor. *Eur. J. Med. Chem.* **2020**, *203*, 112606.

(3) Liang, X.; Xu, L.; Li, C.; Jia, X.; Wei, Y. One-Pot Propagation of (Hetero)Arylamines: Modular Synthesis of Diverse Amino-Di(hetero)arylamines. *Tetrahedron* **2019**, *75*, 721–731.

(4) Duan, J.; Choy, P. Y.; Gan, K. B.; Kwong, F. Y. N-Difluoromethylation of N-Pyridyl-Substituted Anilines with Ethyl Bromodifluoroacetate. *Org. Biomol. Chem.* **2022**, *20*, 1883–1887.

(5) Zheng, D.-Z.; Xiong, H.-G.; Song, A.-X.; Yao, H.-G.; Xu, C. Buchwald-Hartwig Amination of Aryl Esters and Chlorides Catalyzed by the Dianisole-Decorated Pd-NHC Complex. *Org. Biomol. Chem.* **2022**, *20*, 2096–2101.

(6) Wolfe, J. P.; Buchwald, S. L. Scope and Limitations of the Pd/BINAP-Catalyzed Amination of Aryl Bromides. *J. Org. Chem.* **2000**, *65*, 1144–1157.

(7) Wolan, A.; Zaidlewicz, M. Synthesis of Arylboronates by the Palladium Catalysed Cross-Coupling Reaction in Ionic Liquids. *Org. Biomol. Chem.* **2003**, *1*, 3274–3276.10.

(8) Kawamorita, S.; Ohmiya, H.; Hara, K.; Fukuoka, A.; Sawamura, M. Directed Ortho Borylation of Functionalized Arenes Catalyzed by a Silica-Supported Compact Phosphine-Iridium System. *J. Am. Chem. Soc.* **2009**, *131*, 5058–5089.

(9) Ishiyama, T.; Isou, H.; Kikuchi, T.; Miyaura, N. Ortho-C-H Borylation of Benzoate Esters with Bis(pinacolato)diboron Catalyzed by Iridium-Phosphine Complexes. *Chem. Commun.* **2010**, *46*, 159–161.

(10) Ros, A.; Estepa, B.; López-Rodríguez, R.; Álvarez, E.; Fernández, R.; Lassaletta, J. M. Use of Hemilabile N,N Ligands in Nitrogen-Directed Iridium-Catalyzed Borylations of Arenes. *Angew. Chem. Int. Ed Engl.* **2011**, *50*, 11724–11728.

(11) Miller, S. L.; Chotana, G. A.; Fritz, J. A.; Chattopadhyay, B.; Maleczka, R. E., Jr; Smith, M. R., 3rd. C-H Borylation Catalysts That Distinguish Between Similarly Sized Substituents Like Fluorine and Hydrogen. *Org. Lett.* **2019**, *21*, 6388–6392.

(12) Chotana, G. A.; Kallepalli, V. A.; Maleczka, R. E., Jr; Smith, M. R., 3rd. Iridium-Catalyzed Borylation of Thiophenes: Versatile, Synthetic Elaboration Founded on Selective C-H Functionalization. *Tetrahedron* **2008**, *64*. https://doi.org/10.1016/j.tet.2008.02.111.

(13) Wang, G.; Liu, L.; Wang, H.; Ding, Y.-S.; Zhou, J.; Mao, S.; Li, P. N,B-Bidentate Boryl Ligand-Supported Iridium Catalyst for Efficient Functional-Group-Directed C-H Borylation. *J. Am. Chem. Soc.* **2017**, *139*, 91–94.

(14) Kawamorita, S.; Ohmiya, H.; Sawamura, M. Ester-Directed Regioselective Borylation of Heteroarenes Catalyzed by a Silica-Supported Iridium Complex. *J. Org. Chem.* **2010**, *75*, 3855–3858.

(15) Tajuddin, H.; Harrisson, P.; Bitterlich, B.; Collings, J. C.; Sim, N.; Batsanov, A. S.; Cheung, M. S.; Kawamorita, S.; Maxwell, A. C.; Shukla, L.; Morris, J.; Lin, Z.; Marder, T. B.; Steel, P. G. Iridium-Catalyzed C–H Borylation of Quinolines and Unsymmetrical 1,2-Disubstituted Benzenes: Insights into Steric and Electronic Effects on Selectivity. *Chem. Sci.* **2012**, *3*, 3505–3515.

(16) Nishiyama, Y.; Misawa, Y.; Hazama, Y.; Oya, K.; Yoshida, S.; Hosoya, T. SYNTHESIS OF DIVERSE 3-AZIDO-5-(AZIDOMETHYL)BENZENE DERIVATIVES VIA FORMAL C–H AZIDATION AND FUNCTIONAL GROUP-SELECTIVE TRANSFORMATIONS. https://doi.org/10.3987/COM-18-S(F)72.

(17) Li, H.; Tang, X.; Pang, J. H.; Wu, X.; Yeow, E. K. L.; Wu, J.; Chiba, S. Polysulfide Anions as Visible Light Photoredox Catalysts for Aryl Cross-Couplings. *J. Am. Chem. Soc.* **2021**, *143*, 481–487.

(18) Kuninobu, Y.; Ida, H.; Nishi, M.; Kanai, M. A Meta-Selective C–H Borylation Directed by a Secondary Interaction between Ligand and Substrate. *Nat. Chem.* **2015**, *7*, 712–717.